ALMA MATER STUDIORUM · UNIVERSITY OF BOLOGNA

School of Science
Department of Physics and Astronomy
Master Degree in Physics

EXPLORING THE SMEFT IN THE TOP PRODUCTION AT THE LHC

Supervisor: **Submitted by:**
Prof. Fabio Maltoni   Leonardo Guidetti

Academic Year 2021/2022

Sommario

La teoria del campo effettivo del Modello Standard (SMEFT) offre un metodo efficiente di teoria dei campi per raccogliere prove sperimentali della nuova fisica, indipendentemente dalla scelta del modello teorico sottostante. Questo metodo tratta il Modello Standard (SM) come una manifestazione a bassa energia di una teoria fondamentale più ampia e consente di codificare gli effetti a più alta energia aggiungendo alla lagrangiana operatori di dimensione più alta. Pertanto, adattando i coefficienti di questi operatori per mezzo dei dati di alta precisione ottenuti negli esperimenti, è possibile vincolare un insieme di modelli teorici a cui potrebbe appartenere un modello più completo della realtà. Il modo più naturale per cercare effetti di nuova fisica è sicuramente quello di analizzare i dati ottenuti dagli esperimenti ad alta energia del Large Hadron Collider (LHC) e in particolare i dati della produzione del quark top.

In questa tesi, le espressioni delle osservabili chiave, come la sezione d'urto differenziale e totale, sono determinate analiticamente a livello LO nella SMEFT a 6 dimensioni, per la produzione di coppie quark-antiquark top tramite collisioni di protoni all'LHC. Sono inoltre riportate le espressioni non solo per i termini lineari dei coefficienti di Wilson, ma anche per i loro termini quadratici. I dati di simulazione ottenuti con tali osservabili sono poi confrontati con le simulazioni di MadGraph5.

Abstract

The Standard Model Effective Field Theory (SMEFT) offers an efficient field theory method for collecting experimental evidence of the New Physics, regardless of the choice of underlying theoretical model. This method treats the Standard Model (SM) as a low energy manifestation of a broader fundamental theory and allows higher energy effects to be encoded by adding higher-dimensional operators to the Lagrangian. Therefore, by fitting the coefficients of these operators by the high-precision data obtained in experiments, it is possible to constrain a set of theoretical models to which a more complete model of reality might belong. The most natural way to look for New Physics effects is certainly to analyse the data obtained from the high energy experiments at the Large Hadron Collider (LHC) and in particular the data of the top quark production.

In this thesis, the expressions of key observables, such as the differential and total cross section, are determined analytically at the LO level in the 6-dimensional SMEFT, for the production of top quark-antiquark pairs by proton collisions at the LHC. Expressions are found not only for the linear terms of the Wilson coefficients but also for their quadratic terms. The simulation data obtained with these observables are then compared with simulations retrieved with MadGraph5.

"*Nam Myoho Renge Kyo*"
Nichiren Daishonin
Japan, 28 April 1253

Contents

INTRODUCTION

The scope of this dissertation is to study **top quark-antiquark pair** ($t\bar{t}$) production at the **Large Hadron Collider** (LHC) through the lens of the **Standard Model Effective Field Theories** (SMEFT) approach. We perform the computation, at the leading order (LO) in perturbative expansion, of key physical observables characterising the $t\bar{t}$ final state and consider their sensitiveness to new physics effects parametrised by the SMEFT.

After a brief description of the basic physics concepts necessary to frame our work, we detail the methods used to obtain the relevant observables in the production of the $t\bar{t}$ pair at the LHC. Our analytical results are then compared and validated against a fully numerical approach as obtained through **MadGraph5_aMC@NLO**. Finally, we present a first evaluation of the sensitivity of the various SMEFT contributions to these observables.

Why Effective Field Theories?

In the context of High Energy Physics (HEP), the Standard Model (SM) of particles and elementary interactions, based on a gauge quantum field theory, is certainly the most powerful framework to describe the nature of a broad set of phenomena. However, there are several reasons, based on both theoretical as well as experimental and observational arguments, that suggest that the SM might not be complete. Evidence of dark matter and dark energy, the observed asymmetry between matter and antimatter, the strong CP-violation problem, the problem of hierarchy between the Planck and the Electro-Weak (EW) scale, gravity not yet been integrated with the SM and other issues, all point to the existence of physics Beyond the SM (BSM). This leads to many ongoing searches for BSM, often conducted through the development of specific Ultra-Violet (UV) models, highly dependent on theoretical assumptions and very often difficult to characterise.

Run 3 has just started at LHC [1], and no significant evidence for New Physics (NP) has been collected despite the numerous signatures proposed in the context of a variety of BSM models. This suggests using an approach that does not contain such strong assumptions about UV physics, apart from its consistency with the SM at low scales and the general principles of Quantum Field Theory (QFT). This way of attacking the problem is often called model independent.
Among these, **Effective Field Theories** (EFTs) offer an especially powerful tool, being them largely agnostic about UV physics yet capturing low-energy effects consistently. The SMEFT is the EFT associated to consider the SM as a linearly realised gauge theory and extending it to higher dimensions, adding all operators that are consistent with the SM gauge symmetries.

The main idea, implicit in all physical descriptions, is that the phenomena are typically described in a certain range of distances/energy and that such descriptions are by definition only effective theories. A fundamental premise of effective theories is that the dynamics at low energies (or large distances) does not depend on the details of the dynamics at high energies (or short distances). Consequently, low-energy physics can be described using an effective theory that contains only a few necessary degrees of freedom, ignoring the additional degrees present at higher energies. What is relevant in an effective theory is the determination of its scale of application and the dependence of its parameters from the same scale. The underlying purpose behind effective theories is that it is possible to develop a simplified model without knowing the overall exact theory. [2][3]
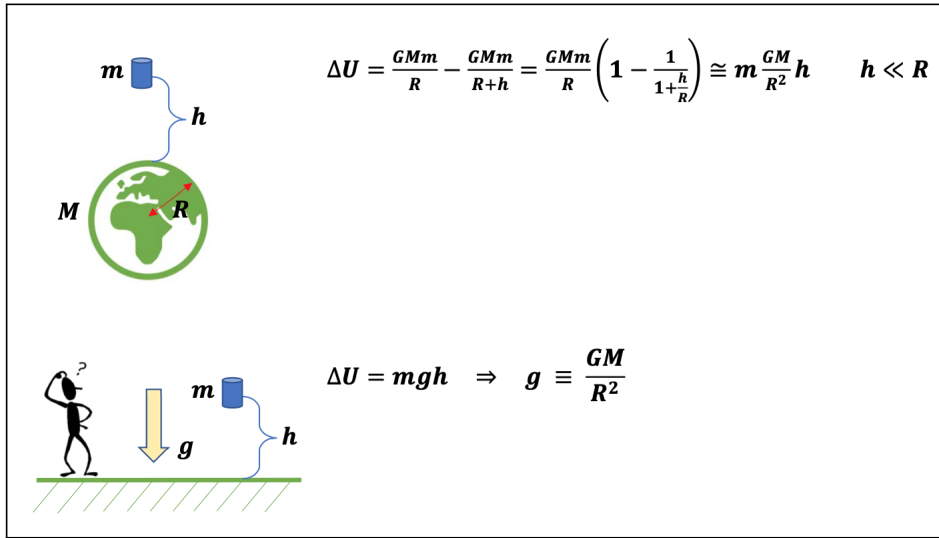
Figure 0.1: For example on the Earth, if the height of an object is less than the Radius scale the gravitational field could be approximated by a uniform function.

Nature contains an abundance of physical scales: from the Hubble scale to the Planck scale. In order to make sense of a given physical problem, we need first to identify the appropriate scale, for example, we do not need to know the composition of planets to calculate their orbital motion or we do not need to know the short-distance properties of Electro-Weak (EW) theory to calculated the Hydrogen energy levels (at least to a very good level of precision). In HEP, we use QFT to compute scattering amplitudes which then enter the determination of collider cross sections, decay rates, etc. In this case, the relevant scales are characterised by particle masses, collider energies, momentum transfers, etc. The key point is to be able to exploit large-scale separations at our advantage, by simply noting that not all of them are relevant to study a specific problem. For example, in a scattering amplitude of two particles with a different mass scale (one light m and one heavy M) with the centre of mass energy E where $E^2 \sim m^2 \ll M^2$, the "heavy physics" should not have a big impact on low energy phenomena but their small contributions could be evaluated with arbitrary precision thanks to power counting expansion terms of m^2/M^2 or E^2/M^2. Theoretical support for this concept is formalised in the *Decoupling Theorem* by Appelquist & Carrazzone (1975) [4].

An EFT efficiently describes phenomena within a certain range as the effects of higher-scale physics are absorbed into parameters of higher-dimensional interactions. The development of an EFT involves two different types of approach: the **top-down** approach by which we start from the knowledge of the theory or models at higher scales and the interest is to more efficiently and reliably

determine results of experiments performed at lower scales and the **bottom-up** approach by which we start from known phenomena and models which describe the data to eventually deduce more complex models capable of describing physics at higher scales. [5]

The EFT is a fully-fledged quantum field theory and, like any other QFT, requires a regularisation and renormalization scheme necessary to deal with ultraviolet (UV) divergences. From this theory, it is then possible to calculate any observable starting from its Lagrangian, without any additional external input, in analogy to what can be done with the Quantum Electrodynamics (QED) theory. In many cases, an EFT is the low energy limit of a more fundamental theory (which could itself be an EFT), often called a "complete theory" or "UV theory". In particular, the SMEFT is an EFT built on top of the SM fields and interactions and is used to analyse the deviations from the SM in order to look for the NP. In general, the scale at which the SMEFT operators are associated is not known but it is still possible to develop calculations in terms of power counting terms relevant to ratios of this scale.

In this work, we have used the SMEFT Lagrangian up to dimension six to develop the expressions of the observables able to be compared with experimental results obtained in the $t\bar{t}$ production process which, at the energy involved at the LHC, is one of the most relevant final states.

Relevance of the top quark

The top quark t is currently the most massive elementary particle ever observed (it is forty times heavier than the bottom quark and at the same scale as the $W^{\pm}$, Z^0 and Higgs bosons). Its mass derives from the Yukawa coupling to the Higgs boson. This coupling, very close to unity, represents the largest of the SM at the SM energy scale. After its prediction in 1977, as the weak isospin partner of the bottom quark and the sixth completion quark of the SM three generations, the top quark was finally discovered in 1995 by the CDF and DØ experiments at the Tevatron collider located in Fermilab (Batavia, US-IL).

The top quark is a spin $1/2$ fermion, has an electrical charge of $+2/3\,e$, has three possible strong colour charges, has a mass value of $(171.77 \pm 0.38)\,\text{GeV}$ (dated April 19, 2022, from 2016 CMS-LHC experimental data [6]). Like other quarks, it participates in all four fundamental interactions: gravitation, electromagnetism, weak interactions and strong interactions, being a quark, it would be subject to colour confinement.

However, due to its large mass, the lifetime of the top quark is roughly $5 \cdot 10^{-25}\,\text{s}$ [7]. This value is about one-twentieth of the time scale of strong interactions, so the top quark decays before starting to have hadronised, as opposed to other quarks, thus giving a unique opportunity to study it individually through its decay products. Its typical low-order decay process by weak force is the following: $t \rightarrow W^+ b$. This characteristic allows us to study experimentally in detail the effects of strong interactions (QCD) in its production.

Another question related to the heavy mass of the top quark is what is called the "stability of the Universe". In fact, the mass of the Higgs boson, whose value determines the absolute stability of the vacuum is strongly dependent on the mass of the top quark. Therefore, it is very important to measure the latter with high precision [8].
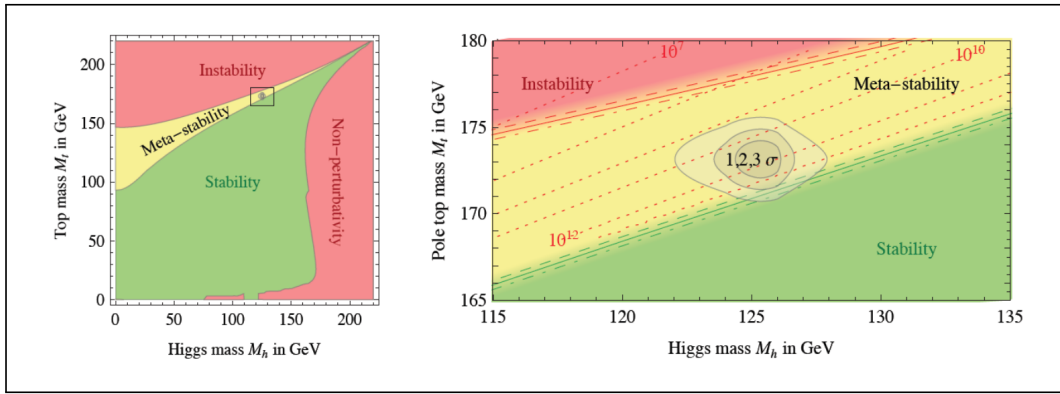
Figure 0.2: Regions of absolute stability, meta-stability and instability of the SM vacuum in the top quark - Higgs boson mass plane [8].

Given their large mass, top quarks can be produced only through very high-energy collisions. These occur naturally in the Earth's upper atmosphere when cosmic rays collide with particles in the air or can be produced in a controlled manner by a particle accelerator. After the Tevatron finished its operations, the Large Hadron Collider remains the only accelerator with enough energy to produce top quarks. There are two main types of production processes: top-pair production and single-top production.

The most common production process is the top-antitop quark pair generation via strong interactions. In a typical collision (i.e. hadron collision as at the LHC), two highly energetic gluons ($gg \to t\bar{t}$) or a highly energetic quark-antiquark pair ($q\bar{q} \to t\bar{t}$) could fuse and turn into a top and antitop pair of quarks, as shown in Figure 0.3. It is also possible to produce pairs of top-antitop through the annihilation of an intermediate virtual photon or Z^0 boson, even if, these processes are predicted to be much rarer and are normally neglected.
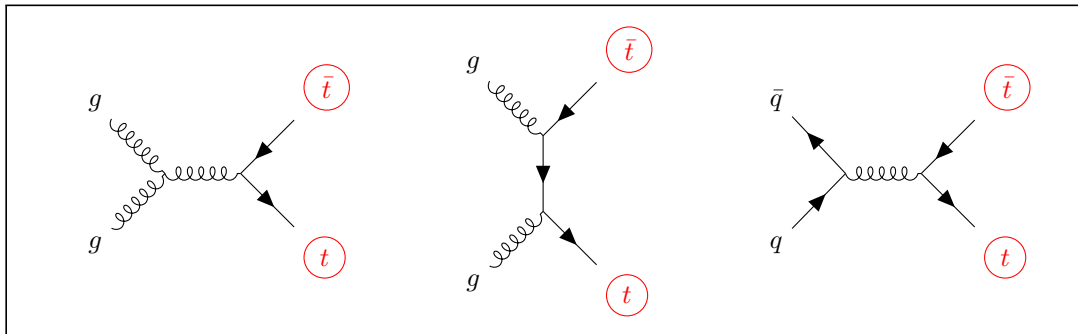
Figure 0.3: Top quark-antiquark pair production at LO, diagrams representing the three different channels (s-, t- and u-channel) for gluon fusion and a single channel for quark-antiquark annihilation are shown.

Although with less frequency than a top pair production, in a hadronic collision of suitable energy, it is possible to produce also single top quarks through weak interaction with processes shown in Figure 0.4.
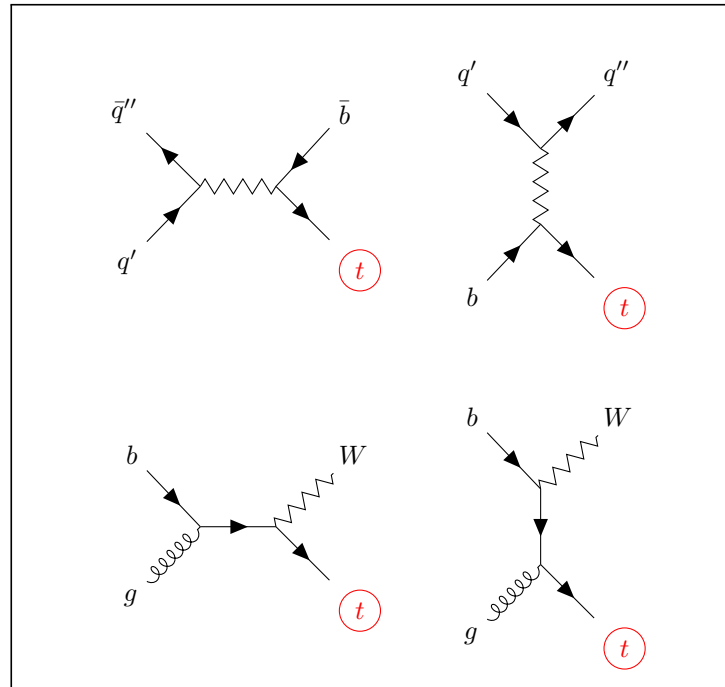
Figure 0.4: Single top quark production at LO, diagrams representing the three different channels (s-, t- and W associated) are shown.

Currently, the goal of the research of the experimental collaborations at the LHC is to improve the level of precision of the measures of the characteristics and interactions of a particle as unique as the top quark, to bring out the signs of new physics.

The Large Hadron Collider

Where can we see signs of the NP in a controlled way? Of course, the Large Hadron Collider (LHC) is a perfect laboratory to explore the HEP phenomena and detect any evidence of undiscovered interactions or resonances.

To date, the LHC synchrotron, at CERN in Geneva, is the largest and most powerful particle accelerator ever built. It is installed inside a $27\,\mathrm{km}$ ring tunnel positioned $100\,\mathrm{m}$ underground in the countryside around Geneva, between Switzerland and France [9]. It is a hadron-hadron (protons or lead ions) collider, where two separated particle beams are injected and repeatedly accelerated in opposite directions inside two dedicated ultrahigh vacuum pipes, reaching a velocity close to the speed of light. These two beams finally collide in four different positions around the ring, corresponding to the four main experiments: CMS, ATLAS, ALICE and LHCb.
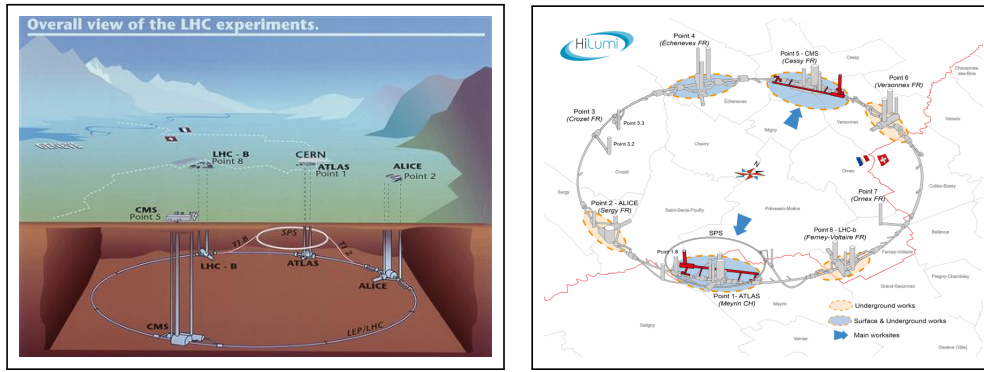
Figure 0.5: LHC scheme - source by CERN.

The two beams are obtained thanks to a complex pre-acceleration system that injects particles into the biggest ring and also thanks to a complex system of radio frequency acceleration cavities and superconducting bending and focusing magnets that allow the boost of protons up to 7 TeV nominal energy per beam ($\sqrt{s} = 14$ TeV mass centre energy of collision). This last part is surely the most delicate, constituted by 9300 multi-pole Ni-Ti alloy superconducting magnets cooled at 1.9 K by hundred tonnes of superfluid helium-4.

In case the colliding particles are protons, nominally, each beam along the ring could hold up to 2808 packets of $1.15 \cdot 10^{11}$ particles, called bunches, for a total of $3 \cdot 10^{14}$ particles per beam. At the maximum collision energy, the elapsed time between two bunches is 25 ns, with a distance between them of 7 m. This corresponds to a collision frequency of 40 MHz.
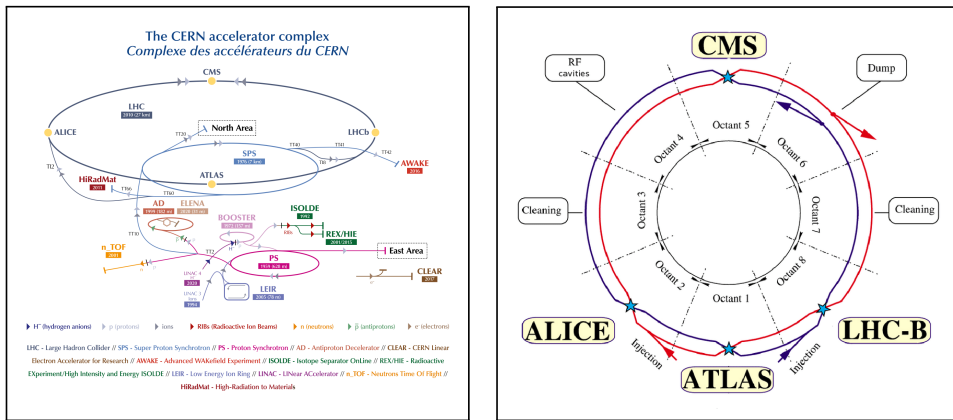
Figure 0.6: Complex chain of accelerators and sectors of the main ring - source by CERN.

Hadrons are not elementary particles, so their collisions at LHC energies are essentially complex interactions between their components, called partons (quarks, antiquarks and gluons). Despite the complexity of the activated processes, it is preferable to use hadrons compared to other elementary particles such as leptons, since having a significantly greater mass than other types of particles, they are less strongly affected by the loss of energy along the acceleration ring. It is known that a charged particle in circular motion loses energy by radiation inversely to the value of the mass of the particle to the fourth.

Each collision (e.g. proton-proton collision) together with all its produced particles is called the event. Many scattering processes take place at each event, as schematised in Figure 0.7. The most interesting part of the event is certainly the hard scattering interaction of the incoming partons of the two proton beams (represented in the figure by a large dark red spot), i.e. the part characterised by high momentum transfer. The outgoing partons, produced by hard scattering, undergo a decay process (small red spots) contributing to forming what is called the partons shower (red filaments). The remaining partons hadronise (light green spots) forming hadrons in a colour singlet state. The unstable hadrons subsequently decay (dark green spots) further into lighter particles. The radiation of photons (yellow filaments) could occur at any stage. At the same time as the hard scattering, the secondary hard scattering process (purple spots) involves the interaction of the remaining partons, that were not directly involved in the primary hard scattering interaction. These processes in the detection phase disturb the tentative reconstruction of the hard scattering process.
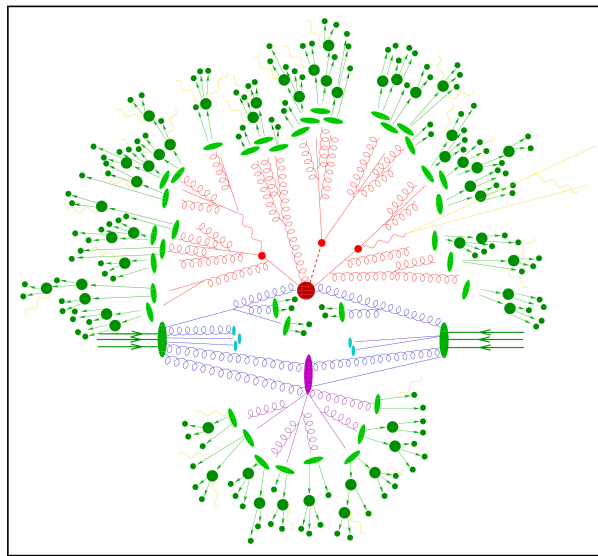
Figure 0.7: LHC event - source by SHERPA [10].

As can be clearly understood, the main parameter of experiments in a collider is the centre of mass energy $\sqrt{s}$ of the colliding particles. The value of this parameter represents an upper limit to the various types of particles that can be produced by the collision or can bring out the interference effects due to hypothetical even heavier particles. The last energy value reached at the LHC during Run II ($\sqrt{s} = 13\,\text{TeV}$) is now superseded by the current new Run III phase value, i.e. $\sqrt{s} = 13.6\,\text{TeV}$.

Another fundamental parameter, for the LHC and in any case for a collider in general, is the instantaneous luminosity L, which provides a measure of the rate of revealed events in a collision experiment. In fact, the number of events of a specific interaction, detected during an elapsed period of time, is given by the product of the instantaneous luminosity, integrated in the same period, by the cross section σ of the interaction process. It is evident that a high luminosity allows the detection of rare processes, a typical characteristic of weak processes. This parameter depends on a lot of factors, i.e. the number of particles per bunch, the number of bunches per beam, the revolution frequency, the velocity of particles and also by the geometric shape of bunching beams, etc. The LHC design instantaneous luminosity is roughly of the order of $L = 1 \cdot 10^{34}\,\text{cm}^{-2}\text{s}^{-1} = 1 \cdot 10^{-2}\,(\text{pb})^{-1}\text{s}^{-1}$. At present, the High-Luminosity Large Hadron Collider (HL-LHC) project is a current program that aims to increase the integrated luminosity by a factor of 10 beyond the LHC design value.

The events generated by the huge number of collisions are identified using large detectors capable of reconstructing the processes involved. The detectors are analogous to three-dimensional digital cameras that can take millions of snapshots per second. For this purpose, the detectors are built with different types of layers, each of them having the task of detecting specific particles together with their kinematic characteristics. Each of the four main LHC experiments, in which particles are made to collide, is essentially constituted of a specific type of detector. These are:

- Compact Muon Solenoid (CMS): is a generic detector designed to observe a wide range of physics and to discover new phenomena;

- A Toroidal LHC Apparatus (ATLAS): is the second general-purpose detector of the LHC with physical objectives similar to CMS, but with a different design and technical implementation;

- A Large Ion Collider Experiment (ALICE): specialises in studying the properties of quark-gluon plasma by analysing lead ion collisions;

- Large Hadron Collider beauty (LHCb): is to study the slight asymmetry between matter and antimatter by analysing the interactions of the bottom quark.

The large number of collision events that arise in each experiment produces an enormous amount of data generated by each individual detector. One of the main problems is certainly represented by the instantaneous processing of all these data in order to identify potentially significant processes. The Trigger system is part of each experiment that uses simple criteria to rapidly decide which is the right one to be recorded. Anyway, collectively, the LHC experiments produce about 15 PB of raw data each year that must be stored, processed, and analysed.

Chapter 1

EFT AND SMEFT APPROACH

In this chapter, we briefly present a summary of the theoretical description of particle physics given by the SM, a short application of EFT and the minimal elements of SMEFT to conduct the calculation for top quark-antiquark pair production.

1.1 Brief summary of the Standard Model (SM)

The SM represents one of the largest and longest efforts in the history of physics to successfully describe and organise the basic constituent elements of Nature. It is a coherent theoretical construction that has been hugely successful in explaining essentially most of the phenomenology of high energy and particle physics. The birth of SM could be traced back to the discoveries of the first elementary particles, which began as early as the end of the 19$^{\text{th}}$ Century, although it is more appropriate to identify its birth with the advent of the first hypotheses on gauge theories, developed between the 1950s and the 1970s. Its great success in the scientific community is certainly due to the self-consistency of the constituent theoretical elements demonstrated so far and mainly to its ability to provide extremely accurate predictions of numerous experimental phenomena. However, some aspects of the SM remain mysterious while some observations seem not to account for the SM framework. This suggests that the SM should be expanded in some way.

The SM of particles and their interactions is a QFT implementation, whose fields, corresponding to the currently discovered particles, are conventionally represented and organised as shown in Figure 1.1. This set of particles is divided into *fermions* (spinorial fields), the basic constituents of matter, and *bosons* (vector fields), mediators of the fundamental forces of Nature as described by gauge interactions: electromagnetic force (*photon* γ), the weak force (three *vector bosons* W^+, W^- and Z^0) and strong force (eight *gluons* g). The Higgs particle, being a scalar, is the carrier of a different force, which we call Yukawa interaction. Fermions are divided into *quarks* (six *flavours* of quarks divided into three generations, each of them further divided into *up* and *down* flavours), which interact through all forces, therefore they are endowed with electric charge, weak charge (weak isospin charge) and strong charge (colour charge) and *leptons* (divided into three generations, each of them

further divided into *neutrinos* and *leptons properly said*), which interact only with the electroweak force and therefore are endowed with an electric charge and a weak charge. In particular, neutrinos have zero electric charge. As already mentioned, a further subdivision of fermions is in *families*, said also *generations*, which have similar characteristics except for the mass of the constituent particles. Finally, there remains the *Higgs boson*, whose interactions with other SM particles are governed by their mass, or rather, it is the interaction with this newly discovered boson that determines the mass of each individual particle.

As predicted by the Dirac theory, each fermion particle has its own anti-particle, with an opposite charge.

Some typical characteristics of the SM particles:

- leptons appear in nature as free particles, although only the electron and neutrinos (apart from the neutrinos oscillation) appear to be stable, while all the others decay via electroweak interactions;

- all quarks (except for the top quark) and gluons can only be studied indirectly since they cannot appear isolated in nature, but only in colourless bound states called *hadrons* (*mesons* and *baryons*), states of two or three quarks "tied" by gluons: this phenomenon is called colour confinement;

- photons are the only long-range stable bosons, the other weak bosons, endowed with mass, also decay due to electroweak interactions.
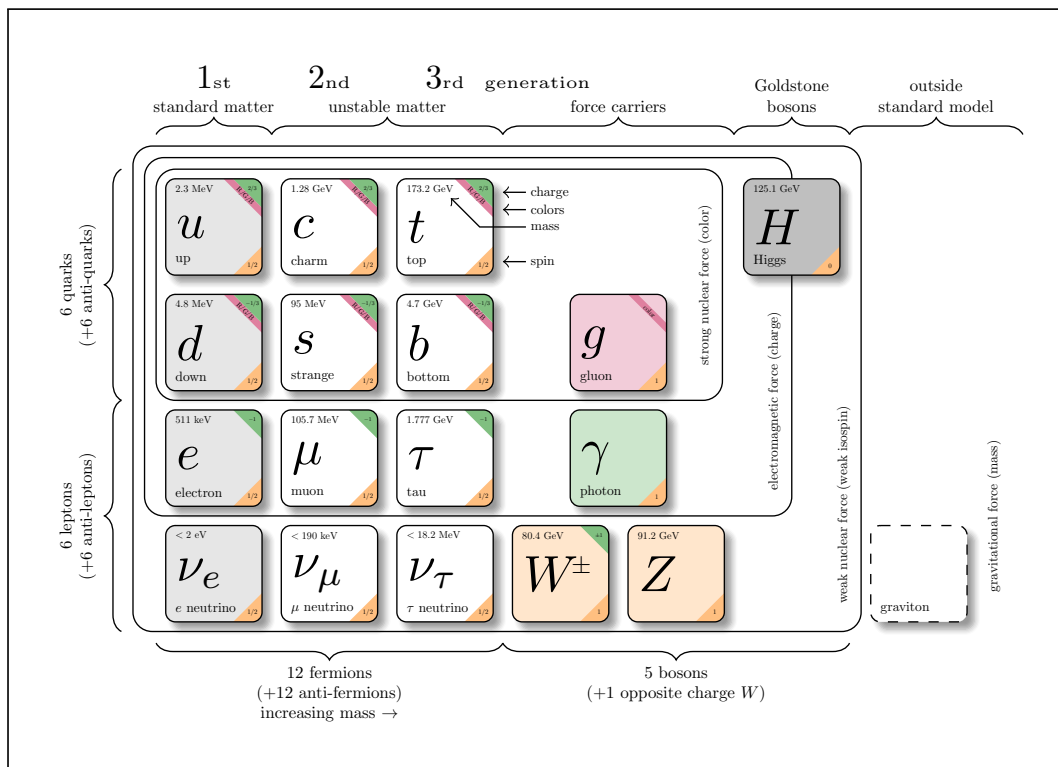

Figure 1.1: Standard Model - source by Carsten Burgard [11].

The SM field theory is a renormalisable non-Abelian gauge symmetry theory based on the transformation groups $SU(3)_C \times SU(2)_L \times U(1)_Y$ [1], with partial symmetry breaking induced by the Brout-Englert-Higgs (BEH) mechanism in the electroweak sector $SU(2)_L \times U(1)_Y$. The bosons are chirally coupled to the three families of fermions and explicit mass terms are not allowed, as these terms would explicitly break the gauge symmetry. For the same reason, mass terms are also not allowed for fermions. The masses of the bosons as well as of fermions emerge from the BEH mechanism. In this strict version, the SM describes massless neutrinos. While we know neutrinos are actually massive, for the sake of the study presented here whose applications are meant for the LHC, this is an extremely good approximation.

To mathematically describe the SM it is necessary to correctly set the parameters in its Lagrangian and to identify its scalar, vector and spinor field components of the Minkowski space-time.

Considering the lepton fields, $l \in \{\nu_e, \nu_\mu, \nu_\tau, e, \mu, \tau\}$, and the quark fields, $q \in \{u, c, t, d, s, b\}$, it is useful to organise them in the following compact *chiral structures*:

- $$
L \equiv \begin{bmatrix} \begin{bmatrix} \nu_e \\ e_L \end{bmatrix} \\ \begin{bmatrix} \nu_\mu \\ \mu_L \end{bmatrix} \\ \begin{bmatrix} \nu_\tau \\ \tau_L \end{bmatrix} \end{bmatrix} \quad
R \equiv \begin{bmatrix} e_R \\ \mu_R \\ \tau_R \end{bmatrix} \quad
Q \equiv \begin{bmatrix} \begin{bmatrix} u_L \\ d_L \end{bmatrix} \\ \begin{bmatrix} c_L \\ s_L \end{bmatrix} \\ \begin{bmatrix} t_L \\ b_L \end{bmatrix} \end{bmatrix} \quad
U \equiv \begin{bmatrix} u_R \\ c_R \\ t_R \end{bmatrix} \quad
D \equiv \begin{bmatrix} d_R \\ s_R \\ b_R \end{bmatrix},
$$

where different dynamics must be considered for each chiral component, *left-handed* $f_L \equiv (1 - \gamma^5)f/2$ and *right-handed* $f_R \equiv (1 + \gamma^5)f/2$, of each fermion field f since SM is supposed to be a chiral theory. Neutrinos are left-handed only.

We have also to take into account that leptons and neutrinos are represented by only one simple Dirac spinorial field, while each quark requires three spinorial fields to represent it, each for all three possible colours. So, a generic quark q can be represented by the following field structure $q \equiv (q^{(r)}, q^{(g)}, q^{(b)})$. Conventionally, the three possible colour charge values are "r": red, "g": green and "b": blue.

All the above fermion fields are measured in $[\text{Energy}]^{1/2} [\text{Length}]^{-1}$ for physical units or in $[\text{Energy}]^{3/2}$ for natural units (where $\hbar = c = 1$) or more simply indicating the only exponent: $[\![f]\!] = 3/2$.

For the force mediators, the following vector fields are considered:

- A_μ for the photon γ;

- W_μ^+ and W_μ^- for the two W^+ and W^- weak bosons and Z_μ for the Z^0 weak boson;

- $\vec{G}_\mu \equiv (G_\mu^1, ..., G_\mu^8)$ for the eight gluons g, corresponding to the eight generators of $SU(3)_C$ group.

Instead of the above-mentioned photon field A_μ and weak fields $W_\mu^\pm, Z_\mu$, for the theory it is preferable to use the following rotating fields, corresponding to the whole electroweak sector:

---

[1]C stands for colour, L stands for left-handed and Y stands for hyper-charge

- $\vec{W}_\mu \equiv (W_\mu^1, W_\mu^2, W_\mu^3)$ and B_μ to cover the four electroweak bosons, corresponding to the four generators of $SU(2)_L \times U(1)_Y$ group:

$$
\begin{cases}
W_\mu^1 \equiv \dfrac{W_\mu^+ + W_\mu^-}{\sqrt{2}} & W_\mu^3 \equiv A_\mu \sin\theta_W + Z_\mu \cos\theta_W \\[2mm]
W_\mu^2 \equiv \dfrac{W_\mu^+ - W_\mu^-}{\sqrt{2}} i & B_\mu \equiv A_\mu \cos\theta_W - Z_\mu \sin\theta_W
\end{cases} ,
$$

where θ_W is the Weinberg angle.

Related to the Higgs boson we have to consider the following complex scalar doublet field (four real scalar fields):

- $\Phi \equiv \begin{bmatrix} \Phi^+ \\ \Phi^0 \end{bmatrix}$.

All of these boson fields are measured in $[\text{Energy}]^{1/2} [\text{Length}]^{-1/2}$ for physical units or in $[\text{Energy}]^1$ for natural units (where $\hbar = c = 1$) or more simply indicating the only exponent: $[\![A_\mu]\!] = [\![W_\mu^\pm]\!] = [\![Z_\mu]\!] = [\![\vec{G}_\mu]\!] = [\![\Phi]\!] = 1$.

1.1.1 Gauge theory

The key point of the SM gauge theory is to ensure the local invariance related to the $SU(3)_C \times SU(2)_L \times U(1)_Y$ transformation group because thanks of this principle emerge the interaction between the constituents of the basic matter and the force mediators. For this purpose it is necessary to assign the following *charge scheme* to each field:

fermions	field generations			charge						
	I	II	III	colour		weak isospin		hyper	electric	
				$\vec{\mathcal{J}}$	$\mathcal{C}$	$\vec{\mathcal{J}}$	$\mathcal{J}^3$	$\mathcal{Y}$	$\mathcal{Q}$	
quarks $\;_{\substack{u\;c\;t \\ d\;s\;b}}$	$\begin{bmatrix} u_L \\ d_L \end{bmatrix}$	$\begin{bmatrix} c_L \\ s_L \end{bmatrix}$	$\begin{bmatrix} t_L \\ b_L \end{bmatrix}$	$\vec{\tau}/2$ $\vec{\tau}/2$	r g b r g b	$\vec{\sigma}/2$	$\begin{cases}+1/2 \\ -1/2\end{cases}$	$+1/3$ $+1/3$	$+2/3$ $-1/3$	
	u_R	c_R	t_R	$\vec{\tau}/2$	r g b	0	0	$+4/3$	$+2/3$	
	d_R	s_R	b_R	$\vec{\tau}/2$	r g b	0	0	$-2/3$	$-1/3$	
leptons $\;_{\substack{\nu_e\;\nu_\mu\;\nu_\tau \\ e\;\;\mu\;\;\tau}}$	$\begin{bmatrix} \nu_e \\ e_L \end{bmatrix}$	$\begin{bmatrix} \nu_\mu \\ \mu_L \end{bmatrix}$	$\begin{bmatrix} \nu_\tau \\ \tau_L \end{bmatrix}$	0 0	$-$ $-$	$\vec{\sigma}/2$	$\begin{cases}+1/2 \\ -1/2\end{cases}$	-1 -1	0 -1	
	e_R	μ_R	τ_R	0	$-$	0	0	-2	-1	

Table 1.1: Charge scheme for fermions.

bosons	fields	charge				
		colour $\mathcal{C}$	weak isospin $\vec{\mathcal{I}}$	$\mathcal{I}^3$	hyper $\mathcal{Y}$	electric $\mathcal{Q}$
eight gluons g	$\vec{G}_\mu$	colour/anticolour	0	0	0	0
photon γ	A_μ	–	0	0	0	0
three weak bosons $W^\pm\ Z^0$	$W_\mu^\pm$ Z_μ	– –	$\vec{\sigma}$	± 1 0	0 0	± 1 0
Higgs boson H	$\begin{bmatrix}\Phi^+\\\Phi^0\end{bmatrix}$	– –	$\vec{\sigma}/2$	$+1/2$ $-1/2$	$+1$ $+1$	$+1$ 0

Table 1.2: Charge scheme for bosons.

The electric charge $\mathcal{Q}$ (not to be confused with the left-handed quark symbol Q) is defined in terms of weak isospin charge $\mathcal{I}^3$ (i.e. the third part of the weak isospin vector) and hyper-charge $\mathcal{Y}$ by the well-known "weak Gell-Mann-Nishijima relation" also said Weinberg relation [2]:

$$\mathcal{Q} \equiv \mathcal{I}^3 + \frac{\mathcal{Y}}{2}\,. \qquad (1.1.1.1)$$

These charge schemes allow the building of the following local transformation, for which the SM theory should be invariant:

$$\mathcal{U} \equiv \exp\left(ig_s\,\vec{\mathcal{J}}\cdot\vec{\vartheta}\ +\ ig\,\vec{\mathcal{I}}\cdot\vec{\eta}\ +\ ig'\,\frac{\mathcal{Y}}{2}\zeta \right)\,, \qquad (1.1.1.2)$$

where $\{g_s, g, g'\}$ are the *gauge coupling*, measured in $[\text{Energy}]^{-1/2}\,[\text{Length}]^{-1/2}$ for physical units or in [1] for natural units (where $\hbar = c = 1$), $\vec{\tau} \equiv (\tau^1, ..., \tau^8)$ are the eight 3×3 Gell-Mann matrices, corresponding to the eight symmetry generators $\vec{\mathcal{J}}$ of the $SU(3)_C$ group, $\vec{\sigma} \equiv (\sigma^1, \sigma^2, \sigma^3)$ are the three 2×2 Pauli matrices, corresponding to the three symmetry generators $\vec{\mathcal{I}}$ of the $SU(2)_L$ group and $\{\vec{\vartheta}, \vec{\eta}, \zeta\}$ are the gauge parameter transformations, varying over space-time.

In order to respect the gauge principle and make the kinetic terms invariant for local transformation in SM Lagrange expression, it is necessary to modify the derivative through the minimal coupling principle, by introducing the following covariant derivative:

$$\mathcal{D}_\mu \equiv \partial_\mu\ -\ ig_s\,\vec{\mathcal{J}}\cdot\vec{G}_\mu\ -\ ig\,\vec{\mathcal{I}}\cdot\vec{W}_\mu\ -\ ig'\,\frac{\mathcal{Y}}{2}B_\mu\,, \qquad (1.1.1.3)$$

hence for each type of field:

$$\begin{cases}
\mathcal{D}_\mu L \equiv \partial_\mu L\ -\ ig\frac{\vec{\sigma}}{2}\cdot\vec{W}_\mu L\ +\ ig'\frac{1}{2}B_\mu L & \Longleftarrow & \vec{\mathcal{J}}(L)=0 \quad \vec{\mathcal{I}}(L)=\frac{\vec{\sigma}}{2} \quad \mathcal{Y}(L)=-1\,, \\[2mm]
\mathcal{D}_\mu R \equiv \partial_\mu R\ +\ ig'B_\mu R & \Longleftarrow & \vec{\mathcal{J}}(R)=0 \quad \vec{\mathcal{I}}(R)=0 \quad \mathcal{Y}(R)=-2\,, \\[2mm]
\mathcal{D}_\mu Q \equiv \partial_\mu Q\ -\ ig_s\frac{\vec{\tau}}{2}\cdot\vec{G}_\mu Q\ -\ ig\frac{\vec{\sigma}}{2}\cdot\vec{W}_\mu Q\ -\ ig'\frac{1}{6}B_\mu Q & \Longleftarrow & \vec{\mathcal{J}}(Q)=\frac{\vec{\tau}}{2} \quad \vec{\mathcal{I}}(Q)=\frac{\vec{\sigma}}{2} \quad \mathcal{Y}(Q)=+\frac{1}{3}\,, \\[2mm]
\mathcal{D}_\mu U \equiv \partial_\mu U\ -\ ig_s\frac{\vec{\tau}}{2}\cdot\vec{G}_\mu U\ -\ ig'\frac{2}{3}B_\mu U & \Longleftarrow & \vec{\mathcal{J}}(U)=\frac{\vec{\tau}}{2} \quad \vec{\mathcal{I}}(U)=0 \quad \mathcal{Y}(U)=+\frac{4}{3}\,, \\[2mm]
\mathcal{D}_\mu D \equiv \partial_\mu D\ -\ ig_s\frac{\vec{\tau}}{2}\cdot\vec{G}_\mu D\ +\ ig'\frac{1}{3}B_\mu D & \Longleftarrow & \vec{\mathcal{J}}(D)=\frac{\vec{\tau}}{2} \quad \vec{\mathcal{I}}(D)=0 \quad \mathcal{Y}(D)=-\frac{2}{3}\,, \\[2mm]
\mathcal{D}_\mu \Phi \equiv \partial_\mu \Phi\ -\ ig\frac{\vec{\sigma}}{2}\cdot\vec{W}_\mu \Phi\ -\ ig'\frac{1}{2}B_\mu \Phi & \Longleftarrow & \vec{\mathcal{J}}(\Phi)=0 \quad \vec{\mathcal{I}}(\Phi)=\frac{\vec{\sigma}}{2} \quad \mathcal{Y}(\Phi)=+1\,.
\end{cases}$$

---

[2]The analysis of broken and un-broken generators of the BEH mechanism leads to this formula.

The above derivative Formula 1.1.1.3 is gauge covariant for transformations like Formula 1.1.1.2 if gauge boson fields transform in the following manner:

$$
\begin{cases}
G_\mu & \longrightarrow \ \mathcal{U} G_\mu \mathcal{U}^{-1} + \dfrac{1}{ig_s} \left(\partial_\mu \mathcal{U} \right) \mathcal{U}^{-1} & \text{where} \quad G_\mu \equiv \vec{\mathcal{J}} \cdot \vec{G}_\mu \quad \text{and} \quad \mathcal{U} \equiv \exp\left(ig_s \, \vec{\mathcal{J}} \cdot \vec{\vartheta} \right), \\[2mm]
W_\mu & \longrightarrow \ \mathcal{U} W_\mu \mathcal{U}^{-1} + \dfrac{1}{ig} \left(\partial_\mu \mathcal{U} \right) \mathcal{U}^{-1} & \text{where} \quad W_\mu \equiv \vec{\mathcal{J}} \cdot \vec{W}_\mu \quad \text{and} \quad \mathcal{U} \equiv \exp\left(ig \, \vec{\mathcal{J}} \cdot \vec{\eta} \right), \\[2mm]
B_\mu & \longrightarrow \ B_\mu + \dfrac{\mathcal{y}}{2} \partial_\mu \zeta & \text{where} \hspace{3.5cm} \mathcal{U} \equiv \exp\left(ig' \, \dfrac{\mathcal{y}}{2} \zeta \right).
\end{cases}
\tag{1.1.1.4}
$$

Imposing the validity of the gauge theory, the fermions kinetic terms $\bar{f} i \slashed{\partial} f$, where $\slashed{\partial} \equiv \gamma^\mu \partial_\mu$, must be changed in the following way:

$$
\bar{f} i \slashed{D} f \,,
\tag{1.1.1.5}
$$

for each chiral structure of fermion fields $f \in \{L, R, Q, U, D\}$ and where $\slashed{D} \equiv \gamma^\mu \mathcal{D}_\mu$.

In addition to kinetic terms, the above covariant derivative also introduces couplings between fermions and bosons and allows mixing between different flavour fermions: $\bar{f}(g_s \vec{\mathcal{J}} \cdot \vec{G}_\mu + g \vec{\mathcal{J}} \cdot \vec{W}_\mu + g' \mathcal{y}/2 \, B_\mu) f$.

For the above relations, boson fields are called *gauge fields* and for each of them it is necessary to introduce the following *strength tensor fields* to take into account the kinetic terms in the Lagrangian expression:

$$
\begin{cases}
G^a_{\mu\nu} & \equiv \ \partial_\mu G^a_\nu \ - \ \partial_\nu G^a_\mu \ + \ g_s f^a_{bc} G^b_\mu G^c_\nu & \text{for } SU(3) \text{ gauge field}, \\[2mm]
W^i_{\mu\nu} & \equiv \ \partial_\mu W^i_\nu \ - \ \partial_\nu W^i_\mu \ + \ g \epsilon^i_{jk} W^j_\mu W^k_\nu & \text{for } SU(2) \text{ gauge field}, \\[2mm]
B_{\mu\nu} & \equiv \ \partial_\mu B_\nu \ - \ \partial_\nu B_\mu & \text{for } U(1) \text{ gauge field},
\end{cases}
\tag{1.1.1.6}
$$

where f^a_{bc} and ϵ^i_{jk} are the constant structure of $SU(3)$ and $SU(2)$ which verify the following commutation relations:

$$
[\tau^a/2 \mid \tau^b/2] \equiv (\tau^a/2)(\tau^b/2) \ - \ (\tau^b/2)(\tau^a/2) \ = \ i f^{ab}_c (\tau^c/2) \quad \text{where} \quad a, b, c = 1, ..., 8 \,,
$$

$$
[\sigma^i/2 \mid \sigma^j/2] \equiv (\sigma^i/2)(\sigma^j/2) \ - \ (\sigma^j/2)(\sigma^i/2) \ = \ i \epsilon^{ij}_k (\sigma^k/2) \quad \text{where} \quad i, j, k = 1, 2, 3 \,.
$$

In Formula 1.1.1.6 we can clearly see non-linear terms, as prescribed by Yang-Mills (YM) theory, typical of non-Abelian $SU(N)$ gauge theories.

For the above YM theory, the kinetic terms for the gauge bosons included in the SM Lagrangian can be written as follows:

$$
-\frac{1}{4} |\vec{G}|^2 - \frac{1}{4} |\vec{W}|^2 - \frac{1}{4} |B|^2 \,,
\tag{1.1.1.7}
$$

where for simplicity we have put: $\quad |\vec{G}|^2 \equiv G^a_{\mu\nu} G^{\mu\nu}_a, \quad |\vec{W}|^2 \equiv W^i_{\mu\nu} W^{\mu\nu}_i, \quad |B|^2 \equiv B_{\mu\nu} B^{\mu\nu}.$

As an additional note, it can be shown that the charge assignment system (Table 1.1 and Table 1.2) of the gauge theory, as set up in the SM, verifies the cancellation of the gauge anomalies, preserving the classical symmetry also at the quantum level and guaranteeing renormalisability.

1.1.2 Spontaneous symmetry breaking

By imposing the gauge principle, it is easy to demonstrate that in the Lagrangian expression, explicit mass terms cannot be present for bosons like $W^{\pm}$ and Z^0 (i.e. $1/2\, m_W^2 |\vec{W}|^2$ or $1/2\, m_B^2 |B|^2$), despite experimental evidence clearly shows they are massive. In fact, the presence of these terms would explicitly "break" the gauge symmetry as they are not gauge invariant. Especially for non-Abelian theories. For this reason, a *spontaneous symmetry-breaking* principle is proposed for the SM in the $SU(2)_L \times U(1)_Y$ sector through the BEH mechanism that brings out the appropriate mass terms while maintaining the gauge invariance.

This mechanism works with complex scalar doublet field Φ and it foresees in the SM Lagrangian a kinetic term $|\mathcal{D}\Phi|^2 \equiv (\mathcal{D}_\mu \Phi)^\dagger \mathcal{D}^\mu \Phi$, where gauge boson mass terms emerge, and a potential term $V(\Phi) \equiv -\mu^2 |\Phi|^2 + \lambda |\Phi|^4$ with $\mu^2, \lambda > 0$, responsible of spontaneous symmetry breaking. For construction, these terms are clearly gauge invariant but, the *ground state* (GS), identified by the minimum of the potential, is not. In this case, it is said the *symmetry is spontaneously broken*. By construction of Φ, the broken symmetry involves only the electroweak sector $SU(2)_L \times U(1)_Y$, since Φ is "transparent" for the strong sector $SU(3)_C$.

The GS is calculated by $\min \{V(\Phi)\}$ giving: $|\Phi_{\mathrm{GS}}|^2 = \mu^2/2\lambda$. It is clearly a degenerate variable, hence for simplicity, we can arbitrarily fix it as:

$$\Phi_{\mathrm{GS}} \coloneqq \begin{bmatrix} 0 \\ v/\sqrt{2} \end{bmatrix}, \quad \text{where} \quad v \equiv \mu/\sqrt{\lambda} \quad \text{with} \quad \mu > 0. \tag{1.1.2.1}$$

This status in not symmetric because for a generic $SU(2)_L \times U(1)_Y$ gauge transformation we obtain:

$$\exp\left(ig\, \frac{\vec{\sigma}}{2} \cdot \vec{\eta} + ig'\, \frac{1}{2}\zeta \right) \Phi_{\mathrm{GS}} \neq \Phi_{\mathrm{GS}}, \tag{1.1.2.2}$$

in fact, reformulating the argument of the exponential in the following way:

$$ig\, \frac{\vec{\sigma}}{2} \cdot \vec{\eta} + ig'\, \frac{1}{2}\zeta = ig\eta_1 \frac{\sigma_1}{2} + ig\eta_2 \frac{\sigma_2}{2} + (ig\eta_3 - ig'\zeta)\frac{\sigma_3 - \mathbb{1}}{4} + (ig\eta_3 + ig'\zeta)\frac{\sigma_3 + \mathbb{1}}{4}, \tag{1.1.2.3}$$

and considering the exponential expansion, we can identify three of the four generators of the symmetry $SU(2)_L \times U(1)_Y$ which instead "break" the symmetry of the GS:

$$\begin{cases} \dfrac{\sigma_1}{2}\Phi_{\mathrm{GS}} \neq 0 \quad \dfrac{\sigma_2}{2}\Phi_{\mathrm{GS}} \neq 0 \quad \dfrac{\sigma_3 - \mathbb{1}}{4}\Phi_{\mathrm{GS}} \neq 0 \quad \text{"broken" generators}, \\[2mm] \dfrac{\sigma_3 + \mathbb{1}}{4}\Phi_{\mathrm{GS}} = 0 \quad \text{"unbroken" generator that suggests Formula 1.1.1.1}. \end{cases} \tag{1.1.2.4}$$

Looking at the above generators, we can re-parameterise around the GS in the following manner:

$$\Phi \coloneqq \exp\left(i\frac{\vec{\chi} \cdot \vec{\sigma}}{v} \right) \begin{bmatrix} 0 \\ \dfrac{v + H}{\sqrt{2}} \end{bmatrix} \quad \text{equivalent to} \quad \Phi \coloneqq \exp\left(i\frac{\vec{\chi} \cdot \vec{\sigma} - \chi_3 \mathbb{1}}{v} \right) \begin{bmatrix} 0 \\ \dfrac{v + H}{\sqrt{2}} \end{bmatrix}, \tag{1.1.2.5}$$

where H and $\vec{\chi} \equiv (\chi_1, \chi_2, \chi_3)$ are four auxiliary fields.

For simplicity, being in a gauge theory, we can work with a gauge transformation of $SU(2)_L \times U(1)_Y$, called *unitary gauge*, which "absorbs" the exponential part of this last parametrization, putting:

$$
\begin{cases}
\vec{\eta} \;:=\; -\dfrac{2\vec{\chi}}{gv}\,, \\[2mm]
\zeta \;:=\; \dfrac{2\chi_3}{g'v}\,.
\end{cases}
\tag{1.1.2.6}
$$

Apply this transformation and consider the rotating boson fields, the mass terms $m_W^2 W_\mu^+ W_-^\mu$ and $1/2\, m_Z^2 Z_\mu Z^\mu$ emerge. Due to the partiality of broken symmetry, the photon has no mass terms, as expected. The BEH mechanism also reveals spurious terms of Higgs boson interactions.

The obtained eigenstates, due to the unitary gauge transformation, are called *gauge eigenstates*.

1.1.3 Yukawa terms

As mentioned above, also the explicit mass terms for the fermions break the $SU(2)_L \times U(1)_Y$ symmetry, hence to introduce masses it is hypothesised the presence of gauge-invariant Yukawa terms in the SM Lagrangian that for leptons is:

$$
-\left(\bar{L}\Phi y^{(L)} R + \text{h.c.} \right),
\tag{1.1.3.1}
$$

where $y^{(L)}$ is the Yukawa coupling matrix.

In general, $y^{(L)}$ is a 3×3 complex matrix, with the same physical dimension of the gauge coupling constants, which could be diagonalised with positive eigenstates thanks to a bi-unitary transformation. This transformation changes the gauge eigenstates in new states called for this occasion *mass eigenstates*.

Thanks to the specific leptons structure, L and R, where neutrinos are assumed to be massless and only left-handled, after applying the unitary gauge transformation and subsequently the bi-unitary transformation to the Formula 1.1.3.1, the leptons mass terms, i.e. $m_l \bar{l}l$ for $l \in \{e, \mu, \tau\}$, emerge. Where, with m_l we have indicated the lepton mass, which can be determinable only by experiments. Due to the BEH mechanism, in addition to the mass terms, also "spurious" Higgs boson coupling terms appear, as $(m_l/v)H\bar{l}l$ for $l \in \{e, \mu, \tau\}$, pointing out the interaction between the massive leptons with Higgs boson.

Despite the transition from gauge eigenstates to mass eigenstates, we can show that the possible interaction between leptons is self-interaction and interaction with their neutrinos [12]. There is no mixing between families.

For the quarks, the presence of mass for the up quarks as well as for the down quarks complicates the structure of the relative Yukawa term, making it necessary to introduce an additional term linked to a complementary field of the complex scalar doublet field, $\tilde{\Phi}$:

$$
-\left(\bar{Q}\Phi y^{(D)} D + \bar{Q}\tilde{\Phi} y^{(U)} U + \text{h.c.} \right),
\tag{1.1.3.2}
$$

where $y^{(D)}$ and $y^{(U)}$ are generic 3×3 complex matrices corresponding to the Yukawa couplings and $\tilde{\Phi} \equiv i\sigma^2 \Phi^* = \left((\Phi^0)^*, -(\Phi^+)^* \right)$ is the complex conjugate of Φ to have $\mathcal{Y}(\tilde{\Phi}) = -1$.

Also, in this case, it is possible to individuate two bi-unitary transformations, one for each Yukawa matrix that diagonalises them, with positive eigenstates. $m_q \bar{q}q$ and $(m_q/v)H\bar{q}q$ with $q \in \{u, c, t, d, s, b\}$ emerge. We have to highlight that these bi-unitary transformations bring out also interaction terms between different quark families. These interaction terms are regulated in the SM Lagrangian by the Cabibbo-Kobayashi-Maskawa (CKM) not diagonal complex matrix $V_{q_u q_d}$ with $q_u \in \{u, c, t\}$ and $q_d \in \{d, s, b\}$, which mixes the flavours of the different quarks. This matrix was introduced for three generations of quarks by Makoto Kobayashi and Toshihide Maskawa, adding one generation to the matrix initially introduced by Nicola Cabibbo.

It is possible to demonstrate that for three families of quarks, the CKM matrix has one complex phase and this implies violation of the CP symmetry, experimentally observed for the first time by the kaon oscillation $K^0 - \bar{K}^0$ system in 1964. Also, this evidence expresses the validity of the SM.

1.1.4   SM Lagrangian

In the end, the SM Lagrangian can be written in the following "compact" manner:

$$
\mathcal{L}_{\text{SM}} \equiv \underbrace{-\frac{1}{4}|\vec{G}|^2 - \frac{1}{4}|\vec{W}|^2 - \frac{1}{4}|B|^2}_{\text{gauge boson kinetic terms}} + \underbrace{\left(\bar{L}i\slashed{D}L + \bar{R}i\slashed{D}R\right) + \left(\bar{Q}i\slashed{D}Q + \bar{U}i\slashed{D}U + \bar{D}i\slashed{D}D\right)}_{\text{fermion kinetic terms including interaction terms with bosons}} +
$$

$$
\underbrace{-\left(\bar{L}\Phi y^{(L)}R + \text{h.c.}\right) - \left(\bar{Q}\Phi y^{(D)}D + \bar{Q}\tilde{\Phi}y^{(U)}U + \text{h.c.}\right)}_{\text{Yukawa interaction terms}} + \underbrace{|\mathcal{D}\Phi|^2 + \mu^2|\Phi|^2 - \lambda|\Phi|^4}_{\text{Higgs boson doublet dynamics}}
$$

$$(1.1.4.1)$$

After the symmetry-breaking and passing to the mass eigenstates, the SM Lagrangian can be written in the following explicit way:

$$\mathcal{L}_{\text{SM}} =$$

$$
\underbrace{-\frac{1}{4}(\partial_\mu G_\nu^a - \partial_\nu G_\mu^a)(\partial^\mu G_a^\nu - \partial^\nu G_a^\mu)}_{\text{gluons pure kinetic term}} \quad \underbrace{-\frac{g_s}{2}f_a^{bc}(\partial_\mu G_\nu^a - \partial_\nu G_\mu^a)G_b^\mu G_c^\nu - \frac{g_s^2}{4}f_{abc}f^{ade}G_\mu^b G_\nu^c G_d^\mu G_e^\nu}_{\text{cubic and quartic gluons self-interaction}} \quad +
$$

$$
\underbrace{-\frac{1}{2}(\partial_\mu W_\nu^+ - \partial_\nu W_\mu^+)(\partial^\mu W_-^\nu - \partial^\nu W_-^\mu)}_{W^\pm \text{ pure kinetic term}} \quad \underbrace{-\frac{1}{4}(\partial_\mu Z_\nu - \partial_\nu Z_\mu)(\partial^\mu Z^\nu - \partial^\nu Z^\mu)}_{Z^0 \text{ pure kinetic term}} \quad +
$$

$$
\underbrace{-\frac{1}{4}(\partial_\mu A_\nu - \partial_\nu A_\mu)(\partial^\mu A^\nu - \partial^\nu A^\mu)}_{\text{photon pure kinetic term}} \quad +
$$

$$-ig_Z \left(W_\mu^+ (\partial^\mu W_-^\nu - \partial^\nu W_-^\mu) Z_\nu - (\partial_\mu W_\nu^+ - \partial_\nu W_\mu^+) W_-^\mu Z^\nu - W_\mu^+ W_\nu^- (\partial^\mu Z^\nu - \partial^\nu Z^\mu) \right) +$$

$$-ig_e \left(W_\mu^+ (\partial^\mu W_-^\nu - \partial^\nu W_-^\mu) A_\nu - (\partial_\mu W_\nu^+ - \partial_\nu W_\mu^+) W_-^\mu A^\nu - W_\mu^+ W_\nu^- (\partial^\mu A^\nu - \partial^\nu A^\mu) \right) +$$

$$-\frac{1}{2} g_e^2 \csc^2 \theta_W \left((W_\mu^+ W_-^\mu)^2 - W_\mu^+ W_\nu^- W_+^\mu W_-^\nu \right) - g_e^2 \cot^2 \theta_W \left(W_\mu^+ W_-^\mu Z_\nu Z^\nu - W_\mu^+ W_\nu^- Z^\mu Z^\nu \right) +$$

$$\underbrace{-g_e^2 \cot \theta_W \left(2 W_\mu^+ W_-^\mu A^\nu Z_\nu - W_\mu^+ W_\nu^- A^\nu Z^\mu - W_\mu^+ W_\nu^- A^\mu Z^\nu \right)}_{\text{cubic and quartic electroweak bosons self-interaction}} \qquad +$$

$$\underbrace{\sum_f \bar{f} \gamma^\mu i \partial_\mu f}_{\text{fermions kinetic term}} \quad + \quad \underbrace{G_\mu^a \sum_q \bar{q} \gamma^\mu \left(g_s \frac{\tau_a}{2} \right) q}_{\text{gluons - quarks interaction}} \quad +$$

$$\underbrace{W_\mu^- \left(\sum_l \bar{\nu}_l \gamma^\mu \left(g_W \frac{1-\gamma^5}{2} \right) l + \sum_q \bar{q}_u \gamma^\mu \left(g_W \frac{1-\gamma^5}{2} V_{q_u q_d}^* \right) q_d \right) + \text{h.c.}}_{\substack{W^\pm \text{ bosons - fermions interaction} \\ \text{(charged currents)}}} \quad +$$

$$\underbrace{A_\mu \sum_f \bar{f} \gamma^\mu \left(g_e \mathcal{Q}(f) \right) f}_{\substack{\text{photon - fermions interaction} \\ \text{(electrical neutral currents QED)}}} \quad + \quad \underbrace{Z_\mu \sum_f \bar{f} \gamma^\mu \left(g_Z \frac{\mathcal{Q}_V(f) - \mathcal{Q}_A(f) \gamma^5}{2} \right) f}_{\substack{Z^0 \text{ boson - fermions interaction} \\ \text{(weak neutral currents)}}} \quad +$$

$$\underbrace{\sum_f m_f \bar{f} f}_{\text{fermions mass term}} \quad + \quad \underbrace{\sum_f \frac{m_f}{v} H \bar{f} f}_{\text{Higgs - fermion interaction}} \quad +$$

$$\underbrace{\frac{1}{2} \partial_\mu H \partial^\mu H - \frac{1}{2} m_H^2 H^2 + \frac{1}{8} m_H^2 v^2}_{\text{Higgs pure kinetic term, mass term and potential}} \quad \underbrace{- \lambda v H^3 - \frac{\lambda}{4} H^4}_{\text{Higgs self-interaction}} \quad +$$

$$\underbrace{m_W^2 W_\mu^+ W_-^\mu + \frac{1}{2} m_Z^2 Z_\mu Z^\mu}_{W^\pm \text{ and } Z^0 \text{ bosons mass terms}} \quad + \quad \underbrace{\frac{1}{2} g_W^2 \left(2vH + H^2 \right) W_\mu^+ W_-^\mu + \frac{1}{8} g_Z^2 \left(2vH + H^2 \right) Z_\mu Z^\mu}_{W^\pm \text{ and } Z^0 \text{ bosons - Higgs boson interaction}} \quad ,$$

$$(1.1.4.2)$$

where,

f	indicates all the fermion fields: $\{\nu_e, \nu_\mu, \nu_\tau, e, \mu, \tau, u, c, t, d, s, b\}$;
l	indicates all the proper lepton fields: $\{e, \mu, \tau\}$;
ν_l	indicates all the neutrino fields: $\{\nu_e, \nu_\mu, \nu_\tau\}$;
q	indicates all the quark fields: $\{u, c, t, d, s, b\}$;
q_u	indicates all the up quark fields only: $\{u, c, t\}$;
q_d	indicates all the down quark fields only: $\{d, s, b\}$;
$g_W \equiv g/\sqrt{2}$	indicates $W^\pm$ boson - fermions coupling constant;
$g_e \equiv g \sin\theta_W = g' \cos\theta_W$	indicates photon - fermions coupling constant: electron charge;
$g_Z \equiv g/\cos\theta_W$	indicates Z^0 boson - fermions coupling constant;
$v \equiv \mu/\sqrt{\lambda}$	indicates GS also said vacuum expectation value (VEV);
$V_{q_u q_d}$	indicates Cabibbo-Kobayashi-Maskawa (CKM) 3×3 matrix;
$\text{diag}(m_l) \equiv (v/\sqrt{2})\, y^{(L)}$	indicates lepton mass 3×3 diagonal matrix, neutrino masses are null;
$\text{diag}(m_{q_{u/d}}) \equiv (v/\sqrt{2})\, X_{(U/D)}^{-1} y^{(U/D)} Y_{(U/D)}$	indicates up or down quark mass 3×3 diagonal matrix;
$X_{(U/D)}$ and $Y_{(U/D)}$	indicates bi-unitary matrices that diagonalise $y^{(U/D)}$;
$m_H \equiv \sqrt{2}\mu = \sqrt{2\lambda}v$	indicates H boson mass;
$m_W \equiv gv/2$	indicates $W^\pm$ boson mass;
$m_Z \equiv \sqrt{g^2 + g'^2}\, v/2 = m_W/\cos\theta_W$	indicates Z^0 boson mass;

$$\mathcal{Q}_V(f) \equiv \begin{cases} +1/2 & \text{for the following fermions: } f \in \{\nu_e, \nu_\mu, \nu_\tau\}; \\ -1/2 + 2\sin^2\theta_W & \text{for the following fermions: } f \in \{e, \mu, \tau\}; \\ +1/2 - 4/3\sin^2\theta_W & \text{for the following fermions: } f \in \{u, c, t\}; \\ -1/2 + 2/3\sin^2\theta_W & \text{for the following fermions: } f \in \{d, s, b\}; \end{cases}$$

$$\mathcal{Q}_A(f) \equiv \begin{cases} +1/2 & \text{for the following fermions: } f \in \{\nu_e, \nu_\mu, \nu_\tau, u, c, t\}; \\ -1/2 & \text{for the following fermions: } f \in \{e, \mu, \tau, d, s, b\}. \end{cases}$$

1.1.5 SM is a renormalisable theory

Most of the experiments in HEP involve a collision of particle beams, inducing particle production and decay. The diffusion data produced by these processes, allow us to study the interactions. The theoretical analysis of such diffusion can take place thanks to the study of the *cross section σ* for the collisions or thanks to the study of the *decay rate Γ*. These two observables express the probability that the diffusion or decay process is detected. These ones, and in particular their differential version, can be calculated by means of the *scattering amplitude matrix $\mathcal{M}$*, also said *matrix element*. As shown below in Formula 1.1.5.1 and Formula 1.1.5.2.

collision:
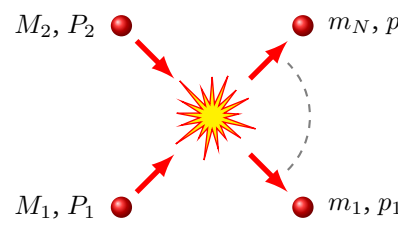
$$d\sigma = \frac{(2\pi)^4}{4\sqrt{(P_1 \cdot P_2)^2 - M_1^2 M_2^2}} \delta^4\left(P_1 + P_2 - \sum_{i=1}^{N} p_i\right) \prod_{i=1}^{N} \frac{d^3\overrightarrow{p_i}}{(2\pi)^3 2E_i}|\mathcal{M}|^2$$

(1.1.5.1)

decay:
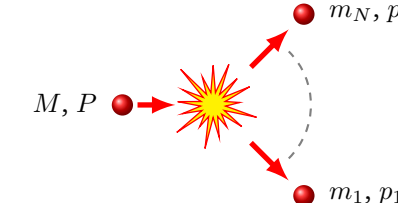
$$d\Gamma = \frac{(2\pi)^4}{2M}\delta^4\left(P - \sum_{i=1}^{N} p_i\right)\prod_{i=1}^{N}\frac{d^3\overrightarrow{p_i}}{(2\pi)^3 2E_i}|\mathcal{M}|^2$$

(1.1.5.2)

One way to calculate the scattering amplitude matrix $\mathcal{M}$, exploits the Lehmann-Symanzik-Zimmermann (LSZ) reduction formula, which leads to the formulation of the so-called *Feynman graphical*

rules in the momentum space, which represent an efficient diagrammatic method for the calculation of the functional integrals involved. Please see Appendix A. These rules lead to describe the scattering amplitude matrices in terms of perturbative expansions of the coupling constants, in which there is a first low-order term of those coupling constants and subsequent higher-order terms that foresee *loop diagrams,* which possibly entail divergent integrals in the momentum space, that need to be first regularised and then renormalised.

Renormalisation techniques were introduced initially around the biennium 1947-1949 in QED and in general in the QFTs to treat these theoretic divergent terms introduced with the loops by Hans Kramers, Hans Bethe, Julian Schwinger, Richard Feynman, Shin'ichiro Tomonaga and systematised by Freeman Dyson at the end.

These techniques require the introduction of *counterterms* in the Lagrangian which compensate for the non-physical divergent terms. In order for the applied QFT to be renormalisable, however, the number of needed counterterms must be finite at each order in perturbation theory. It can be demonstrated that this implies a constraint on the dimensions of the coupling constants, which must have positive or null dimensions. The SM Lagrangian introduced above Formula 1.1.4.2, having just one positive dimension coupling and all the rest being adimensional, is a good candidate for being renormalisable.

1.2   Main characteristics of Effective Field Theories (EFT)

In the context of HEP, experiments, conducted at a certain energy, potentially allow the detection of particles that have masses below this threshold. If the energy at which NP explicitly manifests itself is higher than the maximum available energy of a given experiment, not being able to directly detect its states, one can still try to evaluate their indirect effects. Since, currently, we have no clear idea of what NP might lie at high scales, one is led to adopt the most economical approach, i.e. employing an EFT. A possible example is described in Figure 1.2 here below.
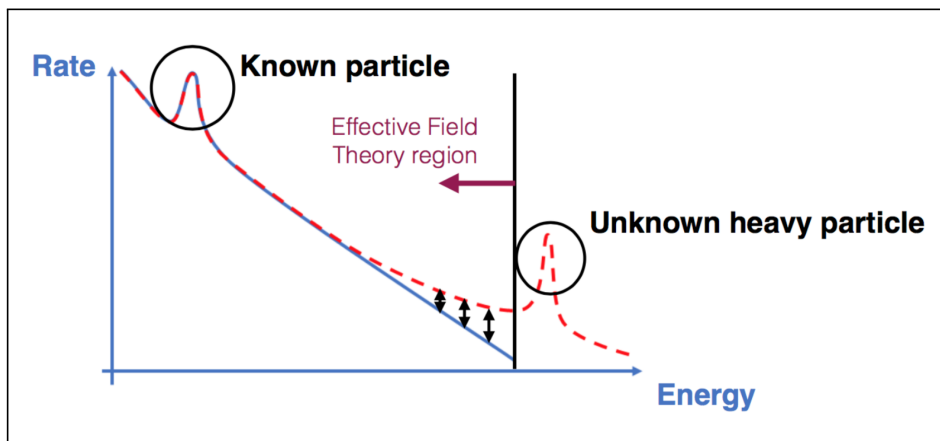
Figure 1.2: Traces of NP (dashed red line) can be studied by the EFT approach, evaluating the deviations from the known theory (solid blue line) in the region of application of EFT, upper bounded by an energy threshold. - source by Eleni Vryonidou [13].

An EFT is a QFT whose range of applicability is by construction limited, which approximates

physical models below a typical scale, usually indicated by Λ. Its power lies in the capability to compute low-energy dynamics without knowing the high-energy complete Lagrangian.

The founding idea is based on the application of the decoupling theorem of Appelquist and Carrazzone [3] [4], which states that the effects of heavy physics, characterised for example by a certain mass M, can be *decoupled* from the effects of low-energy physics, characterised by a certain momentum p. Therefore, in computations, those effects are suppressed by the low-energy renormalisation constants, allowing for a good arbitrary approximation, with order corrections of at least $O(p^2/M^2)$. In this way, phenomena of a hypothetical complete theory (e.g. represented by a Lagrangian $\mathcal{L}_{\text{full}}$), which involves "heavy" fields Φ and "light" fields ϕ, can be approximated below a certain energy scale by EFT (e.g. represented by a Lagrangian $\mathcal{L}_{\text{EFT}}$) containing only "light" fields ϕ: $\mathcal{L}_{\text{full}}(\Phi, \phi) \approx \mathcal{L}_{\text{EFT}}(\phi)$.

To understand intuitively an EFT, it is useful to analyse a classic example concerning the Fermi theory, which explains very well the experimental results of *beta decay* and similarly also those of *muon decay* on a scale of energy below the electroweak scale ($\sim 80\,\text{GeV}$ / $90\,\text{GeV}$).

1.2.1   Fermi theory: one of the most famous EFT applications

Between the 1920s and 1930s, the foundations for the future QED were formulated, but this theory did not include yet the phenomena related to what will later be defined as weak interaction. The *four-fermion interaction* was a "tentative" by Fermi to describe the evidence of such phenomena that, for example for muon decay, could be expressed by the following Lagrangian term, to be added to the currently known theory:

$$\mathcal{L}_{\text{F}} = -\frac{G_{\text{F}}}{\sqrt{2}} \left(\bar{\nu}_\mu \gamma^\mu \left(1 - \gamma^5\right) \mu \right) \left(\bar{e} \gamma_\mu \left(1 - \gamma^5\right) \nu_e \right), \tag{1.2.1.1}$$

where $G_{\text{F}} = 1.167 \cdot 10^{-5}\,\text{GeV}^{-2}$ in natural units, is the Fermi coupling constant.

This theory proved to conform to the experimental results, but not being renormalisable, since $[G_{\text{F}}] = [\text{Energy}]^{-2}$ in natural units, clearly could not be the complete one. Its validity is limited to an energy range much lower than m_W. In fact, comparing the predictions of the Fermi theory in the case of muon decay with the predictions of the more modern EW theory, for the LO case of the perturbative expansion we have the following scattering amplitudes:

$$
\begin{aligned}
i\mathcal{M}_{\text{F}} &= -\frac{iG_{\text{F}}}{\sqrt{2}} \left(\bar{\nu}_\mu \gamma^\mu \left(1 - \gamma^5\right) \mu \right) \left(\bar{e} \gamma_\mu \left(1 - \gamma^5\right) \nu_e \right), \\
i\mathcal{M}_{\text{EW}} &= \left(\frac{-ig}{2\sqrt{2}} \bar{\nu}_\mu \gamma^\mu \left(1 - \gamma^5\right) \mu \right) \left(i \frac{-g_{\mu\nu} + \frac{p_\mu p_\nu}{m_W^2}}{p^2 - m_W^2} \right) \left(\frac{-ig}{2\sqrt{2}} \bar{e} \gamma^\nu \left(1 - \gamma^5\right) \nu_e \right) \approx \\
&\approx -\frac{ig^2}{8m_W^2} \left(\bar{\nu}_\mu \gamma^\mu \left(1 - \gamma^5\right) \mu \right) \left(\bar{e} \gamma^\nu \left(1 - \gamma^5\right) \nu_e \right) \quad \text{with} \quad p^2 \ll m_W^2 .
\end{aligned} \tag{1.2.1.2}
$$

---

[3] the theorem: *For any 1PI Feynman graph with external vector mesons only but containing internal fermions, when all external momenta (i.e. p^2) are small relative to m^2, then apart from coupling constant and field strength renormalisation the graph will be suppressed by some power of m relative to a graph with the same number of external vector mesons but no internal fermions.*
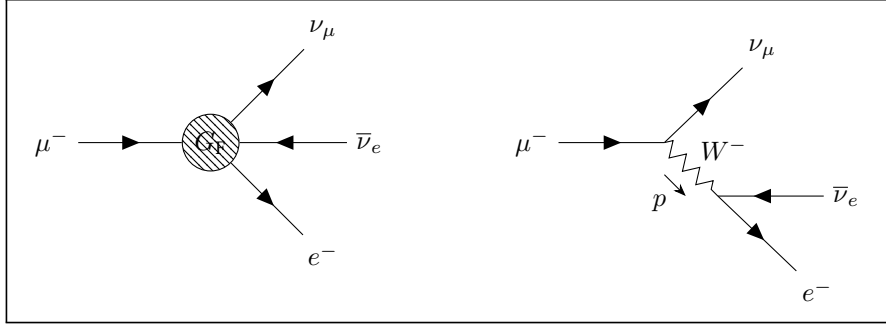
Figure 1.3: Fermi's theory and EW theory of muon decay at LO.

Both theories predict the same physics in the infrared (IR), where $p^2 \ll m_W^2$, but differ in the ultraviolet spectrum (UV), i.e. $p^2 \gtrsim m_W^2$, where on-shell W^- boson can occur. The IR regime is guaranteed by the fact that $m_\mu^2 \ll m_W^2$.

$\mathcal{L}_F$ represents the EFT approximation of the more complete theory $\mathcal{L}_{EW}$. The LO matching fixes the relation between the parameters of the two theories:

$$\mathcal{M}_F(\text{LO}) \coloneqq \mathcal{M}_{EW}(\text{LO}) \text{ at energies much below the UV} \implies G_F = \frac{g^2}{4\sqrt{2}m_W^2} = \frac{1}{\sqrt{2}v} \, .$$

$$(1.2.1.3)$$

1.2.2 EFT expansion

Before to start showing the generic EFT Lagrangian expression, it is useful to remember some dimensional characteristics of the involved elements. Working in natural units (where $\hbar = c = 1$), which implicate $[\text{Energy}] = [\text{Mass}] = [\text{Length}]^{-1}$ and considering a d space-time dimensions, it is understood that starting from a generic QFT functional which involves generic spinorial, scalar and vector fields (i.e. ψ, ϕ, A), the functional $\mathcal{Z} \equiv \int \mathcal{D}(\psi, \phi, A) e^{i\mathcal{S}(\psi,\phi,A)}$ implies that the action $\mathcal{S}$ has to be dimensionless: $[\mathcal{S}] = [\text{Mass}]^0$ and in turn, it implies the Lagrangian density $\mathcal{L}$ ($\mathcal{S} \equiv \int d^d x \mathcal{L}$) and all the additional terms included into it, have to be of d-dimension: $[\mathcal{L}] = [\text{Mass}]^d$, also indicate with $[\![\mathcal{L}]\!] = d$.

As suggested by the previous example and because the effects of any decoupled NP at the high-energy scale could be approximated by higher-dimensional operators at the low-energy scale, it is clear that to extend a giving well-known renormalisable theory $\mathcal{L}_{known}$ in order to cover not explained effects in the IR, we can introduce additional $\mathscr{D}$-dimension operators, with $\mathscr{D} > d$, "effective" below a certain energy scale Λ, in the following way:

$$\mathcal{L}_{EFT} \equiv \mathcal{L}_{known} + \sum_{\substack{1 \leqslant i \leqslant n_{\mathscr{D}} \\ \mathscr{D} > d}} C_i^{(\mathscr{D})} \frac{\mathcal{O}_i^{(\mathscr{D})}}{\Lambda^{\mathscr{D}-d}} \begin{cases} \mathcal{L}_{known} & d\text{-dimension known theory} \\ \mathcal{O}_i^{(\mathscr{D})} & \text{all possible } (n_{\mathscr{D}}) \ \mathscr{D}\text{-dimension operators} \\ C_i^{(\mathscr{D})} & \text{Wilson coefficients, dimensionless} \\ \Lambda & \text{cutoff energy scale} \end{cases} .$$

$$(1.2.2.1)$$

This should realise $\mathcal{L}_{full} \approx \mathcal{L}_{EFT}$ for energies or momenta significantly below the Λ energy scale, where $\mathcal{L}_{full}$ is the Lagrangian of the hypothetical theory whose effects we are trying to simulate.

Clearly, the EFT Lagrangian is a power series expansion of Λ^{-1}, potentially involving an infinite number of operators of arbitrarily high mass dimension that we can truncate to a given order and use to calculate physical observables with desired precision.

Introducing a higher dimension operator, with terms like $C_j^{(\mathscr{D}_j)} \mathcal{O}_j^{(\mathscr{D}_j)} / \Lambda^{\mathscr{D}_j - d}$, contributes with a power factor of the external momenta to the amplitudes. Thus, if we consider a scattering amplitude $i\mathcal{M}_{known}$ in d dimensions, normalised to have zero mass dimension at some typical momentum scale p, then adding with the EFT a single $\mathscr{D}$-dimension operator contributes to the order amplitude of the scattering process in the following way:

$$i\mathcal{M}_{\text{EFT}} \sim \left(\frac{p}{\Lambda}\right)^{\mathscr{D}_j - d} . \tag{1.2.2.2}$$

Instead, adding a set of higher dimension operators $\{\mathcal{O}_j^{(\mathscr{D}_j)}\}$, as stated in Formula 1.2.2.1, leads to scattering amplitude:

$$i\mathcal{M}_{\text{EFT}} \sim \left(\frac{p}{\Lambda}\right)^{\sum_j (\mathscr{D}_j - d)} , \tag{1.2.2.3}$$

where the sum on j is over all the inserted operators.

It is important to highlight Formula 1.2.2.3 that is still valid for any graph, not only for LO diagrams but also for loops [2].

It is well known that a theory that includes $\mathscr{D}$-dimension operators, corresponding to Feynman diagrams with vertices with $\mathscr{D}$ lines, is a renormalisable theory only if $d - \mathscr{D}(d/2 - 1) \geqslant 0$ [14]. Thus, being $\mathscr{D} > d$ and $d > 2$, an EFT appears obviously not renormalisable.
To understand the impact on the difficulty of letting this theory renormalisable, if we consider for example an EFT with two operators of dimension $\mathscr{D}_1$ and $\mathscr{D}_2$ the renormalisation requires counter-terms of a higher dimensional operator of dimension $\mathscr{D}_1 + \mathscr{D}_2$ to cancel divergent piece. In this way, EFTs require an infinite number of counter-terms to cancel divergences to all orders.
Anyway considering that EFT could be usefully truncated to a given order, divergences can be cancelled order-by-order in the Λ parameter, allowing for a predictive theory.

1.2.3   Toy model example

To understand how the EFT analysis of a generic QFT could be developed, let us consider a hypothetical *toy model* theory represented by the following Lagrangian:

$$\mathcal{L}_{\text{full}} := \underbrace{\bar{\psi}(i\not{D} - m)\psi}_{\text{"light" field}} + \underbrace{\frac{1}{2}|\mathcal{D}\phi|^2 - \frac{1}{2}M^2\phi^2}_{\text{"heavy" field}} - \underbrace{\lambda\phi\bar{\psi}\psi}_{\text{coupling}} , \tag{1.2.3.1}$$

where for simplicity we have set $\not{D} \equiv \gamma^\mu \mathcal{D}_\mu$, $|\mathcal{D}\phi|^2 \equiv (\mathcal{D}_\mu \phi)^\dagger \mathcal{D}^\mu \phi$ and $\mathcal{D}_\mu \equiv \partial_\mu - ig_e \mathcal{Q} A_\mu$.

This toy theory, taken as reference from [15], includes an electrically charged massive spinorial field ψ, with mass m, which is assumed to be detectable from experiments and a neutral massive scalar field ϕ, with mass M, which we assume to be $m \ll M$ and not directly detectable by experiments. Considering the electrical charge $\mathcal{Q}$ of the spinorial field, also a gauge vector field A_μ (photon) has been included. We further suppose that the two fields, "light" and "heavy" are coupled by means of a Yukawa coupling term.

We would like to demonstrate how an EFT model can "integrate" the effect of the "heavy" field below its scale M. For example, to achieve this, we can choose two colliding fields, $\psi\psi$, which scatter into two other fields of the same type: $\psi\psi \to \psi\psi$.

For the complete theory here examined at LO expansion, we have:
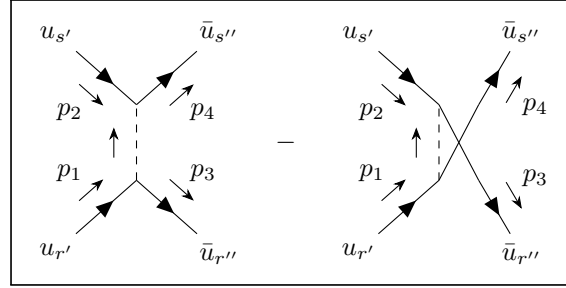
Figure 1.4: Toy model $\psi\psi \to \psi\psi$ scattering due to ϕ interaction.

$$
\begin{aligned}
i\mathcal{M}_{\text{full}} &= \bar{u}_{r''}(p_3)\Big(-i\lambda\Big)u_{r'}(p_1)\left(\frac{i}{(p_1-p_3)^2 - M^2}\right)\bar{u}_{s''}(p_4)\Big(-i\lambda\Big)u_{s'}(p_2) \;-\; \{3 \leftrightarrow 4\} \;= \\
&= \frac{i\lambda^2}{M^2}\left(1 + O\left(\frac{(p_1-p_3)^2}{M^2}\right)\right)\bar{u}_{r''}(p_3)u_{r'}(p_1)\bar{u}_{s''}(p_4)u_{s'}(p_2) \;-\; \{3 \leftrightarrow 4\}\,.
\end{aligned}
$$

$$(1.2.3.2)$$

The ratio $(p_1 - p_3)^2/M^2$ is the expansion parameter and we can construct an effective theory to the desired order in this expansion. Since the effective theory does not include the heavy scalar of mass M, it is clear that the effective theory must break down when the scattering energy approaches M. So, it is natural to fix $\Lambda := M$. A minimum operator that could be added is a 6-dimension operator expressed in the following EFT Lagrangian:

$$
\mathcal{L}_{\text{EFT}} := \underbrace{\bar{\psi}(i\slashed{D} - m)\psi}_{\text{known theory}} \;+\; \underbrace{\frac{C^{(6)}}{\Lambda^2}\frac{1}{2}\left(\bar{\psi}\psi\right)\left(\bar{\psi}\psi\right)}_{\text{EFT 6-dim. operator}}\,.
$$

$$(1.2.3.3)$$
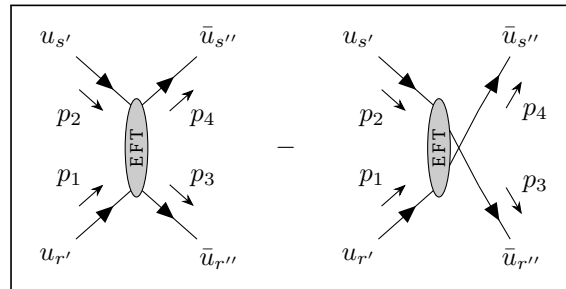
Figure 1.5: Toy model $\psi\psi \to \psi\psi$ scattering studied by EFT interaction.

The matrix element related to the above EFT is the following:

$$
i\mathcal{M}_{\text{EFT}} = \frac{iC^{(6)}}{\Lambda^2}\bar{u}_{r''}(p_3)u_{r'}(p_1)\,\bar{u}_{s''}(p_4)u_{s'}(p_2) \;-\; \{3 \leftrightarrow 4\}\,.
$$

$$(1.2.3.4)$$

So, by matching the two matrix elements Formula 1.2.3.2 and Formula 1.2.3.4 when the module of momentum value much less than M value, we can fix the relevant Wilson coefficient by $C^{(6)} = \lambda^2$.

If we need an extra order of precision in matching with Formula 1.2.3.2, we can improve the EFT model by including operators of higher dimensions as we like. For example, including in the EFT Lagrangian an Formula 1.2.3.3 an 8-dimension operator in the following way:

$$\mathcal{L}_{\text{EFT}} \coloneqq \underbrace{\bar{\psi}(i\slashed{D} - m)\psi}_{\text{known theory}} + \underbrace{\frac{C^{(6)}}{\Lambda^2}\frac{1}{2}\left(\bar{\psi}\psi\right)\left(\bar{\psi}\psi\right)}_{\text{EFT 6-dim. operator}} + \underbrace{\frac{C^{(8)}}{\Lambda^4}(\partial_\mu\bar{\psi}\partial^\mu\psi)(\bar{\psi}\psi)}_{\text{EFT 8-dim. operator}} . \tag{1.2.3.5}$$

For this case the matching has to be performed in the two below matrix elements:

$$
\begin{aligned}
i\mathcal{M}_{\text{full}} &= \frac{i\lambda^2}{M^2}\left(1 + \frac{(p_1 - p_3)^2}{M^2} + O\left(\frac{(p_1 - p_3)^4}{M^4}\right)\right)\bar{u}_{r''}(p_3)u_{r'}(p_1)\bar{u}_{s''}(p_4)u_{s'}(p_2) \ - \ \{3 \leftrightarrow 4\} , \\
i\mathcal{M}_{\text{EFT}} &= \left(\frac{iC^{(6)}}{\Lambda^2} - 2\frac{iC^{(8)}}{\Lambda^4}(p_1 \cdot p_3)\right)\bar{u}_{r''}(p_3)u_{r'}(p_1)\bar{u}_{s''}(p_4)u_{s'}(p_2) \ - \ \{3 \leftrightarrow 4\} .
\end{aligned}
\tag{1.2.3.6}
$$

So, matching the two above matrix elements, after some adjustment calculations, when the module of momentum value is much less than M value, we obtain the two needed Wilson coefficients $C^{(6)} = \lambda^2(1 + 2m^2/M^2)$ and $C^{(8)} = \lambda^2$. This fact is because it is possible to demonstrate EFT can be systematically improved by higher dimension operators and higher order calculations.

A further way to improve the above $\psi\psi \to \psi\psi$ scattering calculation is to compute matching coefficients at one-loop order. As an example, we can examine the additional effects due to fermions coupling to the photon with charge $g_e\mathcal{Q}$ (g_e is the electron electric charge value, whence $\alpha \equiv g_e^2/4\pi$), including Next Leading Order (NLO) QED corrections. This calculation illustrates several important points about matching.
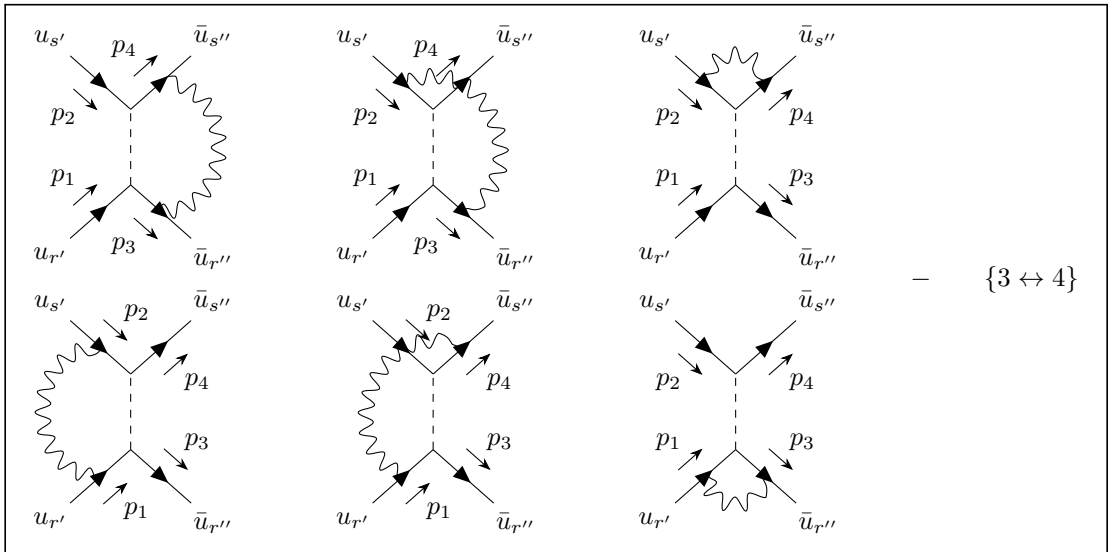
Figure 1.6: Toy model $\psi\psi \to \psi\psi$ scattering due to ϕ and A_μ interaction.

For the EFT the situation becomes:
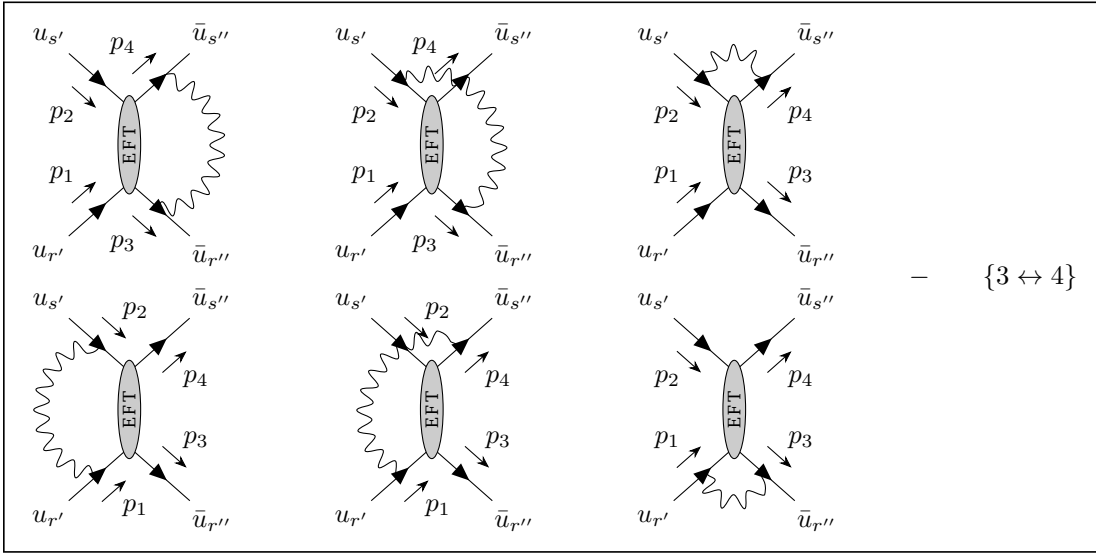
Figure 1.7: Toy model $\psi\psi \to \psi\psi$ scattering studied at NLO by EFT interaction.

To respect the Lorentz structure a new operator for one-loop correction is needed for EFT, thus further to the term with $C^{(6)}$ coefficient of the Formula 1.2.3.3, here below indicated as $C_S^{(6)}$, we need to add a new term with the here below indicated coefficient $C_T^{(6)}$ (refer to [15]):

$$\mathcal{L}_{\text{EFT}} := \underbrace{\bar{\psi}(i\slashed{D} - m)\psi}_{\text{known theory}} + \underbrace{\frac{C_S^{(6)}}{\Lambda^2}\frac{1}{2}\left(\bar{\psi}\psi\right)\left(\bar{\psi}\psi\right) + \frac{C_T^{(6)}}{\Lambda^2}\frac{1}{2}\left(\bar{\psi}\sigma_{\mu\nu}\psi\right)\left(\bar{\psi}\sigma^{\mu\nu}\psi\right)}_{\text{EFT 6-dim. operator}}, \tag{1.2.3.7}$$

where $\sigma^{\mu\nu} \equiv [\gamma^\mu|\gamma^\nu]$,

after the appropriate loop integration for the "full" theory and the EFT, then:

$$\begin{aligned}
i\mathcal{M}_{\text{full}} &= \frac{i\lambda^2}{M^2}\left(1 + \frac{\alpha\mathcal{Q}^2}{\pi}\left(\frac{2}{\epsilon} - 2\ln\frac{m^2}{\mu^2} - 1\right)\right)\bar{u}_{r''}(p_3)u_{r'}(p_1)\bar{u}_{s''}(p_4)u_{s'}(p_2) + \\
&\quad + \frac{i\lambda^2}{M^2}\frac{\alpha\mathcal{Q}^2}{8\pi}\left(-2\ln\frac{m^2}{M^2} - 2\right)\bar{u}_{r''}(p_3)\sigma_{\mu\nu}u_{r'}(p_1)\bar{u}_{s''}(p_4)\sigma^{\mu\nu}u_{s'}(p_2) + \\
&\quad - \{3 \leftrightarrow 4\},
\end{aligned}$$

$$\begin{aligned}
i\mathcal{M}_{\text{EFT}} &= \frac{iC_S^{(6)}}{\Lambda^2}\left(1 + \frac{\alpha\mathcal{Q}^2}{\pi}\left(\frac{2}{\epsilon} - 2\ln\frac{m^2}{\mu^2} - 1\right)\right)\bar{u}_{r''}(p_3)u_{r'}(p_1)\bar{u}_{s''}(p_4)u_{s'}(p_2) + \\
&\quad + \left(\frac{iC_T^{(6)}}{\Lambda^2} + \frac{iC_S^{(6)}}{\Lambda^2}\frac{\alpha\mathcal{Q}^2}{8\pi}\left(\frac{2}{\epsilon} - 2\ln\frac{m^2}{\mu^2} + 1\right)\right)\bar{u}_{r''}(p_3)\sigma_{\mu\nu}u_{r'}(p_1)\bar{u}_{s''}(p_4)\sigma^{\mu\nu}u_{s'}(p_2) + \\
&\quad - \{3 \leftrightarrow 4\},
\end{aligned}$$

$$\tag{1.2.3.8}$$

where μ is the regularisation scale and ϵ is the UV divergent pole related to QED renormalisation. In particular, we can see that in the EFT, the term related to the $\bar{u}_{r''}(p_3)\sigma_{\mu\nu}u_{r'}(p_1)\bar{u}_{s''}(p_4)\sigma^{\mu\nu}u_{s'}(p_2)$

structure leads to a further UV divergent pole terms respect to the full theory, which must be cancelled by a dedicated counter-term in the renormalisation operation.

Matching the two above matrix elements, setting $\mu := M$ and taking into account that both theories predict the same IR behaviour while they are not the same in the UV regime, we have $C_S^{(6)} = \lambda^2$ and $C_T^{(6)} = -3(\alpha \mathcal{Q}^2/8\pi)\lambda^2$. That represents the EFT NLO correction, marching the here analysed full theory in the IR regime.

1.3   Standard Model Effective Field Theories (SMEFT)

Whereas the SM is a fairly well-understood theory around a relatively low energy scale (parametrised the VEV of the Higgs boson), thanks to the presence of a well-defined set of low energy degrees of freedom: $\{\, L,\ R,\ Q,\ U,\ D,\ \gamma,\ W^\pm,\ Z^0,\ g,\ H \,\}$, considering that the LHC data seem to indicate a gap between the results of the SM and those of a presumed BSM Physics, the SM theory it is at least a good EFT theory.

The SMEFT is a consistent EFT extension of the SM, in the sense that its terms respect the essential SM symmetries, which are built on the basis of the $SU_C(3) \times SU_L(2) \times U_Y(1)$ invariant higher dimensional operators, developed by SM fields, described in Section 1.1.
The basic idea is that the SMEFT results should be compliant with the effects at low energy of much heavier NP.

Considering the formulation of a generic EFT Lagrangian and being the SM a four-dimensional theory, the SMEFT Lagrangian can be represented as follows:

$$\boxed{\mathcal{L}_{\text{SMEFT}} \quad \equiv \quad \mathcal{L}_{\text{SM}} \quad + \sum_{\substack{1 \leqslant i \leqslant n_{\mathscr{D}} \\ \mathscr{D} > 4}} C_i^{(\mathscr{D})} \frac{\mathcal{O}_i^{(\mathscr{D})}}{\Lambda^{\mathscr{D}-4}}} , \qquad (1.3.0.1)$$

the non-redundant $n_{\mathscr{D}}$ operators, $\mathcal{O}_i^{(\mathscr{D})}$, are suppressed by $\mathscr{D} - 4$ powers of the cutoff energy scale Λ, which usually is arbitrarily fixed much over the EW scale, while the adimensional Wilson coefficients, $C_i^{(\mathscr{D})}$, must be chosen to fit the experimental results. Obviously, in order to simplify the calculations, the above expansion can be limited to a certain dimension of the additional SMEFT operators.

The additional operators above introduce new Feynman rules to be appended to the Feynman rules of the SM which, for a given process, allow the matrix element of the SMEFT to be calculated as follows:

$$\mathcal{M}_{\text{SMEFT}} \quad \equiv \quad \mathcal{M}_{\text{SM}} \quad + \sum_{\substack{1 \leqslant i \leqslant n_{\mathscr{D}} \\ \mathscr{D} > 4}} C_i^{(\mathscr{D})} \frac{\mathcal{M}_i^{(\mathscr{D})}}{\Lambda^{\mathscr{D}-4}} , \qquad (1.3.0.2)$$

where $\mathcal{M}_i^{(\mathscr{D})}$ is the contribution of the SMEFT to the matrix element of the SM.

Due to the dependency of the cross section σ by the square of the matrix element $|\mathcal{M}|^2$, this observable in the SMEFT could be written in the following way:

$$\sigma_{\text{SMEFT}} \equiv \sigma_{\text{SM}} + \sum_{\substack{1 \leqslant i \leqslant n_{\mathscr{D}} \\ \mathscr{D} > 4}} 2 \operatorname{Re}[C_i^{(\mathscr{D})}] \frac{\sigma_i^{(\mathscr{D})}}{\Lambda^{\mathscr{D}-4}} + \sum_{\substack{1 \leqslant i,j \leqslant n_{\mathscr{D}} \\ \mathscr{D} > 4}} C_i^{(\mathscr{D})*} C_j^{(\mathscr{D})} \frac{\sigma_{ij}^{(\mathscr{D})}}{\Lambda^{2\mathscr{D}-8}} +$$

$$+ \sum_{\substack{1 \leqslant i \leqslant n_{\mathscr{D}}, \mathscr{D} > 4 \\ 1 \leqslant j \leqslant n_{\mathscr{D}'}, \mathscr{D}' > 4 \\ \mathscr{D} \neq \mathscr{D}'}} C_i^{(\mathscr{D})*} C_j^{(\mathscr{D}')} \frac{\sigma_{ij}^{(\mathscr{D}\mathscr{D}')}}{\Lambda^{\mathscr{D}+\mathscr{D}'-8}} , \quad (1.3.0.3)$$

where the quantities $\sigma_i^{(\mathscr{D})}$ are given by the interference between the elements of the matrix SM and the contributions of the operators $\mathcal{O}_i^{(\mathscr{D})}$, while the quantities $\sigma_{ij}^{(\mathscr{D})}$ and $\sigma_{ij}^{(\mathscr{D}\mathscr{D}')}$, including also operators with different dimensions, are produced by squaring the elements of the purely EFT matrix $\mathcal{M}_i^{(\mathscr{D})}$. These last terms seem to represent a greater correction than the terms due to the interference because they are suppressed by a greater power of Λ. Actually, the squared terms grow more with the energy values of the experiment, as evidenced by the results of this thesis, so they cannot be superficially excluded.

A similar situation we have for the decay rate Γ.

1.3.1   Operator basis

In order to develop a higher dimension SMEFT Lagrangian, it is necessary to find a basis of operators, i.e. a set of non-redundant operators, for each dimension, invariant for the SM symmetries. These operators are compounded by the following set of fields:

$$\mathcal{O}^{(\mathscr{D})} \sim \left(\bar{\psi}\Sigma\psi\right)^{N_\psi} \left(X^{\mu\nu}\right)^{N_X} \left(\mathcal{D}_\mu\right)^{N_\mathcal{D}} \left(\phi\right)^{N_\phi} \implies [\![\mathcal{O}^{(\mathscr{D})}]\!] \equiv \mathscr{D} = 3N_\psi + 2N_X + N_\mathcal{D} + N_\phi ,$$
$$(1.3.1.1)$$

where $\bar{\psi}\Sigma\psi$ is a generic bilinear of the spinorial field ψ, $X^{\mu\nu}$ is a gauge field strength, $\mathcal{D}_\mu$ is the covariant derivative and ϕ is a generic scalar field (typically the Higgs field), each one with its relevant power: N_ψ, N_X, $N_\mathcal{D}$ and N_ϕ.

It is useful also to note that Lorentz invariance requires that fermion appears in bilinear forms written in terms of chiral spinorial fields and that the power of dimension of the above fields are: $[\![\psi]\!] = 3/2$, $[\![X^{\mu\nu}]\!] = 2$, $[\![\mathcal{D}_\mu]\!] = 1$ and $[\![\phi]\!] = 1$.

The lowest dimension term in the SMEFT is the unique **five-dimension** with its h.c. term:

$$\mathcal{L}_{\text{SMEFT}}^{(5)} \equiv \mathcal{L}_{\text{SM}} + \underbrace{\frac{C_{mn}^{(5)}}{\Lambda}(\tilde{\Phi}^\dagger L_m)^T \mathcal{C}(\tilde{\Phi}^\dagger L_n)}_{\text{EFT 5-dim. operator}} + \text{h.c.} , \quad (1.3.1.2)$$

where m, n are flavour indices, $\mathcal{C}$ the charge conjugation operator and $C_{mn}^{(5)}$ the relevant Wilson coefficient. It could be demonstrated that Formula 1.3.1.2 is the unique five-dimension term in the SMEFT Lagrangian and it generates a Majorana neutrino mass, proportional to $C_{mn}^{(5)}v^2/\Lambda$ when Higgs field "gets" the VEV. It is important to consider that the unique operator introduced by the 5-dimension SMEFT Lagrangian violates the lepton number by 2 units ($\Delta L = 2$). In fact, it can be shown that invariant operators constructed from SM fields satisfy $(\Delta B - \Delta L)/2 = \mathscr{D} \mod 2$, thus a 5-dimension operator and odd-dimension operators in general, cannot conserve both baryon and lepton number [2]. Considering that we do not have experimental evidence of this violation, i.e. the baryon and

lepton number conservation seems to be a symmetry of the SM, we prefer to pass to SMEFT operators with even-dimension.

The smallest even-dimension theory that includes operators that do not violate lepton or baryon numbers is **six-dimension** SMEFT.

The first historically studied basis in six dimensions is the *Warsaw basis* [16], it has 59 types of independent operators that preserve the number of baryons or leptons and 5 that violate this symmetry. These types are shown in Table 1.3 and Table 1.4 below.

X^3		ϕ^6 and $\phi^4\mathcal{D}^2$		$\phi^3\psi^2$	
$\mathcal{O}_G$	$f^{abc}G_{a\nu}^{\mu}G_{b\rho}^{\nu}G_{c\mu}^{\rho}$	$\mathcal{O}_\Phi$	$(\Phi^\dagger\Phi)^3$	$\mathcal{O}_{\Phi R}$	$(\Phi^\dagger\Phi)(\bar{L}_m\Phi R_n)$
$\mathcal{O}_{\tilde{G}}$	$f^{abc}\tilde{G}_{a\nu}^{\mu}G_{b\rho}^{\nu}G_{c\mu}^{\rho}$	$\mathcal{O}_{\Phi\Box}$	$(\Phi^\dagger\Phi)\Box(\Phi^\dagger\Phi)$	$\mathcal{O}_{\Phi U}$	$(\Phi^\dagger\Phi)(\bar{Q}_m\Phi U_n)$
$\mathcal{O}_W$	$\epsilon^{IJK}W_{I\nu}^{\mu}W_{J\rho}^{\nu}W_{K\rho}^{\rho}$	$\mathcal{O}_{\Phi\mathcal{D}}$	$(\Phi^\dagger\mathcal{D}_\mu\Phi)^*(\Phi^\dagger\mathcal{D}^\mu\Phi)$	$\mathcal{O}_{\Phi D}$	$(\Phi^\dagger\Phi)(\bar{Q}_m\Phi D_n)$
$\mathcal{O}_{\tilde{W}}$	$\epsilon^{IJK}\tilde{W}_{I\nu}^{\mu}W_{J\rho}^{\nu}W_{K\rho}^{\rho}$				

ϕ^2X^2		$\psi^2\phi X$		$\phi^2\psi^2\mathcal{D}$	
$\mathcal{O}_{\Phi G}$	$(\Phi^\dagger\Phi)G_{\mu\nu}^aG_a^{\mu\nu}$	$\mathcal{O}_{RW}$	$(\bar{L}_m\sigma^{\mu\nu}R_n)\dfrac{\sigma_I}{2}\Phi W_{\mu\nu}^I$	$\mathcal{O}_{\Phi L}^{(1)}$	$(\Phi^\dagger i\overset{\leftrightarrow}{\mathcal{D}}_\mu\Phi)(\bar{L}_m\gamma^\mu L_n)$
$\mathcal{O}_{\Phi\tilde{G}}$	$(\Phi^\dagger\Phi)\tilde{G}_{\mu\nu}^aG_a^{\mu\nu}$	$\mathcal{O}_{RB}$	$(\bar{L}_m\sigma^{\mu\nu}R_n)\Phi B_{\mu\nu}$	$\mathcal{O}_{\Phi L}^{(3)}$	$(\Phi^\dagger i\overset{\leftrightarrow}{\mathcal{D}}_{I,\mu}\Phi)(\bar{L}_m\dfrac{\sigma^I}{2}\gamma^\mu L_n)$
$\mathcal{O}_{\Phi W}$	$(\Phi^\dagger\Phi)W_{\mu\nu}^IW_I^{\mu\nu}$	$\mathcal{O}_{UG}$	$(\bar{Q}_m\sigma^{\mu\nu}\dfrac{\tau_a}{2}U_n)\tilde{\Phi}G_{\mu\nu}^a$	$\mathcal{O}_{\Phi R}$	$(\Phi^\dagger i\overset{\leftrightarrow}{\mathcal{D}}_\mu\Phi)(\bar{R}_m\gamma^\mu R_n)$
$\mathcal{O}_{\Phi\tilde{W}}$	$(\Phi^\dagger\Phi)\tilde{W}_{\mu\nu}^IW_I^{\mu\nu}$	$\mathcal{O}_{UW}$	$(\bar{Q}_m\sigma^{\mu\nu}U_n)\dfrac{\sigma_I}{2}\tilde{\Phi}W_{\mu\nu}^I$	$\mathcal{O}_{\Phi Q}^{(1)}$	$(\Phi^\dagger i\overset{\leftrightarrow}{\mathcal{D}}_\mu\Phi)(\bar{Q}_m\gamma^\mu Q_n)$
$\mathcal{O}_{\Phi B}$	$(\Phi^\dagger\Phi)B_{\mu\nu}B^{\mu\nu}$	$\mathcal{O}_{UB}$	$(\bar{Q}_m\sigma^{\mu\nu}U_n)\tilde{\Phi}B_{\mu\nu}$	$\mathcal{O}_{\Phi Q}^{(3)}$	$(\Phi^\dagger i\overset{\leftrightarrow}{\mathcal{D}}_{I,\mu}\Phi)(\bar{Q}_m\dfrac{\sigma^I}{2}\gamma^\mu Q_n)$
$\mathcal{O}_{\Phi\tilde{B}}$	$(\Phi^\dagger\Phi)\tilde{B}_{\mu\nu}B^{\mu\nu}$	$\mathcal{O}_{DG}$	$(\bar{Q}_m\sigma^{\mu\nu}\dfrac{\tau_a}{2}D_n)\Phi G_{\mu\nu}^a$	$\mathcal{O}_{\Phi U}$	$(\Phi^\dagger i\overset{\leftrightarrow}{\mathcal{D}}_\mu\Phi)(\bar{U}_m\gamma^\mu U_n)$
$\mathcal{O}_{\Phi WB}$	$(\Phi^\dagger\dfrac{\sigma_I}{2}\Phi)W_{\mu\nu}^IB^{\mu\nu}$	$\mathcal{O}_{DW}$	$(\bar{Q}_m\sigma^{\mu\nu}D_n)\dfrac{\sigma_I}{2}\Phi W_{\mu\nu}^I$	$\mathcal{O}_{\Phi D}$	$(\Phi^\dagger i\overset{\leftrightarrow}{\mathcal{D}}_\mu\Phi)(\bar{D}_m\gamma^\mu D_n)$
$\mathcal{O}_{\Phi\tilde{W}B}$	$(\Phi^\dagger\dfrac{\sigma_I}{2}\Phi)\tilde{W}_{\mu\nu}^IB^{\mu\nu}$	$\mathcal{O}_{DB}$	$(\bar{Q}_m\sigma^{\mu\nu}D_n)\Phi B_{\mu\nu}$	$\mathcal{O}_{\Phi UD}$	$(\tilde{\Phi}^\dagger i\overset{\leftrightarrow}{\mathcal{D}}_\mu\Phi)(\bar{U}_m\gamma^\mu D_n)$

Table 1.3: Six-dimension not four-fermion operators of Warsaw basis.

	$(\bar{\psi}_L\psi_L)(\bar{\psi}_L\psi_L)$			$(\bar{\psi}_R\psi_R)(\bar{\psi}_R\psi_R)$			$(\bar{\psi}_L\psi_L)(\bar{\psi}_R\psi_R)$
$\mathcal{O}_{LL}$	$(\bar{L}_m\gamma_\mu L_n)(\bar{L}_{m'}\gamma^\mu L_{n'})$		$\mathcal{O}_{RR}$	$(\bar{R}_m\gamma_\mu R_n)(\bar{R}_{m'}\gamma^\mu R_{n'})$		$\mathcal{O}_{LR}$	$(\bar{L}_m\gamma_\mu L_n)(\bar{R}_{m'}\gamma^\mu R_{n'})$
$\mathcal{O}_{QQ}^{(1)}$	$(\bar{Q}_m\gamma_\mu Q_n)(\bar{Q}_{m'}\gamma^\mu Q_{n'})$		$\mathcal{O}_{UU}$	$(\bar{U}_m\gamma_\mu U_n)(\bar{U}_{m'}\gamma^\mu U_{n'})$		$\mathcal{O}_{LU}$	$(\bar{L}_m\gamma_\mu L_n)(\bar{U}_{m'}\gamma^\mu U_{n'})$
$\mathcal{O}_{QQ}^{(3)}$	$(\bar{Q}_m\gamma_\mu\frac{\sigma_I}{2}Q_n)(\bar{Q}_{m'}\gamma^\mu\frac{\sigma^I}{2}Q_{n'})$		$\mathcal{O}_{DD}$	$(\bar{D}_m\gamma_\mu D_n)(\bar{D}_{m'}\gamma^\mu D_{n'})$		$\mathcal{O}_{LD}$	$(\bar{L}_m\gamma_\mu L_n)(\bar{D}_{m'}\gamma^\mu D_{n'})$
$\mathcal{O}_{LQ}^{(1)}$	$(\bar{L}_m\gamma_\mu L_n)(\bar{Q}_{m'}\gamma^\mu Q_{n'})$		$\mathcal{O}_{RU}$	$(\bar{R}_m\gamma_\mu R_n)(\bar{U}_{m'}\gamma^\mu U_{n'})$		$\mathcal{O}_{QR}$	$(\bar{Q}_m\gamma_\mu Q_n)(\bar{R}_{m'}\gamma^\mu R_{n'})$
$\mathcal{O}_{LQ}^{(3)}$	$(\bar{L}_m\gamma_\mu\frac{\sigma_I}{2}L_n)(\bar{Q}_{m'}\gamma^\mu\frac{\sigma^I}{2}Q_{n'})$		$\mathcal{O}_{RD}$	$(\bar{R}_m\gamma_\mu R_n)(\bar{D}_{m'}\gamma^\mu D_{n'})$		$\mathcal{O}_{QU}^{(1)}$	$(\bar{Q}_m\gamma_\mu Q_n)(\bar{U}_{m'}\gamma^\mu U_{n'})$
			$\mathcal{O}_{UD}^{(1)}$	$(\bar{U}_m\gamma_\mu U_n)(\bar{D}_{m'}\gamma^\mu D_{n'})$		$\mathcal{O}_{QU}^{(8)}$	$(\bar{Q}_m\gamma_\mu\frac{\tau_a}{2}Q_n)(\bar{U}_{m'}\gamma^\mu\frac{\tau^a}{2}U_{n'})$
			$\mathcal{O}_{UD}^{(8)}$	$(\bar{U}_m\gamma_\mu\frac{\tau_a}{2}U_n)(\bar{D}_{m'}\gamma^\mu\frac{\tau^a}{2}D_{n'})$		$\mathcal{O}_{QD}^{(1)}$	$(\bar{Q}_m\gamma_\mu Q_n)(\bar{D}_{m'}\gamma^\mu D_{n'})$
						$\mathcal{O}_{QD}^{(8)}$	$(\bar{Q}_m\gamma_\mu\frac{\tau_a}{2}Q_n)(\bar{D}_{m'}\gamma^\mu\frac{\tau^a}{2}D_{n'})$

	$(\bar{\psi}_L\psi_R)(\bar{\psi}_R\psi_L)$ and $(\bar{\psi}_L\psi_R)(\bar{\psi}_L\psi_R)$		B-violating
$\mathcal{O}_{LRDQ}$	$(\bar{L}_{m,\iota}R_n)(\bar{D}_{m'}Q_{n'}^\iota)$	$\mathcal{O}_{DUQ}$	$\epsilon_{ijk}((D_m^i)^T\mathcal{C}U_n^j)((Q_{m'}^{k,\iota})^T\epsilon_{\iota\kappa}\mathcal{C}L_{n'}^\kappa)$
$\mathcal{O}_{QUQD}^{(1)}$	$(\bar{Q}_m^\iota U_n)\epsilon_{\iota\kappa}(\bar{Q}_{m'}^\kappa D_{n'})$	$\mathcal{O}_{QQU}$	$\epsilon_{ijk}((Q_m^{i,\iota})^T\epsilon_{\iota\kappa}\mathcal{C}Q_n^{j,\kappa})((U_{m'}^k)^T\mathcal{C}R_{n'})$
$\mathcal{O}_{QUQD}^{(8)}$	$(\bar{Q}_m^\iota\frac{\tau_a}{2}U_n)\epsilon_{\iota\kappa}(\bar{Q}_{m'}^\kappa\frac{\tau^a}{2}D_{n'})$	$\mathcal{O}_{QQQ}^{(1)}$	$\epsilon_{ijk}((Q_m^{i,\iota})^T\epsilon_{\iota\kappa}\mathcal{C}Q_n^{j,\kappa})((Q_{m'}^{k,\eta})^T\epsilon_{\eta\theta}\mathcal{C}L_{n'}^\theta)$
$\mathcal{O}_{LRQU}^{(1)}$	$(\bar{L}_m^\iota R_n)\epsilon_{\iota\kappa}(\bar{Q}_{m'}^\kappa U_{n'})$	$\mathcal{O}_{QQQ}^{(3)}$	$\epsilon_{ijk}((Q_m^{i,\iota})^T(\tau_I\epsilon)_{\iota\kappa}\mathcal{C}Q_n^{j,\kappa})((Q_{m'}^{k,\eta})^T(\tau^I\epsilon)_{\eta\theta}\mathcal{C}L_{n'}^\theta)$
$\mathcal{O}_{LRQU}^{(3)}$	$(\bar{L}_m^\iota\sigma_{\mu\nu}R_n)\epsilon_{\iota\kappa}(\bar{Q}_{m'}^\kappa\sigma^{\mu\nu}U_{n'})$	$\mathcal{O}_{DUU}$	$\epsilon_{ijk}((D_m^i)^T\mathcal{C}U_n^j)((U_{m'}^k)^T\mathcal{C}R_{n'})$

Table 1.4: Six-dimension four-fermion operators of Warsaw basis.

The following notations have been used for these tables:

- μ, ν, ρ, σ are Lorentzian space-time indices;

- a, b, c are eight-values indices to identify the eight colour status of gluons, corresponding to the adjoined representation of SU(3) symmetry;

- I, J, K are three-values indices corresponding to the adjoined representation of SU(2) symmetry;

- ι, κ, η, θ are three-value indices to identify the three colour status of quarks, corresponding to the representation of SU(3) symmetry;

- i, j, k are two-values indices corresponding to the representation SU(2) symmetry;

- m, n, m', n' are three-values indices to identify the fermion flavour;

- $\tilde{X}_{\mu\nu} \equiv \frac{1}{2}\epsilon_{\mu\nu\rho\sigma}X^{\rho\sigma}$ where $\epsilon_{0123} = +1$;

- $\tilde{\Phi}^i \equiv \epsilon_{ij}\left(\Phi^j\right)^*$ where $\epsilon_{12} = +1$;

- $\Phi^\dagger i \overset{\leftrightarrow}{\mathcal{D}}_\mu \Phi \equiv i\Phi^\dagger\left(\mathcal{D}_\mu\Phi\right) - i\left(\mathcal{D}_\mu\Phi^\dagger\right)\Phi$;

- $\Phi^\dagger i \overset{\leftrightarrow}{\mathcal{D}}_{I,\mu} \Phi \equiv i\Phi^\dagger\frac{\sigma_I}{2}\left(\mathcal{D}_\mu\Phi\right) - i\left(\mathcal{D}_\mu\Phi^\dagger\right)\frac{\sigma_I}{2}\Phi$.

The 59 types of operators preserving B and L allow interaction between all fermion families. Combining all the flavours present in the three fermion families, these types give rise to 2499 operators, denominated *flavour general*, of which 1350 of them conserve the CP-even and 1149 the CP-odd. Considering, on the other hand, the interactions within a single fermion family, denominated *flavour universal*, 76 operators originate, of which 53 of them retain the CP-even and 23 the CP-odd. We remember that for non-Hermitian operators $\mathcal{O}$, $\mathcal{O} + \mathcal{O}^\dagger$ is CP-even, and $\mathcal{O} - \mathcal{O}^\dagger$ is CP-odd. [2]
Following the Table 1.5 with the Number of operators for each type.

Operators	flavor universal			flavor general		
	CP-even	CP-odd	total	CP-even	CP-odd	total
X^3	2	2	4	2	2	4
ϕ^6	1	0	1	1	0	1
$\phi^4 \mathcal{D}^2$	2	0	2	2	0	2
$\phi^2 X^2$	4	4	8	4	4	8
$\phi^3 \psi^2$	3	3	6	27	27	54
$\psi^2 \phi X$	8	8	16	72	72	144
$\phi^2 \psi^2 \mathcal{D}$	8	1	9	51	30	81
$(\bar{\psi}_L \psi_L)(\bar{\psi}_L \psi_L)$	5	0	5	171	126	297
$(\bar{\psi}_R \psi_R)(\bar{\psi}_R \psi_R)$	7	0	7	255	195	450
$(\bar{\psi}_L \psi_L)(\bar{\psi}_R \psi_R)$	8	0	8	360	288	648
$(\bar{\psi}_L \psi_R)(\bar{\psi}_R \psi_L)$+h.c.	1	1	2	81	81	162
$(\bar{\psi}_L \psi_R)(\bar{\psi}_L \psi_R)$+h.c.	4	4	8	324	324	648
total	53	23	76	1350	1149	2499

Table 1.5: Number of conserving B operators of Warsaw basis.

From this basis of operators, only relevant ones will be used to evaluate the impact of the SMEFT at the LO in the top quark pair production process at the LHC, thus following a proton collision.

1.3.2   6-dimension SMEFT operators for top quark pair production

In a proton-proton collision at the LHC, top quark-antiquark pair production involves gluons fusion ($gg \to t\bar{t}$) and quark-antiquark annihilation ($q\bar{q} \to t\bar{t}$) partonic processes. In 6-dimension SMEFT, the above effective operators contribute to both processes, as shown below [17] [18]:

for gluons fusion:

$$\begin{cases} \mathcal{O}_{tG} \equiv (\bar{t}\sigma^{\mu\nu}\tau_a t)\, \tilde{\Phi} G_{\mu\nu}^a & \text{chromomagnetic moment operator} \\[2mm] \mathcal{O}_G \equiv f_{abc} G_\mu^{a\nu} G_\nu^{b\rho} G_\rho^{c\mu} & \text{triple gluon field strength operator} \\[2mm] \mathcal{O}_{\Phi G} \equiv 1/2 \left(\Phi^\dagger \Phi \right) G_{a\mu\nu} G^{a\mu\nu} & \text{Higgs-gluon interaction operator} \end{cases}$$

$$(1.3.2.1)$$

for quark-antiquark annihilation:

$$\begin{cases} \mathcal{O}_{tG} \equiv (\bar{t}\sigma^{\mu\nu}\tau_a t)\, \tilde{\Phi} G_{\mu\nu}^a & \left.\right\} \text{chromomagnetic moment operator} \\[4mm] \mathcal{O}_{Qq}^{(8,1)} \equiv \left(\bar{Q}_{31}\gamma_\mu \tau_a Q_{31} \right) \left(\bar{Q}_1 \gamma^\mu \tau^a Q_1 \right) \quad \mathcal{O}_{Qq}^{(1,1)} \equiv \left(\bar{Q}_{31}\gamma_\mu Q_{31} \right) \left(\bar{Q}_1 \gamma^\mu Q_1 \right) \\[2mm] \mathcal{O}_{Qq}^{(8,3)} \equiv \left(\bar{Q}_{31}\gamma_\mu \tau_a \sigma_I Q_{31} \right) \left(\bar{Q}_1 \gamma^\mu \tau^a \sigma^I Q_1 \right) \quad \mathcal{O}_{Qq}^{(1,3)} \equiv \left(\bar{Q}_{31}\gamma_\mu \sigma_I Q_{31} \right) \left(\bar{Q}_1 \gamma^\mu \sigma^I Q_1 \right) \\[2mm] \mathcal{O}_{tu}^{(8)} \equiv \left(\bar{U}_3\gamma_\mu \tau_a U_3 \right) \left(\bar{U}_1 \gamma^\mu \tau^a U_1 \right) \quad \mathcal{O}_{tu}^{(1)} \equiv \left(\bar{U}_3\gamma_\mu U_3 \right) \left(\bar{U}_1 \gamma^\mu U_1 \right) \\[2mm] \mathcal{O}_{td}^{(8)} \equiv \left(\bar{U}_3\gamma_\mu \tau_a U_3 \right) \left(\bar{D}_1 \gamma^\mu \tau^a D_1 \right) \quad \mathcal{O}_{td}^{(1)} \equiv \left(\bar{U}_3\gamma_\mu U_3 \right) \left(\bar{D}_1 \gamma^\mu D_1 \right) \end{cases}$$

$$\left.\begin{array}{l} \end{array}\right\} \text{8 four-quark operators with LL and RR chiral structure}$$

$$\begin{cases} \mathcal{O}_{Qu}^{(8)} \equiv \left(\bar{Q}_{31}\gamma_\mu \tau_a Q_{31} \right) \left(\bar{U}_1 \gamma^\mu \tau^a U_1 \right) \quad \mathcal{O}_{Qu}^{(1)} \equiv \left(\bar{Q}_{31}\gamma_\mu Q_{31} \right) \left(\bar{U}_1 \gamma^\mu U_1 \right) \\[2mm] \mathcal{O}_{Qd}^{(8)} \equiv \left(\bar{Q}_{31}\gamma_\mu \tau_a Q_{31} \right) \left(\bar{D}_1 \gamma^\mu \tau^a D_1 \right) \quad \mathcal{O}_{Qd}^{(1)} \equiv \left(\bar{Q}_{31}\gamma_\mu Q_{31} \right) \left(\bar{D}_1 \gamma^\mu D_1 \right) \\[2mm] \mathcal{O}_{tq}^{(8)} \equiv \left(\bar{U}_3\gamma_\mu \tau_a U_3 \right) \left(\bar{Q}_1 \gamma^\mu \tau^a Q_1 \right) \quad \mathcal{O}_{tq}^{(1)} \equiv \left(\bar{U}_3\gamma_\mu U_3 \right) \left(\bar{Q}_1 \gamma^\mu Q_1 \right) \end{cases}$$

$$\left.\begin{array}{l} \end{array}\right\} \text{6 four-quark operators with LR and RL chiral structure}$$

$$(1.3.2.2)$$

In this last peculiar case the following convention is used:

- $Q_1 \equiv \left(u_L, d_L \right) \equiv \left(P_L u, P_L d \right)$, $U_1 \equiv u_R \equiv P_R u$ and $D_1 \equiv d_R \equiv P_R d$ where u and d are the "up" quark and "down" quark of the first quark family;

- $Q_3 \equiv \left(t_L, b_L \right) \equiv \left(P_L t, P_L b \right) \implies Q_{31} \equiv t_L \equiv P_L t$ and $U_3 \equiv t_R \equiv P_R t$ where t is the "up" quark of the third quark family.

Further, (L) and (R) denote left-handed and right-handed parts of the fermion field and P_L and P_R are the chiral projectors, also indicated with γ^7 and γ^6.

The operators of this subsection generate Feynman Rules as reported in Section A.4.

Chapter 2

TOP PAIR PRODUCTION AND ITS SMEFT EXTENSION

The production of top quark pair $t\bar{t}$ due to the high-energy collision of hadrons, which occurs e.g. at the LHC through the proton scattering pp, can be mainly described by the perturbative QCD theory of the SM. EW also gives its effects, although less significant. In this scenario, a hard scattering process between two **hadrons** is the result of an interaction of a large number of couples of **partons**, i.e. quarks and gluons that are the constituents of the incoming hadrons. In the collision, each parton possesses a longitudinal momentum $\mathrm{x}p^{\mu}$ that is equal to a fraction $0 \leq \mathrm{x} \leq 1$ of the momentum of its own hadron $p^{\mu} \equiv (E, \overrightarrow{p})$, and the interaction of these partons generates the top quark-antiquark pair $t\bar{t}$, as predicted by the SM.
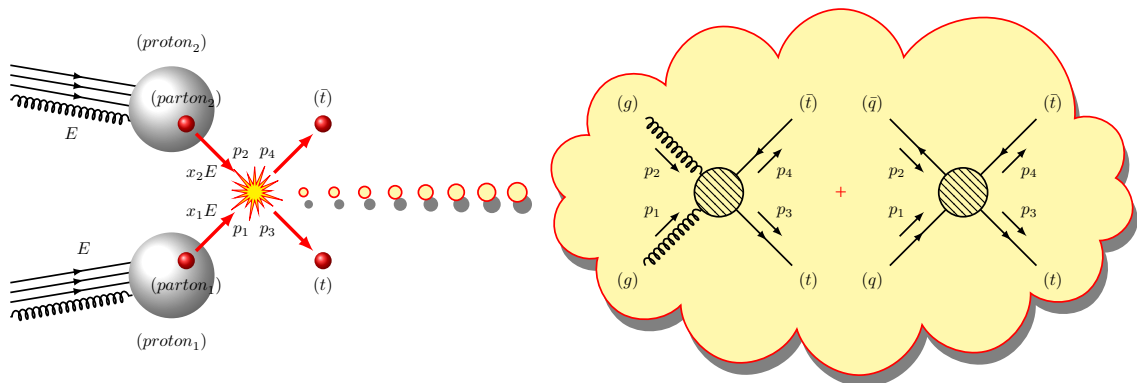
Top quark-antiquark pair production by proton-proton collision

The formation of these top pairs through colliding hadrons can be studied by analysing, for example, the cross section distribution $\mathrm{d}\sigma_{\mathrm{hadronic}}/\mathrm{d}O$ with respect to a chosen observable parameter O, such as the transverse momentum p_T, scattering angle θ, etc. This cross section can be derived from the similar scattering magnitude of individual partons $\mathrm{d}\sigma/\mathrm{d}O$ based on how they are distributed within colliding hadrons.

The *factorisation theorem* expressed as follows comes to the aid of this:

$$\frac{\mathrm{d}\sigma_{\text{hadronic}}}{\mathrm{d}O} = \sum_{ij\in\text{partons}} \int_0^1 \mathrm{d}\mathrm{x}_i\,\mathrm{pdf}_i\left(\mathrm{x}_i,\mu_F^2\right) \int_0^1 \mathrm{d}\mathrm{x}_j\,\mathrm{pdf}_j\left(\mathrm{x}_j,\mu_F^2\right)\ \frac{\mathrm{d}\sigma}{\mathrm{d}O}\left(\mathrm{x}_i\mathrm{x}_j s,\mu_F,\alpha_s\left(\mu_R\right)\right)\ ,$$

where $\mathrm{pdf}_i\left(\mathrm{x}_i,\mu_F^2\right)$ is the Parton Distribution Function (PDF) of a parton i, i.e. the probability density for finding parton i in a hadron carrying momentum x_i, this depends of the fraction of colliding energy passed from the hadron to the parton x_i and function of the energy factorisation scale μ_F. Of course the strong coupling constant $\alpha_s\left(\mu_R\right)$ depends on the renormalisation scale used μ_R.

The hard-scattering cross section $\mathrm{d}\sigma/\mathrm{d}O$, due to the collision of partons, can be calculated through the *Golden Rule* formula:

$$\mathrm{d}^6\sigma = \frac{1}{4\sqrt{(p_1\cdot p_2)^2 - m_1^2 m_2^2}}(2\pi)^4\delta^4\left(p_3 + p_4 - p_1 - p_2\right)\langle|\mathcal{M}|^2\rangle\,\frac{\mathrm{d}^3\overrightarrow{p_3}}{(2\pi)^3 2E_3}\frac{\mathrm{d}^3\overrightarrow{p_4}}{(2\pi)^3 2E_4}\ ,$$

which involves, by means of the *matrix element* $\mathcal{M}$, the SM theory, extensible to the SMEFT.

Starting from the Feynman Rule at LO, it is clear that the partonic processes involved in the collision of protons and which contribute to the formation of top quark-antiquark pairs are the gluon fusion, $gg \to t\bar{t}$ and the quark-antiquark annihilation $q\bar{q} \to t\bar{t}$ as schematised below:
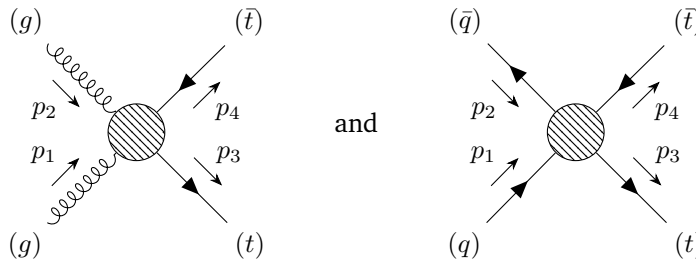
Feynman diagram of whole top quark pair production process by gluon fusion
$gg \to t\bar{t}$ and by quark-antiquark annihilation $q\bar{q} \to t\bar{t}$.

The "blob" depicted above is intended to indicate the contribution of all possible Feynman diagram orders: next to leading order (NLO), next to next to leading order (NNLO), etc. to the tree-level order and all its possible extensions according to SMEFT.

In this chapter, we want to analyse all the elements that allow us to determine the cross sections of the production of the top quark-antiquark pair, on the base of SM, also incorporating the extensions of a possible SMEFT.

We start in a propaedeutic manner, analysing the kinematic aspects of a collision between two particles on their centre of mass frame (CMF), fixed with the laboratory. This study is then extended to the process of a collision between two partons (gg or $q\bar{q}$) which, having different collision energies, possess a centre of mass that appears to be boosted in the direction of the more energetic parton. The kinematic relations obtained are useful to calculate the matrix element $\mathcal{M}$, containing all the information of SM and its SMEFT extension, and its squared average $\langle|\mathcal{M}|^2\rangle$, which are central to the calculation of cross sections.

The SMEFT extension analysed here is introduced by the QCD-related SMEFT operators of dimension 6. This assumption can be made considering that the EW SMEFT extension could probably be of lesser significance given the magnitude of the EW constants compared to QCD.

2.1   Kinematics framework

To analyse a scattering process it is fundamental to set the correct kinematic relations to be used for the calculation of the average square matrix element and to characterise the various observables in general.

For both the processes involved in the top quark-antiquark pair production, by gluons fusion ($gg \rightarrow t\bar{t}$) and light quark-antiquark pair annihilation ($q\bar{q} \rightarrow t\bar{t}$), a **quasi-elastic two particles scattering** is analysed. In Figure 2.1 such processes are represented, the two incoming particles are labelled by (1) and (2), and the two outcoming particles, produced by the interaction during the collision, are labelled by (3) and (4): $(1)(2) \rightarrow (3)(4)$. With p_1, p_2, p_3 and p_4 are indicated the relative four-momenta.
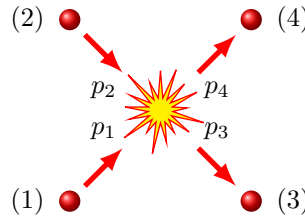

Figure 2.1: Quasi-elastic two particles collision

2.1.1   Momenta scalar product relations and Mandelstam variables

To simplify the calculation of the average square matrix element, it is convenient to reduce the number of momenta scalar products, because not all of them are independent of each other.

Once the momenta are set, from the on-shell mass relations and from the total momentum conservation principle:

$$\begin{cases} p_1^2 = m_1^2 \qquad p_2^2 = m_2^2 & p_1, p_2, m_1, m_2: \text{ incoming particles momenta and masses }, \\ p_3^2 = m_3^2 \qquad p_4^2 = m_4^2 & p_3, p_4, m_3, m_4: \text{ outcoming particles momenta and masses }, \\ p_1 + p_2 = p_3 + p_4 & \text{total momentum conservation principle }, \end{cases}$$

$$(2.1.1.1)$$

the following **momenta scalar product relations** can be obtained:

$$\begin{cases} p_1 \cdot p_4 = p_2 \cdot p_3 + \dfrac{m_1^2 - m_2^2 - m_3^2 + m_4^2}{2} \,, \\ p_2 \cdot p_4 = p_1 \cdot p_3 + \dfrac{-m_1^2 + m_2^2 - m_3^2 + m_4^2}{2} \,, \\ p_3 \cdot p_4 = p_1 \cdot p_2 + \dfrac{m_1^2 + m_2^2 - m_3^2 - m_4^2}{2} \,, \\ p_1 \cdot p_2 = p_1 \cdot p_3 + p_2 \cdot p_3 + \dfrac{-m_1^2 - m_2^2 - m_3^2 + m_4^2}{2} \,. \end{cases}$$

$$(2.1.1.2)$$

From the previous relations it is clear that only two scalar products are independent of the others: in this particular case $p_1 \cdot p_3$ and $p_2 \cdot p_3$ have been chosen.
For simplicity, all the calculations here developed are made in natural units, where $c = 1$ is imposed.

In addition to the previous relations, it is useful to substitute the scalar products with the **Mandelstam variables**, expressing the average squared matrix element in terms of only relativistic invariants:

$$\begin{cases} t \equiv (p_3 - p_1)^2 = (p_2 - p_4)^2 \\ u \equiv (p_3 - p_2)^2 = (p_1 - p_4)^2 \\ s \equiv (p_1 + p_2)^2 = (p_3 + p_4)^2 \end{cases} \implies \begin{cases} p_1 \cdot p_3 = \dfrac{m_1^2 + m_3^2 - t}{2} \\ p_2 \cdot p_3 = \dfrac{m_2^2 + m_3^2 - u}{2} \\ p_1 \cdot p_2 = \dfrac{s - m_1^2 - m_2^2}{2} \end{cases}, \qquad (2.1.1.3)$$

clearly, the following relation is valid $s + t + u = m_1^2 + m_2^2 + m_3^2 + m_4^2$, in this way only two Mandelstam variables are linearly independent.

In particular, considering the top quark-antiquark pair production by gluons fusion ($gg \to t\bar{t}$) or by light quarks pair annihilation ($q\bar{q} \to t\bar{t}$), the masses of the incoming particles are null or however negligible compared to the mass of the produced top quark, while the masses of the outcoming particles are both equal to top quark mass, so the above relations become:

$$\begin{cases} m_1 = m_2 := 0 \\ m_3 = m_4 := m_t \end{cases} \implies \begin{cases} p_1 \cdot p_4 = p_2 \cdot p_3 \\ p_2 \cdot p_4 = p_1 \cdot p_3 \\ p_3 \cdot p_4 = p_1 \cdot p_2 - m_t^2 \\ p_1 \cdot p_2 = p_1 \cdot p_3 + p_2 \cdot p_3 \end{cases} \quad \text{and} \quad \begin{cases} p_1 \cdot p_3 = \dfrac{m_t^2 - t}{2} \\ p_2 \cdot p_3 = \dfrac{m_t^2 - u}{2} \\ p_1 \cdot p_2 = \dfrac{s}{2} \end{cases},$$

$$(2.1.1.4)$$

defining m_t as the top quark mass.

If we do not want to neglect the mass of the incoming quarks, considering the top quarks pair production by quarks pair annihilation ($q\bar{q} \to t\bar{t}$), the above relations become:

$$\begin{cases} m_1 = m_2 := m_q \\ m_3 = m_4 := m_t \end{cases} \implies \begin{cases} p_1 \cdot p_4 = p_2 \cdot p_3 \\ p_2 \cdot p_4 = p_1 \cdot p_3 \\ p_3 \cdot p_4 = p_1 \cdot p_2 + m_q^2 - m_t^2 \\ p_1 \cdot p_2 = p_1 \cdot p_3 + p_2 \cdot p_3 - m_q^2 \end{cases} \quad \text{and} \quad \begin{cases} p_1 \cdot p_3 = \dfrac{m_q^2 + m_t^2 - t}{2} \\ p_2 \cdot p_3 = \dfrac{m_q^2 + m_t^2 - u}{2} \\ p_1 \cdot p_2 = \dfrac{s - 2m_q^2}{2} \end{cases},$$

$$(2.1.1.5)$$

defining m_q as the incoming quark mass.

2.1.2 Observables in fixed CMF

To express the average squared matrix element in terms of observables, it is necessary to fix the "kinematic scene". For the present scope, consider a particles collider system, where two particles, with the same mass $m_2 = m_1$ and the same energy $E_2 = E_1$, but opposite direction $\vec{p_2} = -\vec{p_1}$, interact together in a quasi-elastic collision, where other two particles with same mass $m_3 = m_4$

are generated. In this case, the central mass reference frame (CMF) is fixed and coincides with the laboratory reference frame (LF).

In a collider, the energy of incoming particles is often called **Energy Beam** indicated here as E and the square root of the Mandelstam variable $\sqrt{s} = \sqrt{(p_1 + p_2)^2} = 2E$ is called **Invariant Mass**.

Applying the momenta conservation principle, we obtain: $\vec{p_2} = -\vec{p_1} \implies \vec{p_4} = -\vec{p_3} \implies E_4 = E_3 \implies E_3 = E_1 = E \implies m_3^2 + |\vec{p_3}|^2 = m_1^2 + |\vec{p_1}|^2 = E^2$, hence:

$$|\vec{p_1}| = \frac{\sqrt{s}}{2}\beta_1 \quad |\vec{p_3}| = \frac{\sqrt{s}}{2}\beta_3 , \quad \text{defining} \quad \beta_{1/3} \equiv \sqrt{1 - \frac{4m_{1/3}^2}{s}} . \tag{2.1.2.1}$$

Most experiments in circular colliders, like LHC, utilise a right-handed coordinate Cartesian reference system with the axis z along the direction of the motion of the particles, considering positive the counterclockwise direction looking from above, the axis x directed from the point of collision to the centre of the collider and the axis y perpendicular to the previous ones. The x and z axes are horizontal to the ground where the collider is built while the y axis is vertical. Further, the coordinates are often expressed in a cylindrical coordinate system that reflects the symmetry of the detector. The reference frame is shown in the following Figure 2.2.
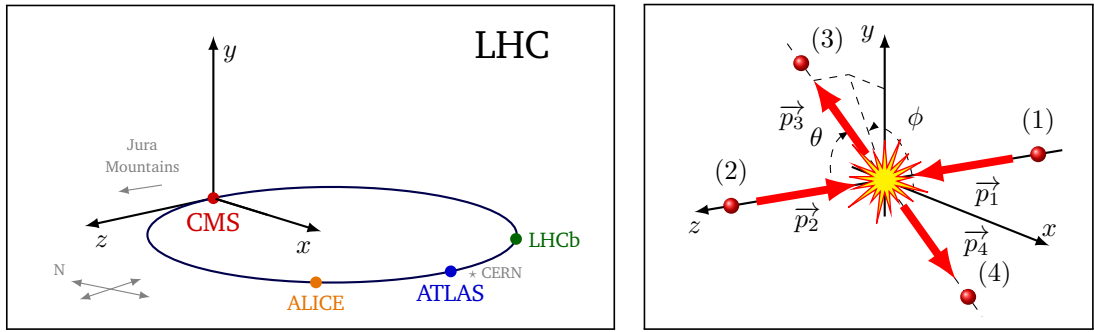
(a) Cartesian coordinates reference frame at LHC   **(b)** Cartesian coordinates reference frame at LHC

Figure 2.2: Coordinate reference system in a collider.

The first intuitive observable is the **Scattering Angle** θ, i.e. the angle between axis z and $\vec{p_3}$, as per figure. The relation between the scalar products or the Mandelstam variable and this observable are the following:

$$\begin{cases} p_1 \cdot p_2 = \sqrt{\left(m_1^2 + |\vec{p_1}|^2\right)\left(m_2^2 + |\vec{p_2}|^2\right)} - \vec{p_1} \cdot \vec{p_2} = m_1^2 + 2|\vec{p_1}|^2 \\ p_1 \cdot p_3 = \sqrt{\left(m_1^2 + |\vec{p_1}|^2\right)\left(m_3^2 + |\vec{p_3}|^2\right)} - \vec{p_1} \cdot \vec{p_3} = m_1^2 + |\vec{p_1}|^2 - |\vec{p_1}||\vec{p_3}|\cos\theta \qquad \implies \\ p_2 \cdot p_3 = \sqrt{\left(m_2^2 + |\vec{p_2}|^2\right)\left(m_3^2 + |\vec{p_3}|^2\right)} - \vec{p_2} \cdot \vec{p_3} = m_1^2 + |\vec{p_1}|^2 + |\vec{p_1}||\vec{p_3}|\cos\theta \end{cases}$$

$$\implies \begin{cases} p_1 \cdot p_2 = \dfrac{s - 2m_1^2}{2} \\ p_1 \cdot p_3 = \dfrac{s}{4}\left(1 - \beta_1\beta_3\cos\theta\right) \\ p_2 \cdot p_3 = \dfrac{s}{4}\left(1 + \beta_1\beta_3\cos\theta\right) \end{cases} \implies \begin{cases} s = 4E^2 \\ m_1^2 + m_3^2 - t = \dfrac{s}{2}\left(1 - \beta_1\beta_3\cos\theta\right) \\ m_1^2 + m_3^2 - u = \dfrac{s}{2}\left(1 + \beta_1\beta_3\cos\theta\right) \end{cases} ,$$

$$\tag{2.1.2.2}$$

for $0 \leqslant \theta \leqslant \pi$.

Another relevant observable is the **Transverse Momentum** p_T of one of the two outcoming particles, for example, particle (3). This quantity is important because in the event that the two incoming particles do not have the same collision energy, the centre of mass frame CMF is pushed in the direction of the particle with the higher energy and it does not coincide with the laboratory frame. Anyway p_T remains a relativistic invariant under Lorentz boosts along the beam direction by construction. The relation between the scalar products or the Mandelstam variable and this observable are the following:

$$p_T \equiv |\vec{p_3}| \sin\theta = \frac{\sqrt{s}}{2}\beta_3 \sin\theta \quad \implies \quad \sin\theta = \frac{2p_T}{\beta_3\sqrt{s}} \quad \implies \quad \cos\theta = \pm\sqrt{1 - \frac{4p_T^2}{s\beta_3^2}} \quad \implies$$

$$\implies \begin{cases} s = 4E^2 \\ m_1^2 + m_3^2 - t = \dfrac{s}{2}\left(1 \mp \beta_1 \sqrt{\beta_3^2 - \dfrac{4p_T^2}{s}}\right) \\ m_1^2 + m_3^2 - u = \dfrac{s}{2}\left(1 \pm \beta_1 \sqrt{\beta_3^2 - \dfrac{4p_T^2}{s}}\right) \end{cases}, \tag{2.1.2.3}$$

for $0 \leqslant p_T \leqslant \frac{\sqrt{s}}{2}\beta_3$ and where the above sign is considered only if $0 \leqslant \theta \leqslant \frac{\pi}{2}$.

In case the centre of mass frame CMF is pushed, the scattering angle does not represent a relativistic invariant quantity, so it is preferable to consider the **Rapidity** y. This, in turn, is not a relativistic invariant quantity, but its transformation law is additive for a constant due to the reference motion $(\mathrm{y}' = \mathrm{y} - \operatorname{arctanh}\beta)$. It is understood that the difference of the rapidity ($\Delta\mathrm{y}$) evaluated at two different points is a relativistic invariant along the z direction. The relation between the scalar products or the Mandelstam variable and this observable are the following:

$$\mathrm{y} \equiv \frac{1}{2}\ln\frac{E_3 + p_{3z}}{E_3 - p_{3z}} = \frac{1}{2}\ln\frac{1 + \dfrac{p_{3z}}{E_3}}{1 - \dfrac{p_{3z}}{E_3}} = \frac{1}{2}\ln\frac{1 + \dfrac{|\vec{p_3}|\cos\theta}{E_3}}{1 - \dfrac{|\vec{p_3}|\cos\theta}{E_3}} = \frac{1}{2}\ln\frac{1 + \beta_3\cos\theta}{1 - \beta_3\cos\theta} = \operatorname{arctanh}\left(\beta_3\cos\theta\right) \quad \implies$$

$$\implies \beta_3\cos\theta = \tanh\mathrm{y} \quad \implies \begin{cases} s = 4E^2 \\ m_1^2 + m_3^2 - t = \dfrac{s}{2}\left(1 - \beta_1\tanh\mathrm{y}\right) \\ m_1^2 + m_3^2 - u = \dfrac{s}{2}\left(1 + \beta_1\tanh\mathrm{y}\right) \end{cases}, \tag{2.1.2.4}$$

for $-\beta_3 \leqslant \tanh\mathrm{y} \leqslant +\beta_3$.

Due to the fact that the rapidity is not easily measured in an experiment, it is preferable to consider the **Pseudo-Rapidity** η that approximates the Rapidity at high energies. In fact in the limit of momenta much larger than the mass of a particle, the Rapidity converges to Pseudo-Rapidity. This quantity of a particle is purely geometrical, it only depends on the polar angle θ. The relation between the scalar products or the Mandelstam variable and this observable are the following:

$$\eta \equiv \frac{1}{2}\ln\frac{|\vec{p_3}| + p_{3z}}{|\vec{p_3}| - p_{3z}} = \frac{1}{2}\ln\frac{1 + \dfrac{p_{3z}}{|\vec{p_3}|}}{1 - \dfrac{p_{3z}}{|\vec{p_3}|}} = \frac{1}{2}\ln\frac{1 + \cos\theta}{1 - \cos\theta} = \operatorname{arctanh}\left(\cos\theta\right) \quad \implies \quad \cos\theta = \tanh\eta \quad \implies$$

$$\implies \begin{cases} s = 4E^2 \\ \\ m_1^2 + m_3^2 - t = \dfrac{s}{2}\left(1 - \beta_1\beta_3\tanh\eta\right) \\ \\ m_1^2 + m_3^2 - u = \dfrac{s}{2}\left(1 + \beta_1\beta_3\tanh\eta\right) \end{cases} , \qquad (2.1.2.5)$$

for $-1 \leqslant \tanh\eta \leqslant +1$.

Also in this case, considering the top quark-antiquark pair production by gluons fusion ($gg \to t\bar{t}$) or by light quarks pair annihilation ($q\bar{q} \to t\bar{t}$), the masses of the incoming particles are null or however negligible compared to the scattering energies, while the masses of the outcoming particles are equal to each other hence, the above relations regarding the Mandelstam variables depending by the here proposed observable become:

$$\begin{cases} s = 4E^2 \quad |\vec{p_1}| = \dfrac{\sqrt{s}}{2} \quad |\vec{p_3}| = \dfrac{\sqrt{s}}{2}\beta \\ \\ m_t^2 - t = \dfrac{s}{2}\left(1 - \beta\cos\theta\right) \qquad \text{for} \quad 0 \leqslant \theta \leqslant \pi \\ \\ m_t^2 - u = \dfrac{s}{2}\left(1 + \beta\cos\theta\right) \end{cases} \qquad (2.1.2.6)$$

or

$$\begin{cases} s = 4E^2 \quad |\vec{p_1}| = \dfrac{\sqrt{s}}{2} \quad |\vec{p_3}| = \dfrac{\sqrt{s}}{2}\beta \\ \\ m_t^2 - t = \dfrac{s}{2}\left(1 \mp \sqrt{\beta^2 - \dfrac{4p_T^2}{s}}\right) \qquad \text{for} \quad 0 \leqslant p_T \leqslant \dfrac{\sqrt{s}}{2}\beta \\ \\ m_t^2 - u = \dfrac{s}{2}\left(1 \pm \sqrt{\beta^2 - \dfrac{4p_T^2}{s}}\right) \end{cases} \qquad (2.1.2.7)$$

or

$$\begin{cases} s = 4E^2 \quad |\vec{p_1}| = \dfrac{\sqrt{s}}{2} \quad |\vec{p_3}| = \dfrac{\sqrt{s}}{2}\beta \\ \\ m_t^2 - t = \dfrac{s}{2}\left(1 - \tanh\mathrm{y}\right) \qquad \text{for} \quad -\beta \leqslant \tanh\mathrm{y} \leqslant +\beta \\ \\ m_t^2 - u = \dfrac{s}{2}\left(1 + \tanh\mathrm{y}\right) \end{cases} \qquad (2.1.2.8)$$
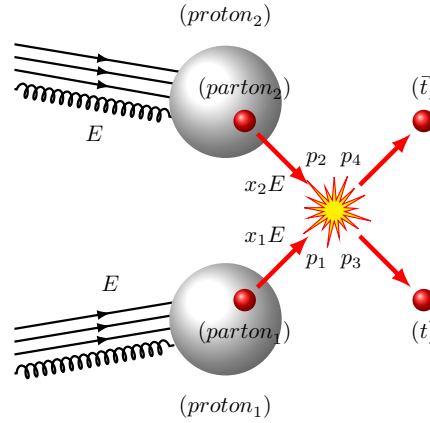
or

$$\begin{cases} s = 4E^2 \quad |\vec{p_1}| = \dfrac{\sqrt{s}}{2} \quad |\vec{p_3}| = \dfrac{\sqrt{s}}{2}\beta \\ \\ m_t^2 - t = \dfrac{s}{2}\left(1 - \beta\tanh\eta\right) \qquad \text{for} \quad -1 \leqslant \tanh\eta \leqslant +1 \\ \\ m_t^2 - u = \dfrac{s}{2}\left(1 + \beta\tanh\eta\right) \end{cases} , \qquad (2.1.2.9)$$

defining $\beta \equiv \sqrt{1 - \dfrac{4m_t^2}{s}}$.

2.1.3   Observables in boosted CMF

According to the parton model, due to the high energy collision of two hadrons, the interactions take place at the level of a single parton constituent, each of which carries with it a certain fraction of the energy of the parent particle.

Figure 2.3: Top quark-antiquark pair production by proton-proton collision

Therefore, even if the two hadrons collide with the same energy, it does not mean that this also happens for the single constituent partons. In general, the centre of mass of the collision of two partons is pushed in the direction of the most energetic parton (boosted CMF $\vec{p_2} \parallel -\vec{p_1}$). To this end, it is advisable to reformulate the previous relations involving observables according to the new kinematic scenario.

To simplify the calculations, we evaluate the case in which the masses of the incoming particles are zero or negligible compared to the energies involved. This is the case of the production of top quark pairs by gluons fusion ($gg \to t\bar{t}$) or by the annihilation of pairs of light quarks ($q\bar{q} \to t\bar{t}$).

Indicating with E the **Energy Beam** of the colliding hadrons, so that the **Invariant Mass** of the hadrons collision is $2E$, at parton level with a high level of energy collision, where the mass of partons could be considered null or negligible, for simplicity we can impose:

$$
\begin{cases}
m_1 = m_2 := 0 \\
m_3 = m_4 := m_t
\end{cases}
\begin{cases}
p_1 := (\mathrm{x}_1 E, 0, 0, +\mathrm{x}_1 E) & p_2 := (\mathrm{x}_2 E, 0, 0, -\mathrm{x}_2 E) \\
p_3 := (E_3, p_{3x}, p_{3y}, p_{3z}) & p_4 := ((\mathrm{x}_1 + \mathrm{x}_2)\,E - E_3, -p_{3x}, -p_{3y}, (\mathrm{x}_1 - \mathrm{x}_2)\,E - p_{3z})
\end{cases} ,
$$

$$(2.1.3.1)$$

where $\mathrm{x}_1, \mathrm{x}_2$, nominated as *Bjorken-x variables*, are the fractions of collision energy of each hadron being passed to the interacting partons, so it is natural to consider the following range: $0 \leqslant \mathrm{x}_1, \mathrm{x}_2 \leqslant 1$ and p_4 is obtained by the total momentum conservation principle, i.e. $p_1 + p_2 = p_3 + p_4$.

Introducing the Mandelstam variables, we can obtain the following relations:

$$\begin{cases} s \equiv (p_1 + p_2)^2 = (p_3 + p_4)^2 \\ t \equiv (p_3 - p_1)^2 \\ u = (p_2 - p_3)^2 \end{cases} \implies \begin{cases} s = 2p_1 \cdot p_2 = 4x_1 x_2 E^2 \quad x_1 x_2 E = (x_1 + x_2) E_3 - (x_1 - x_2) p_{3z} \\ m_t^2 - t = 2p_1 \cdot p_3 = 2x_1 E (E_3 - p_{3z}) \\ m_t^2 - u = 2p_2 \cdot p_3 = 2x_2 E (E_3 + p_{3z}) \end{cases}$$

$$(2.1.3.2)$$

on this way the square root of the Mandelstam variable $\sqrt{s} = \sqrt{(p_1 + p_2)^2} = 2\sqrt{x_1 x_2} E$ is a new quantity called **Invariant Mass of each parton collisions**.

Introducing new variables, m_{12} and y_{12}, instead of x_1 and x_2, by the following relations:

$$\begin{cases} x_1 := \dfrac{m_{12}}{E} e^{+y_{12}} = \dfrac{\sqrt{s}}{2E} e^{+y_{12}} \\ x_2 := \dfrac{m_{12}}{E} e^{-y_{12}} = \dfrac{\sqrt{s}}{2E} e^{-y_{12}} \end{cases} \implies \begin{cases} m_{12}^2 = x_1 x_2 E^2 = \dfrac{s}{4} \\ y_{12} = \dfrac{1}{2} \ln\left(\dfrac{x_1}{x_2}\right) = \operatorname{arctanh}\left(\dfrac{x_1 - x_2}{x_1 + x_2}\right) \end{cases} \implies$$

$$\implies \begin{cases} x_1 + x_2 = \dfrac{2m_{12}}{E} \cosh y_{12} = \dfrac{\sqrt{s}}{E} \cosh y_{12} \\ x_1 - x_2 = \dfrac{2m_{12}}{E} \sinh y_{12} = \dfrac{\sqrt{s}}{E} \sinh y_{12} \end{cases} ,$$

$$(2.1.3.3)$$

the above relation Formula 2.1.3.2 can be reformulated in the following manner:

$$\begin{cases} \dfrac{\sqrt{s}}{2} = E_3 \cosh y_{12} - p_{3z} \sinh y_{12} \\ m_t^2 - t = \sqrt{s} (E_3 - p_{3z}) (\cosh y_{12} + \sinh y_{12}) \\ m_t^2 - u = \sqrt{s} (E_3 + p_{3z}) (\cosh y_{12} - \sinh y_{12}) \end{cases} \cdot$$

$$(2.1.3.4)$$

As in the previous section, it is useful to express the quantities involved with observables that are relativistic invariants, i.e. p_T and y, or for which there may be a geometric symmetry, i.e. ϕ.

Changing the coordinates $\{p_{3x}, p_{3y}, p_{3z}\}$ with the intrinsic coordinates $\{p_T, y, \phi\}$:

$$\begin{cases} p_{3x} := p_T \cos\phi \\ p_{3y} := p_T \sin\phi \\ p_{3z} := m_T \sinh y \\ E_3 = m_T \cosh y \end{cases} \quad \text{defining} \quad m_T \equiv \sqrt{m_t^2 + p_T^2} \,,$$

$$(2.1.3.5)$$

the above relation Formula 2.1.3.4 can be reformulated in the following manner:

$$\boxed{\begin{cases} \dfrac{\sqrt{s}}{2} = \sqrt{m_t^2 + p_T^2} \cosh(y - y_{12}) \implies \dfrac{2p_T}{\sqrt{s}} = \sqrt{\beta^2 - \tanh^2(y - y_{12})} \\\\ m_t^2 - t = \dfrac{s}{2}\left(1 - \tanh(y - y_{12})\right) \qquad\qquad\qquad \text{for } -\beta \leqslant \tanh(y - y_{12}) \leqslant +\beta \\\\ m_t^2 - u = \dfrac{s}{2}\left(1 + \tanh(y - y_{12})\right) \end{cases}}$$

$$(2.1.3.6)$$

and

$$
\begin{cases}
\dfrac{\sqrt{s}}{2} = \sqrt{m_t^2 + p_T^2}\,\cosh\left(\mathrm{y} - \mathrm{y}_{12}\right) \implies \tanh\left(\mathrm{y} - \mathrm{y}_{12}\right) = \pm\sqrt{\beta^2 - \dfrac{4p_T^2}{s}} \\[4ex]
m_t^2 - t = \dfrac{s}{2}\left(1 \mp \sqrt{\beta^2 - \dfrac{4p_T^2}{s}}\right) \qquad\qquad\qquad\qquad \text{for } 0 \leqslant p_T \leqslant \dfrac{\sqrt{s}}{2}\beta \\[4ex]
m_t^2 - u = \dfrac{s}{2}\left(1 \pm \sqrt{\beta^2 - \dfrac{4p_T^2}{s}}\right)
\end{cases}
$$

$$(2.1.3.7)$$

Changing the coordinates $\{p_{3x}, p_{3y}, p_{3z}\}$ with the intrinsic coordinates $\{p_T, \eta, \phi\}$:

$$
\begin{cases}
p_{3x} := p_T \cos\phi \\[1ex]
p_{3y} := p_T \sin\phi \\[1ex]
p_{3z} := p_T \sinh\eta \\[1ex]
|\vec{p_3}| = p_T \cosh\eta
\end{cases}
\qquad \text{where} \quad E_3 = \sqrt{m_t^2 + |\vec{p_3}|^2}\,,
\qquad\qquad (2.1.3.8)
$$

the above relation Formula 2.1.3.4 can be once again reformulated in the following manner:

$$
\begin{cases}
\dfrac{\sqrt{s}}{2} = \sqrt{m_t^2 + p_T^2\cosh^2\eta}\,\cosh\mathrm{y}_{12} - p_T\sinh\eta\sinh\mathrm{y}_{12} \implies \dfrac{2p_T}{\sqrt{s}} = \text{Formula 2.1.3.11} \\[4ex]
m_t^2 - t = \dfrac{s}{2}(1 + \tanh\mathrm{y}_{12})\left(1 - \dfrac{2p_T}{\sqrt{s}}\cosh\eta\sinh\mathrm{y}_{12}(1 - \tanh\mathrm{y}_{12})\right) \qquad \text{for } -\infty < \eta < +\infty \\[4ex]
m_t^2 - u = \dfrac{s}{2}(1 - \tanh\mathrm{y}_{12})\left(1 + \dfrac{2p_T}{\sqrt{s}}\cosh\eta\sinh\mathrm{y}_{12}(1 + \tanh\mathrm{y}_{12})\right)
\end{cases}
$$

$$(2.1.3.9)$$

and

$$
\begin{cases}
\dfrac{\sqrt{s}}{2} = \sqrt{m_t^2 + p_T^2\cosh^2\eta}\,\cosh\mathrm{y}_{12} - p_T\sinh\eta\sinh\mathrm{y}_{12} \implies \sinh\eta = \text{Formula 2.1.3.12} \\[4ex]
m_t^2 - t = \dfrac{s}{2}\left(1 \mp \sqrt{\beta^2 - \dfrac{4p_T^2}{s}}\right) \qquad\qquad\qquad\qquad \text{for } 0 \leqslant p_T \leqslant \dfrac{\sqrt{s}}{2}\beta \\[4ex]
m_t^2 - u = \dfrac{s}{2}\left(1 \pm \sqrt{\beta^2 - \dfrac{4p_T^2}{s}}\right)
\end{cases}
$$

$$(2.1.3.10)$$

Here below are reported the inversion of the above equation to obtain $\frac{2p_T}{\sqrt{s}}$ and $\sinh \eta$:

$$
\frac{2p_T}{\sqrt{s}} = \begin{cases} \dfrac{\tanh \eta \tanh \mathrm{y}_{12} + \sqrt{1 - (1 - \beta^2)\dfrac{1 - \tanh^2 \eta \tanh^2 \mathrm{y}_{12}}{1 - \tanh^2 \mathrm{y}_{12}}}}{\cosh \eta \cosh \mathrm{y}_{12}(1 - \tanh^2 \eta \tanh^2 \mathrm{y}_{12})} \geq 0 \ \text{for} \ \begin{cases} \mathrm{y}_{12}\eta < 0 \ \wedge \ |\tanh \mathrm{y}_{12}| \leq \beta \\[1em] \vee \\[1em] \mathrm{y}_{12}\eta \geq 0 \ \wedge \ |\tanh \eta| \geq \sqrt{\dfrac{1 - \dfrac{\beta^2}{\tanh^2 \mathrm{y}_{12}}}{1 - \beta^2}} \end{cases} \\[5em] \dfrac{\tanh \eta \tanh \mathrm{y}_{12} - \sqrt{1 - (1 - \beta^2)\dfrac{1 - \tanh^2 \eta \tanh^2 \mathrm{y}_{12}}{1 - \tanh^2 \mathrm{y}_{12}}}}{\cosh \eta \cosh \mathrm{y}_{12}(1 - \tanh^2 \eta \tanh^2 \mathrm{y}_{12})} \geq 0 \ \text{for} \ \begin{cases} \mathrm{y}_{12}\eta > 0 \ \wedge \ |\tanh \mathrm{y}_{12}| \geq \beta \\[1em] \wedge \\[1em] |\tanh \eta| \geq \sqrt{\dfrac{1 - \dfrac{\beta^2}{\tanh^2 \mathrm{y}_{12}}}{1 - \beta^2}} \end{cases} \end{cases}
$$
(2.1.3.11)

and

$$
\sinh \eta = \frac{\sqrt{s}}{2p_T}\left(\sinh \mathrm{y}_{12} \pm \cosh \mathrm{y}_{12}\sqrt{\beta^2 - \frac{4p_T^2}{s}}\right) \quad \text{for} \quad 0 \leq p_T \leq \frac{\sqrt{s}}{2}\beta \,,
$$
(2.1.3.12)

where for all the expressions above $\beta \equiv \sqrt{1 - \dfrac{4m_t^2}{s}}$ is considered and of course $s \geq 4m_t^2$.

It is helpful for the calculation of the final observables to translate the above expressions in terms of x_1 and x_2 by using the following relations:

- $\beta^2 = 1 - \dfrac{(m_t/E)^2}{\mathrm{x}_1 \mathrm{x}_2}$,

- $\tanh \mathrm{y}_{12} = \dfrac{\mathrm{x}_1 - \mathrm{x}_2}{\mathrm{x}_1 + \mathrm{x}_2}$,

- $\tanh(\mathrm{y} - \mathrm{y}_{12}) = \dfrac{\mathrm{x}_2 e^{\mathrm{y}} - \mathrm{x}_1 e^{-\mathrm{y}}}{\mathrm{x}_2 e^{\mathrm{y}} + \mathrm{x}_1 e^{-\mathrm{y}}} \implies \dfrac{1}{\cosh^2(\mathrm{y} - \mathrm{y}_{12})} = 1 - \tanh^2(\mathrm{y} - \mathrm{y}_{12}) = \dfrac{4\mathrm{x}_1 \mathrm{x}_2}{(\mathrm{x}_2 e^{\mathrm{y}} + \mathrm{x}_1 e^{-\mathrm{y}})^2}$,

in this way the relative conditions of existence in terms of x_1 and x_2 are:

- $p_T \leq \dfrac{\sqrt{s}}{2}\beta \implies \mathrm{x}_1 \mathrm{x}_2 \geq (m_t/E)^2 + (p_T/E)^2$,

- $|\tanh(\mathrm{y} - \mathrm{y}_{12})| \leq \beta \implies \mathrm{x}_1 \mathrm{x}_2 \geq (m_t/E)\dfrac{\mathrm{x}_2 e^{\mathrm{y}} + \mathrm{x}_1 e^{-\mathrm{y}}}{2}$,

- $\mathrm{y}_{12}\eta < 0 \ \wedge \ |\tanh \mathrm{y}_{12}| \leq \beta \implies \eta \mathrm{x}_1 < \eta \mathrm{x}_2 \ \wedge \ \mathrm{x}_1 \mathrm{x}_2 \geq (m_t/E)\dfrac{\mathrm{x}_2 + \mathrm{x}_1}{2}$,

- $\mathrm{y}_{12}\eta \geq 0 \ \wedge \ |\tanh \eta| \geq \sqrt{\dfrac{1 - \dfrac{\beta^2}{\tanh^2 \mathrm{y}_{12}}}{1 - \beta^2}} \implies$

  $\implies \eta \mathrm{x}_1 \geq \eta \mathrm{x}_2 \ \wedge \ \mathrm{x}_1 \mathrm{x}_2 \geq (m_t/E)\dfrac{\mathrm{x}_2 + \mathrm{x}_1}{2}\sqrt{1 - \left(\dfrac{\mathrm{x}_2 - \mathrm{x}_1}{\mathrm{x}_2 + \mathrm{x}_1}\right)^2 \tanh^2 \eta}$,

- $\mathrm{y}_{12}\eta > 0 \ \wedge \ |\tanh \mathrm{y}_{12}| \geqslant \beta \ \wedge \ |\tanh \eta| \geqslant \sqrt{\dfrac{1 - \dfrac{\beta^2}{\tanh^2 \mathrm{y}_{12}}}{1 - \beta^2}} \quad \Longrightarrow$

$$\Longrightarrow \quad \eta \mathrm{x}_1 > \eta \mathrm{x}_2 \ \wedge \ (m_t/E)\frac{\mathrm{x}_2 + \mathrm{x}_1}{2}\sqrt{1 - \left(\frac{\mathrm{x}_2 - \mathrm{x}_1}{\mathrm{x}_2 + \mathrm{x}_1}\right)^2 \tanh^2 \eta} \leqslant \mathrm{x}_1 \mathrm{x}_2 \leqslant (m_t/E)\frac{\mathrm{x}_2 + \mathrm{x}_1}{2} \ .$$

2.2   Matrix elements

In perturbative theory, for a scattering process, it is essential to calculate its matrix element, also said scattering amplitude, and its average square, to explicitly determine observable quantities such as the cross section and decay rate. This calculation can simply be derived by applying Feynman rules, which contain the model adopted by a certain theory.

In this section, the matrix element and its quadratic mean are calculated for the main processes obtained from proton collisions at the LHC: $gg \to t\bar{t}$ (gluon fusion) and $q\bar{q} \to t\bar{t}$ (quark-antiquark annihilation), extending the SM to the SMEFT but limiting the calculations to the LO alone.
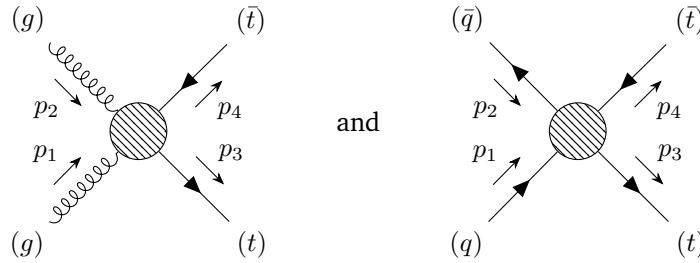
Figure 2.4: Feynman diagram of whole top quark pair production process by gluon fusion $gg \to t\bar{t}$ and by quark-antiquark annihilation $q\bar{q} \to t\bar{t}$.

2.2.1 $gg \to t\bar{t}$ in SM @ LO

For the process $gg \to t\bar{t}$, the matrix element $i\mathcal{M}$, relevant to the SM at the LO, could be calculated by the sum of the following Feynman diagrams:
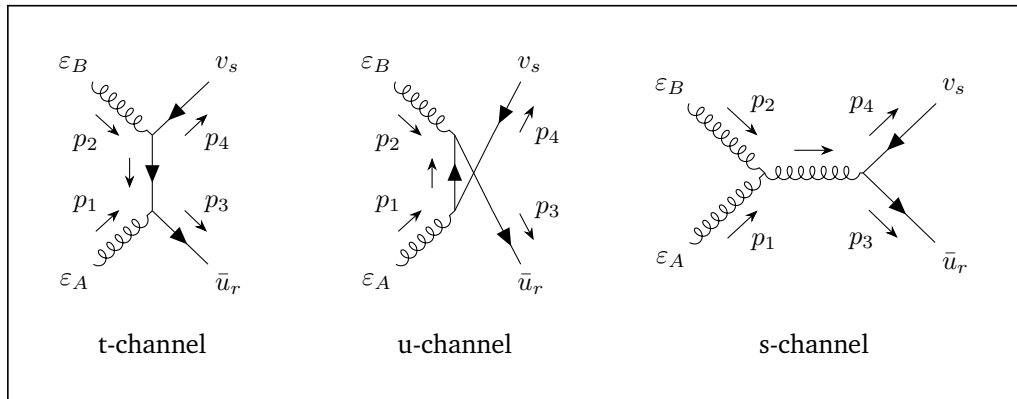
Figure 2.5: Top quark-antiquark pair production by gluons fusion in SM at LO.

directly deducible from the graphical Feynman rules.

$$\boxed{\mathcal{M} \;=\; \mathcal{M}_t \;+\; \mathcal{M}_u \;+\; \mathcal{M}_s} \tag{2.2.1.1}$$

From the above diagrams, it is easy to obtain the following matrix elements by means of Feynman Rule matching:

$$
\begin{aligned}
i\mathcal{M}_t \;&\equiv\; \bar{u}_r(p_3)\left(ig_s\tau^a\gamma^\mu\right)\varepsilon_{A\mu}(p_1)\left(i\frac{\not{p}_3-\not{p}_1+m_t}{(p_3-p_1)^2-m_t^2}\right)\varepsilon_{B\nu}(p_2)\left(ig_s\tau^b\gamma^\nu\right)v_s(p_4) \;=\;\\
&=\; -ig_s^2\tau^a\tau^b\bar{u}_r\not{\varepsilon}_A\frac{\not{p}_3-\not{p}_1+m_t}{(p_3-p_1)^2-m_t^2}\not{\varepsilon}_B v_s \;=\; ig_s^2\tau^a\tau^b\varepsilon_{A\mu}\varepsilon_{B\nu}\bar{u}_r\frac{2p_3^\mu\gamma^\nu-\gamma^\mu\not{p}_1\gamma^\nu}{2(p_1\cdot p_3)}v_s\\[2em]
i\mathcal{M}_u \;&\equiv\; \bar{u}_r(p_3)\left(ig_s\tau^b\gamma^\nu\right)\varepsilon_{B\nu}(p_2)\left(i\frac{\not{p}_3-\not{p}_2+m_t}{(p_3-p_2)^2-m_t^2}\right)\varepsilon_{A\mu}(p_1)\left(ig_s\tau^a\gamma^\mu\right)v_s(p_4) \;=\;\\
&=\; -ig_s^2\tau^b\tau^a\bar{u}_r\not{\varepsilon}_B\frac{\not{p}_3-\not{p}_2+m_t}{(p_3-p_2)^2-m_t^2}\not{\varepsilon}_A v_s \;=\; ig_s^2\tau^b\tau^a\varepsilon_{A\mu}\varepsilon_{B\nu}\bar{u}_r\frac{2p_3^\nu\gamma^\mu-\gamma^\nu\not{p}_2\gamma^\mu}{2(p_2\cdot p_3)}v_s\\[2em]
i\mathcal{M}_s \;&\equiv\; \varepsilon_{A\mu}(p_1)\left(g_s f_c^{ab}\left(g^{\mu\nu}(p_1-p_2)^\rho+g^{\nu\rho}(p_2+p_1+p_2)^\mu+g^{\rho\mu}(-p_1-p_2-p_1)^\nu\right)\right)\varepsilon_{B\nu}(p_2)\\
&\quad\left(\frac{-ig_{\rho\sigma}}{(p_1+p_2)^2}\right)\bar{u}_r(p_3)\left(ig_s\tau^c\gamma^\sigma\right)v_s(p_4) \;=\;\\
&=\; -ig_s^2[\tau^a\mid\tau^b]\bar{u}_r\frac{(\varepsilon_A\cdot\varepsilon_B)(\not{p}_1-\not{p}_2)+\varepsilon_A\cdot(p_1+2p_2)\not{\varepsilon}_B-\varepsilon_B\cdot(2p_1+p_2)\not{\varepsilon}_A}{(p_1+p_2)^2}v_s \;=\;\\
&=\; ig_s^2[\tau^a\mid\tau^b]\varepsilon_{A\mu}\varepsilon_{B\nu}\bar{u}_r\frac{g^{\mu\nu}(\not{p}_2-\not{p}_1)-2p_2^\mu\gamma^\nu+2p_1^\nu\gamma^\mu}{2(p_1\cdot p_2)}v_s
\end{aligned}
$$

$$(2.2.1.2)$$

Due to the gamma matrices anti-commutation relation (i.e., $\not{\varepsilon}_A\not{p}_3 = 2\varepsilon_A\cdot p_3 - \not{p}_3\not{\varepsilon}_A$) and due to the spin-state relation (i.e., $\bar{u}_r(\not{p}_3 - m_t) = 0$), $i\mathcal{M}_t$ has been simplified by the following equation: $\bar{u}_r\not{\varepsilon}_A(\not{p}_3-\not{p}_1+m_t) = \bar{u}_r(2\varepsilon_A\cdot p_3-\not{p}_3\not{\varepsilon}_A-\not{\varepsilon}_A\not{p}_1+m_t\not{\varepsilon}_A) = \bar{u}_r(2\varepsilon_A\cdot p_3-\not{\varepsilon}_A\not{p}_1)-\bar{u}_r(\not{p}_3-m_t)\not{\varepsilon}_A = \bar{u}_r(2\varepsilon_A\cdot p_3-\not{\varepsilon}_A\not{p}_1)$. In the same manner $i\mathcal{M}_u$ has been simplified by: $\bar{u}_r\not{\varepsilon}_B(\not{p}_3-\not{p}_2+m_t) = \bar{u}_r(2\varepsilon_B\cdot p_3-\not{\varepsilon}_B\not{p}_2)$. $i\mathcal{M}_s$ has been simplified by the colour algebra relation $[\tau^a\mid\tau^b] = if_c^{ab}\tau^c$. Furthermore, in order to preserve the colour charge and thus to save Ward's identity for QCD, which justifies the presence of the third term in $i\mathcal{M}_s$, it is necessary for all external gluons to be physical, hence transverse, i.e. $\varepsilon_A\cdot p_1 = \varepsilon_B\cdot p_2 = 0$. This concludes the above simplification for $i\mathcal{M}_s$.

As is well known, in order to determine the cross section of a process, it is necessary to calculate its relative average squared of the matrix elements: $\langle|\mathcal{M}|^2\rangle$. In the proton collision, nothing is known about the colour and polarisation of the interacting parton-gluons and similarly, nothing is known about the colour and spin of the top quarks obtained, so it is useful for the $\langle|\mathcal{M}|^2\rangle$ calculation to

average over all possible states of the incoming parton-gluons and sum over all possible states of the outgoing quarks by the following formula:

$$
\langle |\mathcal{M}|^2 \rangle \equiv \underbrace{\frac{1}{8}\frac{1}{8}\sum_{ab}}_{\substack{\text{8 colour status} \\ \text{for 2 gluons}}} \underbrace{\frac{1}{2}\frac{1}{2}\sum_{AB}}_{\substack{\text{2 polarisation status} \\ \text{for 2 gluons}}} \underbrace{\sum_{ij}}_{\substack{\text{3 colour status} \\ \text{for 2 quarks}}} \underbrace{\sum_{rs}}_{\substack{\text{2 spin status} \\ \text{for 2 quarks}}} \mathcal{M}\mathcal{M}^* =
$$

$$
= \frac{1}{256}\sum_{\substack{ab\ AB \\ ij\ rs}}\left(|\mathcal{M}_t|^2 + |\mathcal{M}_u|^2 + |\mathcal{M}_s|^2 + 2\,\mathrm{Re}[\mathcal{M}_t\mathcal{M}_u^* + \mathcal{M}_u\mathcal{M}_s^* + \mathcal{M}_s\mathcal{M}_t^*] \right)
$$

(2.2.1.3)

All colour states and all polarisation states of the incoming gluons are averaged and all final states of the outcoming top quarks are summed since the colour charge is not detectable and furthermore because we are interested in unpolarised square matrix elements.

To approach this calculation, we note that the first major simplification is to solve the sum over the polarisation of the gluons. In fact, to develop this sum, it is necessary to consider that for QCD the external gluons are transversely polarised, so the following relation should be applied:

$$
\sum_{pol}\varepsilon_{pol}^{\alpha}(p)\varepsilon_{pol}^{\beta *}(p) = -g^{\alpha\beta} + \frac{p^\alpha n^\beta + p^\beta n^\alpha}{p\cdot n} - \frac{n^2 p^\alpha p^\beta}{(p\cdot n)^2} \quad \text{where } n \text{ is an auxiliary vector.} \qquad (2.2.1.4)
$$

Defining for simplicity $\mathcal{M}^{\mu\nu}$ such that $\mathcal{M} = \varepsilon_{A\mu}\varepsilon_{B\nu}\mathcal{M}^{\mu\nu}$, it is quite easy to prove, albeit a bit long that $p_{1\mu}\mathcal{M}^{\mu\nu} = p_{2\nu}\mathcal{M}^{\mu\nu} = 0$ [19] [20], so the sum of polarisation over the two gluons could be hardly simplified in the following way:

$$
\sum_A \varepsilon_{A\mu}\varepsilon_{A\rho}^*\sum_B \varepsilon_{B\nu}\varepsilon_{B\sigma}^*\mathcal{M}^{\mu\nu}\mathcal{M}^{\rho\sigma *} = (-g_{\mu\rho})(-g_{\nu\sigma})\mathcal{M}^{\mu\nu}\mathcal{M}^{\rho\sigma *} = \mathcal{M}_{\mu\nu}\mathcal{M}^{\mu\nu *} \quad \Longrightarrow
$$

$$
\Longrightarrow \quad \langle |\mathcal{M}|^2 \rangle \equiv \frac{1}{256}\sum_{\substack{ab\ AB \\ ij\ rs}}\mathcal{M}\mathcal{M}^* = \frac{1}{256}\sum_{\substack{ab\ ij \\ rs}}\mathcal{M}_{\mu\nu}\mathcal{M}^{\mu\nu *}. \qquad (2.2.1.5)
$$

Regarding all the remaining sums, it is helpful to put in evidence the colour factors from the Dirac factors, rewriting each of three terms, $\mathcal{M}_t$, $\mathcal{M}_u$ and $\mathcal{M}_s$, in the following form:

$$
\mathcal{M}_x^{\mu\nu} = K_x C_x \frac{\bar{u}_r M_x^{\mu\nu} v_s}{D_x} \quad \text{where} \quad \mathcal{M}_x = \varepsilon_{A\mu}\varepsilon_{B\nu}\mathcal{M}_x^{\mu\nu} \quad \text{with} \quad x \in \{t, u, s\} \qquad (2.2.1.6)
$$

and where

$$
K_x : \begin{cases} K_t \equiv g_s^2 \\ K_u \equiv g_s^2 \\ K_s \equiv g_s^2 \end{cases} \qquad C_x : \begin{cases} C_t \equiv (\tau^a\tau^b)_{ij} \\ C_u \equiv (\tau^b\tau^a)_{ij} \\ C_s \equiv ([\tau^a \mid \tau^b])_{ij} \end{cases} \qquad D_x : \begin{cases} D_t \equiv 2(p_1\cdot p_3) \\ D_u \equiv 2(p_2\cdot p_3) \\ D_s \equiv 2(p_1\cdot p_2) \end{cases}
$$

$$
M_x^{\mu\nu} : \begin{cases} M_t^{\mu\nu} \equiv 2p_3^\mu\gamma^\nu - \gamma^\mu\slashed{p}_1\gamma^\nu \\ M_u^{\mu\nu} \equiv 2p_3^\nu\gamma^\mu - \gamma^\nu\slashed{p}_2\gamma^\mu \\ M_s^{\mu\nu} \equiv g^{\mu\nu}(\slashed{p}_2 - \slashed{p}_1) - 2p_2^\mu\gamma^\nu + 2p_1^\nu\gamma^\mu \end{cases} \quad ,
$$

hence:

$$\mathcal{M}^{\mu\nu} = \sum_{x \in \{t,u,s\}} K_x C_x \frac{\bar{u}_r M_x^{\mu\nu} v_s}{D_x} \quad \implies$$

$$\langle |\mathcal{M}|^2 \rangle = \frac{1}{256} \sum_{\substack{ab\ ij \\ rs}} \mathcal{M}_{\mu\nu}\mathcal{M}^{\mu\nu*} = \frac{1}{256} \sum_{xy \in \{t,u,s\}} (K_x K_y)\left(\sum_{ab\ ij} C_x C_y^*\right) \frac{\sum_{rs} (\bar{u}_r M_{x\mu\nu} v_s)(\bar{u}_r M_y^{\mu\nu} v_s)^*}{D_x D_y} .$$

$$(2.2.1.7)$$

Regarding the sum over the spin, it is useful to consider the following formula, sometimes indicated as Casimir trick: $\sum_{rs}(\bar{u}_r(p_m)Av_s(p_n))(\bar{u}_r(p_m)Bv_s(p_n))^* = \mathrm{tr}\left[A(\not{p}_n - m)B^C(\not{p}_m + m)\right]$ where $B^C \equiv \gamma^0 B^\dagger \gamma^0$, hence, the spin sum could be simplified into the following form:

$$\sum_{rs} (\bar{u}_r M_{x\mu\nu} v_s)(\bar{u}_r M_y^{\mu\nu} v_s)^* = \mathrm{tr}\left[M_{x\mu\nu}(\not{p}_4 - m)M_y^{\mu\nu C}(\not{p}_3 + m)\right] \quad \implies$$

$$\langle |\mathcal{M}|^2 \rangle = \frac{1}{256} \sum_{xy \in \{t,u,s\}} (K_x K_y)\left(\sum_{ab\ ij} C_x C_y^*\right) \frac{\mathrm{tr}\left[M_{x\mu\nu}(\not{p}_4 - m)M_y^{\mu\nu C}(\not{p}_3 + m)\right]}{D_x D_y}, \quad (2.2.1.8)$$

which ends the simplification. The remaining step is the colour factor calculation and trace calculation.

Remembering the following properties regarding gamma matrices and traces Appendix B and using the kinematic relations Formula 2.1.1.4, we can obtain for $\mathrm{tr}\left[M_{x\mu\nu}(\not{p}_4 - m)M_y^{\mu\nu C}(\not{p}_3 + m)\right]$:

$$\begin{cases}
\mathrm{tr}\left[M_{t\mu\nu}(\not{p}_4 - m_t)M_t^{\mu\nu C}(\not{p}_3 + m_t)\right] &=& 32\left((p_1 \cdot p_3)(p_2 \cdot p_3) + m_t^2(p_1 \cdot p_3) - m_t^4\right) & \text{for} & |\mathcal{M}_t|^2 \\[2mm]
\mathrm{tr}\left[M_{u\mu\nu}(\not{p}_4 - m_t)M_u^{\mu\nu C}(\not{p}_3 + m_t)\right] &=& 32\left((p_1 \cdot p_3)(p_2 \cdot p_3) + m_t^2(p_2 \cdot p_3) - m_t^4\right) & \text{for} & |\mathcal{M}_u|^2 \\[2mm]
\mathrm{tr}\left[M_{s\mu\nu}(\not{p}_4 - m_t)M_s^{\mu\nu C}(\not{p}_3 + m_t)\right] &=& 64\,(p_1 \cdot p_3)(p_2 \cdot p_3) & \text{for} & |\mathcal{M}_s|^2 \\[2mm]
\mathrm{tr}\left[M_{t\mu\nu}(\not{p}_4 - m_t)M_u^{\mu\nu C}(\not{p}_3 + m_t)\right] &=& 16m_t^2(p_1 \cdot p_2 - 2m_t^2) & \text{for} & 2\,\mathrm{Re}\left[\mathcal{M}_t\mathcal{M}_u^*\right] \\[2mm]
\mathrm{tr}\left[M_{u\mu\nu}(\not{p}_4 - m_t)M_s^{\mu\nu C}(\not{p}_3 + m_t)\right] &=& 16\left(m_t^2(p_2 \cdot p_3 - p_1 \cdot p_3) + 2(p_1 \cdot p_3)(p_2 \cdot p_3)\right) & \text{for} & 2\,\mathrm{Re}\left[\mathcal{M}_u\mathcal{M}_s^*\right] \\[2mm]
\mathrm{tr}\left[M_{s\mu\nu}(\not{p}_4 - m_t)M_t^{\mu\nu C}(\not{p}_3 + m_t)\right] &=& 16\left(m_t^2(p_2 \cdot p_3 - p_1 \cdot p_3) - 2(p_1 \cdot p_3)(p_2 \cdot p_3)\right) & \text{for} & 2\,\mathrm{Re}\left[\mathcal{M}_s\mathcal{M}_t^*\right]
\end{cases}$$

$$(2.2.1.9)$$

For the colour factors, taking into account the conjugation of Gell-Man matrices and the Fierz identity for $SU(3)$: $(\tau^a)_{ij}^* = (\tau^a)_{ij}^T = (\tau^a)_{ji}$ and $(\tau^a)_{ij}(\tau_a)_{kl} \equiv \sum_a (\tau^a)_{ij}(\tau^a)_{kl} = \frac{1}{2}\left(\delta_{il}\delta_{jk} - \frac{1}{3}\delta_{ij}\delta_{kl}\right)$ we obtain for $\sum_{ab\ ij} C_x C_y^*$:

$$\begin{cases}
\sum_{ab\ ij} C_t C_t^* = \sum_{ab}\sum_{ij} \left(\tau^a\tau^b\right)_{ij}\left(\tau^a\tau^b\right)_{ij}^* &=& \frac{16}{3} & \text{for} & |\mathcal{M}_t|^2 \\[2mm]
\sum_{ab\ ij} C_u C_u^* = \sum_{ab}\sum_{ij} \left(\tau^b\tau^a\right)_{ij}\left(\tau^b\tau^a\right)_{ij}^* &=& \frac{16}{3} & \text{for} & |\mathcal{M}_u|^2 \\[2mm]
\sum_{ab\ ij} C_s C_s^* = \sum_{ab}\sum_{ij} \left[\tau^a \mid \tau^b\right]_{ij}\left[\tau^a \mid \tau^b\right]_{ij}^* &=& 12 & \text{for} & |\mathcal{M}_s|^2 \\[2mm]
\sum_{ab\ ij} C_t C_u^* = \sum_{ab}\sum_{ij} \left(\tau^a\tau^b\right)_{ij}\left(\tau^b\tau^a\right)_{ij}^* &=& -\frac{2}{3} & \text{for} & \mathrm{Re}\left[\mathcal{M}_t\mathcal{M}_u^*\right] \\[2mm]
\sum_{ab\ ij} C_u C_s^* = \sum_{ab}\sum_{ij} \left(\tau^b\tau^a\right)_{ij}\left[\tau^a \mid \tau^b\right]_{ij}^* &=& -6 & \text{for} & \mathrm{Re}\left[\mathcal{M}_u\mathcal{M}_s^*\right] \\[2mm]
\sum_{ab\ ij} C_s C_t^* = \sum_{ab}\sum_{ij} \left[\tau^a \mid \tau^b\right]_{ij}\left(\tau^a\tau^b\right)_{ij}^* &=& 6 & \text{for} & \mathrm{Re}\left[\mathcal{M}_s\mathcal{M}_t^*\right]
\end{cases}$$

$$(2.2.1.10)$$

Composing all the above results in terms of Mandelstam variables we have:

$$
\begin{cases}
\dfrac{1}{256} \sum_{\substack{ab\ AB \\ ij\ rs}} |\mathcal{M}_t|^2 & = \quad g_s^4 \dfrac{tu - m_t^2(3t + u) - m_t^4}{6(m_t^2 - t)^2} \\[2.5ex]
\dfrac{1}{256} \sum_{\substack{ab\ AB \\ ij\ rs}} |\mathcal{M}_u|^2 & = \quad g_s^4 \dfrac{tu - m_t^2(3u + t) - m_t^4}{6(m_t^2 - u)^2} \\[2.5ex]
\dfrac{1}{256} \sum_{\substack{ab\ AB \\ ij\ rs}} |\mathcal{M}_s|^2 & = \quad g_s^4 \dfrac{3(m_t^2 - t)(m_t^2 - u)}{4s^2} \\[2.5ex]
\dfrac{1}{256} \sum_{\substack{ab\ AB \\ ij\ rs}} 2\,\mathrm{Re}[\mathcal{M}_t \mathcal{M}_u^*] & = \quad g_s^4 \dfrac{m_t^2(4m_t^2 - s)}{24(m_t^2 - t)(m_t^2 - u)} \\[2.5ex]
\dfrac{1}{256} \sum_{\substack{ab\ AB \\ ij\ rs}} 2\,\mathrm{Re}[\mathcal{M}_u \mathcal{M}_s^*] & = \quad g_s^4 \dfrac{-3(tu - 2m_t^2 u + m_t^4)}{8s(m_t^2 - u)} \\[2.5ex]
\dfrac{1}{256} \sum_{\substack{ab\ AB \\ ij\ rs}} 2\,\mathrm{Re}[\mathcal{M}_s \mathcal{M}_t^*] & = \quad g_s^4 \dfrac{-3(tu - 2m_t^2 t + m_t^4)}{8s(m_t^2 - t)}
\end{cases}
\qquad , \tag{2.2.1.11}
$$

where Formula 2.1.1.4 for Mandelstam variables is used. This last result is perfectly in line with the result reported in [17] for the SM part.

The sum of the above six terms, reducing the Mandelstam variables, gives the final result of $\langle |\mathcal{M}|^2 \rangle$, ending the calculation:

Average Squared of Matrix Element for $gg \to t\bar{t}$ in SM @ LO

$$
\langle |\mathcal{M}|^2 \rangle = \frac{g_s^4 \left(9m_t^4 - 9m_t^2 s + 4s^2 - 9tu\right) \left(-2m_t^8 - m_t^4\left(3s^2 - 4tu\right) + m_t^2 s^3 + tu\left(s^2 - 2tu\right)\right)}{24s^2 \left(m_t^2 - t\right)^2 \left(m_t^2 - u\right)^2}
$$

$$\tag{2.2.1.12}$$

An alternative method to solve the average square matrix element calculation is to include in the polarisation sum also the longitudinal gluons, in this way, the following formula could be considered:

$$
\sum_A \varepsilon_{A\mu} \varepsilon_{A\rho}^* \sum_B \varepsilon_{B\nu} \varepsilon_{B\sigma}^* = (-g_{\mu\rho})(-g_{\nu\sigma}) \, ,
$$

but, it is necessary to include virtual fields named ghosts to obtain the right final result.

To check the correctness of the last result here obtained $\langle |\mathcal{M}|^2 \rangle$, it could be implemented an automatic calculation by FEYNCALC 9.3.1 [21], a WOLFRAM MATHEMATICA package [22] for symbolic evaluation of Feynman diagrams and algebraic calculations in quantum field theory and elementary particle physics. Here below a sample of code to calculate a quick result:

MATHEMATICA Wolfram Notebook (.nb) file listing

```
In[1]:=    ClearAll[a,b,mt,gs];
           ClearAll[p1,p2,p3,p4,t,u,s];
           FCClearScalarProducts[];

           (*Matrix element form*)

           matrixElement1 = (*t-channel*)
               gs^2*SUNT[a,b]*
               SpinorUBar[p3,mt].GS[Polarization[p1]].
               ((GS[p3-p1]+mt)/(2*ScalarProduct[p1,p3])).
               GS[Polarization[p2]].SpinorV[p4,mt];
           matrixElement2 = (*u-channel*)
               gs^2*SUNT[b,a]*
               SpinorUBar[p3,mt].GS[Polarization[p2]].
               ((GS[p3-p2]+mt)/(2*ScalarProduct[p2,p3])).
               GS[Polarization[p1]].SpinorV[p4,mt];
           matrixElement3 = (*s-channel*)
               gs^2*(SUNT[a,b]-SUNT[b,a])*
               SpinorUBar[p3,mt].
               ((ScalarProduct[Polarization[p1],Polarization[p2]]*GS[p2-p1]-
               ScalarProduct[Polarization[p1],p1+2*p2]*GS[Polarization[p2]]+
               ScalarProduct[Polarization[p2],p2+2*p1]*GS[Polarization[p1]])/
               (2*ScalarProduct[p1,p2])).
               SpinorV[p4,mt];
           matrixElement = matrixElement1+matrixElement2+matrixElement3;

           (*Calculation of the average of squared matrix element*)

           ScalarProduct[p1,p1] = 0;
           ScalarProduct[p2,p2] = 0;
           ScalarProduct[p3,p3] = mt^2;
           ScalarProduct[p4,p4] = mt^2;
           ScalarProduct[p1,p4] = ScalarProduct[p2,p3];
           ScalarProduct[p2,p4] = ScalarProduct[p1,p3];
           ScalarProduct[p3,p4] = ScalarProduct[p1,p2]-mt^2;

           SUNN = 3;
           SetOptions[Polarization,Transversality->True];
           n1 = p2;
           n2 = p1;

           matrixElement.ComplexConjugate[matrixElement];
           %//SUNTrace;
           %//FermionSpinSum;
```

```
%//DiracSimplify;
%//DoPolarizationSums[#,p1,n1]&;
%//DoPolarizationSums[#,p2,n2]&;
%*(1/256);
%//ScalarProductExpand;
%//FullSimplify;
%/.{ScalarProduct[p1,p3]->(mt^2-t)/2,
    ScalarProduct[p2,p3]->(mt^2-u)/2,
    ScalarProduct[p1,p2]->(2*mt^2-t-u)/2};
%//FullSimplify;
%/.{u^2->(2*mt^2-s)^2-2*t*u-t^2};
%//FullSimplify;
%/.{(t+u)->(2*mt^2-s)};
%//FullSimplify
```

$$\text{Out[1]}= \frac{gs^4(9mt^4-9mt^2s+4s^2-9tu)(-2mt^8+mt^4(4tu-3s^2)+mt^2s^3+tu(s^2-2tu))}{24s^2(mt^2-t)^2(mt^2-u)^2}$$

perfectly in line with result $\langle|\mathcal{M}|^2\rangle$.

2.2.2 $q\bar{q} \to t\bar{t}$ in SM @ LO

Similar to $gg \to t\bar{t}$, for the process $q\bar{q} \to t\bar{t}$, $i\mathcal{M}$, relevant to the SM at the LO, is the sum of the following contributions:
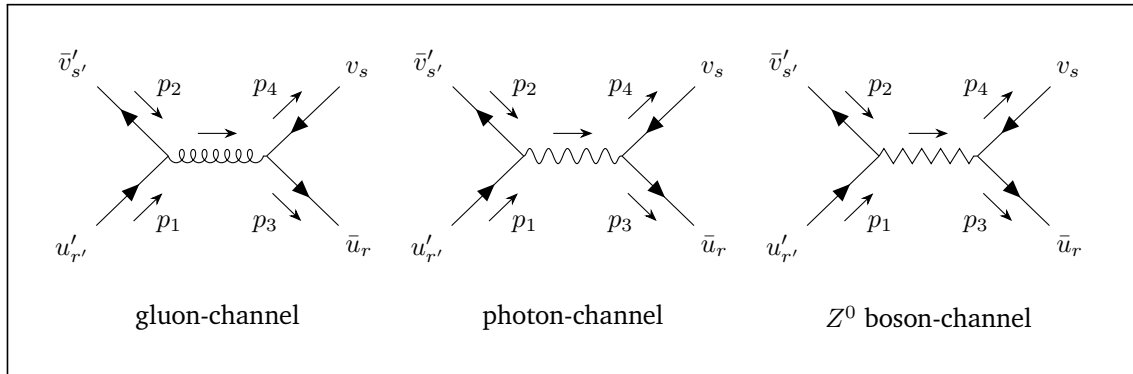
Figure 2.6: Top quark-antiquark pair production by quarks annihilation in SM at LO.

directly deducible from Feynman's graphical rules, but in this case also using EW interactions and not just QCD interactions.

$$\boxed{\mathcal{M} = \mathcal{M}_g + \mathcal{M}_\gamma + \mathcal{M}_Z} \qquad (2.2.2.1)$$

From the above diagrams it is easy to obtain by the correspondence Feynman Rules, the following

matrices:

$$
\begin{aligned}
i\mathcal{M}_g &\equiv \bar{v}'_{s'}(p_2)\left(ig_s\gamma^\mu(\tau^a)_{ij}\right)u'_{r'}(p_1)\left(\frac{-ig_{\mu\nu}\delta_{ab}}{(p_1+p_2)^2}\right)\bar{u}_r(p_3)\left(ig_s\gamma^\nu(\tau^b)_{kl}\right)v_s(p_4) \quad = \\[2mm]
&= i\frac{1}{2}g_s^2\left(\delta_{il}\delta_{jk}-\frac{1}{3}\delta_{ij}\delta_{kl}\right)\frac{(\bar{v}'_{s'}\gamma^\mu u'_{r'})(\bar{u}_r\gamma_\mu v_s)}{2(p_1\cdot p_2)+2m_q^2} \\[4mm]
i\mathcal{M}_\gamma &\equiv \bar{v}'_{s'}(p_2)\left(ig_e\mathcal{Q}(q)\gamma^\mu\delta_{ij}\right)u'_{r'}(p_1)\left(\frac{-ig_{\mu\nu}}{(p_1+p_2)^2}\right)\bar{u}_r(p_3)\left(i\frac{2}{3}g_e\gamma^\nu\delta_{kl}\right)v_s(p_4) \quad = \\[2mm]
&= i\frac{2}{3}g_e^2\mathcal{Q}(q)\delta_{ij}\delta_{kl}\frac{(\bar{v}'_{s'}\gamma^\mu u'_{r'})(\bar{u}_r\gamma_\mu v_s)}{2(p_1\cdot p_2)+2m_q^2} \\[4mm]
i\mathcal{M}_Z &\equiv \bar{v}'_{s'}(p_2)\left(i\frac{g_Z}{2}\gamma^\mu(\mathcal{Q}_V(q)-\mathcal{Q}_A(q)\gamma^5)\delta_{ij}\right)u'_{r'}(p_1)\left(\frac{-ig_{\mu\nu}}{(p_1+p_2)^2-m_Z^2}\right) \\[2mm]
&\quad \bar{u}_r(p_3)\left(i\frac{g_Z}{2}\gamma^\nu(\mathcal{Q}_V(t)-\mathcal{Q}_A(t)\gamma^5)\delta_{kl}\right)v_s(p_4) \quad = \\[2mm]
&= i\frac{1}{4}g_Z^2\delta_{ij}\delta_{kl}\frac{\left(\bar{v}'_{s'}\gamma^\mu(\mathcal{Q}_V(q)-\mathcal{Q}_A(q)\gamma^5)u'_{r'}\right)\left(\bar{u}_r\gamma_\mu(\mathcal{Q}_V(t)-\mathcal{Q}_A(t)\gamma^5)v_s\right)}{2(p_1\cdot p_2)+2m_q^2-m_Z^2}
\end{aligned}
$$

(2.2.2.2)

To simplify the colour algebra for $i\mathcal{M}_g$ the following relation is used: $(\tau^a)_{ij}(\tau_a)_{kl}=\frac{1}{2}\left(\delta_{il}\delta_{jk}-\frac{1}{3}\delta_{ij}\delta_{kl}\right)$. For $i\mathcal{M}_\gamma$, it is understood that $\mathcal{Q}(q)=+2/3$, if q is an up quark or $\mathcal{Q}(q)=-1/3$, if q is a down quark. While for $i\mathcal{M}_Z$, it is understood that $g_Z\equiv g_e/(\cos\theta_W\sin\theta_W)=2\,m_Z/v$ and $\mathcal{Q}_V(q)=+1/2-4/3\sin^2\theta_W$ and $\mathcal{Q}_A(q)=+1/2$, if q is an up quark or $\mathcal{Q}_V(q)=-1/2+2/3\sin^2\theta_W$ and $\mathcal{Q}_A(q)=-1/2$, if q is a down quark. Of course, $\mathcal{Q}_V(t)=+1/2-4/3\sin^2\theta_W$ and $\mathcal{Q}_A(t)=+1/2$.

As is well known, in order to determine the cross section of a process, it is necessary to calculate its relative average squared of the matrix elements: $\langle|\mathcal{M}|^2\rangle$. In the proton collision, nothing is known about the colour of the interacting parton-quarks and similarly, nothing is known about the colour and spin of the top quarks obtained, so it is useful for the $\langle|\mathcal{M}|^2\rangle$ calculation to average over all possible states of the incoming parton-quarks and sum over all possible states of the outgoing quarks by the following formula:

$$
\begin{aligned}
\langle|\mathcal{M}|^2\rangle &\equiv \underbrace{\frac{1}{3}\frac{1}{3}\sum_{ij}}_{\substack{\text{3 color status}\\\text{for 2 in quarks}}}\underbrace{\frac{1}{2}\frac{1}{2}\sum_{r's'}}_{\substack{\text{2 spin status}\\\text{for 2 in quarks}}}\underbrace{\sum_{kl}}_{\substack{\text{3 color status}\\\text{for 2 out quarks}}}\underbrace{\sum_{rs}}_{\substack{\text{2 spin status}\\\text{for 2 out quarks}}}\mathcal{M}\mathcal{M}^* \quad = \\[2mm]
&= \frac{1}{36}\sum_{\substack{ij\ r's'\\kl\ rs}}\left(|\mathcal{M}_g|^2+|\mathcal{M}_\gamma|^2+|\mathcal{M}_Z|^2+2\operatorname{Re}[\mathcal{M}_g\mathcal{M}_\gamma^*+\mathcal{M}_\gamma\mathcal{M}_Z^*+\mathcal{M}_Z\mathcal{M}_g^*]\right)
\end{aligned}
$$

(2.2.2.3)

All colour states and all polarisation states of the incoming gluons are averaged and all final states of the outcoming top quarks are summed since the colour charge is not detectable and furthermore because we are interested in unpolarised square matrix elements.

Also in this case, it is helpful to put in evidence the colour factors from the Dirac factors rewriting each of three terms, $\mathcal{M}_g$, $\mathcal{M}_\gamma$ and $\mathcal{M}_Z$, in the following form:

$$\mathcal{M}_x \quad = \quad K_x C_x \frac{\left(\bar{v}'_{s'} M'^{\,\mu}_x u'_{r'}\right)\left(\bar{u}_r M_{x\,\mu} v_s\right)}{D_x} \quad \text{with} \quad x \in \{g, \gamma, Z\} \tag{2.2.2.4}$$

and where

$$K_x : \begin{cases} K_g \equiv g_s^2 \\ K_\gamma \equiv \frac{2}{3}\mathcal{Q}(q)e^2 \\ K_Z \equiv \frac{1}{4}g_Z^2 \end{cases} \quad C_x : \begin{cases} C_g \equiv \frac{1}{2}\left(\delta_{il}\delta_{jk} - \frac{1}{3}\delta_{ij}\delta_{kl}\right) \\ C_\gamma \equiv \delta_{ij}\delta_{kl} \\ C_Z \equiv \delta_{ij}\delta_{kl} \end{cases} \quad D_x : \begin{cases} D_g \equiv 2(p_1 \cdot p_2) + 2m_q^2 \\ D_\gamma \equiv 2(p_1 \cdot p_2) + 2m_q^2 \\ D_Z \equiv 2(p_1 \cdot p_2) + 2m_q^2 - m_Z^2 \end{cases}$$

$$M'^{\,\mu}_x : \begin{cases} M'^{\,\mu}_g \equiv \gamma^\mu \\ M'^{\,\mu}_\gamma \equiv \gamma^\mu \\ M'^{\,\mu}_Z \equiv \gamma^\mu \left(\mathcal{Q}_V(q) - \mathcal{Q}_A(q)\gamma^5\right) \end{cases} \quad M_x{}^\mu : \begin{cases} M_{g\,\mu} \equiv \gamma_\mu \\ M_{\gamma\,\mu} \equiv \gamma_\mu \\ M_{Z\,\mu} \equiv \gamma_\mu \left(\mathcal{Q}_V(t) - \mathcal{Q}_A(t)\gamma^5\right) \end{cases} \quad ,$$

hence,

$$\left\langle |\mathcal{M}|^2 \right\rangle = \frac{1}{36} \sum_{xy} \left(K_x K_y\right) \left(\sum_{ij\ kl} C_x C_y\right) \frac{\sum_{r's'\ rs} (\bar{v}'_{s'} M'^{\,\mu}_x u'_{r'})(\bar{u}_r M_{x\,\mu} v_s)(\bar{v}'_{s'} M'^{\,\nu}_y u'_{r'})^*(\bar{u}_r M_{y_\nu} v_s)^*}{D_x D_y} \ .$$

$$\tag{2.2.2.5}$$

Regarding the sum over the spin, it is useful to consider the following formula, sometimes indicated as Casimir trick: $\sum_{rs}\left(\bar{v}_s(q)Au_r(q)\right)\left(\bar{v}_s(q)Bu_r(p)\right)^* = \text{tr}\left[A(\slashed{p}+m)B^C(\slashed{q}-m)\right]$ and $\sum_{rs}\left(\bar{u}_r(p)Av_s(q)\right)\left(\bar{u}_r(p)Bv_s(q)\right)^* = \text{tr}\left[A(\slashed{q}-m)B^C(\slashed{p}+m)\right]$ where $B^C \equiv \gamma^0 B^\dagger \gamma^0$, hence, the polarisation sum and the spin sum could be simplified into the following form:

$$\sum_{r's'}(\bar{v}'_{s'} M'^{\,\mu}_x u'_{r'})(\bar{v}'_{s'} M'^{\,\nu}_y u'_{r'})^* = \text{tr}\left[M'^{\,\mu}_x(\slashed{p}_1 + m_q)M'^{\,\nu\,C}_y(\slashed{p}_2 - m_q)\right] \quad \text{and}$$

$$\sum_{rs}(\bar{u}_r M_{x\,\mu} v_s)(\bar{u}_r M_{y_\nu} v_s)^* = \text{tr}\left[M_{x\,\mu}(\slashed{p}_4 - m_t)M_{y_\nu}{}^C(\slashed{p}_3 + m_t)\right] \quad \implies$$

$$\left\langle |\mathcal{M}|^2 \right\rangle = \frac{1}{36} \sum_{xy} \left(K_x K_y\right)\left(\sum_{ij\ kl} C_x C_y\right)$$

$$\frac{\text{tr}\left[M'^{\,\mu}_x(\slashed{p}_1 + m_q)M'^{\,\nu\,C}_y(\slashed{p}_2 - m_q)\right] \text{tr}\left[M_{x\,\mu}(\slashed{p}_4 - m_t)M_{y_\nu}{}^C(\slashed{p}_3 + m_t)\right]}{D_x D_y} \ , \tag{2.2.2.6}$$

which ends the simplification. The remaining step is the colour factor calculation and trace calculation.

Remembering the properties regarding gamma matrices and traces Appendix B and using the kinematic relations Formula 2.1.1.5, we can obtain for $\text{tr}\left[M'^{\,\mu}_x(\slashed{p}_1 + m_q)M'^{\,\nu\,C}_y(\slashed{p}_2 - m_q)\right] \text{tr}\left[M_{x\mu}(\slashed{p}_4 - m_t)M^C_{y\nu}(\slashed{p}_3 + m_t)\right]$:

$$
\begin{cases}
\begin{aligned}
&\operatorname{tr}\left[M_g'^{\mu}(\slashed{p}_1+m_q)M_g'^{\nu\,C}(\slashed{p}_2-m_q)\right]\operatorname{tr}\left[M_{g\,\mu}(\slashed{p}_4-m_t)M_{g\,\nu}{}^C(\slashed{p}_3+m_t)\right] = \\
&= 32\left((p_1\cdot p_3)^2 + (p_2\cdot p_3)^2 + (m_q^2+m_t^2)\big((p_1\cdot p_2)+m_q^2\big)\right) \qquad\qquad \text{for} \quad |\mathcal{M}_g|^2
\end{aligned} \\[2mm]

\begin{aligned}
&\operatorname{tr}\left[M_\gamma'^{\mu}(\slashed{p}_1+m_q)M_\gamma'^{\nu\,C}(\slashed{p}_2-m_q)\right]\operatorname{tr}\left[M_{\gamma\,\mu}(\slashed{p}_4-m_t)M_{\gamma\,\nu}{}^C(\slashed{p}_3+m_t)\right] = \\
&= 32\left((p_1\cdot p_3)^2 + (p_2\cdot p_3)^2 + (m_q^2+m_t^2)\big((p_1\cdot p_2)+m_q^2\big)\right) \qquad\qquad \text{for} \quad |\mathcal{M}_\gamma|^2
\end{aligned} \\[2mm]

\begin{aligned}
&\operatorname{tr}\left[M_Z'^{\mu}(\slashed{p}_1+m_q)M_Z'^{\nu\,C}(\slashed{p}_2-m_q)\right]\operatorname{tr}\left[M_{Z\,\mu}(\slashed{p}_4-m_t)M_{Z\,\nu}{}^C(\slashed{p}_3+m_t)\right] = \\
&= 32\Big(\big((\mathcal{Q}_V^2(q)+\mathcal{Q}_A^2(q))(\mathcal{Q}_V^2(t)+\mathcal{Q}_A^2(t))-4\mathcal{Q}_V(q)\mathcal{Q}_A(q)\mathcal{Q}_V(t)\mathcal{Q}_A(t)\big)(p_1\cdot p_3)^2+ \\
&\quad + \big((\mathcal{Q}_V^2(q)+\mathcal{Q}_A^2(q))(\mathcal{Q}_V^2(t)+\mathcal{Q}_A^2(t))+4\mathcal{Q}_V(q)\mathcal{Q}_A(q)\mathcal{Q}_V(t)\mathcal{Q}_A(t)\big)(p_2\cdot p_3)^2+ \\
&\quad + \big(m_t^2(\mathcal{Q}_V^2(q)+\mathcal{Q}_A^2(q))(\mathcal{Q}_V^2(t)-\mathcal{Q}_A^2(t))+m_q^2(\mathcal{Q}_V^2(q)-\mathcal{Q}_A^2(q))(\mathcal{Q}_V^2(t)+\mathcal{Q}_A^2(t))\big)(p_1\cdot p_2)+ \\
&\quad + m_q^2(\mathcal{Q}_V^2(q)-\mathcal{Q}_A^2(q))\big(m_q^2(\mathcal{Q}_V^2(t)+\mathcal{Q}_A^2(t))+m_t^2(\mathcal{Q}_V^2(t)-3\mathcal{Q}_A^2(t))\big)\Big) \qquad \text{for} \quad |\mathcal{M}_Z|^2
\end{aligned} \\[2mm]

\begin{aligned}
&\operatorname{tr}\left[M_g'^{\mu}(\slashed{p}_1+m_q)M_\gamma'^{\nu\,C}(\slashed{p}_2-m_q)\right]\operatorname{tr}\left[M_{g\,\mu}(\slashed{p}_4-m_t)M_{\gamma\,\nu}{}^C(\slashed{p}_3+m_t)\right] = \\
&= 32\left((p_1\cdot p_3)^2 + (p_2\cdot p_3)^2 + (m_q^2+m_t^2)\big((p_1\cdot p_2)+m_q^2\big)\right) \qquad\qquad \text{for} \quad 2\operatorname{Re}\left[\mathcal{M}_g\mathcal{M}_\gamma^*\right]
\end{aligned} \\[2mm]

\begin{aligned}
&\operatorname{tr}\left[M_\gamma'^{\mu}(\slashed{p}_1+m_q)M_Z'^{\nu\,C}(\slashed{p}_2-m_q)\right]\operatorname{tr}\left[M_{\gamma\,\mu}(\slashed{p}_4-m_t)M_{Z\,\nu}{}^C(\slashed{p}_3+m_t)\right] = \\
&= 32\Big((\mathcal{Q}_V(q)\mathcal{Q}_V(t)-\mathcal{Q}_A(q)\mathcal{Q}_A(t))(p_1\cdot p_3)^2 + (\mathcal{Q}_V(q)\mathcal{Q}_V(t)+\mathcal{Q}_A(q)\mathcal{Q}_A(t))(p_2\cdot p_3)^2+ \\
&\quad + \mathcal{Q}_V(q)\mathcal{Q}_V(t)(m_q^2+m_t^2)\big((p_1\cdot p_2)+m_q^2\big)\Big) \qquad\qquad \text{for} \quad 2\operatorname{Re}\left[\mathcal{M}_\gamma\mathcal{M}_Z^*\right]
\end{aligned} \\[2mm]

\begin{aligned}
&\operatorname{tr}\left[M_Z'^{\mu}(\slashed{p}_1+m_q)M_g'^{\nu\,C}(\slashed{p}_2-m_q)\right]\operatorname{tr}\left[M_{Z\,\mu}(\slashed{p}_4-m_t)M_{g\,\nu}{}^C(\slashed{p}_3+m_t)\right] = \\
&= 32\Big((\mathcal{Q}_V(q)\mathcal{Q}_V(t)-\mathcal{Q}_A(q)\mathcal{Q}_A(t))(p_1\cdot p_3)^2 + (\mathcal{Q}_V(q)\mathcal{Q}_V(t)+\mathcal{Q}_A(q)\mathcal{Q}_A(t))(p_2\cdot p_3)^2+ \\
&\quad + \mathcal{Q}_V(q)\mathcal{Q}_V(t)(m_q^2+m_t^2)\big((p_1\cdot p_2)+m_q^2\big)\Big) \qquad\qquad \text{for} \quad 2\operatorname{Re}\left[\mathcal{M}_Z\mathcal{M}_g^*\right]
\end{aligned}
\end{cases}
\tag{2.2.2.7}
$$

For the colour factors, we obtain for $\sum_{ij\;kl} C_x C_y$:

$$
\begin{cases}
\sum_{ij\;kl} C_g C_g = \sum_{ij}\sum_{kl}\frac{1}{2}\left(\delta_{il}\delta_{jk}-\frac{1}{3}\delta_{ij}\delta_{kl}\right)^2 & = \;2 \;\; \text{for} \;\; |\mathcal{M}_g|^2 \\[2mm]
\sum_{ij\;kl} C_\gamma C_\gamma = \sum_{ij}\sum_{kl}\delta_{ij}^2\delta_{kl}^2 & = \;9 \;\; \text{for} \;\; |\mathcal{M}_\gamma|^2 \\[2mm]
\sum_{ij\;kl} C_Z C_Z = \sum_{ij}\sum_{kl}\delta_{ij}^2\delta_{kl}^2 & = \;9 \;\; \text{for} \;\; |\mathcal{M}_Z|^2 \\[2mm]
\sum_{ij\;kl} C_g C_\gamma = \sum_{ij}\sum_{kl}\frac{1}{2}\left(\delta_{il}\delta_{jk}-\frac{1}{3}\delta_{ij}\delta_{kl}\right)\delta_{ij}\delta_{kl} & = \;0 \;\; \text{for} \;\; 2\operatorname{Re}\left[\mathcal{M}_g\mathcal{M}_\gamma^*\right] \\[2mm]
\sum_{ij\;kl} C_\gamma C_Z = \sum_{ij}\sum_{kl}\delta_{ij}\delta_{kl}\delta_{ij}\delta_{kl} & = \;9 \;\; \text{for} \;\; 2\operatorname{Re}\left[\mathcal{M}_\gamma\mathcal{M}_Z^*\right] \\[2mm]
\sum_{ij\;kl} C_Z C_g = \sum_{ij}\sum_{kl}\delta_{ij}\delta_{kl}\frac{1}{2}\left(\delta_{il}\delta_{jk}-\frac{1}{3}\delta_{ij}\delta_{kl}\right) & = \;0 \;\; \text{for} \;\; 2\operatorname{Re}\left[\mathcal{M}_Z\mathcal{M}_g^*\right]
\end{cases}
\tag{2.2.2.8}
$$

Composing all the above results in terms of Mandelstam variables we have:

$$\begin{cases}
\dfrac{1}{36}\sum_{\substack{ij\ r's'\\kl\ rs}}|\mathcal{M}_g|^2 & = & \dfrac{4g_s^4\left(s^2+2m_t^4-2tu\right)}{9s^2}\\[3em]

\dfrac{1}{36}\sum_{\substack{ij\ r's'\\kl\ rs}}|\mathcal{M}_\gamma|^2 & = & \dfrac{8g_e^4\mathcal{Q}^2(q)\left(s^2+2m_t^4-2tu\right)}{9s^2}\\[3em]

\dfrac{1}{36}\sum_{\substack{ij\ r's'\\kl\ rs}}|\mathcal{M}_Z|^2 & = & \dfrac{g_Z^4\begin{pmatrix}\left(\mathcal{Q}_A^2(q)+\mathcal{Q}_V^2(q)\right)\left(\mathcal{Q}_A^2(t)+\mathcal{Q}_V^2(t)\right)\left(s^2+2m_t^4-2tu\right)+\\-4\left(\mathcal{Q}_A^2(q)+\mathcal{Q}_V^2(q)\right)\mathcal{Q}_A^2(t)m_t^2 s+\\+4\mathcal{Q}_A(q)\mathcal{Q}_A(t)\mathcal{Q}_V(q)\mathcal{Q}_V(t)s\left(t-u\right)\end{pmatrix}}{8\left(m_Z^2-s\right)^2}\\[3em]

\dfrac{1}{36}\sum_{\substack{ij\ r's'\\kl\ rs}}2\,\mathrm{Re}[\mathcal{M}_g\mathcal{M}_\gamma^*] & = & 0\\[2em]

\dfrac{1}{36}\sum_{\substack{ij\ r's'\\kl\ rs}}2\,\mathrm{Re}[\mathcal{M}_\gamma\mathcal{M}_Z^*] & = & \dfrac{2g_e^2 g_Z^2\mathcal{Q}(q)\begin{pmatrix}-\mathcal{Q}_V(q)\mathcal{Q}_V(t)\left(s^2+2m_t^4-2tu\right)+\\-\mathcal{Q}_A(q)\mathcal{Q}_A(t)s(t-u)\end{pmatrix}}{3s\left(m_Z^2-s\right)}\\[3em]

\dfrac{1}{36}\sum_{\substack{ij\ r's'\\kl\ rs}}2\,\mathrm{Re}[\mathcal{M}_Z\mathcal{M}_g^*] & = & 0
\end{cases}$$

$$(2.2.2.9)$$

where Formula 2.1.1.5 for Mandelstam variables is used and it is also applied the following relation:

$$\begin{cases}
\left(m_q^2+m_t^2-t\right)^2+\left(m_q^2+m_t^2-u\right)^2 & = & s^2+2\left(m_q^2+m_t^2\right)^2-2tu-2\left(m_q^2+m_t^2\right)s\\
\left(m_q^2+m_t^2-t\right)^2-\left(m_q^2+m_t^2-u\right)^2 & = & -s\left(t-u\right)
\end{cases},$$

but imposing $m_q=0$ for simplicity.

To obtain $\left\langle|\mathcal{M}|^2\right\rangle$ it is sufficient to sum all the above six terms and this ends the calculation.

Average Squared of Matrix Element for $q\bar{q}\to t\bar{t}$ in SM @ LO

$$\begin{aligned}
\left\langle|\mathcal{M}|^2\right\rangle & = & \dfrac{\left(4g_s^4+8g_e^4\mathcal{Q}^2(q)\right)\left(s^2+2m_t^4-2tu\right)}{9s^2}+\\
& & +\dfrac{g_Z^4\left(\left(\mathcal{Q}_A^2(q)+\mathcal{Q}_V^2(q)\right)\left(\mathcal{Q}_A^2(t)+\mathcal{Q}_V^2(t)\right)\left(s^2+2m_t^4-2tu\right)\right)}{8\left(m_Z^2-s\right)^2}+\\
& & +\dfrac{g_Z^4\left(-4\left(\mathcal{Q}_A^2(q)+\mathcal{Q}_V^2(q)\right)\mathcal{Q}_A^2(t)m_t^2 s+4\mathcal{Q}_A(q)\mathcal{Q}_A(t)\mathcal{Q}_V(q)\mathcal{Q}_V(t)s\left(t-u\right)\right)}{8\left(m_Z^2-s\right)^2}+\\
& & +\dfrac{2g_e^2 g_Z^2\mathcal{Q}(q)\left(-\mathcal{Q}_V(q)\mathcal{Q}_V(t)\left(s^2+2m_t^4-2tu\right)-\mathcal{Q}_A(q)\mathcal{Q}_A(t)s(t-u)\right)}{3s\left(m_Z^2-s\right)}
\end{aligned}$$

$$(2.2.2.10)$$

Also, this result, similar to the $gg\to t\bar{t}$ process in SM at LO, could be verified by a simple code of FeynCalc 9.3.1 [21].

2.2.3 $gg \to t\bar{t}$ in 6-dimension SMEFT @ LO

To extend the $gg \to t\bar{t}$ process with the 6-dimensional SMEFT approach, it is necessary to introduce the operators: $\mathcal{O}_{tG}$, $\mathcal{O}_G$ and $\mathcal{O}_{\phi G}$. These operators lead to new Feynman rules, as shown in Section A.4, through which diagrams are obtained as depicted in Figure 2.7. The calculation of the matrix element $i\mathcal{M}$ must then be conducted by adding these diagrams to those already obtained by considering the effects of the SM alone.
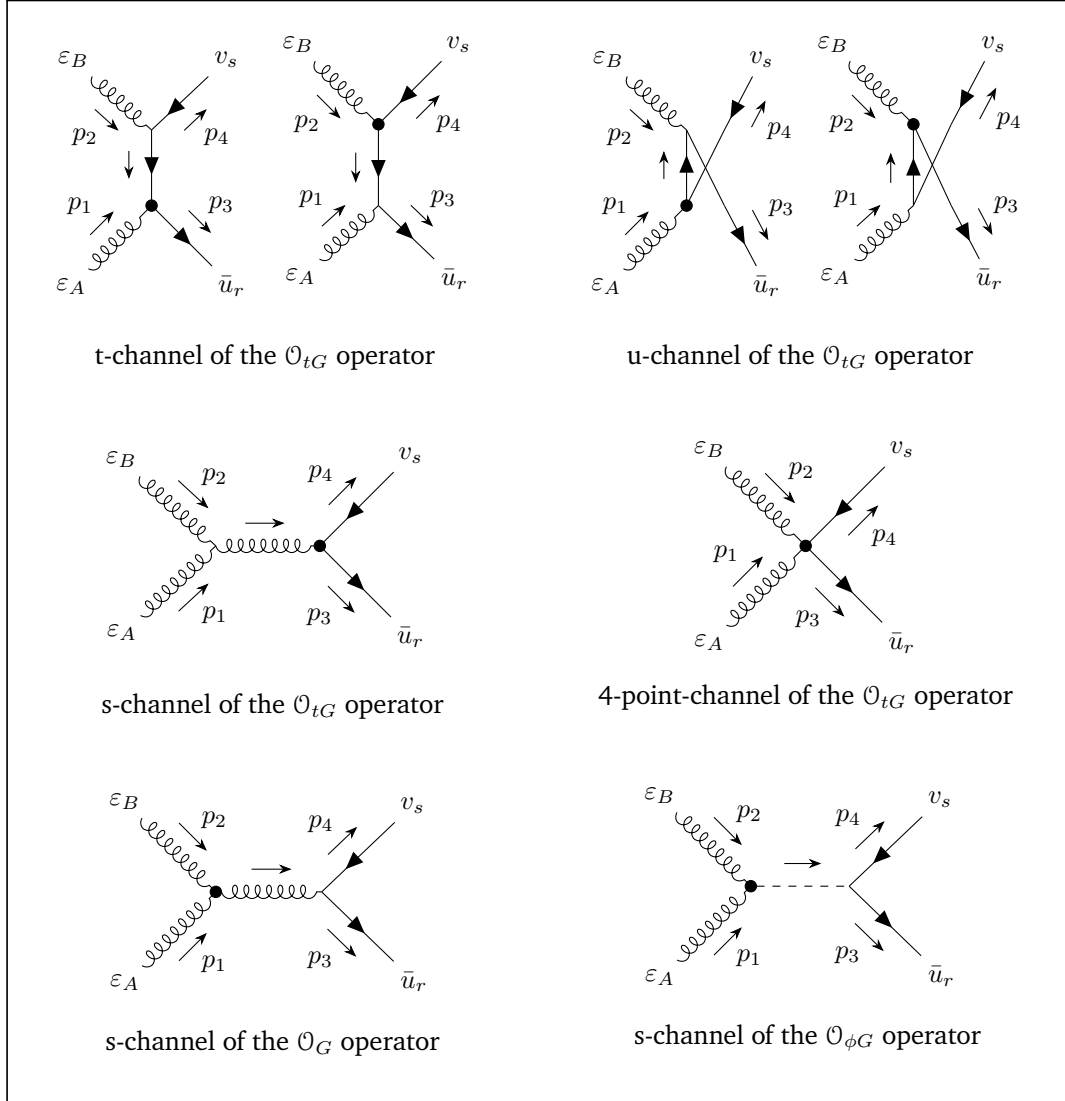
Figure 2.7: Top quark-antiquark pair production by gluons fusion in 6-dim. SMEFT at LO.

$$\mathcal{M}(\mathcal{L}_{\text{SMEFT}}) = \left(\mathcal{M}_t + \mathcal{M}_u + \mathcal{M}_s\right)(\mathcal{L}_{\text{SM}}) + \left(\mathcal{M}_t + \mathcal{M}_u + \mathcal{M}_s + \mathcal{M}_{ggt\bar{t}}\right)(\mathcal{O}_{tG}) + \\ + \left(\mathcal{M}_s\right)(\mathcal{O}_G) + \left(\mathcal{M}_s\right)(\mathcal{O}_{\phi G})$$

$$(2.2.3.1)$$

From the above diagrams, it is easy to obtain the following matrix elements by means of Feynman

Rule matching:

$$
\begin{aligned}
i\mathcal{M}_t(\mathcal{O}_{tG}) \equiv\ & \bar{u}_r(p_3)\left(-i\sqrt{2}\frac{vC_{tG}}{\Lambda^2}\tau^a[\gamma^\mu \mid \slashed{p}_1]\right)\varepsilon_{A\mu}(p_1)\left(i\frac{\slashed{p}_3-\slashed{p}_1+m_t}{(p_3-p_1)^2-m_t^2}\right)\varepsilon_{B\nu}(p_2)\left(-ig_s\tau^b\gamma^\nu\right)v_s(p_4)\ + \\
+\ & \bar{u}_r(p_3)\left(-ig_s\tau^a\gamma^\mu\right)\varepsilon_{A\mu}(p_1)\left(i\frac{\slashed{p}_3-\slashed{p}_1+m_t}{(p_3-p_1)^2-m_t^2}\right)\varepsilon_{B\nu}(p_2)\left(-i\sqrt{2}\frac{vC_{tG}}{\Lambda^2}\tau^b[\gamma^\nu \mid \slashed{p}_2]\right)v_s(p_4)\ = \\[4pt]
=\ & -i\sqrt{2}g_s\frac{vC_{tG}}{\Lambda^2}\tau^a\tau^b\bar{u}_r\left([\slashed{\varepsilon}_A \mid \slashed{p}_1]\frac{\slashed{p}_2-\slashed{p}_4+m_t}{(p_2-p_4)^2-m_t^2}\slashed{\varepsilon}_B - \slashed{\varepsilon}_A\frac{\slashed{p}_3-\slashed{p}_1+m_t}{(p_3-p_1)^2-m_t^2}[\slashed{p}_2 \mid \slashed{\varepsilon}_B]\right)v_s\ = \\[4pt]
=\ & i\sqrt{2}g_s\frac{vC_{tG}}{\Lambda^2}\tau^a\tau^b\varepsilon_{A\mu}\varepsilon_{B\nu}\bar{u}_r\left(\frac{[\gamma^\mu \mid \slashed{p}_1](2p_4^\nu+\gamma^\nu\slashed{p}_2)}{2(p_2\cdot p_4)} + \frac{(2p_3^\mu+\slashed{p}_1\gamma^\mu)[\slashed{p}_2 \mid \gamma^\nu]}{2(p_1\cdot p_3)}\right)v_s
\end{aligned}
$$

$$
\begin{aligned}
i\mathcal{M}_u(\mathcal{O}_{tG}) \equiv\ & \bar{u}_r(p_3)\left(-i\sqrt{2}\frac{vC_{tG}}{\Lambda^2}\tau^b[\gamma^\nu \mid \slashed{p}_2]\right)\varepsilon_{B\nu}(p_2)\left(i\frac{\slashed{p}_3-\slashed{p}_2+m_t}{(p_3-p_2)^2-m_t^2}\right)\varepsilon_{A\mu}(p_1)\left(-ig_s\tau^a\gamma^\mu\right)v_s(p_4)\ + \\
+\ & \bar{u}_r(p_3)\left(-ig_s\tau^b\gamma^\nu\right)\varepsilon_{B\nu}(p_2)\left(i\frac{\slashed{p}_3-\slashed{p}_2+m_t}{(p_3-p_2)^2-m_t^2}\right)\varepsilon_{A\mu}(p_1)\left(-i\sqrt{2}\frac{vC_{tG}}{\Lambda^2}\tau^a[\gamma^\mu \mid \slashed{p}_1]\right)v_s(p_4)\ = \\[4pt]
=\ & -i\sqrt{2}g_s\frac{vC_{tG}}{\Lambda^2}\tau^b\tau^a\bar{u}_r\left([\slashed{\varepsilon}_B \mid \slashed{p}_2]\frac{\slashed{p}_1-\slashed{p}_4+m_t}{(p_1-p_4)^2-m_t^2}\slashed{\varepsilon}_A - \slashed{\varepsilon}_B\frac{\slashed{p}_3-\slashed{p}_2+m_t}{(p_3-p_2)^2-m_t^2}[\slashed{p}_2 \mid \slashed{\varepsilon}_A]\right)v_s\ = \\[4pt]
=\ & i\sqrt{2}g_s\frac{vC_{tG}}{\Lambda^2}\tau^b\tau^a\varepsilon_{A\mu}\varepsilon_{B\nu}\bar{u}_r\left(\frac{[\gamma^\nu \mid \slashed{p}_2](2p_4^\mu+\gamma^\mu\slashed{p}_1)}{2(p_1\cdot p_4)} + \frac{(2p_3^\nu+\slashed{p}_2\gamma^\nu)[\slashed{p}_1 \mid \gamma^\mu]}{2(p_2\cdot p_3)}\right)v_s
\end{aligned}
$$

$$
\begin{aligned}
i\mathcal{M}_s(\mathcal{O}_{tG}) \equiv\ & \varepsilon_{A\mu}(p_1)\left(-g_sf_c^{ab}\left(g^{\mu\nu}(p_1-p_2)^\rho + g^{\nu\rho}(p_2+p_1+p_2)^\mu + g^{\rho\mu}(-p_1-p_2-p_1)^\nu\right)\right)\varepsilon_{B\nu}(p_2) \\
& \left(\frac{-ig_{\rho\sigma}}{(p_1+p_2)^2}\right)\bar{u}_r(p_3)\left(-i\sqrt{2}\frac{vC_{tG}}{\Lambda^2}\tau^c[\gamma^\sigma \mid \slashed{p}_1+\slashed{p}_2]\right)v_s(p_4)\ = \\[4pt]
=\ & i\sqrt{2}g_s\frac{vC_{tG}}{\Lambda^2}[\tau^a \mid \tau^b] \\
& \bar{u}_r\frac{2(\varepsilon_A\cdot\varepsilon_B)[\slashed{p}_1 \mid \slashed{p}_2] + \varepsilon_A\cdot(p_1+2p_2)[\slashed{\varepsilon}_B \mid \slashed{p}_1+\slashed{p}_2] - \varepsilon_B\cdot(2p_1+p_2)[\slashed{\varepsilon}_A \mid \slashed{p}_1+\slashed{p}_2]}{(p_1+p_2)^2}v_s\ = \\[4pt]
=\ & i\sqrt{2}g_s\frac{vC_{tG}}{\Lambda^2}[\tau^a \mid \tau^b]\varepsilon_{A\mu}\varepsilon_{B\nu}\bar{u}_r\frac{g^{\mu\nu}[\slashed{p}_1 \mid \slashed{p}_2] + p_2^\mu[\gamma^\nu \mid \slashed{p}_1+\slashed{p}_2] - p_1^\nu[\gamma^\mu \mid \slashed{p}_1+\slashed{p}_2]}{p_1\cdot p_2}v_s
\end{aligned}
$$

$$
\begin{aligned}
i\mathcal{M}_{ggt\bar{t}}(\mathcal{O}_{tG}) \equiv\ & \varepsilon_{A\mu}(p_1)\bar{u}_r(p_3)\left(i\sqrt{2}g_s\frac{vC_{tG}}{\Lambda^2}[\tau^a \mid \tau^b][\gamma^\mu \mid \gamma^\nu]\right)v_s(p_4)\varepsilon_{B\nu}(p_2)\ = \\[4pt]
=\ & i\sqrt{2}g_s\frac{vC_{tG}}{\Lambda^2}[\tau^a \mid \tau^b]\bar{u}_r[\slashed{\varepsilon}_A \mid \slashed{\varepsilon}_B]v_s\ = \\[4pt]
=\ & i\sqrt{2}g_s\frac{vC_{tG}}{\Lambda^2}[\tau^a \mid \tau^b]\varepsilon_{A\mu}\varepsilon_{B\nu}\bar{u}_r[\gamma^\mu \mid \gamma^\nu]v_s
\end{aligned}
$$

<div align="right">(2.2.3.2)</div>

$$
\begin{aligned}
i\mathcal{M}_s(\mathcal{O}_G) &\equiv \varepsilon_{A\mu}(p_1)\varepsilon_{B\nu}(p_2)\Bigg(-6\frac{C_G}{\Lambda^2}f^{abc}\bigg((p_1+p_2)^\mu p_1^\nu p_2^\rho - p_2^\mu(p_1+p_2)^\nu p_1^\rho+ \\
&\qquad + g^{\mu\nu}\Big(p_1^\rho\big(p_2\cdot(p_1+p_2)\big) - p_2^\rho\big(p_1\cdot(p_1+p_2)\big)\Big)+ \\
&\qquad + g^{\nu\rho}\Big(p_2^\mu\big(p_1\cdot(p_1+p_2)\big) - (p_1+p_2)^\mu\big(p_1\cdot p_2\big)\Big)+ \\
&\qquad + g^{\rho\mu}\Big((p_1+p_2)^\nu(p_1\cdot p_2) - p_1^\nu\big(p_2\cdot(p_1+p_2)\big)\Big)\bigg)\Bigg) \\
&\quad \bigg(i\frac{-g_{\rho\sigma}}{(p_1+p_2)^2}\delta_{cd}\bigg)\bar{u}_r(p_3)\Big(ig_s\gamma^\sigma\tau^d\Big)v_s(p_4) = \\
&= i6g_s\frac{C_G}{\Lambda^2}[\tau^a\mid\tau^b]\bar{u}_r\bigg(\Big((\varepsilon_A\cdot(p_1+p_2)\big)(\varepsilon_B\cdot p_1)\slashed{p}_2 - (\varepsilon_A\cdot p_2)\big(\varepsilon_B\cdot(p_1+p_2)\big)\slashed{p}_1+ \\
&\qquad + (\varepsilon_A\cdot\varepsilon_B)\slashed{p}_1\big(p_2\cdot(p_1+p_2)\big) - (\varepsilon_A\cdot\varepsilon_B)\slashed{p}_2\big(p_1\cdot(p_1+p_2)\big)+ \\
&\qquad + \slashed{\varepsilon}_B(\varepsilon_A\cdot p_2)\big(p_1\cdot(p_1+p_2)\big) - \slashed{\varepsilon}_B\big(\varepsilon_A\cdot(p_1+p_2)\big)(p_1\cdot p_2)+ \\
&\qquad + \slashed{\varepsilon}_A\big(\varepsilon_B\cdot(p_1+p_2)\big)(p_1\cdot p_2) - \slashed{\varepsilon}_A(\varepsilon_B\cdot p_1)\big(p_2\cdot(p_1+p_2)\big)\bigg)v_s \\
&\quad \frac{1}{(p_1+p_2)^2} = \\
&= i3g_s\frac{C_G}{\Lambda^2}[\tau^a\mid\tau^b]\varepsilon_{A\mu}\varepsilon_{B\nu}\frac{p_2^\mu p_1^\nu - g^{\mu\nu}(p_1\cdot p_2)}{p_1\cdot p_2}\bar{u}_r(\slashed{p}_1 - \slashed{p}_2)v_s
\end{aligned}
$$

(2.2.3.3)

$$
\begin{aligned}
i\mathcal{M}_s(\mathcal{O}_{\phi G}) &\equiv \varepsilon_{A\mu}(p_1)\varepsilon_{B\nu}(p_2)\bigg(2i\frac{vC_{\phi G}}{\Lambda^2}\delta^{ab}\Big(p_1^\nu p_2^\mu - (p_1\cdot p_2)g^{\mu\nu}\Big)\bigg)\bigg(\frac{i}{(p_1+p_2)^2 - m_H^2}\bigg)\bigg(-i\frac{m_t}{v}\delta_{ij}\bigg) \\
&\quad \bar{u}_r(p_3)v_s(p_4) = \\
&= 2i\frac{m_t C_{\phi G}}{\Lambda^2}\delta^{ab}\delta_{ij}\frac{(\varepsilon_A\cdot p_2)(\varepsilon_B\cdot p_1) - (\varepsilon_A\cdot\varepsilon_B)(p_1\cdot p_2)}{2(p_1\cdot p_2) - m_H^2}\bar{u}_r v_s = \\
&= 2i\frac{m_t C_{\phi G}}{\Lambda^2}\delta^{ab}\delta_{ij}\varepsilon_{A\mu}\varepsilon_{B\nu}\frac{p_2^\mu p_1^\nu - g^{\mu\nu}(p_1\cdot p_2)}{2(p_1\cdot p_2) - m_H^2}\bar{u}_r v_s
\end{aligned}
$$

(2.2.3.4)

Similar to the SM case Subsection 2.2.1, verifying that also for the matrix elements related to the SMEFT operators are gauge invariant (i.e. $p_{1\mu}\mathcal{M}^{\mu\nu} = p_{2\nu}\mathcal{M}^{\mu\nu} = 0$), hence the total average square matrix could be calculated by the same SM Formula 2.2.1.7.

After tedious calculations involving colour algebra and Dirac algebra, we can obtain:

> **Average Squared of Matrix Element for $gg \to t\bar{t}$ in SMEFT @ LO**
>
> $$\langle |\mathcal{M}|^2 \rangle = \underbrace{\frac{g_s^4(9m_t^4 - 9m_t^2 s + 4s^2 - 9tu)(-2m_t^8 - m_t^4(3s^2 - 4tu) + m_t^2 s^3 + tu(s^2 - 2tu))}{24s^2(m_t^2 - t)^2(m_t^2 - u)^2}}_{\left\langle \left|\mathcal{M}(\mathcal{L}_{\text{SM}})\right|^2 \right\rangle} +$$
>
> $$+ \underbrace{\frac{\sqrt{2}C_{tG}g_s^3 m_t v(9m_t^4 - 9m_t^2 s + 4s^2 - 9tu)}{3(m_t^2 - t)(m_t^2 - u)\Lambda^2}}_{\left\langle 2\,\text{Re}[\mathcal{M}(\mathcal{L}_{\text{SM}})\mathcal{M}(\mathcal{O}_{tG})^*]\right\rangle} + \underbrace{\frac{9C_G g_s^3 m_t^2 (t-u)^2}{8(m_t^2 - t)(m_t^2 - u)\Lambda^2}}_{\left\langle 2\,\text{Re}[\mathcal{M}(\mathcal{L}_{\text{SM}})\mathcal{M}(\mathcal{O}_G)^*]\right\rangle} +$$
>
> $$+ \underbrace{\frac{C_{\phi G}g_s^2 m_t^2 s^2(s - 4m_t^2)}{8(m_H^2 - s)(m_t^2 - t)(m_t^2 - u)\Lambda^2}}_{\left\langle 2\,\text{Re}[\mathcal{M}(\mathcal{L}_{\text{SM}})\mathcal{M}(\mathcal{O}_{\phi G})^*]\right\rangle} +$$
>
> $$+ \underbrace{\frac{C_{tG}^2 g_s^2 v^2\begin{pmatrix}-18m_t^8 + 36m_t^6 s - 3m_t^4(11s^2 - 12tu)+ \\ + m_t^2 s(23s^2 - 36tu) + 3tu(5s^2 - 6tu)\end{pmatrix}}{3s(m_t^2 - t)(m_t^2 - u)\Lambda^4}}_{\left\langle \left|\mathcal{M}(\mathcal{O}_{tG})\right|^2\right\rangle} +$$
>
> $$+ \underbrace{\frac{9C_{tG}C_G g_s^2 m_t v s}{\sqrt{2}\Lambda^4}}_{\left\langle 2\,\text{Re}[\mathcal{M}(\mathcal{O}_{tG})\mathcal{M}(\mathcal{O}_G)^*]\right\rangle} + \underbrace{\frac{C_{tG}C_{\phi G}g_s m_t v s^2(m_t^4 - tu)}{\sqrt{2}(m_H^2 - s)(m_t^2 - t)(m_t^2 - u)\Lambda^4}}_{\left\langle 2\,\text{Re}[\mathcal{M}(\mathcal{O}_{tG})\mathcal{M}(\mathcal{O}_{\phi G})^*]\right\rangle} +$$
>
> $$+ \underbrace{\frac{27C_G^2 g_s^2(m_t^2 - t)(m_t^2 - u)}{4\Lambda^4}}_{\left\langle \left|\mathcal{M}(\mathcal{O}_G)\right|^2\right\rangle} + \underbrace{0}_{\left\langle 2\,\text{Re}[\mathcal{M}(\mathcal{O}_G)\mathcal{M}(\mathcal{O}_{\phi G})^*]\right\rangle} + \underbrace{\frac{3C_{\phi G}^2 m_t^2 s^2(s - 4m_t^2)}{8(m_H^2 - s)^2\Lambda^4}}_{\left\langle \left|\mathcal{M}(\mathcal{O}_{\phi G})\right|^2\right\rangle}$$
>
> $$(2.2.3.5)$$

Also, this calculation could be easily resolved by the use of MATHEMATICA with FEYNCALC 9.3.1 package [21].

2.2.4 $q\bar{q} \to t\bar{t}$ in 6-dimension SMEFT @ LO

To extend the $q\bar{q} \to t\bar{t}$ process with the 6-dimensional SMEFT approach, it is necessary to introduce in addition to the previous operator $\mathcal{O}_{tG}$, and also the 4-quarks operator $\mathcal{O}_{q\bar{q}t\bar{t}}$. These operators lead to new Feynman rules, as shown in Section A.4, through which diagrams are obtained as depicted in Figure 2.8. The calculation of the matrix element $i\mathcal{M}$ must then be conducted by adding these diagrams to those already obtained by considering the effects of the SM alone.
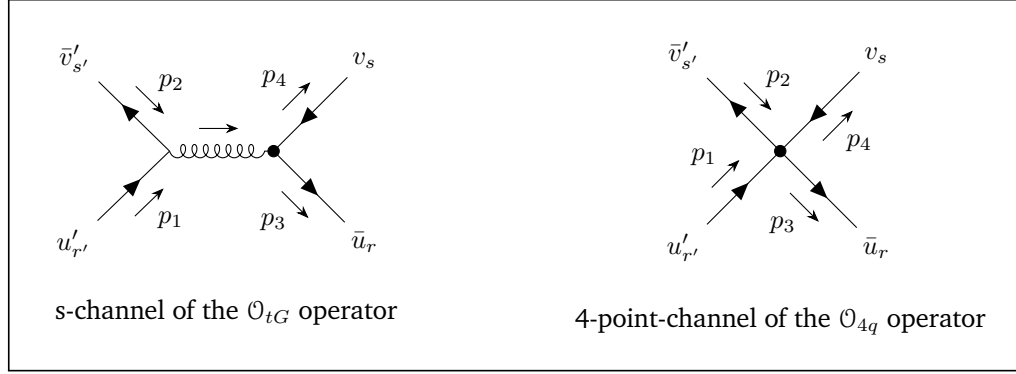
Figure 2.8: Top quark-antiquark pair production by quark annihilation in 6-dim. SMEFT at LO.

The 6-dim. SMEFT matrix element for the present process is given by:

$$
\mathcal{M}(\mathcal{L}_{\text{SMEFT}}) \quad \equiv \quad \left(\mathcal{M}_g + \mathcal{M}_\gamma + \mathcal{M}_Z \right)(\mathcal{L}_{\text{SM}}) + \left(\mathcal{M}_s \right)(\mathcal{O}_{tG}) + \left(\mathcal{M}_{q\bar{q}t\bar{t}} \right)(\mathcal{O}_{4\,\text{quarks}})
$$

$$(2.2.4.1)$$

Where q is mainly an up-quark (u) or a down-quark (d) in a proton-proton collision.

$$
\begin{aligned}
i\mathcal{M}_s(\mathcal{O}_{tG}) &\equiv \bar{v}'_{s'}(p_2)\left(ig_s\gamma^\mu(\tau^a)_{ij}\right)u'_{r'}(p_1)\left(\frac{-ig_{\mu\nu}\delta_{ab}}{(p_1+p_2)^2}\right)\bar{u}_r(p_3)\left(-i\sqrt{2}\frac{vC_{tG}}{\Lambda^2}(\tau^b)_{kl}[\gamma^\nu \mid \not{p}_1 + \not{p}_2]\right)v_s(p_4) = \\
&= -i\frac{\sqrt{2}}{2}g_s\frac{vC_{tG}}{\Lambda^2}\left(\delta_{il}\delta_{jk} - \frac{1}{3}\delta_{ij}\delta_{kl}\right)\frac{(\bar{v}'_{s'}\gamma^\mu u'_{r'})(\bar{u}_r[\gamma_\mu \mid \not{p}_1 + \not{p}_2]v_s)}{2(p_1\cdot p_2) + 2m_q^2}
\end{aligned}
$$

$$(2.2.4.2)$$

$$
\begin{aligned}
\left.\begin{array}{l}
i\mathcal{M}_{u\bar{u}t\bar{t}}(\mathcal{O}_{4\,\text{quarks}}) \\[4pt]
i\mathcal{M}_{d\bar{d}t\bar{t}}(\mathcal{O}_{4\,\text{quarks}})
\end{array}\right\} &\equiv i\left(\frac{C_{Qq}^{(8,1)} \pm C_{Qq}^{(8,3)}}{\Lambda^2}(\tau^a)_{ij}(\tau_a)_{kl} + \frac{C_{Qq}^{(1,1)} \pm C_{Qq}^{(1,3)}}{\Lambda^2}\delta_{ij}\delta_{kl}\right) \\[6pt]
&\qquad\qquad \bar{v}'_{s'}(p_2)(\gamma^6\gamma^\mu\gamma^7)u'_{r'}(p_1)\bar{u}_r(p_3)(\gamma^6\gamma_\mu\gamma^7)v_s(p_4) + \\[6pt]
&+ i\left(\frac{C_{tu/d}^{(8)}}{\Lambda^2}(\tau^a)_{ij}(\tau_a)_{kl} + \frac{C_{tu/d}^{(1)}}{\Lambda^2}\delta_{ij}\delta_{kl}\right)\bar{v}'_{s'}(p_2)(\gamma^7\gamma^\mu\gamma^6)u'_{r'}(p_1)\bar{u}_r(p_3)(\gamma^7\gamma_\mu\gamma^6)v_s(p_4) + \\[6pt]
&+ i\left(\frac{C_{Qu/d}^{(8)}}{\Lambda^2}(\tau^a)_{ij}(\tau_a)_{kl} + \frac{C_{Qu/d}^{(1)}}{\Lambda^2}\delta_{ij}\delta_{kl}\right)\bar{v}'_{s'}(p_2)(\gamma^7\gamma^\mu\gamma^6)u'_{r'}(p_1)\bar{u}_r(p_3)(\gamma^6\gamma_\mu\gamma^7)v_s(p_4) + \\[6pt]
&+ i\left(\frac{C_{tq}^{(8)}}{\Lambda^2}(\tau^a)_{ij}(\tau_a)_{kl} + \frac{C_{tq}^{(1)}}{\Lambda^2}\delta_{ij}\delta_{kl}\right)\bar{v}'_{s'}(p_2)(\gamma^6\gamma^\mu\gamma^7)u'_{r'}(p_1)\bar{u}_r(p_3)(\gamma^7\gamma_\mu\gamma^6)v_s(p_4)
\end{aligned}
$$

$$(2.2.4.3)$$

Similar to the SM case Subsection 2.2.1, the total average square matrix could be calculated by the same SM Formula 2.2.2.6.

After tedious calculations involving colour algebra and Dirac algebra, we can obtain:

Average Squared of Matrix Element for $q\bar{q} \to t\bar{t}$ in SMEFT @ LO

$$\langle |\mathcal{M}|^2 \rangle = \underbrace{\frac{4\left(g_s^4 + 2g_e^4 Q^2(q)\right)\left(s^2 + 2m_t^4 - 2tu\right)}{9s^2}}_{\left\langle \left|\mathcal{M}(\mathcal{L}_{\text{SM}})\right|^2\right\rangle} +$$

$$+ \underbrace{\frac{-2g_e^2 g_Z^2 Q(q)Q_V(q)Q_V(t)(s^2 + 2m_t^4 - 2tu) - 2g_e^2 g_Z^2 Q(q)Q_A(q)Q_A(t)s(t - u)}{3s\left(m_Z^2 - s\right)}}_{\left\langle \left|\mathcal{M}(\mathcal{L}_{\text{SM}})\right|^2\right\rangle} +$$

$$+ \underbrace{\frac{\begin{aligned}&g_Z^4\left(Q_A^2(q) + Q_V^2(q)\right)\left(Q_A^2(t) + Q_V^2(t)\right)\left(s^2 + 2m_t^4 - 2tu\right)+\\&+4g_Z^4 Q_A(q)Q_A(t)Q_V(q)Q_V(t)s(t-u) - 4g_Z^4\left(Q_A^2(q) + Q_V^2(q)\right)Q_A^2(t)m_t^2 s\end{aligned}}{8\left(m_Z^2 - s\right)^2}}_{\left\langle \left|\mathcal{M}(\mathcal{L}_{\text{SM}})\right|^2\right\rangle} +$$

$$+ \underbrace{\frac{32\sqrt{2}C_{tG}g_s^3 m_t v}{9\Lambda^2}}_{\left\langle 2\,\text{Re}[\mathcal{M}(\mathcal{L}_{\text{SM}})\mathcal{M}(\mathcal{O}_{tG})^*]\right\rangle} + \underbrace{\frac{c_{(g+\gamma)q\bar{q}t\bar{t}1}(s^2 + 2m_t^4 - 2tu) + c_{(g+\gamma)q\bar{q}t\bar{t}2}s(t - u)}{9s\Lambda^2}}_{\left\langle 2\,\text{Re}[\mathcal{M}(\mathcal{L}_{\text{SM}})\mathcal{M}(\mathcal{O}_{q\bar{q}t\bar{t}})^*]\right\rangle} +$$

$$+ \underbrace{\frac{c_{Zq\bar{q}t\bar{t}1}(s^2 + 2m_t^4 - 2tu) + c_{Zq\bar{q}t\bar{t}2}s(t - u) + c_{Zq\bar{q}t\bar{t}3}m_t^2 s}{2\left(m_Z^2 - s\right)\Lambda^2}}_{\left\langle 2\,\text{Re}[\mathcal{M}(\mathcal{L}_{\text{SM}})\mathcal{M}(\mathcal{O}_{q\bar{q}t\bar{t}})^*]\right\rangle} +$$

$$+ \underbrace{\frac{64C_{tG}^2 g_s^2 v^2(2m_t^2 s - m_t^4 + tu)}{9s\Lambda^4}}_{\left\langle \left|\mathcal{M}(\mathcal{O}_{tG})\right|^2\right\rangle} + \underbrace{\frac{32\sqrt{2}C_{tG}g_s m_t v\left(C_{qAA}^{(8)}(t - u) + C_{qVV}^{(8)}s\right)}{9\Lambda^4}}_{\left\langle 2\,\text{Re}[\mathcal{M}(\mathcal{O}_{tG})\mathcal{M}(\mathcal{O}_{q\bar{q}t\bar{t}})^*]\right\rangle} +$$

$$+ \underbrace{\frac{\begin{aligned}&4\left(C_{qV+A}^{(8)2} + \tfrac{9}{2}C_{qV+A}^{(1)2}\right)\left(s^2 + 2m_t^4 - 2tu\right)+\\&+8\left(C_{qV*A}^{(8)2} + \tfrac{9}{2}C_{qV*A}^{(1)2}\right)s(t-u) + 8\left(C_{qV\mp A}^{(8)2} + \tfrac{9}{2}C_{qV\mp A}^{(1)2}\right)m_t^2 s\end{aligned}}{9\Lambda^4}}_{\left\langle \left|\mathcal{M}(\mathcal{O}_{q\bar{q}t\bar{t}})\right|^2\right\rangle}$$

$$(2.2.4.4)$$

Also, this calculation could be easily resolved by the use of MATHEMATICA with FEYNCALC 9.3.1 package [21].

Where we have used the following:

$$
\begin{cases}
C_{qVV}^{(x)} \equiv \frac{1}{4}\left(\left(C_{Qq_L}^{(x,1)} \pm C_{Qq_L}^{(x,3)}\right) + C_{tq_R}^{(x)} + C_{tq_L}^{(x)} + C_{Qq_R}^{(x)}\right) \quad "+" \text{ for } q = u \quad "-" \text{ for } q = d \\[2mm]

C_{qVA}^{(x)} \equiv \frac{1}{4}\left(-\left(C_{Qq_L}^{(x,1)} \pm C_{Qq_L}^{(x,3)}\right) + C_{tq_R}^{(x)} - C_{tq_L}^{(x)} + C_{Qq_R}^{(x)}\right) \quad "+" \text{ for } q = u \quad "-" \text{ for } q = d \\[2mm]

C_{qAA}^{(x)} \equiv \frac{1}{4}\left(\left(C_{Qq_L}^{(x,1)} \pm C_{Qq_L}^{(x,3)}\right) + C_{tq_R}^{(x)} - C_{tq_L}^{(x)} - C_{Qq_R}^{(x)}\right) \quad "+" \text{ for } q = u \quad "-" \text{ for } q = d \\[2mm]

C_{qAV}^{(x)} \equiv \frac{1}{4}\left(-\left(C_{Qq_L}^{(x,1)} \pm C_{Qq_L}^{(x,3)}\right) + C_{tq_R}^{(x)} + C_{tq_L}^{(x)} - C_{Qq_R}^{(x)}\right) \quad "+" \text{ for } q = u \quad "-" \text{ for } q = d \\[2mm]

{C_{qV+A}^{(x)}}^2 \equiv {C_{qVV}^{(x)}}^2 + {C_{qVA}^{(x)}}^2 + {C_{qAA}^{(x)}}^2 + {C_{qAV}^{(x)}}^2 \\[2mm]

{C_{qV-A}^{(x)}}^2 \equiv {C_{qVV}^{(x)}}^2 + {C_{qVA}^{(x)}}^2 - {C_{qAA}^{(x)}}^2 - {C_{qAV}^{(x)}}^2 \\[2mm]

{C_{qV\mp A}^{(x)}}^2 \equiv {C_{qV-A}^{(x)}}^2 - {C_{qV+A}^{(x)}}^2 \\[2mm]

{C_{qV*A}^{(x)}}^2 \equiv C_{qVV}^{(x)}C_{qAA}^{(x)} + C_{qVA}^{(x)}C_{qAV}^{(x)} \\[2mm]

c_{(g+\gamma)q\bar{q}t\bar{t}1} \equiv 8\left(g_s^2 C_{qVV}^{(8)} + 3g_e^2 \mathcal{Q}(q)C_{qVV}^{(1)}\right) \\[2mm]

c_{(g+\gamma)q\bar{q}t\bar{t}2} \equiv 8\left(g_s^2 C_{qAA}^{(8)} + 3g_e^2 \mathcal{Q}(q)C_{qAA}^{(1)}\right) \\[2mm]

c_{Zq\bar{q}t\bar{t}1} \equiv g_Z^2\left(-C_{qAA}^{(1)}\mathcal{Q}_A(q)\mathcal{Q}_A(t) + C_{qAV}^{(1)}\mathcal{Q}_A(t)\mathcal{Q}_V(q) + C_{qVA}^{(1)}\mathcal{Q}_A(q)\mathcal{Q}_V(t) - C_{qVV}^{(1)}\mathcal{Q}_V(q)\mathcal{Q}_V(t)\right) \\[2mm]

c_{Zq\bar{q}t\bar{t}2} \equiv g_Z^2\left(-C_{qAA}^{(1)}\mathcal{Q}_V(q)\mathcal{Q}_V(t) + C_{qAV}^{(1)}\mathcal{Q}_A(q)\mathcal{Q}_V(t) + C_{qVA}^{(1)}\mathcal{Q}_V(q)\mathcal{Q}_A(t) - C_{qVV}^{(1)}\mathcal{Q}_A(q)\mathcal{Q}_A(t)\right) \\[2mm]

c_{Zq\bar{q}t\bar{t}3} \equiv 4g_Z^2\mathcal{Q}_A(t)\left(C_{qAA}^{(1)}\mathcal{Q}_A(q) - C_{qAV}^{(1)}\mathcal{Q}_V(q)\right)
\end{cases}
$$

2.3   Cross Sections

The cross section is arguably the most widely used physical observable in collision and in scattering experiments and is a quantity used to describe a process of interaction between particles, assessing the probability of particles changing from an initial state to a new state after the interaction event. It has the size of an area and is usually measured in *barn* or its sub-multiples: $1\,\text{b} = 1 \cdot 10^{-24}\,\text{cm}^2$. Knowing the luminosity of the collider, the **differential cross section** allows calculating the distribution of the events on a kinematics parameter, while the **total cross section** allows counting globally the number of events of a given process.

The previous sessions prepared the theoretical calculation of these observables in the context of the production process of top quark-antiquark pairs in the proton-proton collider experiments at the LHC, where the two parton processes $gg \to t\bar{t}$ and $q\bar{q} \to t\bar{t}$ take place. As said in Subsection 1.1.5, these processes are a quasi-elastic collision between two particles that generates other two scattering particles, $(1)(2) \to (3)(4)$, as represented in Figure 2.1 and the generic differential cross section could

be calculated by the following *Golden Rule* [14]:

$$\mathrm{d}^6\sigma = \frac{1}{4\sqrt{(p_1 \cdot p_2)^2 - m_1^2 m_2^2}} (2\pi)^4 \delta^4 \left(p_3 + p_4 - p_1 - p_2\right) \left\langle |\mathcal{M}|^2 \right\rangle \frac{\mathrm{d}^3\overrightarrow{p_3}}{(2\pi)^3 2E_3} \frac{\mathrm{d}^3\overrightarrow{p_4}}{(2\pi)^3 2E_4} \qquad (2.3.0.1)$$

where p_1, p_2, p_3 and p_4 are the four-vector momenta involved, m_1 and m_2 are the masses of the incoming particles, E_3 and E_4 are the energies of the outcoming particles and $\overrightarrow{p_3}$ and $\overrightarrow{p_4}$ are the spatial part momenta of the outcoming particles. The typology of the involved process is included in the form of $\mathcal{M}$, for the SM theory as well as for the SMEFT.

In the following, the formulae for the cross sections are developed for a simple but theoretically propaedeutic case of particle collisions in a fixed CMF and for the real case of proton-proton collision, which involves the collision of the relevant partons in a CMF that appears to be boosted in the direction of the most energetic parton.

2.3.1   Differential Cross Section

Particle collision in fixed CMF

Considering the simple scenario of the two parton processes, $gg \to t\bar{t}$ and $q\bar{q} \to t\bar{t}$, at the high energies involved, we can put $m_1 = m_2 := 0$ and $m_3 = m_4 := m_t$ and of course, we have $\overrightarrow{p_2} = -\overrightarrow{p_1}$. After some integrations, the Formula 2.3.0.1 becomes:

$$\mathrm{d}^3\sigma = \frac{\left\langle |\mathcal{M}|^2 \right\rangle}{16\pi^2 s^2} \delta\left(E_3 - \frac{\sqrt{s}}{2}\right) \mathrm{d}^3\overrightarrow{p_3}\Bigg|_{E_3 := \frac{\sqrt{s}}{2}}, \qquad (2.3.1.1)$$

changing the coordinates for $\overrightarrow{p_3}$, from (p_{3x}, p_{3y}, p_{3z}) to a generic set (ζ, ξ, χ) one obtains:

$$\mathrm{d}^3\sigma = \frac{\left\langle |\mathcal{M}|^2 \right\rangle}{16\pi^2 s^2} \sum_{\zeta_*: \; E_3 := \frac{\sqrt{s}}{2}} \left(\frac{\delta(\zeta - \zeta_*)}{\left|\frac{\partial E_3}{\partial \zeta}\right|} \right) \left| \det \frac{\partial (p_{3x}, p_{3y}, p_{3z})}{\partial (\zeta, \xi, \chi)} \right| \mathrm{d}\zeta \, \mathrm{d}\xi \, \mathrm{d}\chi \, . \qquad (2.3.1.2)$$

This quantity can then be expressed in various forms by choosing the appropriate set of coordinates, as described below.

- Spherical coordinates $(|\overrightarrow{p_3}|, \theta, \phi)$:

$$\begin{cases} p_{3x} := |\overrightarrow{p_3}| \sin\theta \cos\phi \\ p_{3y} := |\overrightarrow{p_3}| \sin\theta \sin\phi \\ p_{3z} := |\overrightarrow{p_3}| \cos\theta \\ E_3 = \sqrt{m_t^2 + |\overrightarrow{p_3}|^2} \end{cases} \implies \begin{cases} \left| \det \frac{\partial (p_{3x}, p_{3y}, p_{3z})}{\partial (|\overrightarrow{p_3}|, \theta, \phi)} \right| = |\overrightarrow{p_3}|^2 \sin\theta \\ \left| \frac{\partial E_3}{\partial |\overrightarrow{p_3}|} \right| = \frac{|\overrightarrow{p_3}|}{E_3} \\ |\overrightarrow{p_3}|_* = \frac{\sqrt{s}}{2} \beta \end{cases}, \qquad (2.3.1.3)$$

thus the Formula 2.3.1.2 becomes:

$$\mathrm{d}^3\sigma = \frac{\left\langle |\mathcal{M}|^2 \right\rangle}{16\pi^2 s^2} \left(\frac{s}{4} \beta \sin\theta \right) \delta\left(|\overrightarrow{p_3}| - \frac{\sqrt{s}}{2} \beta \right) \mathrm{d}|\overrightarrow{p_3}| \, \mathrm{d}\theta \, \mathrm{d}\phi \qquad \implies$$

$$\implies \boxed{\; \mathrm{d}\sigma \;=\; \frac{\left\langle |\mathcal{M}|^2 \right\rangle}{16\pi^2 s^2} \left(\frac{s}{4}\beta \sin\theta \right) (2\pi)\,\mathrm{d}\theta \;}\;,$$

(2.3.1.4)

where t and u Mandelstam variables are substituted in $\left\langle |\mathcal{M}|^2 \right\rangle$ by:

$$\begin{cases} m_t^2 - t = \dfrac{s}{2}\left(1 - \beta\cos\theta\right) \\[2mm] m_t^2 - u = \dfrac{s}{2}\left(1 + \beta\cos\theta\right) \end{cases}, \quad \text{where} \quad 0 \leqslant \theta \leqslant \pi \;.$$

(2.3.1.5)

- Intrinsic coordinates with scattering angle (p_T, θ, ϕ):

$$\boxed{\begin{cases} p_{3x} := p_T \cos\phi \\[1mm] p_{3y} := p_T \sin\phi \\[1mm] p_{3z} := p_T \cot\theta \\[1mm] E_3 = \sqrt{m_t^2 + p_T^2 \csc^2\theta} \quad \text{and} \quad |\overrightarrow{p_3}| = p_T \csc\theta \end{cases}}$$

$$\implies$$

$$\begin{cases} \left| \det \dfrac{\partial\,(p_{3x}, p_{3y}, p_{3z})}{\partial\,(p_T, \theta, \phi)} \right| = p_T^2 \csc^2\theta = |\overrightarrow{p_3}|^2 \\[3mm] \left| \dfrac{\partial E_3}{\partial \theta} \right| = \dfrac{|\overrightarrow{p_3}|^2 \, |\cot\theta|}{E_3} \quad \text{or} \quad \left| \dfrac{\partial E_3}{\partial p_T} \right| = \dfrac{|\overrightarrow{p_3}| \csc\theta}{E_3} \\[3mm] \beta\cos\theta_* = \pm\sqrt{\beta^2 - \dfrac{4p_T^2}{s}} \quad \text{or} \quad p_{T*} = \dfrac{\sqrt{s}}{2}\beta\sin\theta \end{cases},$$

(2.3.1.6)

thus the Formula 2.3.1.2 becomes:

$$\boxed{\; \mathrm{d}\sigma \;=\; \sum_{\substack{\beta\cos\theta_* := \\ \pm\sqrt{\beta^2 - \frac{4p_T^2}{s}}}} \frac{\left\langle |\mathcal{M}|^2 \right\rangle}{16\pi^2 s^2} \left(\frac{p_T}{\sqrt{\beta^2 - \frac{4p_T^2}{s}}} \right) (2\pi)\,\mathrm{d}p_T \;=\; \frac{\left\langle |\mathcal{M}|^2 \right\rangle}{16\pi^2 s^2} \left(\frac{s}{4}\beta\sin\theta \right) (2\pi)\,\mathrm{d}\theta \;}\;,$$

(2.3.1.7)

where t and u Mandelstam variables are substituted in $\left\langle |\mathcal{M}|^2 \right\rangle$ by:

$$\begin{cases} m_t^2 - t = \dfrac{s}{2}\left(1 - \beta\cos\theta\right) \\[2mm] m_t^2 - u = \dfrac{s}{2}\left(1 + \beta\cos\theta\right) \end{cases}, \quad \text{where} \quad 0 \leqslant \theta \leqslant \pi \;.$$

(2.3.1.8)

- Intrinsic coordinates with rapidity (p_T, y, ϕ):

$$
\begin{cases}
p_{3x} := p_T \cos \phi \\[4pt]
p_{3y} := p_T \sin \phi \\[4pt]
p_{3z} := m_T \sinh \mathrm{y} \\[4pt]
E_3 = m_T \cosh \mathrm{y}
\end{cases}
\quad \text{defining} \quad m_T \equiv \sqrt{m_t^2 + p_T^2} \qquad \Longrightarrow
$$

$$
\begin{cases}
\left| \det \dfrac{\partial \left(p_{3x}, p_{3y}, p_{3z}\right)}{\partial \left(p_T, \mathrm{y}, \phi\right)} \right| = m_t p_T \cosh \mathrm{y} = E_3 p_T \\[10pt]
\left| \dfrac{\partial E_3}{\partial \mathrm{y}} \right| = E_3 \left| \tanh \mathrm{y} \right| \quad \text{or} \quad \left| \dfrac{\partial E_3}{\partial p_T} \right| = \dfrac{p_T \cosh^2 \mathrm{y}}{E_3} \\[10pt]
\tanh \mathrm{y}_* = \pm \sqrt{\beta^2 - \dfrac{4 p_T^2}{s}} \quad \text{or} \quad p_{T*} = \dfrac{\sqrt{s}}{2} \sqrt{\beta^2 - \tanh^2 \mathrm{y}}
\end{cases}
,
$$

$$(2.3.1.9)$$

thus the Formula 2.3.1.2 becomes:

$$
\mathrm{d}\sigma = \sum_{\substack{\tanh \mathrm{y}_* := \\ \pm \sqrt{\beta^2 - \frac{4 p_T^2}{s}}}} \frac{\left\langle |\mathcal{M}|^2 \right\rangle}{16 \pi^2 s^2} \left(\frac{p_T}{\sqrt{\beta^2 - \dfrac{4 p_T^2}{s}}} \right) (2\pi) \, \mathrm{d}p_T = \frac{\left\langle |\mathcal{M}|^2 \right\rangle}{16 \pi^2 s^2} \left(\frac{s}{4 \cosh^2 \mathrm{y}} \right) (2\pi) \, \mathrm{d}\mathrm{y} ,
$$

$$(2.3.1.10)$$

where t and u Mandelstam variables are substituted in $\left\langle |\mathcal{M}|^2 \right\rangle$ by:

$$
\begin{cases}
m_t^2 - t = \dfrac{s}{2} \left(1 - \tanh \mathrm{y}\right) \\[8pt]
m_t^2 - u = \dfrac{s}{2} \left(1 + \tanh \mathrm{y}\right)
\end{cases}
, \quad \text{where} \quad -\beta \leqslant \tanh \mathrm{y} \leqslant +\beta .
\qquad (2.3.1.11)
$$

- Intrinsic coordinates with pseudo-rapidity (p_T, η, ϕ):

$$
\begin{cases}
p_{3x} := p_T \cos \phi \\[4pt]
p_{3y} := p_T \sin \phi \\[4pt]
p_{3z} := p_T \sinh \eta \\[4pt]
|\vec{p_3}| = p_T \cosh \eta
\end{cases}
\quad \text{where} \quad E_3 = \sqrt{m_t^2 + |\vec{p_3}|^2} \qquad \Longrightarrow
$$

$$
\begin{cases}
\left| \det \dfrac{\partial \left(p_{3x}, p_{3y}, p_{3z}\right)}{\partial \left(p_T, \eta, \phi\right)} \right| = |\vec{p_3}| p_T \\[10pt]
\left| \dfrac{\partial E_3}{\partial \eta} \right| = \dfrac{|\vec{p_3}|}{E_3} p_T \left| \sinh \eta \right| \quad \text{or} \quad \left| \dfrac{\partial E_3}{\partial p_T} \right| = \dfrac{|\vec{p_3}|}{E_3} \cosh \eta \\[10pt]
\beta \tanh \eta_* = \pm \sqrt{\beta^2 - \dfrac{4 p_T^2}{s}} \quad \text{or} \quad p_{T*} = \dfrac{\sqrt{s}}{2} \beta \dfrac{1}{\cosh \eta}
\end{cases}
, \qquad (2.3.1.12)
$$

thus the Formula 2.3.1.2 becomes:

$$
\mathrm{d}\sigma \;=\; \sum_{\substack{\beta \tanh \eta_* := \\ \pm\sqrt{\beta^2 - \frac{4p_T^2}{s}}}} \frac{\langle |\mathcal{M}|^2 \rangle}{16\pi^2 s^2} \left(\frac{p_T}{\sqrt{\beta^2 - \frac{4p_T^2}{s}}} \right) (2\pi)\,\mathrm{d}p_T \;=\; \frac{\langle |\mathcal{M}|^2 \rangle}{16\pi^2 s^2} \left(\frac{s\beta}{4\cosh^2 \eta} \right) (2\pi)\,\mathrm{d}\eta \;,
$$

(2.3.1.13)

where t and u Mandelstam variables are substituted in $\langle |\mathcal{M}|^2 \rangle$ by:

$$
\begin{cases} m_t^2 - t = \dfrac{s}{2}\left(1 - \beta \tanh \eta\right) \\[2mm] m_t^2 - u = \dfrac{s}{2}\left(1 + \beta \tanh \eta\right) \end{cases} \;, \quad \text{where} \quad -1 \leqslant \tanh \eta \leqslant +1 \;.
$$

(2.3.1.14)

Here we present the diagrams of the differential cross section distribution of some observables (p_T, θ, y, η) of the processes $gg \to t\bar{t}$ and $u\bar{u}/d\bar{d} \to t\bar{t}$ at $E_{\text{beam}} = 7000$ GeV in SM (i.e. with null Wilson coefficients) and in SMEFT (setting some Wilson coefficients), using the available tools of MATHEMATICA [22].

The typical SM values utilised to plot each differential cross section are reported in Appendix C. In particular, for the SMEFT diagrams, the energy scale is arbitrarily fixed to $\Lambda := 1000$ GeV and, as an example, the following Wilson coefficients are set:

$C_{tG} :=$ 0	$C_G :=$ -0.001	$C_{\phi G} :=$ 0.85	
$C_{qVV}^{(8)} :=$ 0	$C_{qVA}^{(8)} :=$ 0	$C_{qAA}^{(8)} :=$ 0.0002	$C_{qAV}^{(8)} :=$ 0
$C_{qVV}^{(1)} :=$ 0	$C_{qVA}^{(1)} :=$ 0	$C_{qAA}^{(1)} :=$ 0	$C_{qAV}^{(1)} :=$ 0

(a) **Linear** representation
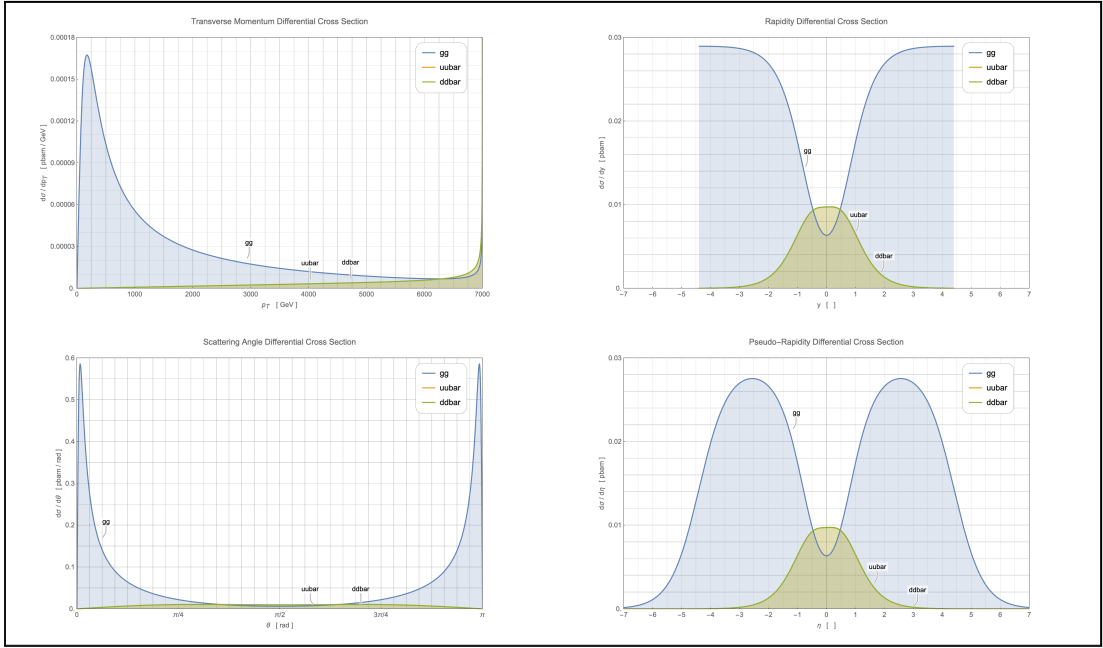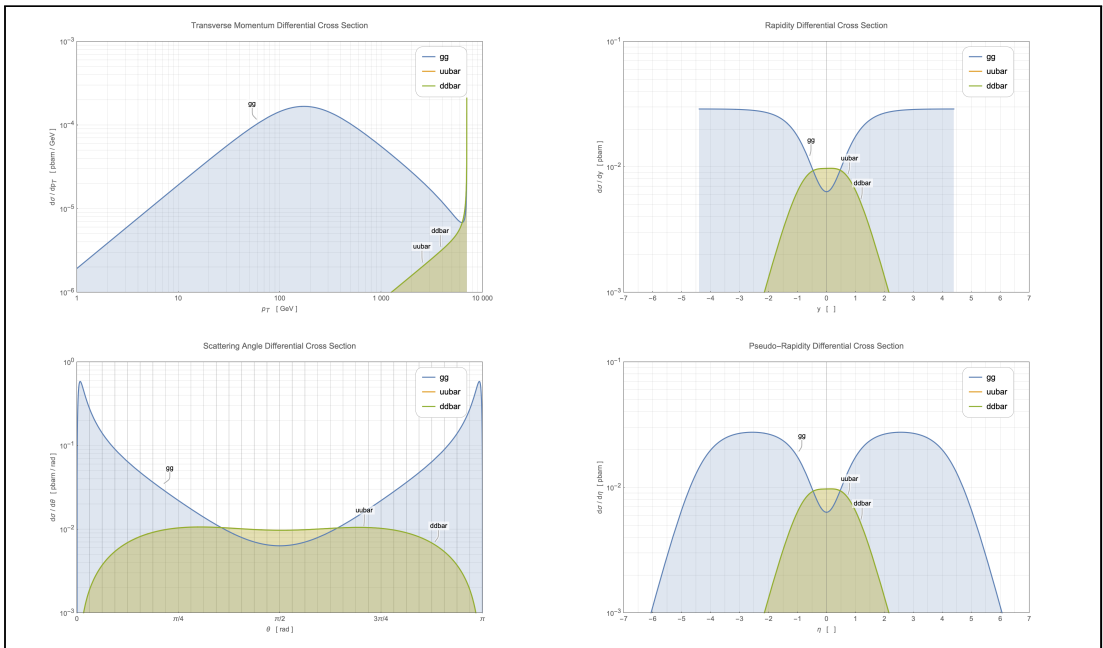
(b) **Logarithmic** representation

Figure 2.9: Distributions for some observables of both processes $gg \rightarrow t\bar{t}$ and $u\bar{u}/d\bar{d} \rightarrow t\bar{t}$ at $E_{\text{beam}} = 7000$ GeV in SM.
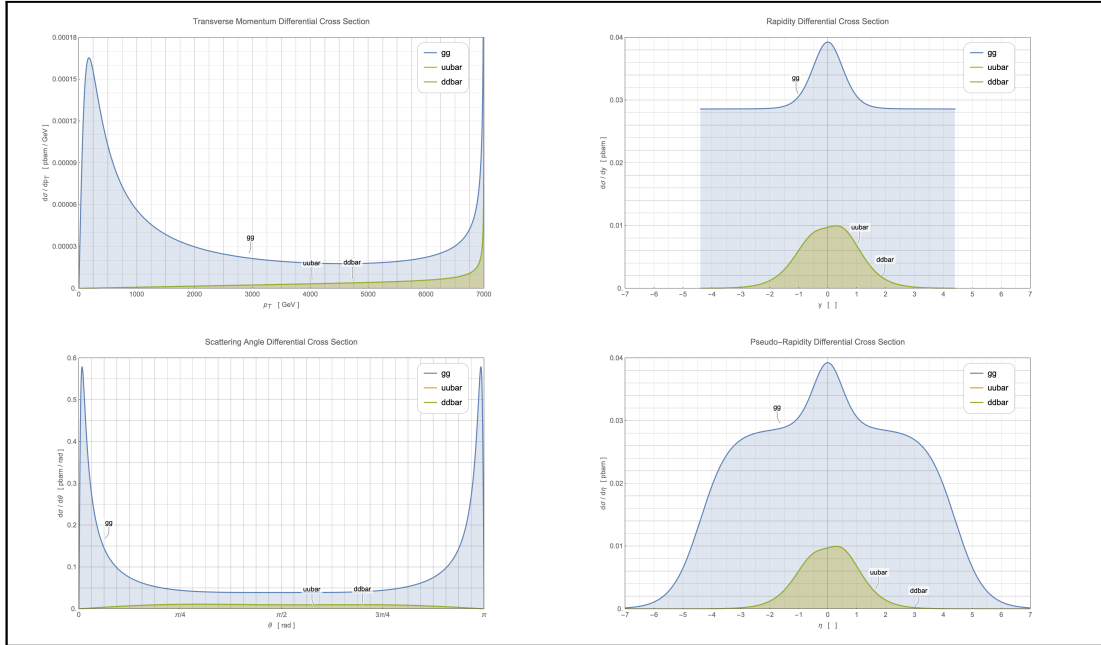
(a) **Linear** representation
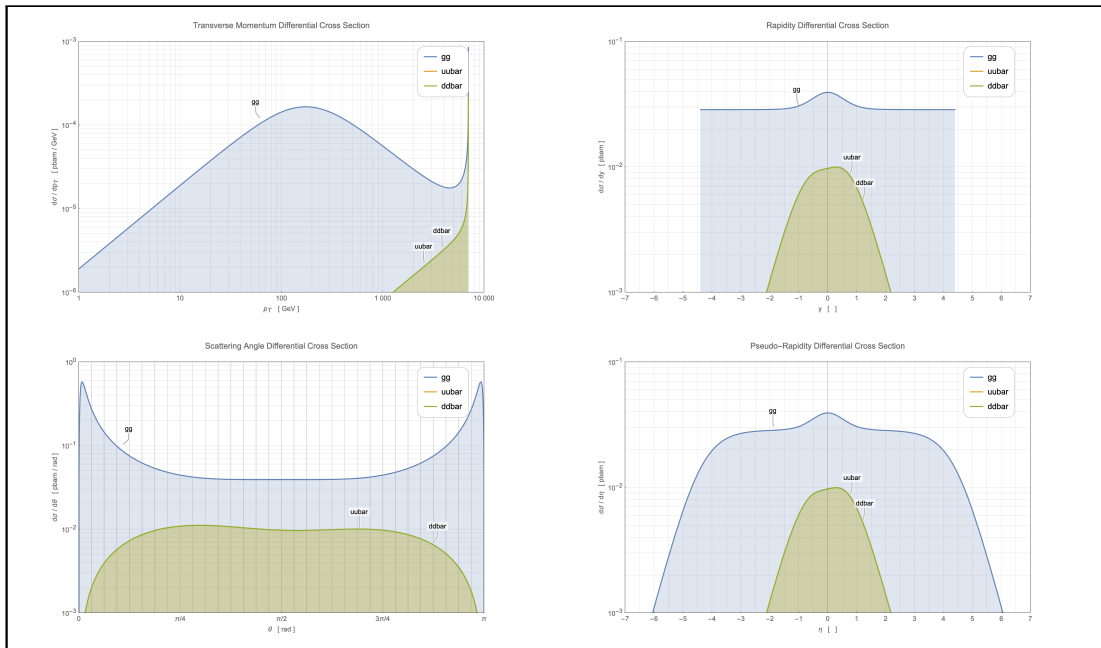
(b) **Logarithmic** representation

Figure 2.10: Distributions for some observables of both processes $gg \rightarrow t\bar{t}$ and $u\bar{u}/d\bar{d} \rightarrow t\bar{t}$ at $E_{\text{beam}} = 7000$ GeV in SMEFT.

Particle collision in boosted CMF - parton interaction of proton collision

In a high-energy proton collision at the LHC, the relevant partons interact by colliding with different energies that are fractions of the energies of the relevant parent protons. These fractional energies are not equal but are distributed according to a suitable distribution function that can be obtained experimentally. This is why the scattering CMF of the partons appears, to the reference system fixed at the collision point, to be pushed in the direction of the most energetic parton.

Considering the scenario of the two processes, $pp \to gg \to t\bar{t}$ and $pp \to q\bar{q} \to t\bar{t}$, at the high energies involved, as before we can put $m_1 = m_2 := 0$ and $m_3 = m_4 := m_t$ in a collider situation with a boosted CMF, where $\vec{p_2} \| -\vec{p_1}$ but not equal, for example, $p_1 := (x_1 E, 0, 0, +x_1 E)$ and $p_2 := (x_2 E, 0, 0, -x_2 E)$. After some integrations, the Formula 2.3.0.1 becomes:

$$\mathrm{d}^3\sigma \;=\; \frac{\langle |\mathcal{M}|^2 \rangle}{32\pi^2 s} \; \frac{\delta(E_3 + E_4 - E(x_1 + x_2))}{E_3 E_4} \; \mathrm{d}^3\vec{p_3} \left|\begin{array}{l} \\ \vec{p_4}_{xy} := -\vec{p_3}_{xy} \\ p_{4z} := E(x_1 - x_2) - p_{3z} \end{array}\right. , \qquad (2.3.1.15)$$

changing the coordinates for $\vec{p_3}$, from (p_{3x}, p_{3y}, p_{3z}) to a generic set (ζ, ξ, χ):

$$\mathrm{d}^3\sigma \;=\; \frac{\langle |\mathcal{M}|^2 \rangle}{32\pi^2 s} \sum_{\substack{\zeta_* \colon E_3 + E_4 := \\ E(x_1 + x_2)}} \left(\frac{\delta(\zeta - \zeta_*)}{E_3 E_4 \left| \dfrac{\partial(E_3 + E_4)}{\partial \zeta} \right|} \right) \left| \det \frac{\partial(p_{3x}, p_{3y}, p_{3z})}{\partial(\zeta, \xi, \chi)} \right| \mathrm{d}\zeta \, \mathrm{d}\xi \, \mathrm{d}\chi , \qquad (2.3.1.16)$$

where, as see in Formula 2.1.3.2, $s = 4x_1 x_2 E^2$.

- Intrinsic coordinates with rapidity (p_T, y, ϕ):

$$\begin{cases} p_{3x} := p_T \cos\phi \\ p_{3y} := p_T \sin\phi \\ p_{3z} := m_T \sinh y \\ E_3 = m_T \cosh y \end{cases} \quad \text{defining} \quad m_T \equiv \sqrt{m_t^2 + p_T^2} \quad \Longrightarrow$$

$$\left| \det \frac{\partial(p_{3x}, p_{3y}, p_{3z})}{\partial(p_T, y, \phi)} \right| = m_t p_T \cosh y = E_3 p_T , \qquad (2.3.1.17)$$

thus the Formula 2.3.1.16 becomes:

$$\mathrm{d}\sigma \;=\; \sum_{\substack{\tanh(y_* - y_{12}) := \\ \pm\sqrt{\beta^2 - \frac{4p_T^2}{s}}}} \frac{\langle |\mathcal{M}|^2 \rangle}{32\pi^2 s} \left(\frac{2p_T}{s\sqrt{\beta^2 - \dfrac{4p_T^2}{s}}} \right) (2\pi)\,\mathrm{d}p_T \;=\; \frac{\langle |\mathcal{M}|^2 \rangle}{32\pi^2 s} \left(\frac{1}{2\cosh^2(y - y_{12})} \right) (2\pi)\,\mathrm{d}y ,$$

$$(2.3.1.18)$$

where t and u Mandelstam variables are substituted in $\langle|\mathcal{M}|^2\rangle$ by:

$$
\begin{cases}
m_t^2 - t = \dfrac{s}{2}\left(1 - \tanh\left(\mathrm{y} - \mathrm{y}_{12}\right)\right) \\[2mm]
m_t^2 - u = \dfrac{s}{2}\left(1 + \tanh\left(\mathrm{y} - \mathrm{y}_{12}\right)\right)
\end{cases}
\quad , \quad \text{where} \quad -\beta \leqslant \tanh\left(\mathrm{y} - \mathrm{y}_{12}\right) \leqslant +\beta \ . \tag{2.3.1.19}
$$

- <u>Intrinsic coordinates with pseudo-rapidity</u> (p_T, η, ϕ):

$$
\begin{cases}
p_{3x} := p_T \cos\phi \\[1mm]
p_{3y} := p_T \sin\phi \\[1mm]
p_{3z} := p_T \sinh\eta \\[1mm]
|\overrightarrow{p_3}| = p_T \cosh\eta
\end{cases}
\quad \text{where} \quad E_3 = \sqrt{m_t^2 + |\overrightarrow{p_3}|^2}
\qquad \Longrightarrow
$$

$$
\left| \det \frac{\partial\left(p_{3x}, p_{3y}, p_{3z}\right)}{\partial\left(p_T, \eta, \phi\right)} \right| = |\overrightarrow{p_3}|\, p_T \ , \tag{2.3.1.20}
$$

thus the Formula 2.3.1.16 becomes:

$$
\begin{aligned}
\mathrm{d}\sigma &= \sum_{\substack{\beta\tanh\eta_* := \\ \pm\sqrt{\beta^2 - \frac{4p_T^2}{s}}}} \frac{\langle|\mathcal{M}|^2\rangle}{32\pi^2 s} \left(\frac{2p_T}{s\sqrt{\beta^2 - \frac{4p_T^2}{s}}} \right) (2\pi)\,\mathrm{d}p_T \ = \\
&= \sum_{\substack{p_{T*} := \\ p_{T+}, p_{T-}}} \left(\sum_{\substack{\beta\tanh\eta := \\ \pm\sqrt{\beta^2 - \frac{4p_T^2}{s}}}} \frac{\langle|\mathcal{M}|^2\rangle}{32\pi^2 s} \right) \left(\frac{4p_T^2/s}{2\sqrt{1 - (1-\beta^2)\dfrac{1 - \tanh^2\eta\,\tanh^2\mathrm{y}_{12}}{1 - \tanh^2\mathrm{y}_{12}}}} \right) (2\pi)\,\mathrm{d}\eta
\end{aligned}
\ ,
$$
$$\tag{2.3.1.21}$$

where t and u Mandelstam variables are substituted in $\langle|\mathcal{M}|^2\rangle$ by:

$$
\begin{cases}
m_t^2 - t = \dfrac{s}{2}\left(1 - \beta\tanh\eta\right) \\[2mm]
m_t^2 - u = \dfrac{s}{2}\left(1 + \beta\tanh\eta\right)
\end{cases}
\quad , \quad \text{where} \quad -1 \leqslant \tanh\eta \leqslant +1 \ . \tag{2.3.1.22}
$$

and where

$$
\begin{cases}
\dfrac{2p_{T+}}{\sqrt{s}} \equiv \dfrac{\tanh\eta \tanh\mathrm{y}_{12} + \sqrt{1 - (1-\beta^2)\dfrac{1 - \tanh^2\eta \tanh^2\mathrm{y}_{12}}{1 - \tanh^2\mathrm{y}_{12}}}}{\cosh\eta \cosh\mathrm{y}_{12}(1 - \tanh^2\eta \tanh^2\mathrm{y}_{12})} \geqslant 0 \quad \text{when} \\[2em]
\qquad \begin{cases} (\mathrm{y}_{12}\eta < 0 \ \wedge \ \tanh^2\mathrm{y}_{12} \leqslant \beta^2) \ \vee \ (\mathrm{y}_{12}\eta \geqslant 0 \ \wedge \ \tanh^2\eta \geqslant \dfrac{1 - \dfrac{\beta^2}{\tanh^2\mathrm{y}_{12}}}{1 - \beta^2}) \end{cases} \\[3em]
\dfrac{2p_{T-}}{\sqrt{s}} \equiv \dfrac{\tanh\eta \tanh\mathrm{y}_{12} - \sqrt{1 - (1-\beta^2)\dfrac{1 - \tanh^2\eta \tanh^2\mathrm{y}_{12}}{1 - \tanh^2\mathrm{y}_{12}}}}{\cosh\eta \cosh\mathrm{y}_{12}(1 - \tanh^2\eta \tanh^2\mathrm{y}_{12})} \geqslant 0 \quad \text{when} \\[2em]
\qquad \begin{cases} \mathrm{y}_{12}\eta > 0 \ \wedge \ \tanh^2\mathrm{y}_{12} \geqslant \beta^2 \ \wedge \ \tanh^2\eta \geqslant \dfrac{1 - \dfrac{\beta^2}{\tanh^2\mathrm{y}_{12}}}{1 - \beta^2} \end{cases}
\end{cases}
$$

$$(2.3.1.23)$$

The above expressions correspond to the hard scattering parton collision cross sections. To obtain the same cross sections relevant to the proton-proton collision, one can use the factorisation theorem by applying the following expression:

$$
\boxed{\mathrm{d}\sigma_{pp\to\mathrm{X}_1\mathrm{X}_2\to t\bar{t}} = \int_0^1 \mathrm{dx}_1\, \mathrm{pdf}_{\mathrm{X}_1}\left(\mathrm{x}_1, \mu_F^2\right) \int_0^1 \mathrm{dx}_2\, \mathrm{pdf}_{\mathrm{X}_2}\left(\mathrm{x}_2, \mu_F^2\right)\, \mathrm{d}\sigma_{\mathrm{X}_1\mathrm{X}_2\to t\bar{t}}(\mathrm{x}_1, \mathrm{x}_2, E)}, \qquad (2.3.1.24)
$$

where we have indicated with X_1 and X_2 the two interacting partons of the two colliding protons pp, hence $\mathrm{X}_1\mathrm{X}_2$ are gg or $u\bar{u}$ or $d\bar{d}$. The contribution of other types of partons, as c, s, etc. at energies used in LHC, experimentally seams irrelevant. $\mathrm{pdf}_{\mathrm{X}_i}\left(\mathrm{x}_i, \mu_F^2\right)$ is the Parton Distribution Function (PDF) of a parton X_i, x_i is the fraction of the proton momentum passed to its relative parton X_i and function of the energy factorisation scale μ_F.

Here we present the differential cross section distribution of some observables (p_T, θ, y, η) of the processes $gg \to t\bar{t}$ and $u\bar{u}/d\bar{d} \to t\bar{t}$ at $E_{\mathrm{beam}} = 7000$ GeV in SM only (i.e. with null Wilson coefficients), in pp collision, using the available tools of Mathematica [22].
It is important to notice that for the application of the PDF a peculiar interface developed for Mathematica has been used [23]. This tool was developed by NNPDF, a research group collaborating with the aim of determining the proton structure and evaluating the PDF using modern artificial intelligence methods [24].

The values utilised to plot each differential cross section are the same as used before in the CMF fixed frame: Appendix C. For the NNPDF interface, the "NNPDF23_lo_as_0130_qed_mem0" grid of value is used.
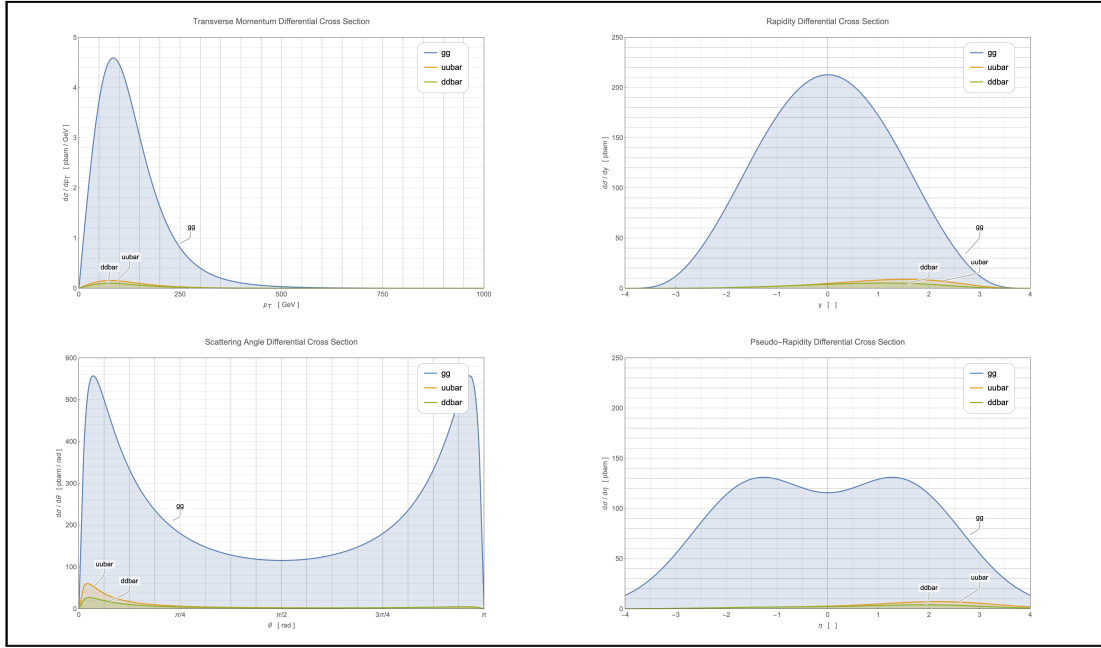
(a) **Linear** representation
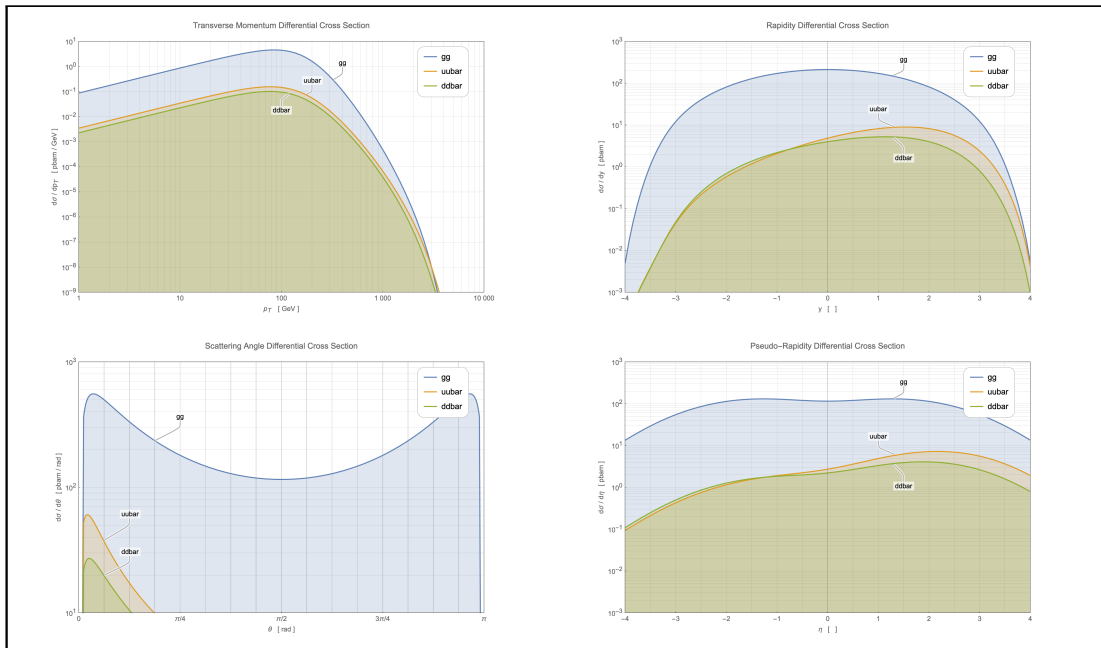
(b) **Logarithmic** representation

Figure 2.11: Distributions for some observables of both processes $pp \to gg \to t\bar{t}$ and $pp \to u\bar{u}/d\bar{d} \to t\bar{t}$ at $E_{\text{beam}} = 7000$ GeV in SM.
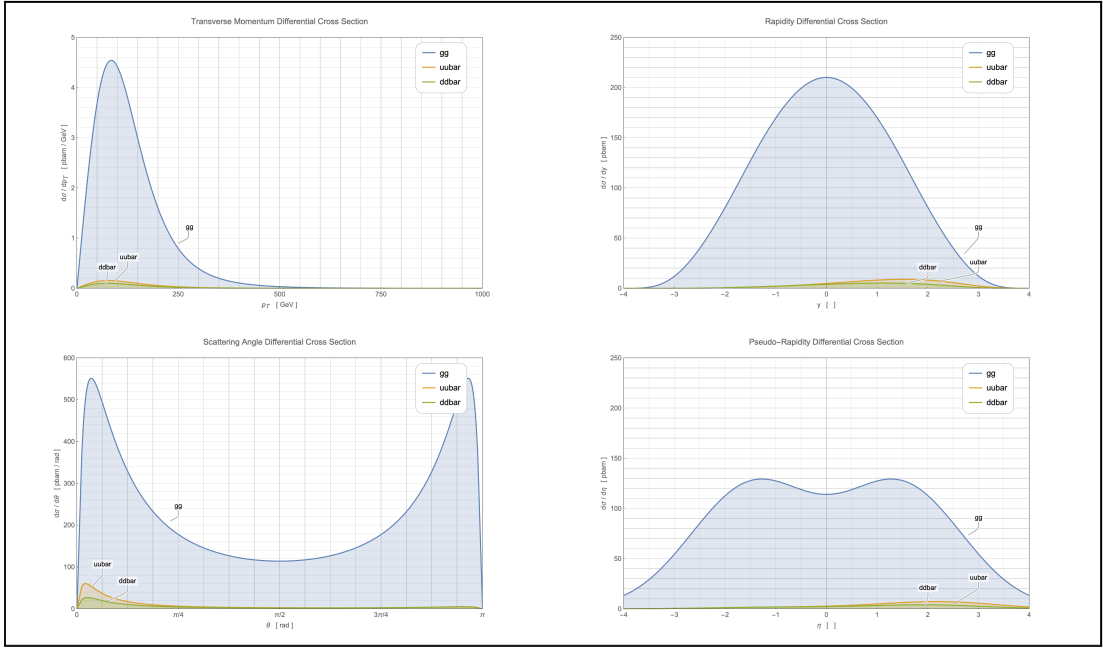
(a) **Linear** representation
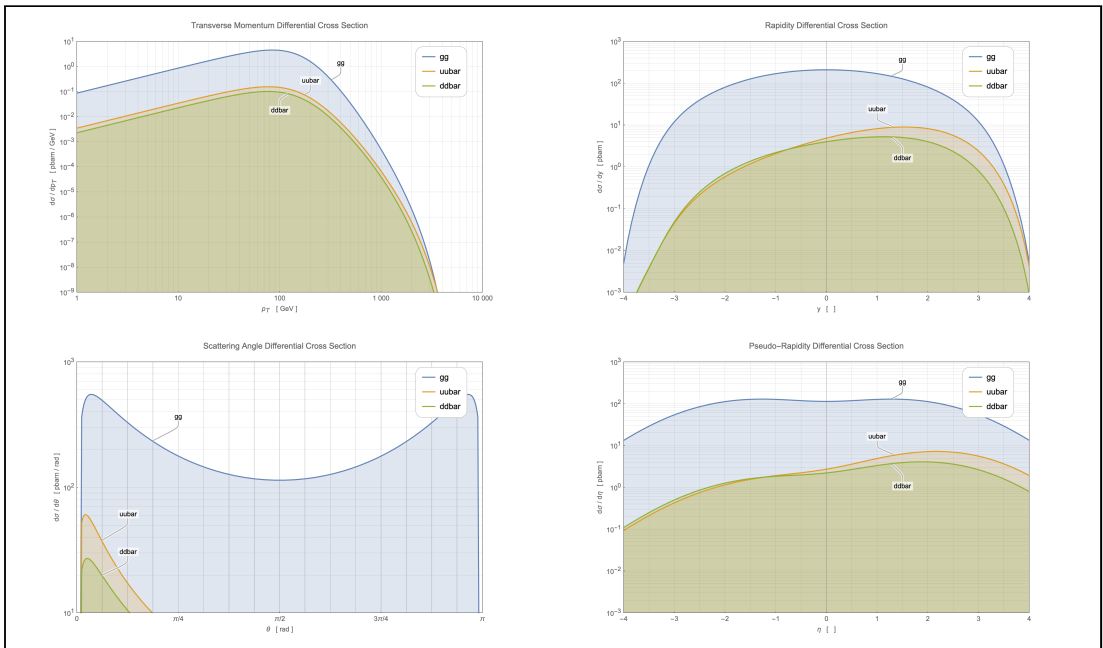
(b) **Logarithmic** representation

Figure 2.12: Distributions for some observables of both processes $pp \to gg \to t\bar{t}$ and $pp \to u\bar{u}/d\bar{d} \to t\bar{t}$ at $E_{\text{beam}} = 7000$ GeV in SMEFT.

2.3.2 Total cross section

To calculate the total cross section, it is necessary to choose an observable, express $\langle |\mathcal{M}|^2 \rangle$ as a function of this chosen observable, via the Mandelstam variables, and integrate the differential cross section in the appropriate limits.

Particle collision in fixed CMF

Considering the processes $gg \to t\bar{t}$ or $q\bar{q} \to t\bar{t}$ (where $q\bar{q}$ is $u\bar{u}$ or $d\bar{d}$), also including the SMEFT contribution to LO, the simplest way to integrate the differential cross section is to substitute the Mandelstam variables as a function of y and use this observable as the integration variable:

$$
\begin{cases}
m_t^2 - t = \dfrac{s}{2}\left(1 - \tanh \mathrm{y}\right) \\[2mm]
m_t^2 - u = \dfrac{s}{2}\left(1 + \tanh \mathrm{y}\right)
\end{cases}
\quad \text{where} \quad -\beta \leqslant \tanh \mathrm{y} \leqslant +\beta \,,
\tag{2.3.2.1}
$$

then the integration could be simply done by:

$$
\boxed{\sigma = \int_{\tanh \mathrm{y}=-\beta}^{\tanh \mathrm{y}=+\beta} \frac{\langle |\mathcal{M}|^2 \rangle}{16\pi^2 s^2} \left(\frac{s}{4\cosh^2 \mathrm{y}} \right) (2\pi)\, \mathrm{dy} = \int_{-\beta}^{+\beta} \frac{\langle |\mathcal{M}|^2 \rangle}{32\pi s}\, \mathrm{d}\left(\tanh \mathrm{y}\right)}\,.
\tag{2.3.2.2}
$$

This integral could be quite tedious applying it to the SM or SMEFT $\langle |\mathcal{M}|^2 \rangle$ expressions, but it could be easily resolved by use of MATHEMATICA obtaining:

Total Cross Section for $gg \to t\bar{t}$ in SMEFT @ LO

$$
\sigma = \underbrace{\frac{\pi\alpha_s^2\left(\beta\left(31\beta^2 - 59\right) + 2\left(\beta^4 - 18\beta^2 + 33\right)\operatorname{arctanh}\beta\right)}{48s}}_{\left\langle \left|\mathcal{M}(\mathcal{L}_{\mathrm{SM}})\right|^2 \right\rangle} +
$$

$$
+ C_{tG}\underbrace{\frac{\sqrt{\frac{\pi}{2}}\alpha_s^{\frac{3}{2}} v \sqrt{1-\beta^2}\left(16\operatorname{arctanh}\beta - 9\beta\right)}{6\sqrt{s}\Lambda^2}}_{\left\langle 2\operatorname{Re}[\mathcal{M}(\mathcal{L}_{\mathrm{SM}})\mathcal{M}(\mathcal{O}_{tG})^*]\right\rangle} + C_G\underbrace{\frac{9\sqrt{\pi}\alpha_s^{\frac{3}{2}}\left(1-\beta^2\right)\left(\operatorname{arctanh}\beta - \beta\right)}{16\Lambda^2}}_{\left\langle 2\operatorname{Re}[\mathcal{M}(\mathcal{L}_{\mathrm{SM}})\mathcal{M}(\mathcal{O}_G)^*]\right\rangle} +
$$

$$
+ C_{\phi G}\underbrace{\frac{\alpha_s\beta^2\left(\beta^2 - 1\right)\operatorname{arctanh}\beta}{32\delta^2\Lambda^2}}_{\left\langle 2\operatorname{Re}[\mathcal{M}(\mathcal{L}_{\mathrm{SM}})\mathcal{M}(\mathcal{O}_{\phi G})^*]\right\rangle} + C_{tG}^2\underbrace{\frac{\alpha_s v^2\left(3\beta\left(\beta^2 + 7\right) + 16\left(1-\beta^2\right)\operatorname{arctanh}\beta\right)}{24\Lambda^4}}_{\left\langle \left|\mathcal{M}(\mathcal{O}_{tG})\right|^2 \right\rangle} +
$$

$$
+ C_{tG}C_G\underbrace{\frac{9\alpha_s v\beta\sqrt{1-\beta^2}\sqrt{s}}{8\sqrt{2}\Lambda^4}}_{\left\langle 2\operatorname{Re}[\mathcal{M}(\mathcal{O}_{tG})\mathcal{M}(\mathcal{O}_G)^*]\right\rangle} + C_{tG}C_{\phi G}\underbrace{\frac{\sqrt{\alpha_s} v\sqrt{1-\beta^2}\left(\beta - \left(1-\beta^2\right)\operatorname{arctanh}\beta\right)\sqrt{s}}{16\sqrt{2\pi}\delta^2\Lambda^4}}_{\left\langle 2\operatorname{Re}[\mathcal{M}(\mathcal{O}_{tG})\mathcal{M}(\mathcal{O}_{\phi G})^*]\right\rangle} +
$$

$$
+ C_G^2\underbrace{\frac{9\alpha_s\beta\left(3-\beta^2\right)s}{64\Lambda^4}}_{\left\langle \left|\mathcal{M}(\mathcal{O}_G)\right|^2 \right\rangle} + \underbrace{0}_{\left\langle 2\operatorname{Re}[\mathcal{M}(\mathcal{O}_G)\mathcal{M}(\mathcal{O}_{\phi G})^*]\right\rangle} + C_{\phi G}^2\underbrace{\frac{3\beta^3\left(1-\beta^2\right)s}{512\pi\delta^4\Lambda^4}}_{\left\langle \left|\mathcal{M}(\mathcal{O}_{\phi G})\right|^2 \right\rangle}
$$

$$
\tag{2.3.2.3}
$$

Total Cross Section for $q\bar{q} \to t\bar{t}$ in SMEFT @ LO

$$
\begin{aligned}
\sigma \;=\; & \frac{4\pi\alpha_s^2\beta\left(3-\beta^2\right)}{27s} + \frac{8\pi\alpha^2\mathcal{Q}^2(q)\beta\left(3-\beta^2\right)}{27s} + \frac{\alpha\mathcal{Q}(q)g_Z^2\mathcal{Q}_V(q)\mathcal{Q}_V(t)\beta\left(3-\beta^2\right)}{18\epsilon^2 s} + \\
& + \underbrace{\frac{g_Z^4\left(\mathcal{Q}_A^2(q)+\mathcal{Q}_V^2(q)\right)\left(\mathcal{Q}_V^2(t)\beta\left(3-\beta^2\right)+\mathcal{Q}_A^2(t)2\beta^3\right)}{384\pi\epsilon^4 s}}_{\left\langle\left|\mathcal{M}(\mathcal{L}_{\mathrm{SM}})\right|^2\right\rangle} +
\end{aligned}
$$

$$
+ \underbrace{C_{tG}\frac{8\alpha_s\sqrt{2\pi\alpha_s s}\,v\beta\sqrt{1-\beta^2}}{9s\Lambda^2}}_{\left\langle 2\,\mathrm{Re}[\mathcal{M}(\mathcal{L}_{\mathrm{SM}})\mathcal{M}(\mathcal{O}_{tG})^*]\right\rangle} +
$$

$$
\begin{aligned}
& + C_{qVV}^{(8)}\frac{\alpha_s\beta\left(3-\beta^2\right)}{27\Lambda^2} + C_{qVV}^{(1)}\frac{\alpha\mathcal{Q}(q)\beta\left(3-\beta^2\right)}{9\Lambda^2} + \\
& + \frac{g_Z^2\mathcal{Q}_V(t)\left(\mathcal{Q}_V(q)C_{qVV}^{(1)}-\mathcal{Q}_A(q)C_{qVA}^{(1)}\right)\beta\left(3-\beta^2\right)}{96\pi\epsilon^2\Lambda^2} + \\
& + \underbrace{\frac{g_Z^2\mathcal{Q}_A(t)\left(\mathcal{Q}_A(q)C_{qAA}^{(1)}-\mathcal{Q}_V(q)C_{qAV}^{(1)}\right)2\beta^3}{96\pi\epsilon^2\Lambda^2}}_{\left\langle 2\,\mathrm{Re}[\mathcal{M}(\mathcal{L}_{\mathrm{SM}})\mathcal{M}(\mathcal{O}_{q\bar{q}t\bar{t}})^*]\right\rangle} +
\end{aligned}
$$

$$
+ \underbrace{C_{tG}^2\frac{8\alpha_s v^2\beta\left(3-2\beta^2\right)}{27\Lambda^4}}_{\left\langle\left|\mathcal{M}(\mathcal{O}_{tG})\right|^2\right\rangle} + \underbrace{C_{tG}C_{qVV}^{(8)}\frac{\sqrt{2\pi\alpha_s s}\,v\beta\sqrt{1-\beta^2}}{9\pi\Lambda^4}}_{\left\langle 2\,\mathrm{Re}[\mathcal{M}(\mathcal{O}_{tG})\mathcal{M}(\mathcal{O}_{q\bar{q}t\bar{t}})^*]\right\rangle} +
$$

$$
\begin{aligned}
& + \frac{\left(9C_{qVA}^{(1)\,2}+9C_{qVV}^{(1)\,2}+2C_{qVA}^{(8)\,2}+2C_{qVV}^{(8)\,2}\right)\beta\left(3-\beta^2\right)s}{216\pi\Lambda^4} + \\
& + \underbrace{\frac{2\left(9C_{qAV}^{(1)\,2}+9C_{qAA}^{(1)\,2}+2C_{qAV}^{(8)\,2}+2C_{qAA}^{(8)\,2}\right)2\beta^3 s}{216\pi\Lambda^4}}_{\left\langle\left|\mathcal{M}(\mathcal{O}_{q\bar{q}t\bar{t}})\right|^2\right\rangle}
\end{aligned}
$$

$$(2.3.2.4)$$

where for both the expressions we use $\beta \equiv \sqrt{1-4m_t^2/s}$, $\delta \equiv \sqrt{1-m_H^2/s}$ and $\epsilon \equiv \sqrt{1-m_Z^2/s}$.

Alternatively, for the case $gg \to t\bar{t}$, we can also choose p_T as the integrating variable and integrate within its positive limits, getting the same right result because $\left\langle\left|\mathcal{M}\right|^2\right\rangle$ does not change by swapping the Mandelstam variables t and u. However, this operation is incorrect for the other case $q\bar{q} \to t\bar{t}$, which is instead sensitive to exchanging the Mandelstam variables t and u.

Here we present the values of the total cross section of both processes $gg \to t\bar{t}$ and $u\bar{u}/d\bar{d} \to t\bar{t}$ at $E_{\mathrm{beam}} = 7000$ GeV and at SMEFT energy scale of $\Lambda = 1000$ GeV, expressed in the quadratic form

"$\Sigma \, (\_ \cdot \_)$" of Wilson coefficients:

$$
\sigma_{gg \to t\bar{t}} \;=\; \left(
\begin{array}{c|cccc}
\Sigma \, (\_ \cdot \_) & 1 & C_{tG} & C_G & C_{\phi G} \\
\hline
1 & 0.20397300 & 0.0439190 & 0.0163091 & -0.00192548 \\
C_{tG} & 0.04391900 & 2.7893700 & 1.5564200 & 0.14164600 \\
C_G & 0.01630910 & 1.5564200 & 2532.8200 & 0 \\
C_{\phi G} & -0.00192548 & 0.14164600 & 0 & 0.08687560
\end{array}
\right) \quad \text{pbarn}
$$

$$
\sigma_{u\bar{u} \to t\bar{t}} \;=\; \left(
\begin{array}{c|cccccc}
\Sigma \, (\_ \cdot \_) & 1 & C_{tG} & C_{qVV}^{(8)} & C_{qAA}^{(8)} & C_{qAV}^{(8)} & C_{qVA}^{(8)} \\
\hline
1 & 0.0259519 & 0.00764032 & 3.40346 & 0 & 0 & 0 \\
C_{tG} & 0.00764032 & 0.826076 & 1.00989 & 0 & 0 & 0 \\
C_{qVV}^{(8)} & 3.40346 & 1.00989 & 449.868 & 0 & 0 & 0 \\
C_{qAA}^{(8)} & 0 & 0 & 0 & 449.456 & 0 & 0 \\
C_{qAV}^{(8)} & 0 & 0 & 0 & 0 & 449.456 & 0 \\
C_{qVA}^{(8)} & 0 & 0 & 0 & 0 & 0 & 449.868 \\
C_{qVV}^{(1)} & 0.494112 & 0 & 0 & 0 & 0 & 0 \\
C_{qAA}^{(1)} & 0.353864 & 0 & 0 & 0 & 0 & 0 \\
C_{qAV}^{(1)} & -0.144144 & 0 & 0 & 0 & 0 & 0 \\
C_{qVA}^{(1)} & -0.144276 & 0 & 0 & 0 & 0 & 0
\end{array}
\right.
$$

$$
\left.
\begin{array}{cccc}
C_{qVV}^{(1)} & C_{qAA}^{(1)} & C_{qAV}^{(1)} & C_{qVA}^{(1)} \\
\hline
0.494112 & 0.353864 & -0.144144 & -0.144276 \\
0 & 0 & 0 & 0 \\
0 & 0 & 0 & 0 \\
0 & 0 & 0 & 0 \\
0 & 0 & 0 & 0 \\
0 & 0 & 0 & 0 \\
2024.41 & 0 & 0 & 0 \\
0 & 2022.55 & 0 & 0 \\
0 & 0 & 2022.55 & 0 \\
0 & 0 & 0 & 2024.41
\end{array}
\right) \quad \text{pbarn}
$$

$$\sigma_{d\bar{d}\to t\bar{t}} =$$

$\Sigma\,(\_\cdot\_)$	1	C_{tG}	$C_{qVV}^{(8)}$	$C_{qAA}^{(8)}$	$C_{qAV}^{(8)}$	$C_{qVA}^{(8)}$	$C_{qVV}^{(1)}$	$C_{qAA}^{(1)}$	$C_{qAV}^{(1)}$	$C_{qVA}^{(1)}$
1	0.025902	0.00764032	3.40346	0	0	0	−0.319194	−0.353864	0.249004	0.144276
C_{tG}	0.00764032	0.826076	1.00989	0	0	0	0	0	0	0
$C_{qVV}^{(8)}$	3.40346	1.00989	449.868	0	0	0	0	0	0	0
$C_{qAA}^{(8)}$	0.	0	0	449.456	0	0	0	0	0	0
$C_{qAV}^{(8)}$	0.	0	0	0	449.456	0	0	0	0	0
$C_{qVA}^{(8)}$	0.	0	0	0	0	449.868	0	0	0	0
$C_{qVV}^{(1)}$	−0.319194	0	0	0	0	0	2024.41	0	0	0
$C_{qAA}^{(1)}$	−0.353864	0	0	0	0	0	0	2022.55	0	0
$C_{qAV}^{(1)}$	0.249004	0	0	0	0	0	0	0	2022.55	0
$C_{qVA}^{(1)}$	0.144276	0	0	0	0	0	0	0	0	2024.41

pbarn

Also here, as in the previous Section, the typical SM values utilised to calculate each total cross section are reported in Appendix C.

The symbol "$\Sigma\,(\_\cdot\_)$" was used to indicate the following quadratic expression:

$$\sigma_{\text{SMEFT}} \equiv \sigma_{\text{SM}} + 2\sum_i C_i \frac{\sigma_i}{\Lambda^2} + \sum_{i,j} C_i C_j \frac{\sigma_{ij}}{\Lambda^4},$$

where
$$C_i, C_j \in \begin{cases} \{C_{tG}, C_G, C_{\phi G}\} & \text{for} \quad gg \to t\bar{t} \\ \{C_{tG}, C_{qVV}^{(x)}, C_{qAA}^{(x)}, C_{qAV}^{(x)}, C_{qVA}^{(x)}\} & \text{for} \quad u\bar{u}/d\bar{d} \to t\bar{t} \end{cases},$$

Analysing the above values, it seems clear that for the σ_{SMEFT} all the non-zero terms should be considered, i.e. the interference terms σ_i/Λ^2 and also the quadratic terms σ_{ij}/Λ^4, at least with the parameters here used and with the here chosen energy scale $\Lambda = 1000$ GeV . The contribution of quadratic terms becomes negligible for energy scale $\Lambda \gg 1000$ GeV .

Particle collision in boosted CMF - parton interaction of proton collision

Also in this case to calculate the total cross section considering the parton distribution within the proton (PDF) we can apply the factorisation theorem:

$$\sigma_{pp \to X_1 X_2 \to t\bar{t}} = \int_0^1 dx_1 \, pdf_{X_1}\left(x_1, \mu_F^2\right) \int_0^1 dx_2 \, pdf_{X_2}\left(x_2, \mu_F^2\right) \, \sigma_{X_1 X_2 \to t\bar{t}}(x_1, x_2, E) \, , \qquad (2.3.2.5)$$

Here we present the values of the total cross section of both processes $pp \to gg \to t\bar{t}$ and $pp \to u\bar{u}/d\bar{d} \to t\bar{t}$ (evaluated by the proper PDF) at $E_{\text{beam}} = 7000$ GeV and at SMEFT energy scale of $\Lambda = 1000$ GeV , expressed by the quadratic form "$\Sigma\,(\_\cdot\_)$" of Wilson coefficients:

$$\sigma_{pp \to gg \to t\bar{t}} =$$

$\Sigma\,(\_\cdot\_)$	1	C_{tG}	C_G	$C_{\phi G}$
1	744.640	189.119	27.3203	-5.99650
C_{tG}	189.119	116.656	49.6421	2.00712
C_G	27.3203	49.6421	225.551	0
$C_{\phi G}$	-5.99650	2.00712	0	1.51565

pbarn

$$\sigma_{pp \to u\bar{u} \to t\bar{t}} =$$

$\Sigma\,(\_\cdot\_)$	1	C_{tG}	$C_{qVV}^{(8)}$	$C_{qAA}^{(8)}$	$C_{qAV}^{(8)}$	$C_{qVA}^{(8)}$	$C_{qVV}^{(1)}$	$C_{qAA}^{(1)}$	$C_{qAV}^{(1)}$	$C_{qVA}^{(1)}$
1	26.3977	5.85966	4.94647	0	0	0	0.654012	0.256850	-0.104626	-0.195674
C_{tG}	5.85966	1.75184	1.18408	0	0	0	0	0	0	0
$C_{qVV}^{(8)}$	4.94647	1.18408	2.28230	0	0	0	0	0	0	0
$C_{qAA}^{(8)}$	0	0	0	1.82203	0	0	0	0	0	0
$C_{qAV}^{(8)}$	0	0	0	0	1.82203	0	0	0	0	0
$C_{qVA}^{(8)}$	0	0	0	0	0	2.28230	0	0	0	0
$C_{qVV}^{(1)}$	0.654012	0	0	0	0	0	10.2704	0	0	0
$C_{qAA}^{(1)}$	0.256850	0	0	0	0	0	0	8.19914	0	0
$C_{qAV}^{(1)}$	-0.104626	0	0	0	0	0	0	0	8.19914	0
$C_{qVA}^{(1)}$	-0.195674	0	0	0	0	0	0	0	0	10.2704

pbarn

$$\sigma_{pp\to d\bar{d}\to t\bar{t}} = \left(\begin{array}{c|cccccc}
\Sigma(\_\cdot\_) & 1 & C_{tG} & C_{qVV}^{(8)} & C_{qAA}^{(8)} & C_{qAV}^{(8)} & C_{qVA}^{(8)} \\
\hline
1 & 16.9912 & 3.77374 & 3.14296 & 0 & 0 & 0 \\
C_{tG} & 3.77374 & 1.11787 & 0.750507 & 0 & 0 & 0 \\
C_{qVV}^{(8)} & 3.14296 & 0.750507 & 1.37490 & 0 & 0 & 0 \\
C_{qAA}^{(8)} & 0 & 0 & 0 & 1.08316 & 0 & 0 \\
C_{qAV}^{(8)} & 0 & 0 & 0 & 0 & 1.08316 & 0 \\
C_{qVA}^{(8)} & 0 & 0 & 0 & 0 & 0 & 1.37490 \\
C_{qVV}^{(1)} & -0.269980 & 0 & 0 & 0 & 0 & 0 \\
C_{qAA}^{(1)} & -0.161363 & 0 & 0 & 0 & 0 & 0 \\
C_{qAV}^{(1)} & 0.113547 & 0 & 0 & 0 & 0 & 0 \\
C_{qVA}^{(1)} & 0.124382 & 0 & 0 & 0 & 0 & 0
\end{array}\right.$$

$$\left.\begin{array}{cccc}
C_{qVV}^{(1)} & C_{qAA}^{(1)} & C_{qAV}^{(1)} & C_{qVA}^{(1)} \\
-0.269980 & -0.161363 & 0.113547 & 0.124382 \\
0 & 0 & 0 & 0 \\
0 & 0 & 0 & 0 \\
0 & 0 & 0 & 0 \\
0 & 0 & 0 & 0 \\
0 & 0 & 0 & 0 \\
6.18703 & 0 & 0 & 0 \\
0 & 4.87422 & 0 & 0 \\
0 & 0 & 4.87422 & 0 \\
0 & 0 & 0 & 6.18703
\end{array}\right) \text{pbarn}$$

The values utilised to calculate the total cross section are the same as used before in the CMF fixed frame: Appendix C. In particular, to implement the calculation with the PDF it is used the NNPDF MATHEMATICA interface with the specific "NNPDF23_lo_as_0130_qed_mem0" value grid.

Also in this case, for the σ_{SMEFT} all the non-zero terms should be considered, i.e. the interference terms σ_i/Λ^2 and also the quadratic terms σ_{ij}/Λ^4, at least with the parameters here used and with the here chosen energy scale $\Lambda = 1000$ GeV .

Chapter 3

MADGRAPH SIMULATIONS

To check the correctness of the formulae obtained in the previous chapter regarding the differential cross sections distribution and the total cross sections, we can compare the calculated results for a fixed energy beam of collision with the data obtained by simulations of the MADGRAPH5_aMC@NLO [25]. The version of MADGRAPH5_aMC@NLO here used is "2.8.0" dated 2020-08-21.

What is MadGraph? The MadGraph software and its actual version MadGraph 5, written in the Python programming language, is a Monte Carlo event generator for simulating particle collision experiments. It is currently being used extensively to simulate events at the LHC, as predicted by the SM. However, it is possible to extend the simulation model to other BSM theories and thus can also include the SMEFT models.

Through the generation of hard collision events, MadGraph enables the calculation of cross sections and, thanks to the integration with other analysis tools, allows the distribution of appropriate observable quantities.
Processes can be simulated with LO accuracy for any user-defined model, and with NLO accuracy in the case of models that support this type of calculation.
The **MadGraph5_aMCNLO** is the current version of the MadGraph software family which includes both MadGraph5 and aMCNLO that unifies the LO and NLO lines of development of automated tools within the MadGraph family.

For SMEFT at LO simulations, MADGRAPH5_aMC@NLO can import an appropriate model that extends the SM. In this case, the Universal FeynRules Output (UFO) format **SMEFTsim** [26] [27] model is used. The SMEFTsim package contains a set of models written in FeynRules and pre-exported to the UFO format.

3.1 Differential cross sections

To analyse the differential cross section of a given observable, it is necessary to elaborate the *Les Houches event file* [28] generated by the MADGRAPH5_aMC@NLO simulation and tagged with the extension ".lha".

For the present scope, we have developed a MATHEMATICA procedure to extract from this .lha file the values (E, p_x, p_y, p_z) of each of the 10000 events generated by the MADGRAPH5_aMC@NLO default set. From each event then, it is easy to calculate the observable $(p_T, \text{y}, \eta, \theta)$ in the following way:

$$ p_T \equiv \sqrt{p_x^2 + p_y^2} $$

Transverse Momentum

$$ \text{y} \equiv \frac{1}{2} \log\left(\frac{E + p_z}{E - p_z} \right) $$

Rapidity

$$ \theta \equiv \arccos\left(\frac{p_z}{\sqrt{p_x^2 + p_y^2 + p_z^2}} \right) $$

Scattering Angle

$$ \eta \equiv \frac{1}{2} \log\left(\frac{\sqrt{p_x^2 + p_y^2 + p_z^2} + p_z}{\sqrt{p_x^2 + p_y^2 + p_z^2} - p_z} \right) $$

Pseudo-Rapidity

After that these calculated values are grouped for convenience into 40 bins, obtaining a distribution of the events relevant to the observable. This distribution could be then overlapped with the differential cross section coming from the models developed so far, and manipulated in the following way:

<u>continue distribution</u> (indicated by blue line in the graphics here reported)

$$ \left(\frac{\text{number of events}}{\text{total cross section}} \right) \cdot \left(\frac{\text{observable max variation}}{\text{number of bins}} \right) \cdot \left(\text{observable differential cross section} \right) $$

<u>discrete distribution</u> (indicated by blue points in the graphics here reported)

$$ \left(\frac{\text{number of events}}{\text{total cross section}} \right) \cdot \int\limits_{\substack{\text{within} \\ \text{the bin}}} \left(\text{observable differential cross section} \right) $$

Below is the overlap between what was calculated by the present work and the simulation result obtained by MADGRAPH5_aMC@NLO for the SM and SMEFT.

3.1.1 $gg \to t\bar{t}$ and $u\bar{u}/d\bar{d} \to t\bar{t}$ in CMF

SM & SMEFT @ LO $gg \to t\bar{t}$ **and** $u\bar{u}/d\bar{d} \to t\bar{t}$ **collision @** 7000 **GeV**

$gg \to t\bar{t}$ @ LO in SM

Transverse Momentum Distribution

Rapidity Distribution

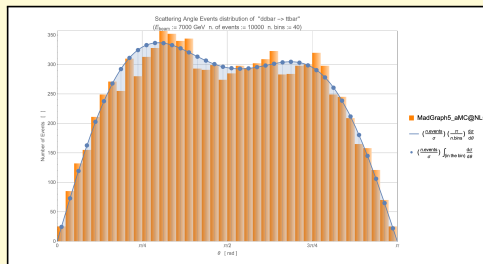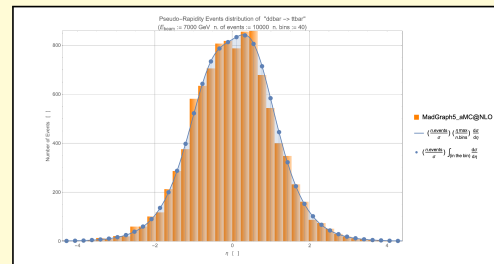Scattering Angle Distribution

Pseudo-Rapidity Distribution

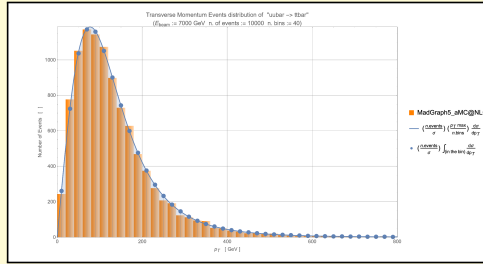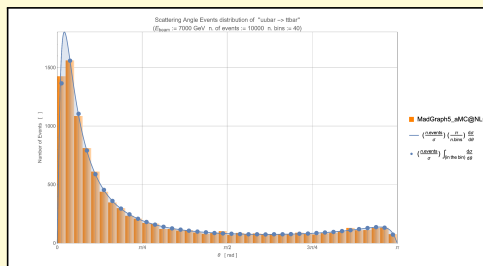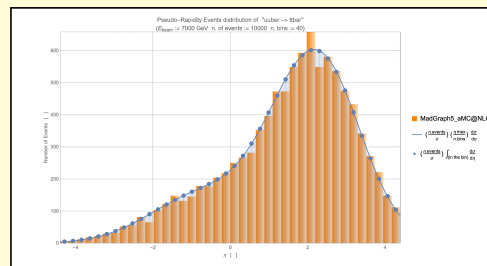$gg \to t\bar{t}$ @ LO in SMEFT with: $\Lambda = 1000$ GeV $C_{tG} = -0.0325$ $C_G = -0.0035$ $C_{\phi G} = 0.4$

Transverse Momentum Distribution

Rapidity Distribution

Scattering Angle Distribution

Pseudo-Rapidity Distribution
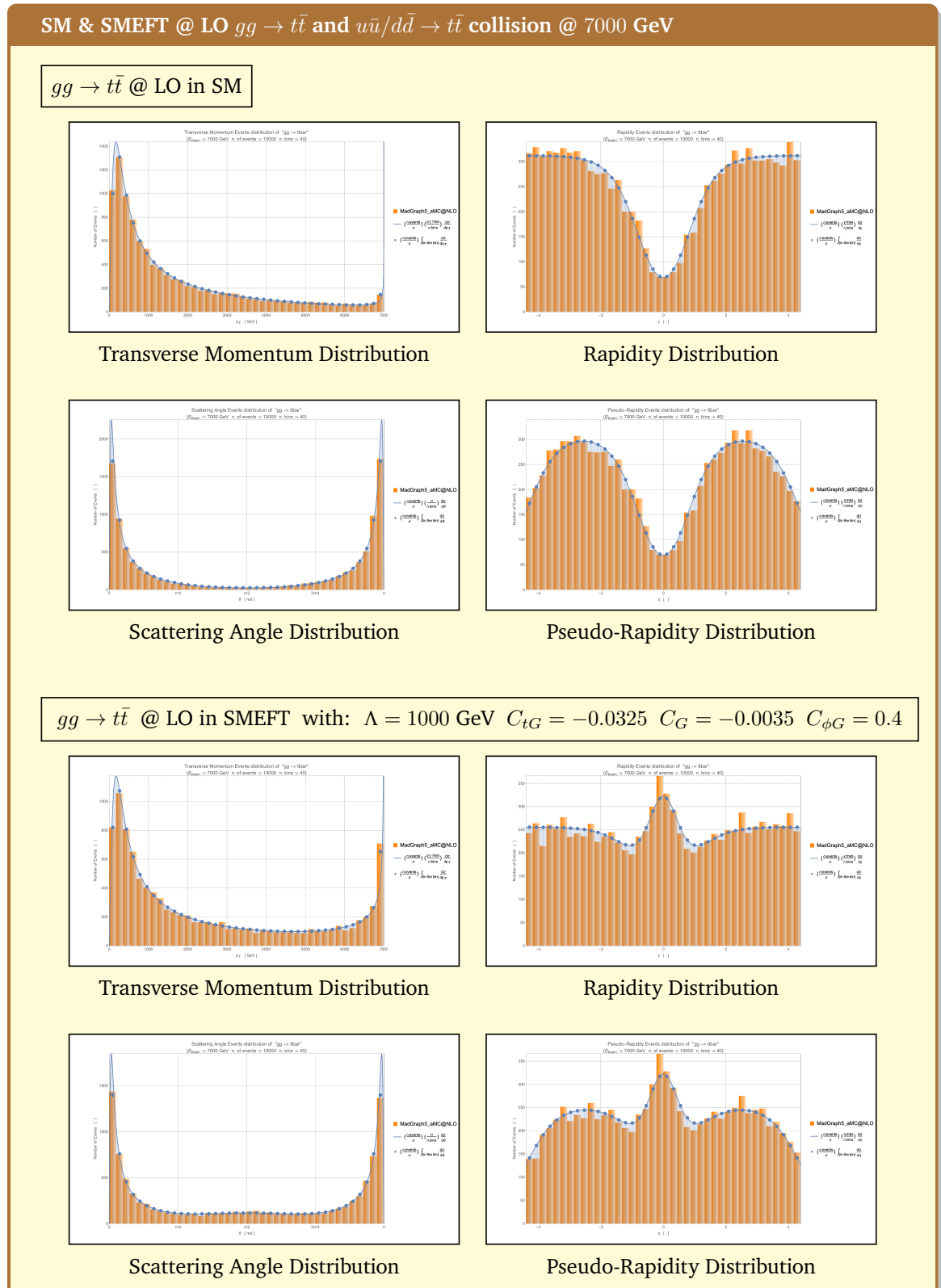
SM & SMEFT @ LO $gg \to t\bar{t}$ and $u\bar{u}/d\bar{d} \to t\bar{t}$ collision @ 7000 GeV

$u\bar{u} \to t\bar{t}$ @ LO in SM (QCD+QED+EW)
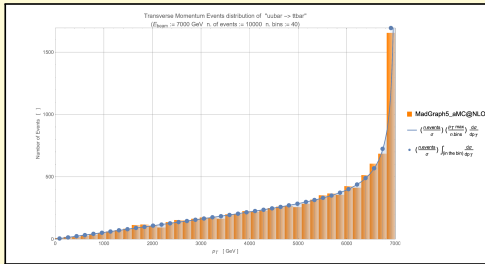
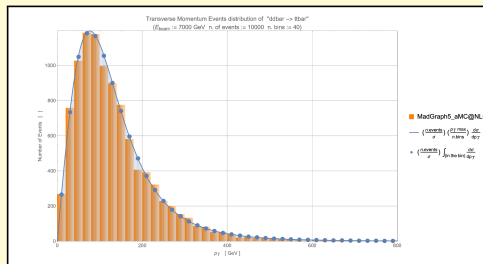

Transverse Momentum Distribution
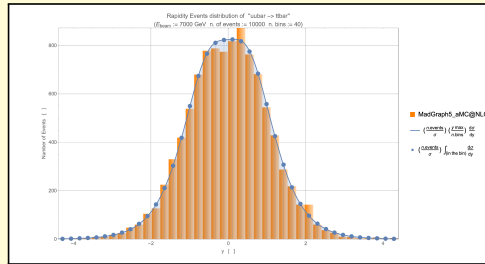
Rapidity Distribution
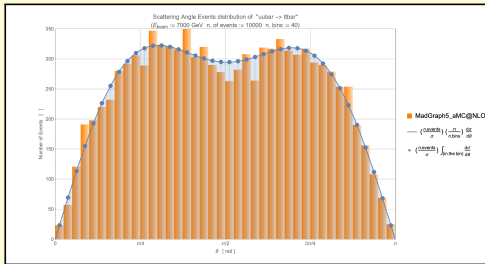
Scattering Angle Distribution
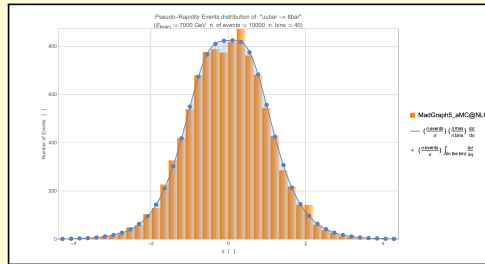
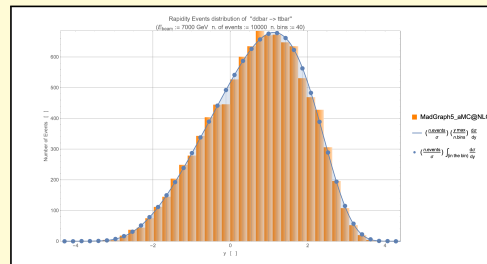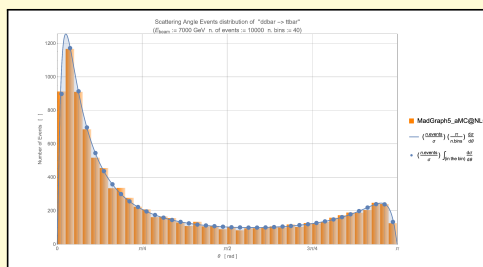
Pseudo-Rapidity Distribution

$u\bar{u} \to t\bar{t}$ @ LO in SMEFT with: $\Lambda = 1000$ GeV $C_{qAA}^{(8)} = 0.0002$ the other are set to zero
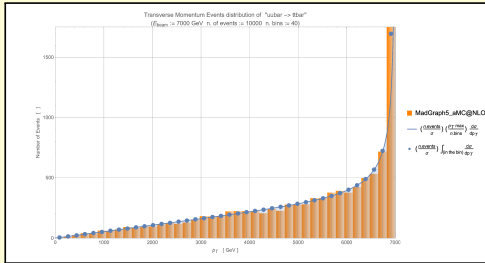
Transverse Momentum Distribution
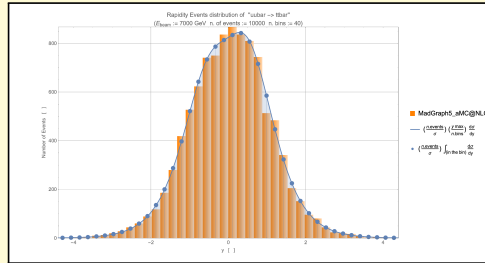
Rapidity Distribution
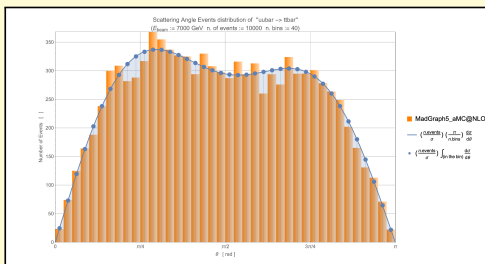
Scattering Angle Distribution
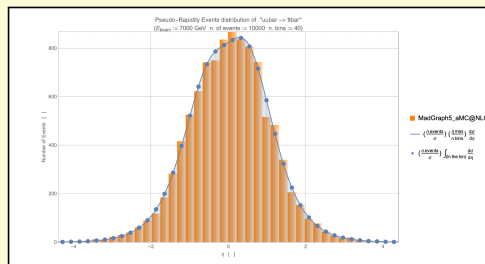
Pseudo-Rapidity Distribution

SM & SMEFT @ LO $gg \to t\bar{t}$ and $u\bar{u}/d\bar{d} \to t\bar{t}$ collision @ 7000 GeV

$d\bar{d} \to t\bar{t}$ @ LO in SM (QCD+QED+EW)
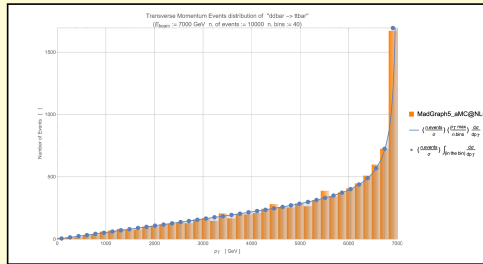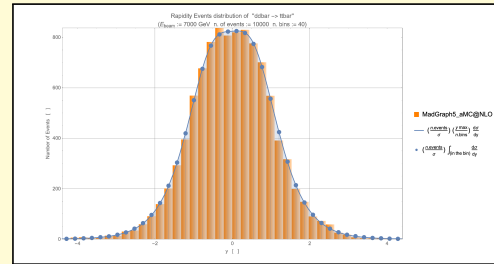
Transverse Momentum Distribution

Rapidity Distribution
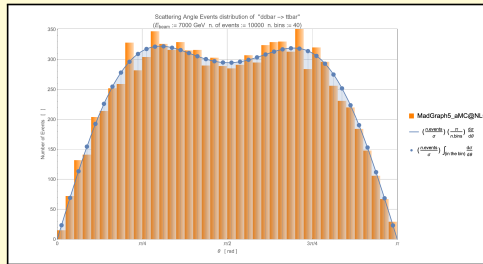
Scattering Angle Distribution
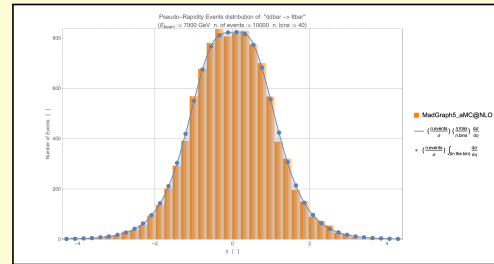
Pseudo-Rapidity Distribution

$d\bar{d} \to t\bar{t}$ @ LO in SMEFT with: $\Lambda = 1000$ GeV $C_{qAA}^{(8)} = 0.0002$ the other are set to zero
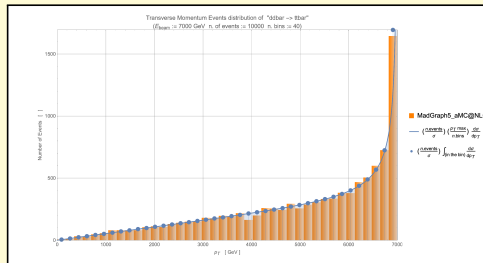
Transverse Momentum Distribution
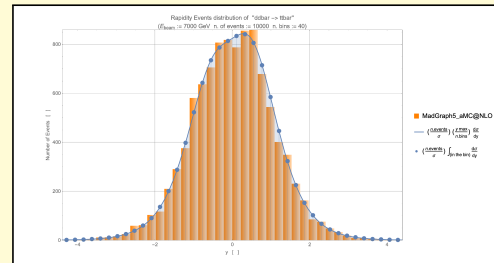
Rapidity Distribution

Scattering Angle Distribution

Pseudo-Rapidity Distribution

The above simulations are provided by the script reported in Appendix D

3.1.2 $gg \to t\bar{t}$ and $u\bar{u}/d\bar{d} \to t\bar{t}$ by proton collision

Collision @ $Ebeam$ 7000 GeV for $gg \to t\bar{t}$ and $u\bar{u}/d\bar{d} \to t\bar{t}$ in SM @ LO

$gg \to t\bar{t}$ @ LO in SM

Transverse Momentum Distribution

Rapidity Distribution

Scattering Angle Distribution

Pseudo-Rapidity Distribution
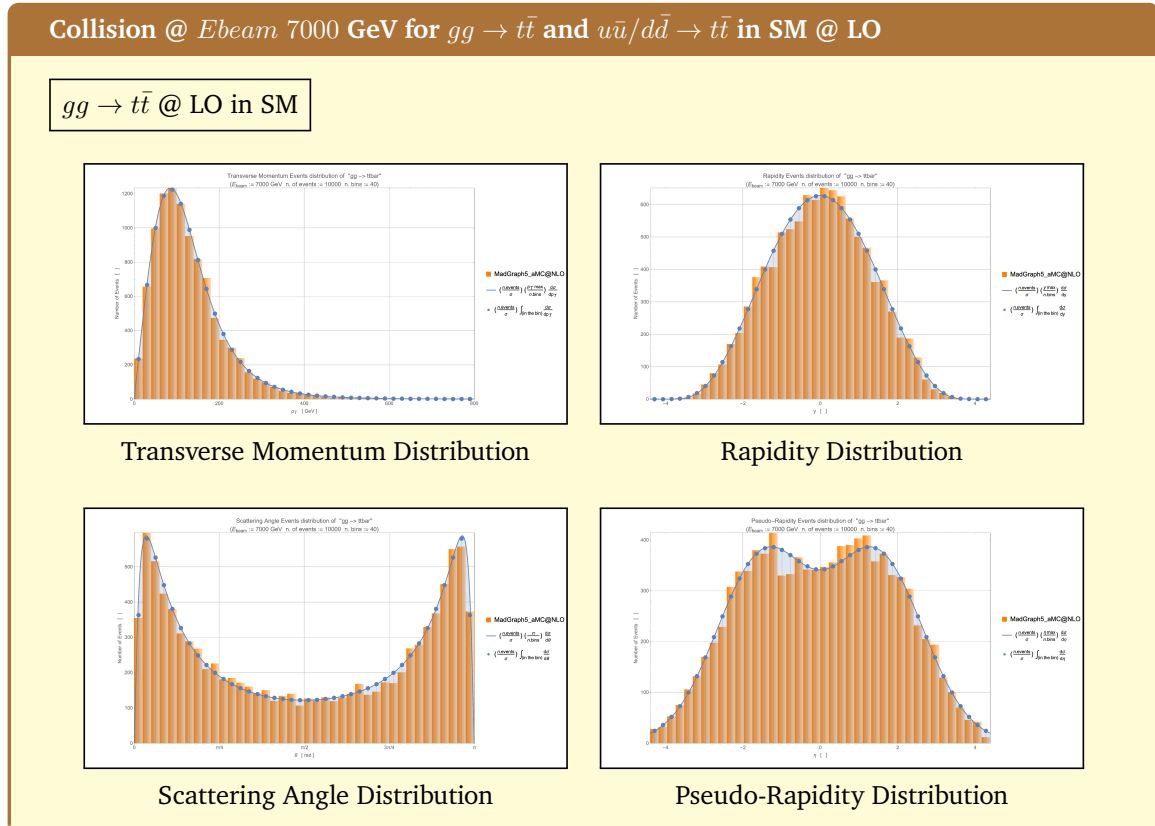
Collision @ E_{beam} 7000 GeV for $gg \to t\bar{t}$ and $u\bar{u}/d\bar{d} \to t\bar{t}$ in SM @ LO

$u\bar{u} \to t\bar{t}$ @ LO in SM QCD+QED+EW
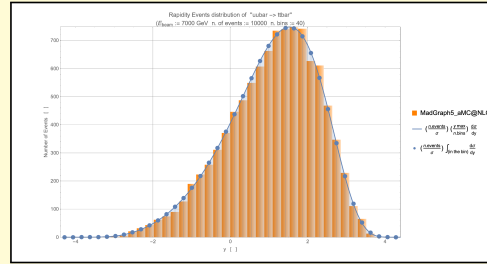
Transverse Momentum Distribution

Rapidity Distribution

Scattering Angle Distribution

Pseudo-Rapidity Distribution

$d\bar{d} \to t\bar{t}$ @ LO in SM QCD+QED+EW

Transverse Momentum Distribution

Rapidity Distribution

Scattering Angle Distribution
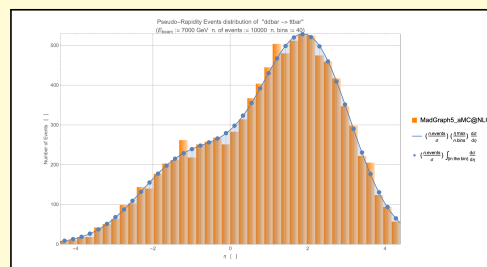
Pseudo-Rapidity Distribution

3.2   Total cross sections

SMEFT @ LO $gg \to t\bar{t}$ and $u\bar{u}/d\bar{d} \to t\bar{t}$ cross section elements @ 7000 GeV

$\boxed{gg \to t\bar{t} \text{ @ LO in SMEFT}}$

$$\begin{cases} \sigma_{\text{calculated}} \\ \sigma_{\textsc{MadGraph5\_aMC@NLO}} \end{cases} =$$

$\Sigma\,(\_\cdot\_)$	1	C_{tG}	C_G
1	$\begin{cases} \mathbf{2.03973 \cdot 10^{-1}} \\ \mathbf{(2.03960 \pm 0.00116) \cdot 10^{-1}} \end{cases}$	$\begin{cases} \mathbf{4.39190 \cdot 10^{-2}} \\ \mathbf{(4.38600 \pm 0.00891) \cdot 10^{-2}} \end{cases}$	$\begin{cases} \mathbf{1.63091 \cdot 10^{-2}} \\ \mathbf{(1.63360 \pm 0.00433) \cdot 10^{-2}} \end{cases}$
C_{tG}	...	$\begin{cases} \mathbf{2.78937 \cdot 10^{0}} \\ \mathbf{(2.79270 \pm 0.00475) \cdot 10^{0}} \end{cases}$	$\begin{cases} \mathbf{1.55642 \cdot 10^{0}} \\ \mathbf{(1.55600 \pm 0.00208) \cdot 10^{0}} \end{cases}$
C_G	...	...	$\begin{cases} \mathbf{2.53282 \cdot 10^{3}} \\ \mathbf{(2.53250 \pm 0.00337) \cdot 10^{3}} \end{cases}$
$C_{\phi G}$	...	...	...

$\Sigma\,(\_\cdot\_)$	$C_{\phi G}$	
1	$\begin{cases} \mathbf{-1.92548 \cdot 10^{-3}} \\ \mathbf{(-1.92720 \pm 0.00245) \cdot 10^{-3}} \end{cases}$	
C_{tG}	$\begin{cases} \mathbf{1.41646 \cdot 10^{-1}} \\ \mathbf{(1.41320 \pm 0.00129) \cdot 10^{-1}} \end{cases}$	pbarn
C_G	0	
$C_{\phi G}$	$\begin{cases} \mathbf{8.68756 \cdot 10^{-2}} \\ \mathbf{(8.67990 \pm 0.01210) \cdot 10^{-2}} \end{cases}$	

Where "..." indicates that the element is equal to its symmetric.

SMEFT @ LO $gg \to t\bar{t}$ and $u\bar{u}/d\bar{d} \to t\bar{t}$ cross section elements @ 7000 GeV

$\boxed{u\bar{u} \to t\bar{t} \text{ @ LO in SMEFT}}$

$$\begin{cases} \sigma_{\text{calculated}} \\ \sigma_{\text{MadGraph5\_aMC@NLO}} \end{cases} =$$

$\Sigma\,(\_\cdot\_)$	1	C_{tG}	$C_{uVV}^{(8)}$
1	$\begin{cases} \mathbf{2.59519 \cdot 10^{-2}} \\ \mathbf{(2.59260 \pm 0.00287) \cdot 10^{-2}} \end{cases}$	$\begin{cases} \mathbf{7.64032 \cdot 10^{-3}} \\ \mathbf{(7.63920 \pm 0.00851) \cdot 10^{-3}} \end{cases}$	$\begin{cases} \mathbf{3.40346 \cdot 10^{0}} \\ \mathbf{(3.40120 \pm 0.00410) \cdot 10^{0}} \end{cases}$
C_{tG}	...	$\begin{cases} \mathbf{8.26076 \cdot 10^{-1}} \\ \mathbf{(8.27440 \pm 0.01250) \cdot 10^{-1}} \end{cases}$	$\begin{cases} \mathbf{1.00989 \cdot 10^{0}} \\ \mathbf{(1.00960 \pm 0.00124) \cdot 10^{0}} \end{cases}$
$C_{uVV}^{(8)}$	...	...	$\begin{cases} \mathbf{4.49868 \cdot 10^{2}} \\ \mathbf{(4.49980 \pm 0.00664) \cdot 10^{2}} \end{cases}$
$C_{uAA}^{(8)}$	...	...	...
$C_{uAV}^{(8)}$	...	...	...
$C_{uVA}^{(8)}$	...	...	...
$C_{uVV}^{(1)}$	...	...	...
$C_{uAA}^{(1)}$	...	...	...
$C_{uAV}^{(1)}$	...	...	...
$C_{uVA}^{(1)}$	...	...	...

$\Sigma\,(\_\cdot\_)$	$C_{uAA}^{(8)}$	$C_{uAV}^{(8)}$	$C_{uVA}^{(8)}$
1	0	0	0
C_{tG}	0	0	0
$C_{uVV}^{(8)}$	0	0	0
$C_{uAA}^{(8)}$	$\begin{cases} \mathbf{4.49456 \cdot 10^{2}} \\ \mathbf{(4.49150 \pm 0.00730) \cdot 10^{2}} \end{cases}$	0	0
$C_{uAV}^{(8)}$	...	$\begin{cases} \mathbf{4.49456 \cdot 10^{2}} \\ \mathbf{(4.49290 \pm 0.00591) \cdot 10^{2}} \end{cases}$	0
$C_{uVA}^{(8)}$	...	...	$\begin{cases} \mathbf{4.49868 \cdot 10^{2}} \\ \mathbf{(4.50610 \pm 0.00704) \cdot 10^{2}} \end{cases}$
$C_{uVV}^{(1)}$	...	...	...
$C_{uAA}^{(1)}$	...	...	...
$C_{uAV}^{(1)}$	...	...	...
$C_{uVA}^{(1)}$	...	...	...

SMEFT @ LO $gg \to t\bar{t}$ and $u\bar{u}/d\bar{d} \to t\bar{t}$ cross section elements @ 7000 GeV

$\Sigma\,(\_\cdot\_)$	$C^{(1)}_{uVV}$	$C^{(1)}_{uAA}$	$C^{(1)}_{uAV}$
1	$\begin{cases} \mathbf{4.94112 \cdot 10^{-1}} \\ \mathbf{(4.94070 \pm 0.00644)\cdot 10^{-1}} \end{cases}$	$\begin{cases} \mathbf{3.53864 \cdot 10^{-1}} \\ \mathbf{(3.53890 \pm 0.00611)\cdot 10^{-1}} \end{cases}$	$\begin{cases} \mathbf{-1.44144 \cdot 10^{-1}} \\ \mathbf{(-1.44930 \pm 0.00743)\cdot 10^{-1}} \end{cases}$
C_{tG}	0	0	0
$C^{(8)}_{uVV}$	0	0	0
$C^{(8)}_{uAA}$	0	0	0
$C^{(8)}_{uAV}$	0	0	0
$C^{(8)}_{uVA}$	0	0	0
$C^{(1)}_{uVV}$	$\begin{cases} \mathbf{2.02441 \cdot 10^{3}} \\ \mathbf{(2.02370 \pm 0.00267)\cdot 10^{3}} \end{cases}$	0	0
$C^{(1)}_{uAA}$	...	$\begin{cases} \mathbf{2.02255 \cdot 10^{3}} \\ \mathbf{(2.02240 \pm 0.00253)\cdot 10^{3}} \end{cases}$	0
$C^{(1)}_{uAV}$	...	...	$\begin{cases} \mathbf{2.02255 \cdot 10^{3}} \\ \mathbf{(\ 2.02210 \pm 0.00247)\cdot 10^{3}} \end{cases}$
$C^{(1)}_{uVA}$	...	...	...

$\Sigma\,(\_\cdot\_)$	$C^{(1)}_{uVA}$	
1	$\begin{cases} \mathbf{-1.44276 \cdot 10^{-1}} \\ \mathbf{(-1.42330 \pm 0.00549)\cdot 10^{-1}} \end{cases}$	
C_{tG}	0	
$C^{(8)}_{uVV}$	0	
$C^{(8)}_{uAA}$	0	
$C^{(8)}_{uAV}$	0	pbarn
$C^{(8)}_{uVA}$	0	
$C^{(1)}_{uVV}$	0	
$C^{(1)}_{uAA}$	0	
$C^{(1)}_{uAV}$	0	
$C^{(1)}_{uVA}$	$\begin{cases} \mathbf{2.02441 \cdot 10^{3}} \\ \mathbf{(\ 2.02550 \pm 0.00253)\cdot 10^{3}} \end{cases}$	

Where "..." indicates that the element is equal to its symmetric.

SMEFT @ LO $gg \to t\bar{t}$ and $u\bar{u}/d\bar{d} \to t\bar{t}$ cross section elements @ 7000 GeV

$\boxed{d\bar{d} \to t\bar{t} \text{ @ LO in SMEFT}}$

$$\begin{cases} \sigma_{\text{calculated}} \\ \sigma_{\text{MadGraph5\_aMC@NLO}} \end{cases} =$$

$\Sigma\,(\_\cdot\_)$	1	C_{tG}	$C_{dVV}^{(8)}$
1	$\begin{cases} \mathbf{2.59020 \cdot 10^{-2}} \\ \mathbf{(2.58750 \pm 0.00333) \cdot 10^{-2}} \end{cases}$	$\begin{cases} \mathbf{7.64032 \cdot 10^{-3}} \\ \mathbf{(7.63920 \pm 0.00851) \cdot 10^{-3}} \end{cases}$	$\begin{cases} \mathbf{3.40346 \cdot 10^{0}} \\ \mathbf{(3.40430 \pm 0.00348) \cdot 10^{0}} \end{cases}$
C_{tG}	...	$\begin{cases} \mathbf{8.26076 \cdot 10^{-1}} \\ \mathbf{(8.27440 \pm 0.01250) \cdot 10^{-1}} \end{cases}$	$\begin{cases} \mathbf{1.00989 \cdot 10^{0}} \\ \mathbf{(1.00990 \pm 0.00177) \cdot 10^{0}} \end{cases}$
$C_{dVV}^{(8)}$	...	...	$\begin{cases} \mathbf{4.49868 \cdot 10^{2}} \\ \mathbf{(4.50260 \pm 0.01140) \cdot 10^{2}} \end{cases}$
$C_{dAA}^{(8)}$	...	...	...
$C_{dAV}^{(8)}$	...	...	...
$C_{dVA}^{(8)}$	...	...	...
$C_{dVV}^{(1)}$	...	...	...
$C_{dAA}^{(1)}$	...	...	...
$C_{dAV}^{(1)}$	...	...	...
$C_{dVA}^{(1)}$	...	...	...

$\Sigma\,(\_\cdot\_)$	$C_{dAA}^{(8)}$	$C_{dAV}^{(8)}$	$C_{dVA}^{(8)}$
1	0	0	0
C_{tG}	0	0	0
$C_{dVV}^{(8)}$	0	0	0
$C_{dAA}^{(8)}$	$\begin{cases} \mathbf{4.49456 \cdot 10^{2}} \\ \mathbf{(4.49750 \pm 0.01270) \cdot 10^{2}} \end{cases}$	0	0
$C_{dAV}^{(8)}$	...	$\begin{cases} \mathbf{4.49456 \cdot 10^{2}} \\ \mathbf{(4.50590 \pm 0.01110) \cdot 10^{2}} \end{cases}$	0
$C_{dVA}^{(8)}$	...	...	$\begin{cases} \mathbf{4.49868 \cdot 10^{2}} \\ \mathbf{(4.50830 \pm 0.01150) \cdot 10^{2}} \end{cases}$
$C_{dVV}^{(1)}$	...	...	...
$C_{dAA}^{(1)}$	...	...	...
$C_{dAV}^{(1)}$	...	...	...
$C_{dVA}^{(1)}$	...	...	...

SMEFT @ LO $gg \to t\bar{t}$ and $u\bar{u}/d\bar{d} \to t\bar{t}$ cross section elements @ 7000 GeV

$\Sigma\,(\_\cdot\_)$	$C^{(1)}_{dVV}$	$C^{(1)}_{dAA}$	$C^{(1)}_{dAV}$
1	$\begin{cases} -3.19194\cdot 10^{-1} \\ (-3.18940\pm 0.00506)\cdot 10^{-1} \end{cases}$	$\begin{cases} -3.53864\cdot 10^{-1} \\ (-3.53520\pm 0.00458)\cdot 10^{-1} \end{cases}$	$\begin{cases} 2.49004\cdot 10^{-1} \\ (2.49450\pm 0.00455)\cdot 10^{-1} \end{cases}$
C_{tG}	0	0	0
$C^{(8)}_{dVV}$	0	0	0
$C^{(8)}_{dAA}$	0	0	0
$C^{(8)}_{dAV}$	0	0	0
$C^{(8)}_{dVA}$	0	0	0
$C^{(1)}_{dVV}$	$\begin{cases} 2.02441\cdot 10^{3} \\ (\;2.02270\pm 0.00478)\cdot 10^{3} \end{cases}$	0	0
$C^{(1)}_{dAA}$	...	$\begin{cases} 2.02255\cdot 10^{3} \\ (\;2.02390\pm 0.00443)\cdot 10^{3} \end{cases}$	0
$C^{(1)}_{dAV}$	...	...	$\begin{cases} 2.02255\cdot 10^{3} \\ (2.02460\pm 0.00447)\cdot 10^{3} \end{cases}$
$C^{(1)}_{dVA}$	...	...	...

$\Sigma\,(\_\cdot\_)$	$C^{(1)}_{dVA}$	
1	$\begin{cases} 1.44276\cdot 10^{-1} \\ (1.45230\pm 0.00447)\cdot 10^{-1} \end{cases}$	
C_{tG}	0	
$C^{(8)}_{dVV}$	0	
$C^{(8)}_{dAA}$	0	
$C^{(8)}_{dAV}$	0	pbarn
$C^{(8)}_{dVA}$	0	
$C^{(1)}_{dVV}$	0	
$C^{(1)}_{dAA}$	0	
$C^{(1)}_{dAV}$	0	
$C^{(1)}_{dVA}$	$\begin{cases} 2.02441\cdot 10^{3} \\ (2.02050\pm 0.00482)\cdot 10^{3} \end{cases}$	

Where "..." indicates that the element is equal to its symmetric.

The total cross sections here calculated are in perfect agreement with the data obtained by the simulation of MADGRAPH5_aMC@NLO.

The above simulations are provided by the script reported in Appendix D.

CONCLUSIONS

As mentioned at the beginning of this thesis, astrophysical and cosmological observations, together with a number of theoretical arguments, suggest the existence of new physics beyond that currently described by the standard model of fundamental interactions. Among the many avenues to search for new physics is that of considering modifications of the interactions between the known particles and in particular among those whose mass resides at the EW scale. Among these, the top quark stands out due to its peculiar characteristics which can be studied in the experiments at the Large Hadron Collider (LHC), currently the largest energy accelerator in the world.

Given the information at hand, it is difficult to hypothesise a model that can describe phenomena not covered by the SM and at the same time explain all the current limitations and experimental observations, so it seems clear that an approach independent of the chosen theory may be more powerful. The effective theory of the Standard Model (SMEFT) can help with this. Indeed, by comparing predictions of such an effective theory to the high-precision data from the LHC, it is possible to constrain a quite general set of new models beyond the SM.

In this dissertation, we have considered the effects of the 6-dimensional SMEFT operators in the production of top quark-antiquark pairs in proton collisions at the LHC. The aim was to identify theoretical formulae for total and differential cross sections related to the relevant physical observables at the lowest order in perturbation theory.

We started by determining the matrix elements related to the SM and then introduced the contributions of the 6-dimensional operators of the SMEFT, expressed through the appropriate Feynman rules. The average square matrix element calculations, although not excessively complex, appear to be quite long and tedious, and for this purpose in the present work we made use of automatic tools provided by the FEYNCALC 9.3.1 package developed for the WOLFRAM MATHEMATICA environment. It should be noted that the $gg \to t\bar{t}$ process at LO level according to the SM is a process involving only strong interactions (QCD) and consequently the contributions of the 6-dimensional SMEFT operators also reflect the same characteristic. Whereas, as far as the and $q\bar{q} \to t\bar{t}$ process at the LO level is concerned, the SM also includes the contribution of electroweak interactions (Quantum Electro Dynamics: QED + Electro-Weak: EW), which obviously have a smaller incidence than the contributions of the strong interactions, but represent a useful and necessary correction that cannot be neglected if the models obtained are to be adapted to the high-precision data of the LHC. While not neglecting this part, the contributions of SMEFT operators related to this production channel have not been considered in this paper.

The effects of the 6-dimension SMEFT operators on the total and differential cross sections can be written in the following form:

$$\sigma_{\text{SMEFT}} \equiv \sigma_{\text{SM}} + 2 \sum_i C_i \frac{\sigma_i}{\Lambda^2} + \sum_{i,j} C_i C_j \frac{\sigma_{ij}}{\Lambda^4}.$$

Obviously, the second term is derived from the SMEFT operators interfering with the SM amplitude and goes as Λ^{-2}. The third term, on the other hand, derives from the square of the amplitude of the SMEFT operators and the mixed products of these and is further suppressed by the large scale Λ, going as Λ^{-4}. Because of this dependence, one might think that this term is negligible, however, on has to take into account also the weights σ_i and σ_{ij}.

In the case discussed here, at the collision energies ($E_{\text{beam}} = 7000$ GeV) and for the energy scale set ($\Lambda = 1000$ GeV), it is found that, given the current limits, the quadratic terms must also be included in the analysis. This situation occurs both at the parton level and with the Parton Distribution Functions (PDF).

A large part of the work in this thesis was devoted to comparing theoretically obtained data with the leading software for simulating particle collision events, MADGRAPH5_aMC@NLO, both using the SM rules and its 6-dimensional extension SMEFT, via the SMEFTsim package, which contains a series of models written in FeynRules and pre-exported in UFO format.

This comparison was carried out using MATHEMATICA routines, which acquired the data from MADGRAPH5. As far as the purely partonic process was concerned, the comparison was relatively easy and yielded results in agreement. Whereas for hadronic collision processes, the use of routines available in MATHEMATICA environment such as NNPDF2.3 and the use of embedded numerical integrations made the calculation more involved. Yet the comparison was successful and the validation of the analytic formulas was fully completed.

The original part of this work, i.e., the analytic computation of the squared terms, will be useful for further studies, e.g., the developments proposed in [29].

Appendix A

Feynman rules

In the QFT, the matrix element $\mathcal{M}$ of a scattering process is necessary to calculate the total cross section or the differential cross section relevant to an observable. The simplest way to compute the $i\mathcal{M}$ is obviously to analyse the scattering processes drawing its relevant Feynman diagram by using the following graphical Feynman rules. This method introduced by Richard Feynman in 1948, allowed a graphical representation of the mathematical expressions describing the behaviour and interaction of particle fields.

Feynman Rule 1 - External Lines: all the incoming and outcoming fermions or boson field particles of a process are represented by a peculiar line named *External Lines*. For the calculation of $i\mathcal{M}$ this means introducing a spinor for each fermion and a polarisation vector for each vector boson and eventually their colour status. For scalar bosons, no factor is needed.

Feynman Rule 2 - Internal Lines: all the virtual fields not observable in a process are drawn by specific lines named *Internal Lines*. For the calculation of $i\mathcal{M}$ this means introducing a relevant propagator factor.

Feynman Rule 3 - Vertices: to indicate all the possible interactions inside the event, *Vertices* between the lines are drawn. These interactions are the results of gauge principles, YM theory, BEH mechanism and Youkawa's coupling and could be deducted starting from the Lagrangian expression in the following way:

- search for all terms which contain a certain selection of the fields, e.g.:
$-ig\left(\partial_{\mu}A_{\nu}\right)A^{\mu}B^{\nu} = -ig\left(\partial_{\mu}A^{\rho}\right)g_{\nu\rho}A^{\mu}B^{\nu}$

- replace all derivatives by i times the incoming momenta of the respective fields in Fourier Transform:
$-ig\left(\partial_{\mu}A^{\rho}(a)\right)g_{\nu\rho}A^{\mu}\left(a'\right)B^{\nu}(b) \ \rightarrow \ -gq_{\mu}g_{\nu\rho}A^{\rho}(q)A^{\mu}\left(q'\right)B^{\nu}(p)$

- symmetrise indices of all identical boson fields:
$-gq_{\mu}g_{\nu\rho}A^{\rho}A^{\mu}B^{\nu} \ \rightarrow \ -g\left(q_{\mu}g_{\nu\rho} + q'_{\rho}g_{\mu\nu}\right)A^{\rho}(q)A^{\mu}(q')B^{\nu}(p)$

- multiply by i and at the end the Feynman vertex:

$$-ig\left(q_\mu g_{\nu\rho} + q'_\rho g_{\mu\nu}\right)$$

Feynman Rule 4 - Momentum Assignment and Loops: The momenta of external lines are fixed by experimental conditions. Then, at each vertex, the energy-momenta is conserved. The energy-momentum conservation constrains that the sum of all energy-momenta of external lines have to vanish assuming all the external momenta are inward going. It also fixes all the momenta for tree diagrams that do not contain loops. Each loop leaves one momentum unconstrained and has to be integrated, leading to divergent integrals. The integration includes a sum over spinor indices and polarisation, depending on the particle species that form the loop. For each closed fermion loop, an extra sign (-1) has to be attached. It is a result of the anti-commutativity of the fermion fields.

Here below the Feynman graphic rules for the SM Lagrangian. Most of the results and conventions used here refer to "Peskin" [30], "Nagashima" [31] and to [32]. For the last reference we have fixed $\eta_s = 1$, $\eta = -1$, $\eta_Y = 1/2$, $\eta_Z = 1$, $\eta_\theta = 1$, $\eta_e = -1$.

A.1   Incoming and outcoming fields: external lines

To take into account all the fields involved in a process or in an experiment, the following schemes are used, which represent all the incoming and outcoming particles:

incoming gluon:

$$\varepsilon^\mu_{A,a} \qquad\equiv\qquad \varepsilon^\mu_{A,a}(p) \quad \text{polarization vector}$$

outcoming gluon:

$$\varepsilon^{\mu*}_{A,a} \qquad\equiv\qquad \varepsilon^{\mu*}_{A,a}(p) \quad \text{polarization vector}$$

incoming photon:

$$\varepsilon^\mu_A \qquad\equiv\qquad \varepsilon^\mu_A(p) \quad \text{polarization vector}$$

outcoming photon:

$$\varepsilon^{\mu*}_A \qquad\equiv\qquad \varepsilon^{\mu*}_A(p) \quad \text{polarization vector}$$

incoming $W^\pm/Z^0$ boson:		$\equiv$	$\varepsilon_A^\mu(p)$	polarization vector
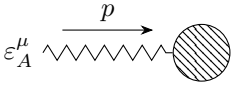
outcoming $W^\pm/Z^0$ boson:		$\equiv$	$\varepsilon_A^{\mu*}(p)$	polarization vector
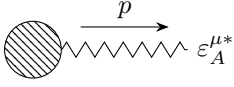
incoming fermion:		$\equiv$	$u_r^{\alpha,\iota}(p)$	spinor
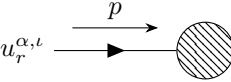
incoming antifermion:		$\equiv$	$\bar{v}_s^{\beta,\kappa}(p)$	spinor
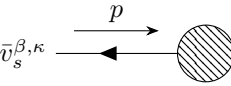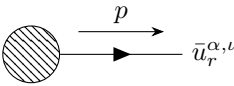
outcoming fermion:		$\equiv$	$\bar{u}_r^{\alpha,\iota}(p)$	spinor

outcoming antifermion:		$\equiv$	$v_s^{\beta,\kappa}(p)$	spinor
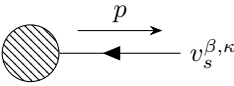
A.2 Propagators: internal lines

gluon propagator:
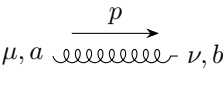
$$\mu,a\ \text{\Lleftarrow}\ \nu,b \quad \equiv \quad i\frac{-g^{\mu\nu}+(1-\xi)\frac{p^\mu p^\nu}{p^2+i0^+}}{p^2+i0^+}\delta^{ab}$$

photon propagator:
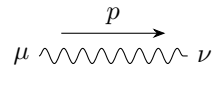
$$\mu\ \text{\Lleftarrow}\ \nu \quad \equiv \quad i\frac{-g^{\mu\nu}+(1-\xi)\frac{p^\mu p^\nu}{p^2+i0^+}}{p^2+i0^+}$$

$W^\pm/Z^0$ boson propagator:
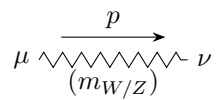
$$\mu\ \underset{(m_{W/Z})}{\text{\Lleftarrow}}\ \nu \quad \equiv \quad i\frac{-g^{\mu\nu}+(1-\xi)\frac{p^\mu p^\nu}{p^2-\xi m_{W/Z}^2+i0^+}}{p^2-m_{W/Z}^2+i0^+}$$

Higgs boson propagator:

$$\equiv \quad \frac{i}{p^2 - m_H^2 + i0^+}$$

fermion propagator:

$$\equiv \quad i\frac{(\not{p})_{\alpha\beta} + m_f}{p^2 - m_f^2 + i0^+}\delta_{\iota\kappa}$$
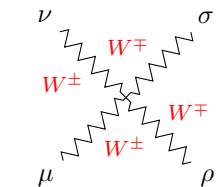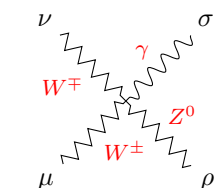
A.3   Interactions: SM vertices

3-gluon:
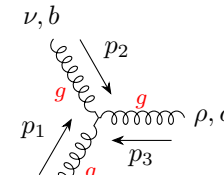
$$\equiv \quad g_s f^{abc}\begin{pmatrix} g^{\mu\nu}(p_1 - p_2)^\rho + \\ g^{\nu\rho}(p_2 - p_3)^\mu + \\ g^{\rho\mu}(p_3 - p_1)^\nu \end{pmatrix}$$

4-gluon:
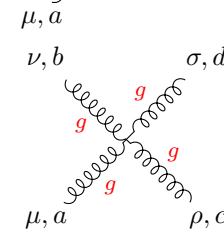
$$\equiv \quad -ig_s^2\begin{pmatrix} f^{abe}f^{cde}\left(g^{\mu\rho}g^{\nu\sigma} - g^{\mu\sigma}g^{\nu\rho}\right) + \\ f^{ace}f^{bde}\left(g^{\mu\nu}g^{\rho\sigma} - g^{\mu\sigma}g^{\rho\nu}\right) + \\ f^{ade}f^{bce}\left(g^{\mu\nu}g^{\sigma\rho} - g^{\mu\rho}g^{\sigma\nu}\right) \end{pmatrix}$$

2-$W^\pm$ boson - photon:
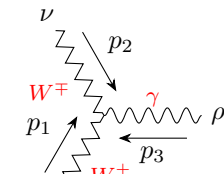
$$\equiv \quad ig_e\begin{pmatrix} g^{\mu\nu}(p_1 - p_2)^\rho + \\ g^{\nu\rho}(p_2 - p_3)^\mu + \\ g^{\rho\mu}(p_3 - p_1)^\nu \end{pmatrix}$$

2-$W^\pm$ boson - Z^0 boson:
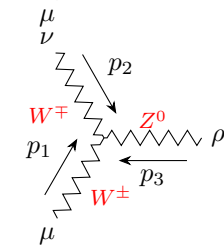
$$\equiv \quad ig_Z\cos^2\theta_W\begin{pmatrix} g^{\mu\nu}(p_1 - p_2)^\rho + \\ g^{\nu\rho}(p_2 - p_3)^\mu + \\ g^{\rho\mu}(p_3 - p_1)^\nu \end{pmatrix}$$

4-$W^\pm$ boson:

$$\equiv \quad i2g_W^2\begin{pmatrix} 2g^{\mu\nu}g^{\rho\sigma} + \\ -g^{\mu\rho}g^{\nu\sigma} + \\ -g^{\mu\sigma}g^{\nu\rho} \end{pmatrix}$$

2-$W^\pm$ boson - Z^0 boson - photon:

$$\equiv \quad -ig_e g_Z\cos^2\theta_W\begin{pmatrix} 2g^{\mu\nu}g^{\rho\sigma} + \\ -g^{\mu\rho}g^{\nu\sigma} + \\ -g^{\mu\sigma}g^{\nu\rho} \end{pmatrix}$$

2-$W^\pm$ boson - 2-photon:
$$\equiv \quad -ig_e \begin{pmatrix} 2g^{\mu\nu}g^{\rho\sigma}+ \\ -g^{\mu\rho}g^{\nu\sigma}+ \\ -g^{\mu\sigma}g^{\nu\rho} \end{pmatrix}$$

2-$W^\pm$ boson - 2-Z^0 boson:
$$\equiv \quad -ig_Z^2 \cos^4\theta_W \begin{pmatrix} 2g^{\mu\nu}g^{\rho\sigma}+ \\ -g^{\mu\rho}g^{\nu\sigma}+ \\ -g^{\mu\sigma}g^{\nu\rho} \end{pmatrix}$$

2-quark - gluon:
$$\equiv \quad ig_s(\gamma^\mu)_{\alpha\beta}(\tau^a)_{\iota\kappa} \quad \text{same flavor quarks}$$

2-fermion - photon:
$$\equiv \quad ig_e\left(\gamma^\mu \mathcal{Q}(f)\right)_{\alpha\beta} \delta_{\iota\kappa} \quad \text{same flavor fermions}$$

2-fermion - Z^0 boson:
$$\equiv \quad ig_Z\left(\gamma^\mu \frac{\mathcal{Q}_V(f)-\mathcal{Q}_A(f)\gamma^5}{2}\right)_{\alpha\beta}\delta_{\iota\kappa} \quad \text{same lepton families}$$

2-lepton - $W^\pm$ boson:
$$\equiv \quad ig_W\left(\gamma^\mu \frac{1-\gamma^5}{2}\right)_{\alpha\beta} \quad \text{same lepton families}$$
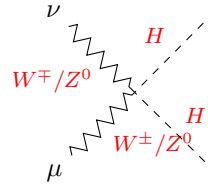
2-quark - $W^\pm$ boson:
$$\equiv \quad ig_W\left(\gamma^\mu \frac{1-\gamma^5}{2}\right)_{\alpha\beta} \begin{cases} V_{q_u q_d} \\ V_{q_u q_d}^* \end{cases} \delta_{\iota\kappa}$$
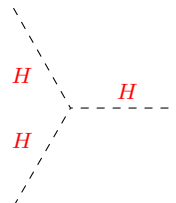
2-$W^\pm/Z^0$ boson - Higgs boson:
$$\equiv \quad i\frac{m_{W/Z}^2}{v}g^{\mu\nu}$$
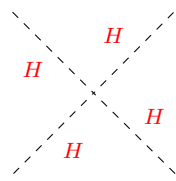
2-$W^\pm/Z^0$ boson - Higgs boson:

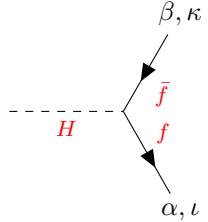$$\equiv\; 2i\frac{m_{W/Z}^2}{v^2}g^{\mu\nu}$$

3-Higgs boson:

$$\equiv\; -3i\frac{m_H^2}{v}$$

4-Higgs boson:

$$\equiv\; -3i\frac{m_H^2}{v^2}$$

2-fermion - Higgs boson:

$$\equiv\; -i\frac{m_f}{v}\delta_{\iota\kappa}\quad\text{same flavor fermions}$$

A.4 Interactions: 6-dimension SMEFT vertices interesting the $gg/q\bar{q}\rightarrow t\bar{t}$ processes
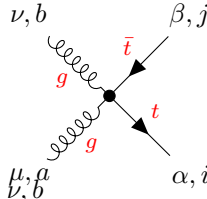
The new 6-dimension SMEFT operators introduce new Feynman rules, in particular, the operator $\mathcal{O}_{tG}$ changes the SM $gt\bar{t}$ coupling and also generates a new $ggt\bar{t}$ interaction. $\mathcal{O}_G$ affects the three-point gluon vertex in QCD. $\mathcal{O}_{\phi G}$ generates a new diagram with an s-channel Higgs boson. The 14 four-quarks operators generate a new vertex $q\bar{q}t\bar{t}$. We have checked the here presented rules with the "Dedes article" [33], but with the conventions used in "Peskin" [30] and "Cen Zhang article" [17]. In particular, attention is focused on the extension of the SM that preserves CP symmetry, thus assuming that all Wilson coefficients are real and thus neglecting CP-violating interactions as proposed in the article by "I.Brivio et All" [18]. Taking Wilson coefficients as real and denoting by v the vacuum expectation value, the following Feynman rules are obtained:
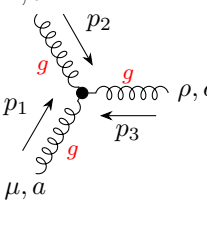
2 tops - gluon:
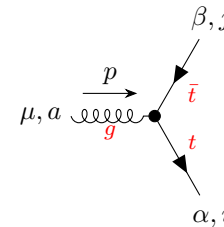
$$\equiv\; -i\sqrt{2}\frac{vC_{tG}}{\Lambda^2}(\tau^a)_{ij}\left(\left[\gamma^\mu\mid\slashed{p}\right]\right)_{\alpha\beta}$$

2 quarks - 2 gluons:

$$\equiv \quad -i\sqrt{2}g_s \frac{vC_{tG}}{\Lambda^2}\left(\left[\tau^a \mid \tau^b\right]\right)_{ij}\left(\left[\gamma^\mu \mid \gamma^\nu\right]\right)_{\alpha\beta}$$

3 gluons:

$$\equiv \quad -6\frac{C_G}{\Lambda^2}f^{abc}\Big(p_3^\mu p_1^\nu p_2^\rho - p_2^\mu p_3^\nu p_1^\rho +$$
$$+ g^{\mu\nu}\Big(p_1^\rho\left(p_2\cdot p_3\right) - p_2^\rho\left(p_1\cdot p_3\right)\Big)+$$
$$+ g^{\nu\rho}\Big(p_2^\mu\left(p_1\cdot p_3\right) - p_3^\mu\left(p_1\cdot p_2\right)\Big)+$$
$$+ g^{\rho\mu}\Big(p_3^\nu\left(p_1\cdot p_2\right) - p_1^\nu\left(p_2\cdot p_3\right)\Big)\Big)$$

2 gluons - Higgs:
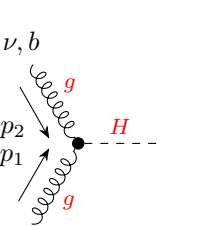
$$\equiv \quad 2i\frac{vC_{\phi G}}{\Lambda^2}\delta^{ab}\Big(p_1^\nu p_2^\mu - (p_1\cdot p_2)g^{\mu\nu}\Big)$$

4 quarks:

$$\equiv$$
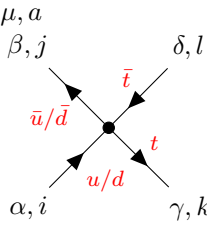
$$\equiv \quad i\left(\frac{C_{Qq}^{(8,1)}\pm C_{Qq}^{(8,3)}}{\Lambda^2}\left(\tau^a\right)_{ij}\left(\tau_a\right)_{kl} + \frac{C_{Qq}^{(1,1)}\pm C_{Qq}^{(1,3)}}{\Lambda^2}\delta_{ij}\delta_{kl}\right)\left(\gamma^6\gamma^\mu\gamma^7\right)_{\beta\alpha}\left(\gamma^6\gamma_\mu\gamma^7\right)_{\gamma\delta} +$$

$$+ i\left(\frac{C_{tu/d}^{(8)}}{\Lambda^2}\left(\tau^a\right)_{ij}\left(\tau_a\right)_{kl} + \frac{C_{tu/d}^{(1)}}{\Lambda^2}\delta_{ij}\delta_{kl}\right)\left(\gamma^7\gamma^\mu\gamma^6\right)_{\beta\alpha}\left(\gamma^7\gamma_\mu\gamma^6\right)_{\gamma\delta} +$$

$$+ i\left(\frac{C_{Qu/d}^{(8)}}{\Lambda^2}\left(\tau^a\right)_{ij}\left(\tau_a\right)_{kl} + \frac{C_{Qu/d}^{(1)}}{\Lambda^2}\delta_{ij}\delta_{kl}\right)\left(\gamma^7\gamma^\mu\gamma^6\right)_{\beta\alpha}\left(\gamma^6\gamma_\mu\gamma^7\right)_{\gamma\delta} +$$

$$+ i\left(\frac{C_{tq}^{(8)}}{\Lambda^2}\left(\tau^a\right)_{ij}\left(\tau_a\right)_{kl} + \frac{C_{tq}^{(1)}}{\Lambda^2}\delta_{ij}\delta_{kl}\right)\left(\gamma^6\gamma^\mu\gamma^7\right)_{\beta\alpha}\left(\gamma^7\gamma_\mu\gamma^6\right)_{\gamma\delta}$$

A.5   Conventions used for Feynman rules

Here the following conventions are used:

- p, p_1, p_2, p_3 are various momenta vectors;

- $m_{W/Z/H}$, m_f are respectively the mass of the involved $W^\pm/Z^0/H$ bosons and f fermions where

$$\begin{cases} m_W \equiv gv/2 & W^\pm \text{ boson mass} \\ m_Z \equiv \sqrt{g^2 + g'^2}\,v/2 = m_W/\cos\theta_W & Z^0 \text{ boson mass} \\ m_H \equiv \sqrt{2}\mu = \sqrt{2\lambda}v & H \text{ boson mass} \\ m_{f=\nu_l} \equiv 0 & \nu_l \text{ neutrino mass} \\ m_{f=l} \equiv v/\sqrt{2}\,\text{diag}(y^{(L)})_l & l \text{ lepton mass} \\ m_{f=q} \equiv v/\sqrt{2}\,\text{diag}(U_{(U/D)}^{-1}y^{(U/D)}V_{(U/D)})_q & q \text{ quark mass} \end{cases} \quad ;$$

- μ, ν, ρ, σ are Lorentzian space-time indices;
- A, B are two-value indices to identify the two polarisation states of physical vector bosons;
- a, b, c are eight-values indices to identify the eight colour status of gluons;
- α, β are spinorial indices;
- r, s are two-value indices to identify the two spin-states polarisation of fermions;
- ι, κ are three-values indices to identify the three colour status of quarks;
- g_s is the strong interaction coupling parameter;
- $g_e \equiv g\sin\theta_W$ is the electromagnetic interaction coupling parameter;
- $\mathcal{Q}(f)$ is the fermion electric charge where

$$\mathcal{Q}(f) \equiv \begin{cases} 0 & f = \text{neutrino/anti-neutrino} \\ \mp 1 & f = \text{lepton/anti-lepton} \\ \pm 2/3 & f = \text{up/anti-up quark} \\ \mp 1/3 & f = \text{down/anti-down quark} \end{cases} ;$$

- $g_W \equiv g/\sqrt{2}$ is the $W^{\pm}$ bosons weak interaction coupling parameter;
- $g_Z \equiv g/\cos\theta_W$ is the Z^0 boson weak interaction coupling parameter and $\mathcal{Q}_V(f)$ and $\mathcal{Q}_A(f)$ the relevant vector and axial coefficients, where

$$\mathcal{Q}_V(f) \equiv \begin{cases} +1/2 & f \in \{\nu_e\nu_\mu\nu_\tau\} \\ -1/2 + 2\sin^2\theta_W & f \in \{e,\mu,\tau\} \\ +1/2 - 4/3\sin^2\theta_W & f \in \{u,c,t\} \\ -1/2 + 2/3\sin^2\theta_W & f \in \{d,s,b\} \end{cases}$$

$$\mathcal{Q}_A(f) \equiv \begin{cases} +1/2 & f \in \{\nu_e\nu_\mu\nu_\tau, u,c,t\} \\ -1/2 & f \in \{e,\mu,\tau,d,s,b\} \end{cases}$$

- ξ is the gauge choice that for simplicity, but without loss of generality one can always put $\xi = 1$, named Feynman gauge;
- γ^μ are the four Dirac Gamma matrices;
- τ^a are the eight Gell-Mann matrices divided by 2;
- f^{abc} are the structure constants.

Appendix B

Dirac Gamma matrices properties

Here below some properties of Gamma matrices and their traces, useful for average squared matrix element calculation.

- $\{\gamma^\mu \mid \gamma^\nu\} = 2g^{\mu\nu}$ $\implies$ $\{\not p \mid \not q\} = 2(p \cdot q)$ $\implies$ $\not p \not p = p^2$

- $\gamma_\mu \gamma^\mu = 4$

- $\gamma_\mu \gamma^\alpha \gamma^\mu = -2\gamma^\alpha$ $\implies$ $\gamma_\mu \not p \gamma^\mu = -2\not p$

- $\gamma_\mu \gamma^\alpha \gamma^\beta \gamma^\mu = 4g^{\alpha\beta}$ $\implies$ $\gamma_\mu \not p \not q \gamma^\mu = 4(p \cdot q)$

- $\gamma_\mu \gamma^\alpha \gamma^\beta \gamma^\gamma \gamma^\mu = -2\gamma^\gamma \gamma^\beta \gamma^\alpha$ $\implies$ $\gamma_\mu \not p \not q \not k \gamma^\mu = -2\not k \not q \not p$

- $(\gamma^\mu)^\dagger = \gamma^0 \gamma^\mu \gamma^0$

- $\text{tr}[1] = 4$

- $\text{tr}[\gamma^\mu \gamma^\nu] = 4g^{\mu\nu}$ $\implies$ $\text{tr}[\not p \not q] = 4(p \cdot q)$

- $\text{tr}[\gamma^\mu \gamma^\nu \gamma^\rho \gamma^\sigma] = 4\left(g^{\mu\nu}g^{\rho\sigma} - g^{\mu\rho}g^{\nu\sigma} + g^{\mu\sigma}g^{\nu\rho}\right)$ $\implies$ $\text{tr}[\not p \not q \not k \not h] = 4\big((p \cdot q)(k \cdot h) - (p \cdot k)(q \cdot h) + (p \cdot h)(q \cdot k)\big)$

- $\text{tr}[\text{odd number of } \gamma] = \text{tr}[\text{odd number of } /] = 0$

Appendix C

Values of the SM parameters used

The values of the SM parameters used for each calculation and plot are the following:

$$
\begin{aligned}
(\hbar c)^2 &= 0.3893793721 \cdot 10^9 \text{ GeV}^2\text{pbarn} &&\text{natural constant} \\
m_t &= 173.000 \text{ GeV} &&\text{top quark mass} \\
m_Z &= 91.188 \text{ GeV} &&\text{Z boson mass} \\
m_W &= 80.419 \text{ GeV} &&\text{W boson mass} \\
\alpha &= 1/132.507 &&\text{electromagnetic constant} \\
G_F &= 1.16639 \cdot 10^{-5} \text{ GeV}^{-2} &&\text{Fermi's constant} \\
\alpha_s &= 0.118 &&\text{strong constant} \\
m_H &= 125.000 \text{ GeV} &&\text{Higgs boson mass} \\
\\
g_e &= \sqrt{4\pi\alpha} &&\text{QED coupling constant} \\
g_s &= \sqrt{4\pi\alpha_s} &&\text{QCD coupling constant} \\
v &= 1/\sqrt{\sqrt{2}\,G_F} &&\text{vacuum expectation value} \\
\sin^2(\theta_W) &= \pi\alpha/(\sqrt{2}G_F m_W^2) &&\text{squared sine of Weinberg angle} \\
g_Z &= 2\,m_Z/v &&\text{weak charge for the Z} \\
\mathcal{Q}_V(t/u) &= +1/2 - 4/3\,\sin^2(\theta_W) &&\text{vector coefficient for top and up quarks} \\
\mathcal{Q}_A(t/u) &= +1/2 &&\text{axial coefficient for top and up quarks} \\
\mathcal{Q}_V(d) &= -1/2 + 2/3\,\sin^2(\theta_W) &&\text{vectorial coefficient for down quark} \\
\mathcal{Q}_A(d) &= -1/2 &&\text{axial coefficient for down quark}
\end{aligned}
$$

where all the numerical values are fixed as per MadGraph5_aMC@NLO 'param_card.dat' default set.

We have to take into account that $\{\alpha, G_F, m_Z, m_W\}$ are not fully independent, the following relations are valid:

$$
\begin{cases}
m_W = \dfrac{m_Z}{\sqrt{2}}\sqrt{1 + \sqrt{1 - \dfrac{2\sqrt{2}\pi\alpha}{G_F m_Z^2}}} & \text{in case of \textbf{"Alpha scheme"}, where } \{G_F, m_Z, \alpha\} \text{ are fixed;} \\
\\
\alpha = \dfrac{\sqrt{2}G_F m_W^2}{\pi}\left(1 - \dfrac{m_W^2}{m_Z^2}\right) & \text{in case of \textbf{"Mw scheme"}, where } \{G_F, m_Z, m_W\} \text{ are fixed.}
\end{cases}
$$

Appendix D

MADGRAPH5_aMC@NLO script listings

To launch the desired process simulation by the MADGRAPH5_aMC@NLO the efficient way is to develop a script file with the proper MADGRAPH5_aMC@NLO instructions.

Here below the macOS bash file ("mg5py2_RUN_with_mg5_input.sh") used to launch the MADGRAPH5_aMC@NLO program ("mg5_aMC") in python2 ambient with a script file ("mg5_input.txt"), which give the instructions for the simulation:

"mg5py2_RUN_with_mg5_input.sh": MADGRAPH5_aMC@NLO (mg5_aMC) bash file

```
#!/bin/sh
python2 /Users/leonardoguidetti/mg5amcnlo/bin/mg5_aMC
↪    /Users/leonardoguidetti/Documents/MadGraph/MadGraph5/Work/mg5_input.txt
```

Here below is the script file used for the process simulations.

D.1 Script for differential cross sections simulation

"mg5_input.txt": SM & SMEFT @ LO $gg \to t\bar{t}$ and $u\bar{u}/d\bar{d} \to t\bar{t}$ collision @ 7000 GeV - MADGRAPH5_aMC@NLO (mg5_aMC) input script file

```
##########################################################################
##### SM & SMEFT gg/uubar/ddbar -> ttbar parton collisions @ 7000 GeV #####
##########################################################################
```

"mg5_input.txt": SM & SMEFT @ LO $gg \to t\bar{t}$ and $u\bar{u}/d\bar{d} \to t\bar{t}$ collision @ 7000 GeV - MadGraph5_aMC@NLO (mg5_aMC) input script file

```
import model SMEFTsim_top_MwScheme_UFO


### gg ################################################################

set automatic_html_opening True

generate g g > t t~ QCD<=2 QED<=2 NP<=1 SMHLOOP=0 NPshifts=0 NPprop=0 NPcpv=0 @1

output /Users/.../MadGraph5/Simulations/Collision_SM-SMEFT/gg -f

launch -n SM
#-- 'param_card.dat' --#
set mt 173.000
set mz 91.1880
set mw 80.4190
set mh 125.000
set md 0
set mu 0
set gf 1.16639e-05
set as 0.11800
#-- Wilson Coefficients --#
set ctGRe  0
set cG     0
set cHG    0
#-- 'run_card.dat' --#
set lpp1 0
set lpp2 0
set ebeam1 7000
set ebeam2 7000
set fixed_ren_scale true
set fixed_fac_scale true
#set use_syst False
done

launch -n SMEFT
#-- Wilson Coefficients --#
set ctGRe  0
set cG     0.001
set cHG    0.425
done

#open index.html


### uubar ###########################################################
```

"mg5_input.txt": SM & SMEFT @ LO $gg \to t\bar{t}$ **and** $u\bar{u}/d\bar{d} \to t\bar{t}$ **collision @ 7000 GeV -** **MADGRAPH5_aMC@NLO (mg5_aMC) input script file**

```
set automatic_html_opening True

generate u u~ > t t~ /H QCD<=2 QED<=2 NP<=1 SMHLOOP=0 NPshifts=0 NPprop=0 NPcpv=0
↪   NPcuG=0 NPctB=0 NPctW=0 NPcHl3=0 NPcll1=0 NPcHDD=0 NPcHWB=0
    NPcHt=0 NPcHQ1=0 NPcHQ3=0 NPcHu=0 NPcHj1=0 NPcHj3=0 @2

output /Users/.../MadGraph5/Simulations/Collision_SM-SMEFT/uubar -f

launch -n SM
#-- 'param_card.dat' --#
set mt 173.000
set mz 91.1880
set mw 80.4190
set mh 125.000
set md 0
set mu 0
set gf 1.16639e-05
set as 0.11800
#-- Wilson Coefficients --#
set ctGRe  0
set cQj18  0
set cQj38  0
set ctu8   0
set cQu8   0
set ctj8   0
set cQj11  0
set cQj31  0
set ctu1   0
set cQu1   0
set ctj1   0
#-- 'run_card.dat' --#
set lpp1 0
set lpp2 0
set ebeam1 7000
set ebeam2 7000
set fixed_ren_scale true
set fixed_fac_scale true
#set use_syst False
done

launch -n SMEFT
#-- Wilson Coefficients --#
set ctGRe  0
set cQj18  0.0001
set cQj38  0.0001
set ctu8   0.0002
```

"mg5_input.txt": SM & SMEFT @ LO $gg \to t\bar{t}$ and $u\bar{u}/d\bar{d} \to t\bar{t}$ collision @ 7000 GeV - MADGRAPH5_aMC@NLO (mg5_aMC) input script file

```
set cQu8   -0.0002
set ctj8   -0.0002
set cQj11  0
set cQj31  0
set ctu1   0
set cQu1   0
set ctj1   0
done


#open index.html



### ddbar ###############################################################

set automatic_html_opening True

generate d d~ > t t~ /H QCD<=2 QED<=2 NP<=1 SMHLOOP=0 NPshifts=0 NPprop=0 NPcpv=0
→   NPcuG=0 NPctB=0 NPctW=0 NPcHl3=0 NPcll1=0 NPcHDD=0 NPcHWB=0
    NPcHt=0 NPcHQ1=0 NPcHQ3=0 NPcHu=0 NPcHj1=0 NPcHj3=0 @3

output /Users/.../MadGraph5/Simulations/Collision_SM-SMEFT/ddbar -f

launch -n SM
#-- 'param_card.dat' --#
set mt 173.000
set mz 91.1880
set mw 80.4190
set mh 125.000
set md 0
set mu 0
set gf 1.16639e-05
set as 0.11800
#-- Wilson Coefficients --#
set ctGRe  0
set cQj18  0
set cQj38  0
set ctd8   0
set cQd8   0
set ctj8   0
set cQj11  0
set cQj31  0
set ctd1   0
set cQd1   0
set ctj1   0
#-- 'run_card.dat' --#
set lpp1 0
set lpp2 0
```

"mg5_input.txt": SM & SMEFT @ LO $gg \to t\bar{t}$ **and** $u\bar{u}/d\bar{d} \to t\bar{t}$ **collision @ 7000 GeV - MADGRAPH5_aMC@NLO (mg5_aMC) input script file**

```
set ebeam1 7000
set ebeam2 7000
set fixed_ren_scale true
set fixed_fac_scale true
#set use_syst False
done

launch -n SMEFT
#-- Wilson Coefficients --#
set ctGRe  0
set cQj18  0.0003
set cQj38  0.0001
set ctd8   0.0002
set cQd8   -0.0002
set ctj8   -0.0002
set cQj11  0
set cQj31  0
set ctd1   0
set cQd1   0
set ctj1   0
done


#open index.html


! cp /Users/leonardoguidetti/Documents/MadGraph/MadGraph5/Work/mg5_input.txt
↪  /Users/.../MadGraph5/Simulations/Collision_SM-SMEFT
```

D.2   Script for total cross sections simulation

"mg5_input.txt": SMEFT @ LO $gg \to t\bar{t}$ **and** $u\bar{u}/d\bar{d} \to t\bar{t}$ **total cross section elements @ 7000 GeV - MADGRAPH5_aMC@NLO (mg5_aMC) input script file**

```
################################################################################
## SMEFT gg/uubar/ddbar -> ttbar total cross section elements @ 7000 GeV ##
################################################################################



import model SMEFTsim_top_MwScheme_UFO



### gg ####################################################################
```

"mg5_input.txt": SMEFT @ LO $gg \to t\bar{t}$ **and** $u\bar{u}/d\bar{d} \to t\bar{t}$ **total cross section elements @ 7000 GeV - MADGRAPH5_AMC@NLO (mg5_aMC) input script file**

```
### gg SM ###

set automatic_html_opening True

generate g g > t t~ QCD<=2 QED<=2 NP=0 SMHLOOP=0 NPshifts=0 NPprop=0 NPcpv=0
↪   @1

output /Users/.../MadGraph5/Simulations/Sigma_Elements_SMEFT/gg/1_SM -f

launch -n SM
#-- 'param_card.dat' --#
set mt 173.000
set mz 91.1880
set mw 80.4190
set mh 125.000
set md 0
set mu 0
set gf 1.16639e-05
set as 0.11800
#-- Wilson Coefficients --#
set ctGRe   0
set cG      0
set cHG     0
#-- 'run_card.dat' --#
set lpp1 0
set lpp2 0
set ebeam1 7000
set ebeam2 7000
set fixed_ren_scale true
set fixed_fac_scale true
#set use_syst False
done

launch -i
print_results
↪   -path=/Users/.../MadGraph5/Simulations/Sigma_Elements_SMEFT/sigma_gg_1.txt
exit


### gg first row ###
```

"mg5_input.txt": SMEFT @ LO $gg \to t\bar{t}$ and $u\bar{u}/d\bar{d} \to t\bar{t}$ total cross section elements @ 7000 GeV - MadGraph5_aMC@NLO (mg5_aMC) input script file

```
set automatic_html_opening True

generate g g > t t~ QCD<=2 QED<=2 NP<=1 NP^2==1 SMHLOOP=0 NPshifts=0
↪   NPprop=0 NPcpv=0 @2

output /Users/.../MadGraph5/Simulations/Sigma_Elements_SMEFT/gg/2_firstrow
↪   -f

launch -n CtG
#-- 'param_card.dat' --#
set mt 173.000
set mz 91.1880
set mw 80.4190
set mh 125.000
set md 0
set mu 0
set gf 1.16639e-05
set as 0.11800
#-- Wilson Coefficients --#
set ctGRe -1
set cG     0
set cHG    0
#-- 'run_card.dat' --#
set lpp1 0
set lpp2 0
set ebeam1 7000
set ebeam2 7000
set fixed_ren_scale true
set fixed_fac_scale true
#set use_syst False
done
launch -n CG
#-- Wilson Coefficients --#
set ctGRe  0
set cG    -0.5
set cHG    0
done
launch -n CHG
#-- Wilson Coefficients --#
set ctGRe  0
set cG     0
set cHG    0.25
done
```

"mg5_input.txt": SMEFT @ LO $gg \to t\bar{t}$ and $u\bar{u}/d\bar{d} \to t\bar{t}$ total cross section elements @ 7000 GeV - MadGraph5_aMC@NLO (mg5_aMC) input script file

```
launch -i
print_results
↪   -path=/Users/.../MadGraph5/Simulations/Sigma_Elements_SMEFT/sigma_gg_2.txt
exit


### gg diagonal ###

set automatic_html_opening True

generate g g > t t~ QCD<=2 QED<=2 NP==1 SMHLOOP=0 NPshifts=0 NPprop=0
↪   NPcpv=0 @3

output /Users/.../MadGraph5/Simulations/Sigma_Elements_SMEFT/gg/3_diagonal
↪   -f

launch -n CtG^2
#-- 'param_card.dat' --#
set mt 173.000
set mz 91.1880
set mw 80.4190
set mh 125.000
set md 0
set mu 0
set gf 1.16639e-05
set as 0.11800
#-- Wilson Coefficients --#
set ctGRe -2
set cG     0
set cHG     0
#-- 'run_card.dat' --#
set lpp1 0
set lpp2 0
set ebeam1 7000
set ebeam2 7000
set fixed_ren_scale true
set fixed_fac_scale true
#set use_syst False
done

launch -n CG^2
#-- Wilson Coefficients --#
```

"mg5_input.txt": SMEFT @ LO $gg \to t\bar{t}$ and $u\bar{u}/d\bar{d} \to t\bar{t}$ total cross section elements @ 7000 GeV - MADGRAPH5_aMC@NLO (mg5_aMC) input script file

```
set ctGRe   0
set cG     -1
set cHG     0
done


launch -n CHG^2
#-- Wilson Coefficients --#
set ctGRe   0
set cG      0
set cHG    0.5
done
launch -i
print_results
→  -path=/Users/.../MadGraph5/Simulations/Sigma_Elements_SMEFT/sigma_gg_3.txt
exit



### gg interferences ###


set automatic_html_opening True


generate g g > t t~ QCD<=2 QED<=2 NP<=1 NP^2==2 NPctG^2==1 SMHLOOP=0
→  NPshifts=0 NPprop=0 NPcpv=0 @4

output
→  /Users/.../MadGraph5/Simulations/Sigma_Elements_SMEFT/gg/4_interferences
→  -f

launch -n CtGxCG
#-- 'param_card.dat' --#
set mt 173.000
set mz 91.1880
set mw 80.4190
set mh 125.000
set md 0
set mu 0
set gf 1.16639e-05
set as 0.11800
#-- Wilson Coefficients --#
set ctGRe -1
set cG     -1
set cHG     0
#-- 'run_card.dat' --#
```

"mg5_input.txt": SMEFT @ LO $gg \to t\bar{t}$ and $u\bar{u}/d\bar{d} \to t\bar{t}$ total cross section elements @ 7000 GeV - MADGRAPH5_aMC@NLO (mg5_aMC) input script file

```
set lpp1 0
set lpp2 0
set ebeam1 7000
set ebeam2 7000
set fixed_ren_scale true
set fixed_fac_scale true
#set use_syst False
done

launch -n CtGxCHG
#-- Wilson Coefficients --#
set ctGRe -1
set cG     0
set cHG    0.5
done
launch -i
print_results
↪   -path=/Users/.../MadGraph5/Simulations/Sigma_Elements_SMEFT/sigma_gg_4.txt
exit




### uubar
↪   ##########################################################################


### uubar SM ###

set automatic_html_opening True

generate u u~ > t t~ /H QCD<=2 QED<=2 NP=0 SMHLOOP=0 NPshifts=0 NPprop=0
↪   NPcpv=0 NPcuG=0 NPctB=0 NPctW=0 NPcHl3=0 NPcll1=0 NPcHDD=0 NPcHWB=0
    NPcHt=0 NPcHQ1=0 NPcHQ3=0 NPcHu=0 NPcHj1=0 NPcHj3=0

output /Users/.../MadGraph5/Simulations/Sigma_Elements_SMEFT/uubar/1_SM -f

launch -n SM
#-- 'param_card.dat' --#
set mt 173.000
set mz 91.1880
set mw 80.4190
set mh 125.000
set md 0
```

"mg5_input.txt": SMEFT @ LO $gg \to t\bar{t}$ and $u\bar{u}/d\bar{d} \to t\bar{t}$ total cross section elements @ 7000 GeV - MADGRAPH5_aMC@NLO (mg5_aMC) input script file

```
set mu 0
set gf 1.16639e-05
set as 0.11800
#-- Wilson Coefficients --#
set ctGRe  0
set cQj18  0
set cQj38  0
set ctu8   0
set cQu8   0
set ctj8   0
set cQj11  0
set cQj31  0
set ctu1   0
set cQu1   0
set ctj1   0
#-- 'run_card.dat' --#
set lpp1 0
set lpp2 0
set ebeam1 7000
set ebeam2 7000
set fixed_ren_scale true
set fixed_fac_scale true
#set use_syst False
done

launch -i
print_results
→   -path=/Users/.../MadGraph5/Simulations/Sigma_Elements_SMEFT/sigma_uubar_1.txt
exit


### uubar first row ###

set automatic_html_opening True

generate u u~ > t t~ /H QCD<=2 QED<=2 NP<=1 NP^2==1 SMHLOOP=0 NPshifts=0
→   NPprop=0 NPcpv=0 NPcuG=0 NPctB=0 NPctW=0 NPcHl3=0 NPcll1=0 NPcHDD=0
    NPcHWB=0 NPcHt=0 NPcHQ1=0 NPcHQ3=0 NPcHu=0 NPcHj1=0 NPcHj3=0

output
→   /Users/.../MadGraph5/Simulations/Sigma_Elements_SMEFT/uubar/2_firstrow
→   -f
```

"mg5_input.txt": SMEFT @ LO $gg \to t\bar{t}$ and $u\bar{u}/d\bar{d} \to t\bar{t}$ total cross section elements @ 7000 GeV - MadGraph5_aMC@NLO (mg5_aMC) input script file

```
launch -n CtG
#-- 'param_card.dat' --#
set mt 173.000
set mz 91.1880
set mw 80.4190
set mh 125.000
set md 0
set mu 0
set gf 1.16639e-05
set as 0.11800
#-- Wilson Coefficients --#
set ctGRe -1
set cQj18  0
set cQj38  0
set ctu8   0
set cQu8   0
set ctj8   0
set cQj11  0
set cQj31  0
set ctu1   0
set cQu1   0
set ctj1   0
#-- 'run_card.dat' --#
set lpp1 0
set lpp2 0
set ebeam1 7000
set ebeam2 7000
set fixed_ren_scale true
set fixed_fac_scale true
#set use_syst False
done

launch -n CuVV8
#-- Wilson Coefficients --#
set ctGRe  0
set cQj18  0.25
set cQj38  0.25
set ctu8   0.5
set cQu8   0.5
set ctj8   0.5
set cQj11  0
set cQj31  0
set ctu1   0
```

"mg5_input.txt": SMEFT @ LO $gg \to t\bar{t}$ and $u\bar{u}/d\bar{d} \to t\bar{t}$ total cross section elements @ 7000 GeV - MADGRAPH5_aMC@NLO (mg5_aMC) input script file

```
set cQu1   0
set ctj1   0
done

launch -n CuVV1
#-- Wilson Coefficients --#
set ctGRe  0
set cQj18  0
set cQj38  0
set ctu8   0
set cQu8   0
set ctj8   0
set cQj11  0.25
set cQj31  0.25
set ctu1   0.5
set cQu1   0.5
set ctj1   0.5
done

launch -n CuAA1
#-- Wilson Coefficients --#
set ctGRe  0
set cQj18  0
set cQj38  0
set ctu8   0
set cQu8   0
set ctj8   0
set cQj11  0.25
set cQj31  0.25
set ctu1   0.5
set cQu1   -0.5
set ctj1   -0.5
done

launch -n CuAV1
#-- Wilson Coefficients --#
set ctGRe  0
set cQj18  0
set cQj38  0
set ctu8   0
set cQu8   0
set ctj8   0
set cQj11  -0.25
```

"mg5_input.txt": SMEFT @ LO $gg \to t\bar{t}$ **and** $u\bar{u}/d\bar{d} \to t\bar{t}$ **total cross section elements @ 7000 GeV - MadGraph5_aMC@NLO (mg5_aMC) input script file**

```
set cQj31 -0.25
set ctu1   0.5
set cQu1  -0.5
set ctj1   0.5
done


launch -n CuVA1
#-- Wilson Coefficients --#
set ctGRe  0
set cQj18  0
set cQj38  0
set ctu8   0
set cQu8   0
set ctj8   0
set cQj11 -0.25
set cQj31 -0.25
set ctu1   0.5
set cQu1   0.5
set ctj1  -0.5
done


launch -i
print_results
↪   -path=/Users/.../MadGraph5/Simulations/Sigma_Elements_SMEFT/sigma_uubar_2.txt
exit



### uubar diagonal ###


set automatic_html_opening True


generate u u~ > t t~ /H QCD<=2 QED<=2 NP==1 SMHLOOP=0 NPshifts=0 NPprop=0
↪   NPcpv=0 NPcuG=0 NPctB=0 NPctW=0 NPcHl3=0 NPcll1=0 NPcHDD=0 NPcHWB=0
    NPcHt=0 NPcHQ1=0 NPcHQ3=0 NPcHu=0 NPcHj1=0 NPcHj3=0 NPctG^2==2

add process u u~ > t t~ /H QCD<=2 QED<=2 NP==1 SMHLOOP=0 NPshifts=0 NPprop=0
↪   NPcpv=0 NPcuG=0 NPctB=0 NPctW=0 NPcHl3=0 NPcll1=0 NPcHDD=0 NPcHWB=0
    NPcHt=0 NPcHQ1=0 NPcHQ3=0 NPcHu=0 NPcHj1=0 NPcHj3=0 NPcQj18^2==2

add process u u~ > t t~ /H QCD<=2 QED<=2 NP==1 SMHLOOP=0 NPshifts=0 NPprop=0
↪   NPcpv=0 NPcuG=0 NPctB=0 NPctW=0 NPcHl3=0 NPcll1=0 NPcHDD=0 NPcHWB=0
    NPcHt=0 NPcHQ1=0 NPcHQ3=0 NPcHu=0 NPcHj1=0 NPcHj3=0 NPcQj38^2==2
```

"mg5_input.txt": SMEFT @ LO $gg \to t\bar{t}$ and $u\bar{u}/d\bar{d} \to t\bar{t}$ total cross section elements @ 7000 GeV - MADGRAPH5_aMC@NLO (mg5_aMC) input script file

```
add process u u~ > t t~ /H QCD<=2 QED<=2 NP==1 SMHLOOP=0 NPshifts=0 NPprop=0
↪  NPcpv=0 NPcuG=0 NPctB=0 NPctW=0 NPcHl3=0 NPcll1=0 NPcHDD=0 NPcHWB=0
   NPcHt=0 NPcHQ1=0 NPcHQ3=0 NPcHu=0 NPcHj1=0 NPcHj3=0 NPctu8^2==2

add process u u~ > t t~ /H QCD<=2 QED<=2 NP==1 SMHLOOP=0 NPshifts=0 NPprop=0
↪  NPcpv=0 NPcuG=0 NPctB=0 NPctW=0 NPcHl3=0 NPcll1=0 NPcHDD=0 NPcHWB=0
   NPcHt=0 NPcHQ1=0 NPcHQ3=0 NPcHu=0 NPcHj1=0 NPcHj3=0 NPcQu8^2==2

add process u u~ > t t~ /H QCD<=2 QED<=2 NP==1 SMHLOOP=0 NPshifts=0 NPprop=0
↪  NPcpv=0 NPcuG=0 NPctB=0 NPctW=0 NPcHl3=0 NPcll1=0 NPcHDD=0 NPcHWB=0
   NPcHt=0 NPcHQ1=0 NPcHQ3=0 NPcHu=0 NPcHj1=0 NPcHj3=0 NPctj8^2==2

add process u u~ > t t~ /H QCD<=2 QED<=2 NP==1 SMHLOOP=0 NPshifts=0 NPprop=0
↪  NPcpv=0 NPcuG=0 NPctB=0 NPctW=0 NPcHl3=0 NPcll1=0 NPcHDD=0 NPcHWB=0
   NPcHt=0 NPcHQ1=0 NPcHQ3=0 NPcHu=0 NPcHj1=0 NPcHj3=0 NPcQj18^2==1
     ↪  NPcQj38^2==1

add process u u~ > t t~ /H QCD<=2 QED<=2 NP==1 SMHLOOP=0 NPshifts=0 NPprop=0
↪  NPcpv=0 NPcuG=0 NPctB=0 NPctW=0 NPcHl3=0 NPcll1=0 NPcHDD=0 NPcHWB=0
   NPcHt=0 NPcHQ1=0 NPcHQ3=0 NPcHu=0 NPcHj1=0 NPcHj3=0 NPcQj18^2==1
     ↪  NPctj8^2==1

add process u u~ > t t~ /H QCD<=2 QED<=2 NP==1 SMHLOOP=0 NPshifts=0 NPprop=0
↪  NPcpv=0 NPcuG=0 NPctB=0 NPctW=0 NPcHl3=0 NPcll1=0 NPcHDD=0 NPcHWB=0
   NPcHt=0 NPcHQ1=0 NPcHQ3=0 NPcHu=0 NPcHj1=0 NPcHj3=0 NPcQj38^2==1
     ↪  NPctj8^2==1

add process u u~ > t t~ /H QCD<=2 QED<=2 NP==1 SMHLOOP=0 NPshifts=0 NPprop=0
↪  NPcpv=0 NPcuG=0 NPctB=0 NPctW=0 NPcHl3=0 NPcll1=0 NPcHDD=0 NPcHWB=0
   NPcHt=0 NPcHQ1=0 NPcHQ3=0 NPcHu=0 NPcHj1=0 NPcHj3=0 NPctu8^2==1
     ↪  NPcQu8^2==1

add process u u~ > t t~ /H QCD<=2 QED<=2 NP==1 SMHLOOP=0 NPshifts=0 NPprop=0
↪  NPcpv=0 NPcuG=0 NPctB=0 NPctW=0 NPcHl3=0 NPcll1=0 NPcHDD=0 NPcHWB=0
   NPcHt=0 NPcHQ1=0 NPcHQ3=0 NPcHu=0 NPcHj1=0 NPcHj3=0 NPcQj11^2==2

add process u u~ > t t~ /H QCD<=2 QED<=2 NP==1 SMHLOOP=0 NPshifts=0 NPprop=0
↪  NPcpv=0 NPcuG=0 NPctB=0 NPctW=0 NPcHl3=0 NPcll1=0 NPcHDD=0 NPcHWB=0
   NPcHt=0 NPcHQ1=0 NPcHQ3=0 NPcHu=0 NPcHj1=0 NPcHj3=0 NPcQj31^2==2

add process u u~ > t t~ /H QCD<=2 QED<=2 NP==1 SMHLOOP=0 NPshifts=0 NPprop=0
↪  NPcpv=0 NPcuG=0 NPctB=0 NPctW=0 NPcHl3=0 NPcll1=0 NPcHDD=0 NPcHWB=0
   NPcHt=0 NPcHQ1=0 NPcHQ3=0 NPcHu=0 NPcHj1=0 NPcHj3=0 NPctu1^2==2
```

"mg5_input.txt": SMEFT @ LO $gg \to t\bar{t}$ and $u\bar{u}/d\bar{d} \to t\bar{t}$ total cross section elements @ 7000 GeV - MadGraph5_aMC@NLO (mg5_aMC) input script file

```
add process u u~ > t t~ /H QCD<=2 QED<=2 NP==1 SMHLOOP=0 NPshifts=0 NPprop=0
↪   NPcpv=0 NPcuG=0 NPctB=0 NPctW=0 NPcHl3=0 NPcll1=0 NPcHDD=0 NPcHWB=0
    NPcHt=0 NPcHQ1=0 NPcHQ3=0 NPcHu=0 NPcHj1=0 NPcHj3=0 NPcQu1^2==2

add process u u~ > t t~ /H QCD<=2 QED<=2 NP==1 SMHLOOP=0 NPshifts=0 NPprop=0
↪   NPcpv=0 NPcuG=0 NPctB=0 NPctW=0 NPcHl3=0 NPcll1=0 NPcHDD=0 NPcHWB=0
    NPcHt=0 NPcHQ1=0 NPcHQ3=0 NPcHu=0 NPcHj1=0 NPcHj3=0 NPctj1^2==2

add process u u~ > t t~ /H QCD<=2 QED<=2 NP==1 SMHLOOP=0 NPshifts=0 NPprop=0
↪   NPcpv=0 NPcuG=0 NPctB=0 NPctW=0 NPcHl3=0 NPcll1=0 NPcHDD=0 NPcHWB=0
    NPcHt=0 NPcHQ1=0 NPcHQ3=0 NPcHu=0 NPcHj1=0 NPcHj3=0 NPcQj11^2==1
      ↪   NPcQj31^2==1

add process u u~ > t t~ /H QCD<=2 QED<=2 NP==1 SMHLOOP=0 NPshifts=0 NPprop=0
↪   NPcpv=0 NPcuG=0 NPctB=0 NPctW=0 NPcHl3=0 NPcll1=0 NPcHDD=0 NPcHWB=0
    NPcHt=0 NPcHQ1=0 NPcHQ3=0 NPcHu=0 NPcHj1=0 NPcHj3=0 NPcQj11^2==1
      ↪   NPctj1^2==1

add process u u~ > t t~ /H QCD<=2 QED<=2 NP==1 SMHLOOP=0 NPshifts=0 NPprop=0
↪   NPcpv=0 NPcuG=0 NPctB=0 NPctW=0 NPcHl3=0 NPcll1=0 NPcHDD=0 NPcHWB=0
    NPcHt=0 NPcHQ1=0 NPcHQ3=0 NPcHu=0 NPcHj1=0 NPcHj3=0 NPcQj31^2==1
      ↪   NPctj1^2==1

add process u u~ > t t~ /H QCD<=2 QED<=2 NP==1 SMHLOOP=0 NPshifts=0 NPprop=0
↪   NPcpv=0 NPcuG=0 NPctB=0 NPctW=0 NPcHl3=0 NPcll1=0 NPcHDD=0 NPcHWB=0
    NPcHt=0 NPcHQ1=0 NPcHQ3=0 NPcHu=0 NPcHj1=0 NPcHj3=0 NPctu1^2==1
      ↪   NPcQu1^2==1

output
↪   /Users/.../MadGraph5/Simulations/Sigma_Elements_SMEFT/uubar/3_diagonal
↪   -f

launch -n CtG^2
#-- 'param_card.dat' --#
set mt 173.000
set mz 91.1880
set mw 80.4190
set mh 125.000
set md 0
set mu 0
set gf 1.16639e-05
set as 0.11800
```

"mg5_input.txt": SMEFT @ LO $gg \to t\bar{t}$ and $u\bar{u}/d\bar{d} \to t\bar{t}$ total cross section elements @ 7000 GeV - MADGRAPH5_aMC@NLO (mg5_aMC) input script file

```
#-- Wilson Coefficients --#
set ctGRe -2
set cQj18  0
set cQj38  0
set ctu8   0
set cQu8   0
set ctj8   0
set cQj11  0
set cQj31  0
set ctu1   0
set cQu1   0
set ctj1   0
#-- 'run_card.dat' --#
set lpp1 0
set lpp2 0
set ebeam1 7000
set ebeam2 7000
set fixed_ren_scale true
set fixed_fac_scale true
#set use_syst False
done

launch -n CuVV8^2
#-- Wilson Coefficients --#
set ctGRe  0
set cQj18  0.5
set cQj38  0.5
set ctu8   1
set cQu8   1
set ctj8   1
set cQj11  0
set cQj31  0
set ctu1   0
set cQu1   0
set ctj1   0
done

launch -n CuAA8^2
#-- Wilson Coefficients --#
set ctGRe  0
set cQj18  0.5
set cQj38  0.5
set ctu8   1
```

"mg5_input.txt": SMEFT @ LO $gg \rightarrow t\bar{t}$ **and** $u\bar{u}/d\bar{d} \rightarrow t\bar{t}$ **total cross section elements @ 7000 GeV - MadGraph5_aMC@NLO (mg5_aMC) input script file**

```
set cQu8  -1
set ctj8  -1
set cQj11  0
set cQj31  0
set ctu1   0
set cQu1   0
set ctj1   0
done


launch -n CuAV8^2
#-- Wilson Coefficients --#
set ctGRe  0
set cQj18 -0.5
set cQj38 -0.5
set ctu8   1
set cQu8  -1
set ctj8   1
set cQj11  0
set cQj31  0
set ctu1   0
set cQu1   0
set ctj1   0
done


launch -n CuVA8^2
#-- Wilson Coefficients --#
set ctGRe  0
set cQj18 -0.5
set cQj38 -0.5
set ctu8   1
set cQu8   1
set ctj8  -1
set cQj11  0
set cQj31  0
set ctu1   0
set cQu1   0
set ctj1   0
done


launch -n CuVV1^2
#-- Wilson Coefficients --#
set ctGRe  0
set cQj18  0
```

"mg5_input.txt": SMEFT @ LO $gg \to t\bar{t}$ and $u\bar{u}/d\bar{d} \to t\bar{t}$ total cross section elements @ 7000 GeV - MADGRAPH5_aMC@NLO (mg5_aMC) input script file

```
set cQj38  0
set ctu8   0
set cQu8   0
set ctj8   0
set cQj11  0.5
set cQj31  0.5
set ctu1   1
set cQu1   1
set ctj1   1
done

launch -n CuAA1^2
#-- Wilson Coefficients --#
set ctGRe  0
set cQj18  0
set cQj38  0
set ctu8   0
set cQu8   0
set ctj8   0
set cQj11  0.5
set cQj31  0.5
set ctu1   1
set cQu1   -1
set ctj1   -1
done

launch -n CuAV1^2
#-- Wilson Coefficients --#
set ctGRe  0
set cQj18  0
set cQj38  0
set ctu8   0
set cQu8   0
set ctj8   0
set cQj11  -0.5
set cQj31  -0.5
set ctu1   1
set cQu1   -1
set ctj1   1
done

launch -n CuVA1^2
#-- Wilson Coefficients --#
```

"mg5_input.txt": SMEFT @ LO $gg \to t\bar{t}$ and $u\bar{u}/d\bar{d} \to t\bar{t}$ total cross section elements @ 7000 GeV - MadGraph5_aMC@NLO (mg5_aMC) input script file

```
set ctGRe  0
set cQj18  0
set cQj38  0
set ctu8   0
set cQu8   0
set ctj8   0
set cQj11 -0.5
set cQj31 -0.5
set ctu1   1
set cQu1   1
set ctj1  -1
done


launch -i
print_results
↪  -path=/Users/.../MadGraph5/Simulations/Sigma_Elements_SMEFT/sigma_uubar_3.txt
exit



### uubar interferences ###

set automatic_html_opening True

generate u u~ > t t~ /H QCD<=2 QED<=2 NPctG^2==1 SMHLOOP=0 NPshifts=0
↪  NPprop=0 NPcpv=0 NPcuG=0 NPctB=0 NPctW=0 NPcHl3=0 NPcll1=0 NPcHDD=0
   NPcHWB=0 NPcHt=0 NPcHQ1=0 NPcHQ3=0 NPcHu=0 NPcHj1=0 NPcHj3=0
   ↪  NPcQj18^2==1

add process u u~ > t t~ /H QCD<=2 QED<=2 NPctG^2==1 SMHLOOP=0 NPshifts=0
↪  NPprop=0 NPcpv=0 NPcuG=0 NPctB=0 NPctW=0 NPcHl3=0 NPcll1=0 NPcHDD=0
   NPcHWB=0 NPcHt=0 NPcHQ1=0 NPcHQ3=0 NPcHu=0 NPcHj1=0 NPcHj3=0
   ↪  NPcQj38^2==1

add process u u~ > t t~ /H QCD<=2 QED<=2 NPctG^2==1 SMHLOOP=0 NPshifts=0
↪  NPprop=0 NPcpv=0 NPcuG=0 NPctB=0 NPctW=0 NPcHl3=0 NPcll1=0 NPcHDD=0
   NPcHWB=0 NPcHt=0 NPcHQ1=0 NPcHQ3=0 NPcHu=0 NPcHj1=0 NPcHj3=0 NPctu8^2==1

add process u u~ > t t~ /H QCD<=2 QED<=2 NPctG^2==1 SMHLOOP=0 NPshifts=0
↪  NPprop=0 NPcpv=0 NPcuG=0 NPctB=0 NPctW=0 NPcHl3=0 NPcll1=0 NPcHDD=0
   NPcHWB=0 NPcHt=0 NPcHQ1=0 NPcHQ3=0 NPcHu=0 NPcHj1=0 NPcHj3=0 NPcQu8^2==1

add process u u~ > t t~ /H QCD<=2 QED<=2 NPctG^2==1 SMHLOOP=0 NPshifts=0
↪  NPprop=0 NPcpv=0 NPcuG=0 NPctB=0 NPctW=0 NPcHl3=0 NPcll1=0 NPcHDD=0
```

"mg5_input.txt": SMEFT @ LO $gg \to t\bar{t}$ and $u\bar{u}/d\bar{d} \to t\bar{t}$ total cross section elements @ 7000 GeV - MADGRAPH5_aMC@NLO (mg5_aMC) input script file

```
    NPcHWB=0 NPcHt=0 NPcHQ1=0 NPcHQ3=0 NPcHu=0 NPcHj1=0 NPcHj3=0 NPctj8^2==1


output
↪  /Users/.../MadGraph5/Simulations/Sigma_Elements_SMEFT/uubar/4_interferences
↪  -f

launch -n CtGxCuVV8
#-- 'param_card.dat' --#
set mt 173.000
set mz 91.1880
set mw 80.4190
set mh 125.000
set md 0
set mu 0
set gf 1.16639e-05
set as 0.11800
#-- Wilson Coefficients --#
set ctGRe -1
set cQj18  0.5
set cQj38  0.5
set ctu8   1
set cQu8   1
set ctj8   1
set cQj11  0
set cQj31  0
set ctu1   0
set cQu1   0
set ctj1   0
#-- 'run_card.dat' --#
set lpp1 0
set lpp2 0
set ebeam1 7000
set ebeam2 7000
set fixed_ren_scale true
set fixed_fac_scale true
#set use_syst False
done

launch -i
print_results
↪  -path=/Users/.../MadGraph5/Simulations/Sigma_Elements_SMEFT/sigma_uubar_4.txt
exit
```

"mg5_input.txt": SMEFT @ LO $gg \to t\bar{t}$ **and** $u\bar{u}/d\bar{d} \to t\bar{t}$ **total cross section elements @ 7000 GeV - MADGRAPH5_aMC@NLO (mg5_aMC) input script file**

```
### ddbar
↪   ######################################################################


### ddbar SM ###

set automatic_html_opening True

generate d d~ > t t~ /H QCD<=2 QED<=2 NP=0 SMHLOOP=0 NPshifts=0 NPprop=0
↪   NPcpv=0 NPcdG=0 NPctB=0 NPctW=0 NPcHl3=0 NPcll1=0 NPcHDD=0 NPcHWB=0
    NPcHt=0 NPcHQ1=0 NPcHQ3=0 NPcHd=0 NPcHj1=0 NPcHj3=0

output /Users/.../MadGraph5/Simulations/Sigma_Elements_SMEFT/ddbar/1_SM -f

launch -n SM
#-- 'param_card.dat' --#
set mt 173.000
set mz 91.1880
set mw 80.4190
set mh 125.000
set md 0
set mu 0
set gf 1.16639e-05
set as 0.11800
#-- Wilson Coefficients --#
set ctGRe  0
set cQj18  0
set cQj38  0
set ctd8   0
set cQd8   0
set ctj8   0
set cQj11  0
set cQj31  0
set ctd1   0
set cQd1   0
set ctj1   0
#-- 'run_card.dat' --#
set lpp1 0
set lpp2 0
set ebeam1 7000
set ebeam2 7000
```

"mg5_input.txt": SMEFT @ LO $gg \to t\bar{t}$ and $u\bar{u}/d\bar{d} \to t\bar{t}$ total cross section elements @ 7000 GeV - MadGraph5_aMC@NLO (mg5_aMC) input script file

```
set fixed_ren_scale true
set fixed_fac_scale true
#set use_syst False
done


launch -i
print_results
↪   -path=/Users/.../MadGraph5/Simulations/Sigma_Elements_SMEFT/sigma_ddbar_1.txt
exit



### ddbar first row ###


set automatic_html_opening True

generate d d~ > t t~ /H QCD<=2 QED<=2 NP<=1 NP^2==1 SMHLOOP=0 NPshifts=0
↪   NPprop=0 NPcpv=0 NPcdG=0 NPctB=0 NPctW=0 NPcHl3=0 NPcll1=0 NPcHDD=0
    NPcHWB=0 NPcHt=0 NPcHQ1=0 NPcHQ3=0 NPcHd=0 NPcHj1=0 NPcHj3=0

output
↪   /Users/.../MadGraph5/Simulations/Sigma_Elements_SMEFT/ddbar/2_firstrow
↪   -f

launch -n CtG
#-- 'param_card.dat' --#
set mt 173.000
set mz 91.1880
set mw 80.4190
set mh 125.000
set md 0
set mu 0
set gf 1.16639e-05
set as 0.11800
#-- Wilson Coefficients --#
set ctGRe -1
set cQj18  0
set cQj38  0
set ctd8   0
set cQd8   0
set ctj8   0
set cQj11  0
set cQj31  0
set ctd1   0
```

"mg5_input.txt": SMEFT @ LO $gg \to t\bar{t}$ and $u\bar{u}/d\bar{d} \to t\bar{t}$ total cross section elements @ 7000 GeV - MadGraph5_aMC@NLO (mg5_aMC) input script file

```
set cQd1   0
set ctj1   0
#-- 'run_card.dat' --#
set lpp1 0
set lpp2 0
set ebeam1 7000
set ebeam2 7000
set fixed_ren_scale true
set fixed_fac_scale true
#set use_syst False
done

launch -n CdVV8
#-- Wilson Coefficients --#
set ctGRe  0
set cQj18  0.75
set cQj38  0.25
set ctd8   0.5
set cQd8   0.5
set ctj8   0.5
set cQj11  0
set cQj31  0
set ctd1   0
set cQd1   0
set ctj1   0
done

launch -n CdVV1
#-- Wilson Coefficients --#
set ctGRe  0
set cQj18  0
set cQj38  0
set ctd8   0
set cQd8   0
set ctj8   0
set cQj11  0.75
set cQj31  0.25
set ctd1   0.5
set cQd1   0.5
set ctj1   0.5
done

launch -n CdAA1
```

"mg5_input.txt": SMEFT @ LO $gg \to t\bar{t}$ and $u\bar{u}/d\bar{d} \to t\bar{t}$ total cross section elements @ 7000 GeV - MADGRAPH5_aMC@NLO (mg5_aMC) input script file

```
#-- Wilson Coefficients --#
set ctGRe  0
set cQj18  0
set cQj38  0
set ctd8   0
set cQd8   0
set ctj8   0
set cQj11  0.75
set cQj31  0.25
set ctd1   0.5
set cQd1   -0.5
set ctj1   -0.5
done

launch -n CdAV1
#-- Wilson Coefficients --#
set ctGRe  0
set cQj18  0
set cQj38  0
set ctd8   0
set cQd8   0
set ctj8   0
set cQj11 -0.75
set cQj31 -0.25
set ctd1   0.5
set cQd1   -0.5
set ctj1   0.5
done

launch -n CdVA1
#-- Wilson Coefficients --#
set ctGRe  0
set cQj18  0
set cQj38  0
set ctd8   0
set cQd8   0
set ctj8   0
set cQj11 -0.75
set cQj31 -0.25
set ctd1   0.5
set cQd1   0.5
set ctj1   -0.5
done
```

"mg5_input.txt": SMEFT @ LO $gg \to t\bar{t}$ and $u\bar{u}/d\bar{d} \to t\bar{t}$ total cross section elements @ 7000 GeV - MADGRAPH5_aMC@NLO (mg5_aMC) input script file

```
launch -i
print_results
↪  -path=/Users/.../MadGraph5/Simulations/Sigma_Elements_SMEFT/sigma_ddbar_2.txt
exit


### ddbar diagonal ###

set automatic_html_opening True

generate d d~ > t t~ /H QCD<=2 QED<=2 NP==1 SMHLOOP=0 NPshifts=0 NPprop=0
↪  NPcpv=0 NPcdG=0 NPctB=0 NPctW=0 NPcHl3=0 NPcll1=0 NPcHDD=0 NPcHWB=0
   NPcHt=0 NPcHQ1=0 NPcHQ3=0 NPcHd=0 NPcHj1=0 NPcHj3=0 NPctG^2==2

add process d d~ > t t~ /H QCD<=2 QED<=2 NP==1 SMHLOOP=0 NPshifts=0 NPprop=0
↪  NPcpv=0 NPcdG=0 NPctB=0 NPctW=0 NPcHl3=0 NPcll1=0 NPcHDD=0 NPcHWB=0
   NPcHt=0 NPcHQ1=0 NPcHQ3=0 NPcHd=0 NPcHj1=0 NPcHj3=0 NPcQj18^2==2

add process d d~ > t t~ /H QCD<=2 QED<=2 NP==1 SMHLOOP=0 NPshifts=0 NPprop=0
↪  NPcpv=0 NPcdG=0 NPctB=0 NPctW=0 NPcHl3=0 NPcll1=0 NPcHDD=0 NPcHWB=0
   NPcHt=0 NPcHQ1=0 NPcHQ3=0 NPcHd=0 NPcHj1=0 NPcHj3=0 NPcQj38^2==2

add process d d~ > t t~ /H QCD<=2 QED<=2 NP==1 SMHLOOP=0 NPshifts=0 NPprop=0
↪  NPcpv=0 NPcdG=0 NPctB=0 NPctW=0 NPcHl3=0 NPcll1=0 NPcHDD=0 NPcHWB=0
   NPcHt=0 NPcHQ1=0 NPcHQ3=0 NPcHd=0 NPcHj1=0 NPcHj3=0 NPctd8^2==2

add process d d~ > t t~ /H QCD<=2 QED<=2 NP==1 SMHLOOP=0 NPshifts=0 NPprop=0
↪  NPcpv=0 NPcdG=0 NPctB=0 NPctW=0 NPcHl3=0 NPcll1=0 NPcHDD=0 NPcHWB=0
   NPcHt=0 NPcHQ1=0 NPcHQ3=0 NPcHd=0 NPcHj1=0 NPcHj3=0 NPcQd8^2==2

add process d d~ > t t~ /H QCD<=2 QED<=2 NP==1 SMHLOOP=0 NPshifts=0 NPprop=0
↪  NPcpv=0 NPcdG=0 NPctB=0 NPctW=0 NPcHl3=0 NPcll1=0 NPcHDD=0 NPcHWB=0
   NPcHt=0 NPcHQ1=0 NPcHQ3=0 NPcHd=0 NPcHj1=0 NPcHj3=0 NPctj8^2==2

add process d d~ > t t~ /H QCD<=2 QED<=2 NP==1 SMHLOOP=0 NPshifts=0 NPprop=0
↪  NPcpv=0 NPcdG=0 NPctB=0 NPctW=0 NPcHl3=0 NPcll1=0 NPcHDD=0 NPcHWB=0
   NPcHt=0 NPcHQ1=0 NPcHQ3=0 NPcHd=0 NPcHj1=0 NPcHj3=0 NPcQj18^2==1
      ↪  NPcQj38^2==1

add process d d~ > t t~ /H QCD<=2 QED<=2 NP==1 SMHLOOP=0 NPshifts=0 NPprop=0
↪  NPcpv=0 NPcdG=0 NPctB=0 NPctW=0 NPcHl3=0 NPcll1=0 NPcHDD=0 NPcHWB=0
```

"mg5_input.txt": SMEFT @ LO $gg \to t\bar{t}$ and $u\bar{u}/d\bar{d} \to t\bar{t}$ total cross section elements @ 7000 GeV - MADGRAPH5_aMC@NLO (mg5_aMC) input script file

```
    NPcHt=0 NPcHQ1=0 NPcHQ3=0 NPcHd=0 NPcHj1=0 NPcHj3=0 NPcQj18^2==1
    ↪  NPctj8^2==1

add process d d~ > t t~ /H QCD<=2 QED<=2 NP==1 SMHLOOP=0 NPshifts=0 NPprop=0
↪  NPcpv=0 NPcdG=0 NPctB=0 NPctW=0 NPcHl3=0 NPcll1=0 NPcHDD=0 NPcHWB=0
    NPcHt=0 NPcHQ1=0 NPcHQ3=0 NPcHd=0 NPcHj1=0 NPcHj3=0 NPcQj38^2==1
    ↪  NPctj8^2==1

add process d d~ > t t~ /H QCD<=2 QED<=2 NP==1 SMHLOOP=0 NPshifts=0 NPprop=0
↪  NPcpv=0 NPcdG=0 NPctB=0 NPctW=0 NPcHl3=0 NPcll1=0 NPcHDD=0 NPcHWB=0
    NPcHt=0 NPcHQ1=0 NPcHQ3=0 NPcHd=0 NPcHj1=0 NPcHj3=0 NPctd8^2==1
    ↪  NPcQd8^2==1

add process d d~ > t t~ /H QCD<=2 QED<=2 NP==1 SMHLOOP=0 NPshifts=0 NPprop=0
↪  NPcpv=0 NPcdG=0 NPctB=0 NPctW=0 NPcHl3=0 NPcll1=0 NPcHDD=0 NPcHWB=0
    NPcHt=0 NPcHQ1=0 NPcHQ3=0 NPcHd=0 NPcHj1=0 NPcHj3=0 NPcQj11^2==2

add process d d~ > t t~ /H QCD<=2 QED<=2 NP==1 SMHLOOP=0 NPshifts=0 NPprop=0
↪  NPcpv=0 NPcdG=0 NPctB=0 NPctW=0 NPcHl3=0 NPcll1=0 NPcHDD=0 NPcHWB=0
    NPcHt=0 NPcHQ1=0 NPcHQ3=0 NPcHd=0 NPcHj1=0 NPcHj3=0 NPcQj31^2==2

add process d d~ > t t~ /H QCD<=2 QED<=2 NP==1 SMHLOOP=0 NPshifts=0 NPprop=0
↪  NPcpv=0 NPcdG=0 NPctB=0 NPctW=0 NPcHl3=0 NPcll1=0 NPcHDD=0 NPcHWB=0
    NPcHt=0 NPcHQ1=0 NPcHQ3=0 NPcHd=0 NPcHj1=0 NPcHj3=0 NPctd1^2==2

add process d d~ > t t~ /H QCD<=2 QED<=2 NP==1 SMHLOOP=0 NPshifts=0 NPprop=0
↪  NPcpv=0 NPcdG=0 NPctB=0 NPctW=0 NPcHl3=0 NPcll1=0 NPcHDD=0 NPcHWB=0
    NPcHt=0 NPcHQ1=0 NPcHQ3=0 NPcHd=0 NPcHj1=0 NPcHj3=0 NPcQd1^2==2

add process d d~ > t t~ /H QCD<=2 QED<=2 NP==1 SMHLOOP=0 NPshifts=0 NPprop=0
↪  NPcpv=0 NPcdG=0 NPctB=0 NPctW=0 NPcHl3=0 NPcll1=0 NPcHDD=0 NPcHWB=0
    NPcHt=0 NPcHQ1=0 NPcHQ3=0 NPcHd=0 NPcHj1=0 NPcHj3=0 NPctj1^2==2

add process d d~ > t t~ /H QCD<=2 QED<=2 NP==1 SMHLOOP=0 NPshifts=0 NPprop=0
↪  NPcpv=0 NPcdG=0 NPctB=0 NPctW=0 NPcHl3=0 NPcll1=0 NPcHDD=0 NPcHWB=0
    NPcHt=0 NPcHQ1=0 NPcHQ3=0 NPcHd=0 NPcHj1=0 NPcHj3=0 NPcQj11^2==1
    ↪  NPcQj31^2==1

add process d d~ > t t~ /H QCD<=2 QED<=2 NP==1 SMHLOOP=0 NPshifts=0 NPprop=0
↪  NPcpv=0 NPcdG=0 NPctB=0 NPctW=0 NPcHl3=0 NPcll1=0 NPcHDD=0 NPcHWB=0
    NPcHt=0 NPcHQ1=0 NPcHQ3=0 NPcHd=0 NPcHj1=0 NPcHj3=0 NPcQj11^2==1
    ↪  NPctj1^2==1
```

"mg5_input.txt": SMEFT @ LO $gg \to t\bar{t}$ and $u\bar{u}/d\bar{d} \to t\bar{t}$ total cross section elements @ 7000 GeV - MadGraph5_aMC@NLO (mg5_aMC) input script file

```
add process d d~ > t t~ /H QCD<=2 QED<=2 NP==1 SMHLOOP=0 NPshifts=0 NPprop=0
↪   NPcpv=0 NPcdG=0 NPctB=0 NPctW=0 NPcHl3=0 NPcll1=0 NPcHDD=0 NPcHWB=0
    NPcHt=0 NPcHQ1=0 NPcHQ3=0 NPcHd=0 NPcHj1=0 NPcHj3=0 NPcQj31^2==1
    ↪   NPctj1^2==1

add process d d~ > t t~ /H QCD<=2 QED<=2 NP==1 SMHLOOP=0 NPshifts=0 NPprop=0
↪   NPcpv=0 NPcdG=0 NPctB=0 NPctW=0 NPcHl3=0 NPcll1=0 NPcHDD=0 NPcHWB=0
    NPcHt=0 NPcHQ1=0 NPcHQ3=0 NPcHd=0 NPcHj1=0 NPcHj3=0 NPctd1^2==1
    ↪   NPcQd1^2==1

output
↪   /Users/.../MadGraph5/Simulations/Sigma_Elements_SMEFT/ddbar/3_diagonal
↪   -f

launch -n CtG^2
#-- 'param_card.dat' --#
set mt 173.000
set mz 91.1880
set mw 80.4190
set mh 125.000
set md 0
set mu 0
set gf 1.16639e-05
set as 0.11800
#-- Wilson Coefficients --#
set ctGRe -2
set cQj18  0
set cQj38  0
set ctd8   0
set cQd8   0
set ctj8   0
set cQj11  0
set cQj31  0
set ctd1   0
set cQd1   0
set ctj1   0
#-- 'run_card.dat' --#
set lpp1 0
set lpp2 0
set ebeam1 7000
set ebeam2 7000
set fixed_ren_scale true
set fixed_fac_scale true
```

"mg5_input.txt": SMEFT @ LO $gg \to t\bar{t}$ and $u\bar{u}/d\bar{d} \to t\bar{t}$ total cross section elements @ 7000 GeV - MadGraph5_aMC@NLO (mg5_aMC) input script file

```
#set use_syst False
done


launch -n CdVV8^2
#-- Wilson Coefficients --#
set ctGRe  0
set cQj18  1.5
set cQj38  0.5
set ctd8   1
set cQd8   1
set ctj8   1
set cQj11  0
set cQj31  0
set ctd1   0
set cQd1   0
set ctj1   0
done


launch -n CdAA8^2
#-- Wilson Coefficients --#
set ctGRe  0
set cQj18  1.5
set cQj38  0.5
set ctd8   1
set cQd8  -1
set ctj8  -1
set cQj11  0
set cQj31  0
set ctd1   0
set cQd1   0
set ctj1   0
done


launch -n CdAV8^2
#-- Wilson Coefficients --#
set ctGRe  0
set cQj18 -1.5
set cQj38 -0.5
set ctd8   1
set cQd8  -1
set ctj8   1
set cQj11  0
set cQj31  0
```

"mg5_input.txt": SMEFT @ LO $gg \to t\bar{t}$ and $u\bar{u}/d\bar{d} \to t\bar{t}$ total cross section elements @ 7000 GeV - MadGraph5_aMC@NLO (mg5_aMC) input script file

```
set ctd1   0
set cQd1   0
set ctj1   0
done

launch -n CdVA8^2
#-- Wilson Coefficients --#
set ctGRe  0
set cQj18 -1.5
set cQj38 -0.5
set ctd8   1
set cQd8   1
set ctj8  -1
set cQj11  0
set cQj31  0
set ctd1   0
set cQd1   0
set ctj1   0
done

launch -n CdVV1^2
#-- Wilson Coefficients --#
set ctGRe  0
set cQj18  0
set cQj38  0
set ctd8   0
set cQd8   0
set ctj8   0
set cQj11  1.5
set cQj31  0.5
set ctd1   1
set cQd1   1
set ctj1   1
done

launch -n CdAA1^2
#-- Wilson Coefficients --#
set ctGRe  0
set cQj18  0
set cQj38  0
set ctd8   0
set cQd8   0
set ctj8   0
```

"mg5_input.txt": SMEFT @ LO $gg \to t\bar{t}$ and $u\bar{u}/d\bar{d} \to t\bar{t}$ total cross section elements @ 7000 GeV - MadGraph5_aMC@NLO (mg5_aMC) input script file

```
set cQj11  1.5
set cQj31  0.5
set ctd1   1
set cQd1   -1
set ctj1   -1
done

launch -n CdAV1^2
#-- Wilson Coefficients --#
set ctGRe  0
set cQj18  0
set cQj38  0
set ctd8   0
set cQd8   0
set ctj8   0
set cQj11 -1.5
set cQj31 -0.5
set ctd1   1
set cQd1   -1
set ctj1   1
done

launch -n CdVA1^2
#-- Wilson Coefficients --#
set ctGRe  0
set cQj18  0
set cQj38  0
set ctd8   0
set cQd8   0
set ctj8   0
set cQj11 -1.5
set cQj31 -0.5
set ctd1   1
set cQd1   1
set ctj1   -1
done

launch -i
print_results
→  -path=/Users/.../MadGraph5/Simulations/Sigma_Elements_SMEFT/sigma_ddbar_3.txt
exit
```

> **"mg5_input.txt": SMEFT @ LO** $gg \to t\bar{t}$ **and** $u\bar{u}/d\bar{d} \to t\bar{t}$ **total cross section elements @ 7000 GeV - MadGraph5_aMC@NLO (mg5_aMC) input script file**

```
### ddbar interferences ###

set automatic_html_opening True

generate d d~ > t t~ /H QCD<=2 QED<=2 NPctG^2==1 SMHLOOP=0 NPshifts=0
↪   NPprop=0 NPcpv=0 NPcdG=0 NPctB=0 NPctW=0 NPcHl3=0 NPcll1=0 NPcHDD=0
    NPcHWB=0 NPcHt=0 NPcHQ1=0 NPcHQ3=0 NPcHd=0 NPcHj1=0 NPcHj3=0
    ↪   NPcQj18^2==1

add process d d~ > t t~ /H QCD<=2 QED<=2 NPctG^2==1 SMHLOOP=0 NPshifts=0
↪   NPprop=0 NPcpv=0 NPcdG=0 NPctB=0 NPctW=0 NPcHl3=0 NPcll1=0 NPcHDD=0
    NPcHWB=0 NPcHt=0 NPcHQ1=0 NPcHQ3=0 NPcHd=0 NPcHj1=0 NPcHj3=0
    ↪   NPcQj38^2==1

add process d d~ > t t~ /H QCD<=2 QED<=2 NPctG^2==1 SMHLOOP=0 NPshifts=0
↪   NPprop=0 NPcpv=0 NPcdG=0 NPctB=0 NPctW=0 NPcHl3=0 NPcll1=0 NPcHDD=0
    NPcHWB=0 NPcHt=0 NPcHQ1=0 NPcHQ3=0 NPcHd=0 NPcHj1=0 NPcHj3=0 NPctd8^2==1

add process d d~ > t t~ /H QCD<=2 QED<=2 NPctG^2==1 SMHLOOP=0 NPshifts=0
↪   NPprop=0 NPcpv=0 NPcdG=0 NPctB=0 NPctW=0 NPcHl3=0 NPcll1=0 NPcHDD=0
    NPcHWB=0 NPcHt=0 NPcHQ1=0 NPcHQ3=0 NPcHd=0 NPcHj1=0 NPcHj3=0 NPcQd8^2==1

add process d d~ > t t~ /H QCD<=2 QED<=2 NPctG^2==1 SMHLOOP=0 NPshifts=0
↪   NPprop=0 NPcpv=0 NPcdG=0 NPctB=0 NPctW=0 NPcHl3=0 NPcll1=0 NPcHDD=0
    NPcHWB=0 NPcHt=0 NPcHQ1=0 NPcHQ3=0 NPcHd=0 NPcHj1=0 NPcHj3=0 NPctj8^2==1

output
↪   /Users/.../MadGraph5/Simulations/Sigma_Elements_SMEFT/ddbar/4_interferences
↪   -f

launch -n CtGxCdVV8
#-- 'param_card.dat' --#
set mt 173.000
set mz 91.1880
set mw 80.4190
set mh 125.000
set md 0
set mu 0
set gf 1.16639e-05
set as 0.11800
#-- Wilson Coefficients --#
set ctGRe -1
set cQj18  1.5
```

"mg5_input.txt": SMEFT @ LO $gg \to t\bar{t}$ and $u\bar{u}/d\bar{d} \to t\bar{t}$ total cross section elements @ 7000 GeV - MADGRAPH5_aMC@NLO (mg5_aMC) input script file

```
set cQj38  0.5
set ctd8   1
set cQd8   1
set ctj8   1
set cQj11  0
set cQj31  0
set ctd1   0
set cQd1   0
set ctj1   0
#-- 'run_card.dat' --#
set lpp1 0
set lpp2 0
set ebeam1 7000
set ebeam2 7000
set fixed_ren_scale true
set fixed_fac_scale true
#set use_syst False
done

launch -i
print_results
↪  -path=/Users/.../MadGraph5/Simulations/Sigma_Elements_SMEFT/sigma_ddbar_4.txt
exit


! cat /Users/.../MadGraph5/Simulations/Sigma_Elements_SMEFT/sigma_gg_1.txt
    /Users/.../MadGraph5/Simulations/Sigma_Elements_SMEFT/sigma_gg_2.txt
    /Users/.../MadGraph5/Simulations/Sigma_Elements_SMEFT/sigma_gg_3.txt
    /Users/.../MadGraph5/Simulations/Sigma_Elements_SMEFT/sigma_gg_4.txt >
    /Users/.../MadGraph5/Simulations/Sigma_Elements_SMEFT/sigma_gg.txt
! rm -f /Users/.../MadGraph5/Simulations/Sigma_Elements_SMEFT/sigma_gg_1.txt
! rm -f /Users/.../MadGraph5/Simulations/Sigma_Elements_SMEFT/sigma_gg_2.txt
! rm -f /Users/.../MadGraph5/Simulations/Sigma_Elements_SMEFT/sigma_gg_3.txt
! rm -f /Users/.../MadGraph5/Simulations/Sigma_Elements_SMEFT/sigma_gg_4.txt

! cat
↪  /Users/.../MadGraph5/Simulations/Sigma_Elements_SMEFT/sigma_uubar_1.txt
    /Users/.../MadGraph5/Simulations/Sigma_Elements_SMEFT/sigma_uubar_2.txt
    /Users/.../MadGraph5/Simulations/Sigma_Elements_SMEFT/sigma_uubar_3.txt
    /Users/.../MadGraph5/Simulations/Sigma_Elements_SMEFT/sigma_uubar_4.txt
        ↪  >
    /Users/.../MadGraph5/Simulations/Sigma_Elements_SMEFT/sigma_uubar.txt
```

"mg5_input.txt": SMEFT @ LO $gg \to t\bar{t}$ and $u\bar{u}/d\bar{d} \to t\bar{t}$ total cross section elements @ 7000 GeV - MadGraph5_aMC@NLO (mg5_aMC) input script file

```
! rm -f
↪   /Users/.../MadGraph5/Simulations/Sigma_Elements_SMEFT/sigma_uubar_1.txt
! rm -f
↪   /Users/.../MadGraph5/Simulations/Sigma_Elements_SMEFT/sigma_uubar_2.txt
! rm -f
↪   /Users/.../MadGraph5/Simulations/Sigma_Elements_SMEFT/sigma_uubar_3.txt
! rm -f
↪   /Users/.../MadGraph5/Simulations/Sigma_Elements_SMEFT/sigma_uubar_4.txt

! cat
↪   /Users/.../MadGraph5/Simulations/Sigma_Elements_SMEFT/sigma_ddbar_1.txt
    /Users/.../MadGraph5/Simulations/Sigma_Elements_SMEFT/sigma_ddbar_2.txt
    /Users/.../MadGraph5/Simulations/Sigma_Elements_SMEFT/sigma_ddbar_3.txt
    /Users/.../MadGraph5/Simulations/Sigma_Elements_SMEFT/sigma_ddbar_4.txt
    ↪   >
    /Users/.../MadGraph5/Simulations/Sigma_Elements_SMEFT/sigma_ddbar.txt
! rm -f
↪   /Users/.../MadGraph5/Simulations/Sigma_Elements_SMEFT/sigma_ddbar_1.txt
! rm -f
↪   /Users/.../MadGraph5/Simulations/Sigma_Elements_SMEFT/sigma_ddbar_2.txt
! rm -f
↪   /Users/.../MadGraph5/Simulations/Sigma_Elements_SMEFT/sigma_ddbar_3.txt
! rm -f
↪   /Users/.../MadGraph5/Simulations/Sigma_Elements_SMEFT/sigma_ddbar_4.txt

! cp /Users/leonardoguidetti/Documents/MadGraph/MadGraph5/Work/mg5_input.txt
    /Users/.../MadGraph5/Simulations/Sigma_Elements
```

BIBLIOGRAPHY AND REFERENCES

[1] CERN. *Large Hadron Collider restarts*. Conseil Européen pour la Recherche Nucléaire (CERN). URL: https://home.web.cern.ch/news/news/accelerators/large-hadron-collider-restarts (visited on 04/22/2022).

[2] Aneesh V. Manohar. «Introduction to Effective Field Theories». In: *arXiv e-prints*, arXiv:1804.05863 (Apr. 2018), arXiv:1804.05863. arXiv: 1804.05863 [hep-ph].

[3] Aneesh V. Manohar. «Effective field theories». In: 479 (1997). Ed. by H. Latal and W. Schweiger, p. 311. DOI: 10.1007/BFb0104294.

[4] Thomas Appelquist and J. Carazzone. «Infrared singularities and massive fields». In: *Phys. Rev. D* 11 (10 May 1975), pp. 2856–2861. DOI: 10.1103/PhysRevD.11.2856. URL: https://link.aps.org/doi/10.1103/PhysRevD.11.2856.

[5] Philip Bechtle et al. «Bottoms Up: Standard Model Effective Field Theory from a Model Perspective». In: *arXiv e-prints*, arXiv:2201.08819 (Jan. 2022), arXiv:2201.08819. arXiv: 2201.08819 [physics.hist-ph].

[6] *CMS measures the mass of the top quark with unparalleled accuracy*. URL: https://home.cern/news/news/physics/cms-measures-mass-top-quark-unparalleled-accuracy.

[7] M. Tanabashi et al. «Review of Particle Physics». In: *Phys. Rev. D* 98 (3 Aug. 2018), p. 030001. DOI: 10.1103/PhysRevD.98.030001. URL: https://link.aps.org/doi/10.1103/PhysRevD.98.030001.

[8] Giuseppe Degrassi et al. «Higgs mass and vacuum stability in the Standard Model at NNLO». In: *Journal of High Energy Physics* 2012, 98 (Aug. 2012), p. 98. DOI: 10.1007/JHEP08(2012)098. arXiv: 1205.6497 [hep-ph].

[9] *Taking a closer look at LHC*. URL: http://lhc-closer.es/taking_a_closer_look_at_lhc/1.lhc.

[10] T. Gleisberg et al. «Event generation with SHERPA 1.1». In: *Journal of High Energy Physics* 2009.2, 007 (Feb. 2009), p. 007. DOI: 10.1088/1126-6708/2009/02/007. arXiv: 0811.4622 [hep-ph].

[11] Carsten Burgard. *Standard model of physics*. URL: https://texample.net/tikz/examples/model-physics/ (visited on 12/31/2016).

[12] Alexandr Kamenchtchik Michele Cicoli. *76344 - CAMPI E PARTICELLE*. Secondo ciclo AA 2015/2016.

[13] Vryonidou Eleni. *EFT for New Physics (Online HEFT school, 11/04/21)*. URL: https://indico.ihep.ac.cn/event/13633/contribution/5/material/slides/0.pdf.

[14] Roberto Soldati. *Supplement of Theoretical Physics - Advances in Quantum Field Theory*. Dec. 2019.

[15] Ken Mimatsu. *Searching for new physics with effective field theories I - Madgraph School 2019 (India)*. Nov. 2019. URL: https://indico.cern.ch/event/829653/contributions/3568548/.

[16] B. Grzadkowski et al. «Dimension-six terms in the Standard Model Lagrangian». In: *Journal of High Energy Physics* 2010, 85 (Oct. 2010), p. 85. DOI: 10.1007/JHEP10(2010)085. arXiv: 1008.4884 [hep-ph].

[17] Cen Zhang and Scott Willenbrock. «Effective-field-theory approach to top-quark production and decay». In: \prd 83.3, 034006 (Feb. 2011), p. 034006. DOI: 10.1103/PhysRevD.83.034006. arXiv: 1008.3869 [hep-ph].

[18] Ilaria Brivio et al. «O new physics, where art thou? A global search in the top sector». In: *Journal of High Energy Physics* 2020.2, 131 (Feb. 2020), p. 131. DOI: 10.1007/JHEP02(2020)131. arXiv: 1910.03606 [hep-ph].

[19] Michelangelo L. Mangano. *INTRODUCTION TO QCD*. URL: https://cds.cern.ch/record/454171/files/p53.pdf.

[20] Notes from Carlo Olearis lectures. *Introduction to perturbative QCD*. URL: https://virgilio.mib.infn.it/~oleari/public/QCD/appunti_corso/Oleari_QCD-2014-05-04.pdf (visited on 05/04/2014).

[21] Vladyslav Shtabovenko, Rolf Mertig, and Frederik Orellana. «FeynCalc 9.3: New features and improvements». In: *Computer Physics Communications* 256, 107478 (Nov. 2020), p. 107478. DOI: 10.1016/j.cpc.2020.107478. arXiv: 2001.04407 [hep-ph].

[22] Wolfram Research Inc. *Mathematica, Version 12.0*. Champaign, IL, 2019.

[23] Nathan P. Hartland and Emanuele R. Nocera. «A Mathematica interface to NNPDFs». In: *Nuclear Physics B Proceedings Supplements* 234 (Jan. 2013), pp. 54–57. DOI: 10.1016/j.nuclphysbps.2012.11.013. arXiv: 1209.2585 [hep-ph].

[24] NNPDF. *NNPDF*. URL: https://nnpdf.mi.infn.it.

[25] J. Alwall et al. «The automated computation of tree-level and next-to-leading order differential cross sections, and their matching to parton shower simulations». In: *Journal of High Energy Physics* 2014, 79 (July 2014), p. 79. DOI: 10.1007/JHEP07(2014)079. arXiv: 1405.0301 [hep-ph].

[26] Ilaria Brivio, Yun Jiang, and Michael Trott. «The SMEFTsim package, theory and tools». In: *Journal of High Energy Physics* 2017.12, 70 (Dec. 2017), p. 70. DOI: 10.1007/JHEP12(2017)070. arXiv: 1709.06492 [hep-ph].

[27] Ilaria Brivio. «SMEFTsim 3.0 a practical guide». In: *Journal of High Energy Physics* 2021.4, 73 (Apr. 2021), p. 73. DOI: 10.1007/JHEP04(2021)073. arXiv: 2012.11343 [hep-ph].

[28] J. Alwall et al. «A standard format for Les Houches Event Files». In: *Computer Physics Communications* 176.4 (Feb. 2007), pp. 300–304. DOI: 10.1016/j.cpc.2006.11.010. arXiv: hep-ph/0609017 [hep-ph].

[29] Rafael Aoude et al. «Quantum SMEFT tomography: Top quark pair production at the LHC». In: *Phys. Rev. D* 106.5, 055007 (Sept. 2022), p. 055007. DOI: 10.1103/PhysRevD.106.055007. arXiv: 2203.05619 [hep-ph].

[30]   Michael Edward Peskin and Daniel V. Schroeder. *An Introduction to Quantum Field Theory*. Reading, USA: Addison-Wesley (1995) 842 p. Westview Press, 1995.

[31]   Yorikiyo Nagashima. *Elementary particle physics Volume 2: Foundations of the Standard Model*. Wiley-VCH, 2012.

[32]   Jorge C. Romão and João P. Silva. «a Resource for Signs and Feynman Diagrams of the Standard Model». In: *International Journal of Modern Physics A* 27.26, 1230025 (Oct. 2012), p. 1230025. DOI: 10.1142/S0217751X12300256. arXiv: 1209.6213 [hep-ph].

[33]   A. Dedes et al. «Feynman rules for the Standard Model Effective Field Theory in R $_\xi$-gauges». In: *Journal of High Energy Physics* 2017.6, 143 (June 2017), p. 143. DOI: 10.1007/JHEP06(2017)143. arXiv: 1704.03888 [hep-ph].